

Elucidating the effects of selected antibiotics and artificial sweeteners on the intestinal microbiota and related fecal and plasma metabolomes of young adult Wistar rats

Aishwarya Murali



Propositions

1. The effects of chemicals on the gut microbiome cannot be adequately assessed without knowledge on the baseline variability.
(this thesis)
2. A strong reduction of urinary hippuric acid is a non-invasive parameter that indicates changes in the gut microbiome.
(this thesis)
3. Changing the intestinal microbiome can be a new strategy for pest management.
4. The introduction of stem cell therapy in underdeveloped countries needs to be accompanied by financial support from the companies providing the service.
5. Generation Z's obsession with early retirement will bear significant consequences on society, its economy and consequently their own children.
6. The attractiveness for Indian students to study abroad is not only for scientific reasons but also to escape the harsh reality of the country.

Propositions belonging to the thesis, entitled

'Elucidating the effects of selected antibiotics and artificial sweeteners on the intestinal microbiota and related fecal and plasma metabolomes of young adult Wistar rats'.

Aishwarya Murali

Wageningen, 09.10.2023

**Elucidating the effects of selected antibiotics
and artificial sweeteners on the intestinal
microbiota and related fecal and plasma
metabolomes of young adult Wistar rats**

Aishwarya Murali

Thesis committee

Promotor

Prof. Dr B. van Ravenzwaay

Special Professor, Reproduction and Development Toxicology

Wageningen University & Research

Former Senior Vice President of Experimental Toxicology and Ecology, BASF SE

Ludwigshafen, Germany

Co-promotor

Prof. Dr I.M.C.M. Rietjens

Professor of Toxicology

Wageningen University & Research

Other members

Dr T. Tralau, German Federal Institute for Risk Assessment, Berlin, Germany

Dr J. Louisse, Wageningen University & Research

Dr R. Landsiedel, BASF SE, Ludwigshafen, Germany

Prof. Dr S. Kersten, Wageningen University & Research

This research was conducted under the auspices of VLAG Graduate School (Biobased, Biomolecular, Chemical, Food and Nutrition Sciences)

Elucidating the effects of selected antibiotics and artificial sweeteners on the intestinal microbiota and related fecal and plasma metabolomes of young adult Wistar rats

Aishwarya Murali

Thesis

submitted in fulfilment of the requirements for the degree of doctor

at Wageningen University

by the authority of the Rector Magnificus,

Prof. Dr A.P.J. Mol,

in the presence of the

Thesis Committee appointed by the Academic Board

to be defended in public

on Monday 9 October 2023

at 4 p.m. in the Omnia Auditorium.

Aishwarya Murali

Elucidating the effects of selected antibiotics and artificial sweeteners on the intestinal microbiota and related fecal and plasma metabolomes of young adult Wistar rats,

215 pages.

PhD thesis, Wageningen University, Wageningen, the Netherlands (2023)

With references, with summary in English

ISBN: 978-94-6447-839-6

DOI: <https://doi.org/10.18174/636512>

Table of Contents

Chapter 1. General introduction	8
Chapter 2. Elucidating the Relations between Gut Bacterial Composition and the Plasma and Fecal Metabolomes of Antibiotic Treated Wistar Rats	26
Chapter 3. Connecting Gut Microbial Diversity with Plasma Metabolome and Fecal Bile Acid Changes Induced by the Antibiotics Tobramycin and Colistin Sulfate	76
Chapter 4. Gut Microbiota as Well as Metabolomes of Wistar Rats Recover within Two Weeks after Doripenem Antibiotic Treatment	112
Chapter 5. Investigating the gut microbiome and metabolome following treatment with artificial sweeteners acesulfame potassium and saccharin in young adult Wistar rats	150
Chapter 6. General Discussion and Future Perspectives	178
Chapter 7. Summary	202
Acknowledgements	206
About the Author	212





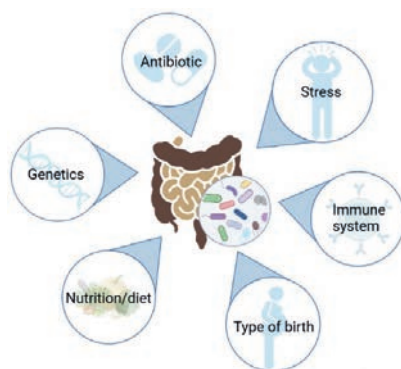
CHAPTER 1:

GENERAL INTRODUCTION

1.1. Background information on gut microbiota and associated metabolism

Mammalian host-microbial interactions have gained substantial attention in the past decades. It is estimated that the number of microorganisms populating a mammalian host, such as a human body, is in the same order as the number of mammalian cells in the host [1]. These microbes are present in numerous organs of the human body, including the skin, upper respiratory tract, vagina, gastrointestinal (GI) tract and several others. A vast majority of these microbes are known to colonize the GI tract where they compete with one another for survival and co-evolve with the host species [2]. These microbes are known as the gut microbiota, and include bacteria, archaea and eukaryotes, out of which bacteria are the predominant colonizers that are known to have co-evolved with the human host for over thousands of years to form a stable symbiotic relationship [3].

In the extensive analysis of human microbiota by the Human Microbiome Project (HMP), it has been estimated that bacteria are the predominant species dominating the human GI tract, exceeding by about 2-3 orders of magnitude the other prokaryotes, eukaryotes and archaea present. Bacteroidetes and Firmicutes are the most prominent phyla in the human gut microbiota, followed by Proteobacteria, Verrucomicrobia, Actinobacteria, Fusobacteria and Cyanobacteria [3, 4]. The diversity and composition of the gut bacteria are known to be rather stable up to phylum level and more species-specific at genus or species levels [5]. As shown in figure 1.1, several factors are known to influence the microbial population in the GI tract, including host diet, nutrition, host genetics, exposure to medications, immune system, method of delivery at birth and many others [2]. When the host is exposed to xenobiotics, such as antibiotics, not only harmful bacteria are targeted but also the host-associated 'good' bacterial communities can be affected, hence potentially affecting host health in a negative manner. One of the key limitations of antibiotic therapies is the resulting decreased bacterial diversity in the gut microbiota and the fact that this alteration may also affect the co-dependent colonizers, resulting in a potential increase in colonization by opportunistic pathogens leading to loss of host homeostasis [6].



Figures 1.1: Overview of different factors that influence the composition and functions of a healthy gut microbiota.

Gut bacteria are known to perform several vital bio-transformations of molecules that are ingested via host diet, in order to maintain host homeostasis [7]. These vital reactions include extraction of calories from the host diet, synthesis of essential vitamins and amino acids, bile acid and lipid metabolism, support of host immune functions, maintaining the energy balance and preventing infections [8]. The ability to perform these vital functions to maintain host health and prevent diseases have high relevance in the fields of toxicology, pharmacology, oncology and many others [9]. Specific microbial (bio)transformation reactions for xenobiotics and other dietary constituents include processes like reduction, hydrolysis, removal of succinate groups, dehydroxylation, (de)acetylation, reductive cleavage of azo bonds, proteolysis, and denitration [10-13]. These reactions may significantly alter, that is, increase as well as decrease, the toxicity of the respective compounds. Furthermore, some forms of microbial dysbiosis are associated with human diseases such as Crohn's disease, colon cancer, diabetes, allergies, Alzheimer's and Parkinson's disease, depression, stroke, and many more [14, 15]. Therefore, the microbiota can significantly impact the host health, but the functional relevance of dysbiosis and the processes a perturbed microbiota mediates are poorly understood, since experimental systems to address these complex processes are also lacking.

Further, the huge inter-individual differences in microbiota composition may also hamper the interpretation of the consequences of compositional changes of the microbiota. Thus, it is important to perform both the taxonomic profiling to capture inter- and intraspecies differences as well as to analyze microbial metabolic functionality [16-18]. Integrative research approaches will advance knowledge about how taxonomic differences drive intestinal metabolic capacity. To increase our mechanistic understanding of how the microbiota influences host health, there is a need to integrate knowledge of the composition of the gut microbiota with its functionality in terms of microbiota-mediated metabolic processes. Given the complexity of this system, the integration of omics technologies represents a well fit approach towards a functional and mechanistic understanding of the complex dynamics of host-microbiome interactions [19].

Aim of this thesis

The main objective of the present thesis was to extend knowledge of the gut microbiota mediated production of small molecules or endogenous metabolites via metabolism, with the help of integrated omics approaches using young adult rat models. To address this objective, an OECD 407 guideline type of study design was used where rats were orally administered a variety of test compounds, from antibiotics to artificial sweeteners and blood and feces samplings were conducted to analyze the extent of the role of gut microbiota on the host metabolic patterns. The test compounds and their dosage were selected in order to induce perturbations in the gut microbiota but avoiding systemic toxic effects. The reason for doing this was to not have any interferences in the targeted metabolome profiles as a result of a systemic response to the administered compounds. At first, antibiotics were selected to study the

changes induced in the metabolism via the perturbed gut microbiota as they are known to cause an antibacterial response. In addition, two different non-caloric artificial sweeteners were selected to study their effects on the gut microbiota and the corresponding changes induced in the gut microbiota-mediated metabolism. The effects of the compounds on the gut composition as well as on the metabolic output (functions) were analyzed and several key biomarkers or metabolites associated with a perturbed gut microbiota were identified. Furthermore, the ability of spontaneous restoration of the gut microbiota and associated metabolism post antibiotic exposure was investigated in order to better understand natural recovery of the gut microbiota and functions without any external or therapeutic intervention. The results obtained will contribute to the understanding of the metabolic contribution of the gut microbiota.

1.2. Impact of gut microbiota on host health

The most frequently discussed phyla that are associated with the human gut microbiota are Firmicutes, Bacteroidetes, Actinobacteria, and Proteobacteria, as these four phyla constitute up to 99% of intestinal microbiota in healthy adults with Firmicutes and Bacteroidetes being predominant (~ 90%) [20, 21]. Apart from these key bacterial phyla, the homeostasis and host health are defined by the gut bacterial specific diversity or richness. Gut resilience acts against any deviation from the healthy state in order to not compromise host health and hence, any change in the levels of specific phyla or a reduction in species diversity could indicate a perturbed gut and potentially result in deviation from a healthy state.

Gut bacterial homeostasis is necessary to maintain host health. As mentioned in the previous section, a variety of factors can induce a disruption of this homeostatic state. A shift in the gut bacterial composition and/or metabolic functions, is known to affect host health by contributing to many host diseases [22]. GI-associated diseases such as Crohn's disease and ulcerative colitis are the most prevalent forms of inflammatory bowel disease [10-15]. It has been shown that a reduced intestinal microbial diversity, including an increase in Bacteroidetes and a reduction in Firmicutes are observed in patients suffering from Crohn's disease and ulcerative colitis. Furthermore, other conditions such as metabolic disorders, obesity, and type 2 diabetes have been associated with gut dysbiosis. In obese humans and rodent models, an increase in the relative abundances of Firmicutes and a reduction in Bacteroidetes levels have been observed, making gut dysbiosis a gold standard in prediction of metabolic diseases [23, 24]. A stable Firmicutes/Bacteroidetes ratio is widely accepted to have an overall key influence in maintaining a healthy gut homeostasis [25, 26]. A change in this ratio has been associated with obesity, gut inflammation, increasing the risk of systemic bacterial infections [27, 28].

Studies with germ-free rodent models that possess no microorganisms in or on them, showed that the absence of gut microbes has consequences for the regulation of fat storage and metabolism, highlighting the metabolic functionality of the intestinal microbiota [29, 30]. A dysbiotic state of human gut

microbiota has an overall impact on the metabolome of the microbial community as well as consequently on the host metabolome.

Reduced levels of vital commensal bacteria (commensalism is where one species gains benefit while the other species neither benefits nor is harmed) may lead to open ‘niches’ available for pathogenic bacteria to grow, potentially leading to overgrowth of certain harmful pathogens such as *Clostridium difficile*, thereby compromising the immune functions of the host [31]. Nevertheless, doubts still persist whether gut dysbiosis is a direct cause for metabolic-related disorders or rather a consequence. Hence, further studies are necessary to understand this causal versus consequence relationship of dysbiosis and disease.

1.3. Relevance of gut microbiota in the field of toxicology

The contribution of intestinal microbial biotransformation to the overall host metabolism is not well studied, but nevertheless an important field for toxicology. Toxicity studies routinely investigate many organs/target sites including the liver, kidney, lungs, thyroid system and many others (toxicodynamics), while including absorption, distribution, metabolism (in most cases in the liver) and excretion of a compound (toxicokinetics), while the role of gut-mediated metabolism is still poorly characterized [16, 18]. The plethora of bacterial species that colonize the gut microbiota may have important contributions in (de)toxification of chemical compounds and/or the production of endogenous metabolites. Therefore, it is important to understand the metabolic capabilities of the intestinal microbiota and to consider how changes in their composition could play a role in altered metabolism of chemicals and pharmaceuticals. Further, chemicals may be absorbed and transported to the liver, where they are conjugated and excreted back into the gut through bile secretion for subsequent microbial metabolism. The metabolic functions of intestinal microbes can influence the absorption, distribution, metabolism and excretion (ADME) of a specific compound [32]. The interaction of intestinal microbiota with chemical compounds is bidirectional. First, the chemical compound can induce changes in the gut community structure and second, there can be changes induced by the gut community on the compound itself. To address the first aspect, a combination of omics approaches would be of use [33].

In regulatory toxicological studies, rodents and in particular rats are commonly used to assess chemical safety for humans and have significantly contributed to delineating correlations between the intestinal microbiome and diseases [34, 35]. Analyses of rat intestinal microbiota revealed bacterial diversity exceeding that of the human gut by 2-3 orders of magnitude [1]. The microbiota of rats, the gold standard model in toxicology, appear to be more representative of the human gut microbiota than mice microbiota [21, 36]. Even though there are overlaps in microbiota composition between species, it is not clear to which extent differences in the microbiota contribute to species differences in responses to toxicant exposure. The gut microbiota and its metabolic capacity can be studied by inducing an artificial shift in the composition through exposure to xenobiotics. Consequently, microbiota-derived metabolites

need to be assessed. As these mechanistic studies are generally performed on rodent models, there is a need to understand the inter-individual variability in the composition of the gut microbiota of rodents, as well as inter-species differences of the microbiome in order to extrapolate the data to humans.

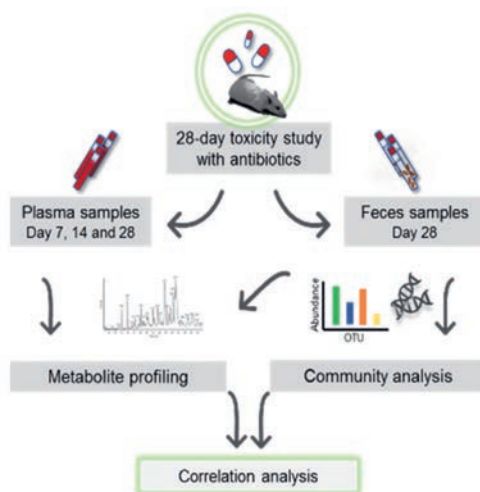


Figure 1.2: Schematic diagram of experimental design overview. The study design followed a 28-day repeated dose oral study with young adult Wistar rats where blood sampling was conducted on days 7, 14 and 28 and feces collection on day 28 of the study. Both the sampled matrices were used for metabolomics and feces was also used for 16S marker gene sequence analysis.

In vivo toxicological studies, specifically short term acute and subacute studies such as for example 28 days repeated oral dose toxicity studies compliant to OECD 407 guidelines are a practical streamlined setup to study the effects of orally (by gavage) administered compounds in rat models (Figure 1.2). Such studies may be used to analyse the impacts of orally administered test substances (such as xenobiotics) during a limited period of time [37]. These guidelines are specific for rats and indicate that at least 10 animals (five per sex) have to be used per dose group and that there should be at least three test groups including controls. Clinical parameters including regular measurements of body weights and food/water consumption need to be noted throughout the study followed by gross necropsy and histopathology once the 28 days of the study are over. This study design also fits well with the in-house database that is used to upload and analyse metabolome profiles which accepts data from a 28-day study design.

1.4. Importance of multi-omics technologies

To better understand the gut microorganisms as well as their derived metabolites necessary for host health, integrated omics approaches help to explain the complexities of the gut bacteria-host interactions. First of all, in order to understand the changes induced by a particular chemical compound on the gut community structure, Next Generation Sequencing (NGS) may be applied [38, 39]. Developments in NGS have aided in many breakthroughs of taxonomic or phylogenetic profiling of the gut microbiota. For example, the use of 16S rDNA gene sequencing

has been the standard to study bacterial phylogeny and taxonomy [40, 41]. Gut dysbiosis can be easily assessed by determining alterations in the levels of gut bacterial families via 16S rDNA gene sequencing. Using this method, along with bioinformatics analysis, identification of intestinal bacterial genus and/or species could be determined [41].

Further, analysis of the metabolic potential of gut microbiota is possible via identification of gut bacteria-derived metabolites that may alter host physiology and pathology. Metabolomics is a technique which involves detection of a broad range of metabolites from a biological matrix (such as urine, blood, tissue samples, feces among others). These metabolites could be of any class including carbohydrates, fatty acids, amino acids, energy metabolites, bile acids and their derivatives. Sensitive mass spectrometry-based methods including LC-MS and GC-MS offer the possibility to detect and quantify relevant metabolites [16, 19]. In the last decades, metabolomics has been regarded as a vital tool in risk assessment in the field of toxicology. By using this approach in toxicology as a screening tool, various metabolite patterns for adverse effects on different toxicological targets (liver, kidney, thyroid system, testes, blood, nervous system and endocrine system) and various modes of action were established in the BASF MetaMapTox (MMT) database [42-45].

The MMT database consists of metabolite profiles as well as toxicity data of over 1000 chemicals, agrochemicals and drugs. MMT is an in-house database that consists of metabolic profiles from highly standardized studies that are OECD 407 guidelines compliant. MMT has been successfully used as a tool for the identification and prediction of toxicological modes of action of new compounds [46]. In addition, applicability to improve the quality of read across cases has been shown thus reducing the need for animal testing [42-45, 47, 48]. Metabolic patterns have been generated using well characterized reference compounds and their respective toxicological endpoints which can be used to predict the toxicity of chemicals based on their specific metabolome [42]. In summary after exposing rats to a specific chemical, via the MTT database, changes in the metabolite profiles can be linked to (the absence of) toxicological effects. We have used this experimental set up to study the effects of various compounds, assumed to affect the microbiome, on subsequent changes in the fecal and plasma metabolome. The MMT database was used to assess if exposure to the substances investigated in this thesis may have produced systemic toxicity [46].

The metabolites produced by the gut bacteria are known to be absorbed across the intestinal cell wall and can be further modified by the liver, ending up circulating in the blood stream of the host [49]. The metabolic patterns may be measured with the help of metabolomics, that can serve as a tool for assessing the functional output of the microbiome beyond genomics. Metabolites that are produced by the microbiota and are available for uptake by the host may potentially affect the host organism systemically. Since the blood plasma metabolite profile consists of both the microbiota-derived metabolites as well as the endogenous metabolites, combined metabolome analysis of both blood plasma and feces of control as well as antibiotic treated rats would help to find out which metabolites

were derived specifically from the gut bacteria and to determine their impact on the host metabolite profile. Using the integrative genomics and metabolomics approaches as well as the existing knowledge from the MMT database, gut microbial functionality may be studied after treatment with substances which are known to induce an artificial shift in the microbial community.

1.5. Complex ecological dynamics of gut microbiota

A healthy or 'normal' gut microbiota composition is hard to be defined due to a high inter-individual and inter-species variability of the bacteria colonizing the GI tract. It is known that the gut bacterial composition stays conserved only up to phyla levels and beyond that taxonomy, it is known to be rather unique to individuals. The inter- and intra-individual variability in gut microbiota composition may occur predominantly due to external factors as previously mentioned. Hence, analyzing the differences in the gut microbiota across a population and correlating this variability with variability in specific metabolic functions is necessary to understand the gut-mediated host metabolism. The huge inter-individual differences in microbiota composition may further hamper the interpretation of compositional changes. Gut microbiota dynamics is complex and diverse across ecological communities which includes inter- and intra-individual fluctuations. These fluctuations may be short or long term and therefore it is important to understand to what extent a variation may be defined as 'normal'. And in case of abnormal temporal fluctuations of a specific taxa, it could be considered as a biomarker for any form of clinically relevant illness [50, 51]. Thus, it is important to perform both the taxonomic profiling to capture inter- and intraspecies differences as well as to analyze the resulting variability in gut microbiota-mediated metabolic functions [50].

Antibiotic administration shifts the gut microbiota to a different state, causing a dysbiosis and a natural restoration of the gut microbiota after cessation of the treatment towards a healthy pre-dysbiosis state indicates resilience. The present knowledge on the ability of the gut microbiota to recover spontaneously post-antibiotic cessation is not well studied. However, it is not only necessary to understand this restoration patterns of gut bacterial strains following antibiotic treatment but also to characterize the associated metabolite recoveries in order to understand full functional restoration. This knowledge may be an important factor to maintain or restore long-term host health, as it lays the basis for rationale strategies that could reduce long-term effects of antibiotic treatment on gut health. Although the antibiotic treatments are normally short-term, they might shift the gut microbiota to long term dysbiosis states, which may consequently induce permanent loss of useful commensal bacteria and hence increased colonization of pathogenic bacteria and eventually promoting adverse effects on the host leading to diseases including colorectal adenoma [52], risk of type 2 diabetes [53], Parkinson's disease [54] and several others.

1.6. Gut microbiota-derived metabolites

The gut microbiota interacts with the host primarily through metabolites. These are small molecules produced as intermediates or end products during intestinal microbial metabolism. Bacteria may produce metabolites by metabolically modifying dietary substrates, or directly by modifying host molecules, such as bile acids [55]. The short chain fatty acids (SCFAs) are intestinally produced from dietary fibers. SCFAs may also be produced via protein fermentation but they are mainly derived from branched chain fatty acids, such as, isobutyrate and 2-methylbutyrate [56]. Acetate, propionate and butyrate are the highly abundant SCFAs, making up almost 95% of the total SCFAs [57]. 95% of these SCFAs produced in the cecum and large intestine are known to be rapidly absorbed into the systemic circulation, whereas the remaining 5% get eliminated from the system. Any perturbation in the gut microbiome may affect the concentration threshold of these vital SCFAs in the host [58].

Other metabolites such as hippuric acid, indole derivatives and glycerol are also established as key plasma biomarkers of a perturbed gut microbiome [59, 60]. Indoles are metabolites from the bacterial tryptophan metabolism pathway and these metabolites function as signaling molecules in the gut homeostasis where they may regulate bacterial biofilm production, motility, antibiotic resistance mechanisms and secretion of virulence factors [61]. One of the indole derivatives, indole-3-propionic acid or IPA, is involved in both tryptophan and indole metabolism. This metabolite is known to be a potent antioxidant, which is produced by gut bacterial species, and is then introduced into the bloodstream of the host for further functions [62]. Another indole derivative, indole-3-acetic acid or IAA originates from dietary tryptophan metabolism by intestinal bacteria. The source of tryptophan is either from dietary protein degradation or directly from the intestinal bacteria [63]. The bacterial tryptophanase enzyme may degrade tryptophan to produce skatole and indole, where indole gets absorbed directly from the intestine into the bloodstream and is further metabolized in the liver [64]. Another indole derivative indoxyl sulfate is produced from intestinally generated indole, in the liver [61]. This metabolite has only been found in the serum of animals that harbor microbes and hence is a great candidate for a gut perturbation associated key biomarker, as a gut bacterial reduction subsequently leads to loss of the necessary bacterial enzymes that further aid in the production of this metabolite.

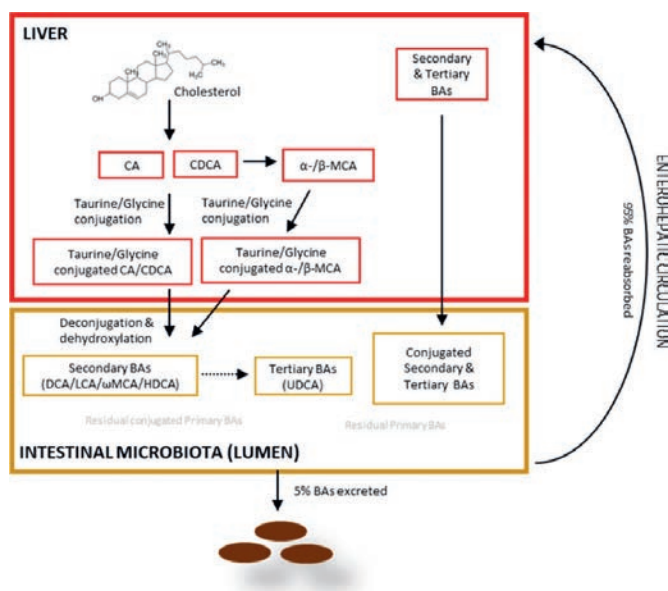


Figure 1.3: Schematic diagram showing bile acid metabolism. Bile acids in red boxes are the primary bile acids that are produced in the liver and/or enter into the liver via the enterohepatic circulation (portal vein). Presented in brown boxes are the secondary and tertiary bile acids that are produced from primary bile acids, and 95% of these conjugated and/or unconjugated bile acids are reabsorbed from the colon walls and re-enter the liver via enterohepatic circulation to tightly regulate the BA pool [65].

Secondary or tertiary bile acids are known to be produced from primary bile acids, by the gut bacteria via bacterial deconjugation and dehydroxylation reactions (Figure 1.3). Primary bile acids, i.e., cholic acid and chenodeoxycholic acid are synthesized in the liver from cholesterol and are subsequently conjugated with amino acids (taurine or glycine). They are further secreted into the bile and finally reach the small intestine for lipid metabolism and emulsification reactions. About 95% of these bile acids enter the enterohepatic circulation and hence are reabsorbed in the ileum while the rest (~5%) reach the colon and are further excreted in the feces [66, 67]

In the intestine, taurine or glycine conjugated primary bile acids are converted by bacterial enzymes to their unconjugated forms and further undergo a cascade of reactions including dehydroxylation reactions to produce secondary (deoxycholic acid, lithocholic acid, omega muricholic acid and hyodeoxycholic acid) and tertiary bile acids (ursodeoxycholic acid). Bacterial bile salt hydrolases are enzymes that catalyze deconjugation reactions performed by obligate anaerobes that is the first step to convert primary to secondary bile acids [68].

1.7. Test compounds to study the gut microbiome

In the present thesis six different test compounds were selected to study the gut microbiota and its metabolic functions in Wistar rats. The selection of the antibiotics and the dose selection were performed based on three main criteria. First, the test compound should be known to alter the gut

microbiota composition. Second, the compound should have low or no systemic bioavailability and finally, the dosage of the compounds selected should not induce any form of systemic or organ-specific toxicity. Four antibiotics belonging to three different antibiotic classes were used to change the gut microbiome and to elucidate the consequences thereof on the gut (fecal) and the plasma metabolome in treated rats. Having established this test system, two different artificial sweeteners were selected to study their effects. The antibiotics selected for the 28-day oral study using young adult Wistar rats were tobramycin, colistin sulfate, meropenem trihydrate and doripenem hydrate. Further, two artificial sweeteners namely, acesulfame potassium and saccharin were selected because there is widespread human oral exposure to these substances. The effects of these noncaloric sweeteners were analyzed on the gut microbiota and the resulting metabolites. The dosage and form of preparation of these compounds are presented in Table 1.1.

Table 1.1: List of test compounds used in this thesis, their dose levels and forms of preparation. All the compounds were administered orally by gavage.

Treatment	Low Dose (mg/kg bw/d) ^a	High Dose (mg/kg bw/d) ^a	Form of Preparation
Tobramycin	100	1000	in deionized water
Colistin sulfate	10	100	in deionized water
Meropenem trihydrate	100	300	in deionized water
Doripenem hydrate	100	1000	in deionized water
Acesulfame potassium	40	120	in deionized water
Saccharin	20	100	In 0,5% CMC ^b

^a mg/kg body weight/day. ^b carboxymethyl cellulose

1.7.1. Antibiotics

Antibiotics are well known and widely used in medicine for their antimicrobial properties, hence, making them good candidates to study consequences of effects on the gut microbiota [69]. Tobramycin is an aminoglycoside antibiotic which is known to be a broad spectrum antibiotic and to be active against Gram negative bacteria including Enterobacteriaceae spp., *Escherichia coli*, *Klebsiella pneumoniae*, *Pseudomonas aeruginosa* and several others and also against a few Gram positives including *Staphylococcus* spp., *Streptococcus* spp. and *Mycobacterium* spp. [70]. The mode of action of this antibiotic is via inhibition of protein synthesis in cells of Gram negative and positive bacteria. It is a poorly bioavailable antibiotic with almost 90% being eliminated from the system via feces [71]. Colistin sulfate on the other hand, is a Polymyxin antibiotic whose mode of action is by penetrating through the bacterial cell membrane and disrupting it. It is also a poorly bioavailable antibiotic and hence is less likely to be absorbed and have a systemic influence on the host [72, 73]. The two carbapenem antibiotics, meropenem trihydrate and doripenem hydrate are broad-spectrum antibiotics that are active against both Gram positive and negative bacteria [74, 75]. These antibiotics cause bacterial cell death after inhibiting the penicillin-binding proteins, which are bacterial enzymes that are otherwise responsible for peptidoglycan cross-linking during the process of bacterial cell wall synthesis [74] [76]. Both the carbapenems are known to be poorly bioavailable [77, 78].

1.7.2. Artificial sweeteners

In recent years, the harmful effects of sugars such as obesity, diabetes, other metabolic diseases like non-alcoholic fatty liver disease, hypertension, to name a few are well known and this has significantly increased the consumption of synthetic or artificial sweeteners as the latter have no caloric value [79-81]. Several studies have shown that these sweeteners may cause gut dysbiosis leading to inflammation and gastrointestinal diseases [82-84]. These compounds are also known to reduce the useful commensal bacteria and hereby, potentially increase the abundance of pathogenic bacteria in the gut such as for example of *Escherichia coli* leading to health risks in the host organism [85, 86]. Both acesulfame potassium (Ace-K) and saccharin are approved as low-caloric artificial sweeteners, where both have been considered as safe [87-89]. Although many studies have addressed the effects of these two sweeteners on the gut composition, none of those studies relate the changes in the gut composition to the metabolic functions of the host.

1.8. Thesis outline

Since the last decades, gut bacteria and their crosstalk with the host organism and related consequences for host health have been extensively studied using various techniques. The aim of this thesis was to associate changes in the gut composition with metabolic functionality in the host. This was achieved by altering the gut microbiome by exposure of rats to antibiotics. Given the complexity of the system, a combined omics approach was considered the best way to understand the complex dynamics of the host-microbiota interactions. The objectives of the thesis were (1) to explore the interrelationship between microbiome composition and host fecal and plasma metabolome, (2) to identify metabolic biomarkers that may govern these interactions between the gut bacteria and host, (3) to investigate reversibility of the gut microbiome and associated metabolites following cessation of treatment. Finally, the experimental set up used for the antibiotics was applied to investigate the effects of two artificial sweeteners as case studies.

Chapter 1 provides an overall introduction on the topic of the thesis, which includes background information about the approach and methodologies used to study the metabolic potential of the gut microbiota in rats, as well as an overview of the importance of the gut microbiota for host health, the consequences of dysbiosis and the microbial metabolites that are important for the host metabolome. The aim of the thesis is defined, and an overview of the compounds used in the studies to address the aim is outlined in this chapter followed by an outline of the thesis.

In **Chapter 2**, the correlations between altered gut bacterial families and fecal and plasma metabolites were investigated upon exposure of rats to a series of selected antibiotics. Antibiotics from different classes and with a different activity spectrum were used to induce an artificial shift in the gut composition and functions. These perturbations were then used to define correlations between altered

gut bacterial families and the fecal and plasma metabolites in order to elucidate which bacterial families are responsible for the formation of fecal or plasma metabolites.

In **Chapter 3**, two additional antibiotics belonging to different classes were used to elucidate their effects on the fecal and host plasma metabolomes via an effect on intestinal microbial metabolic capacity, specifically that of the bile acids, using the same 28-day exposure rodent model. Tobramycin and colistin sulfate were selected based on their low bioavailability and their ability to cause a gut microbial perturbation. As such a comprehensive analysis of the effects on the gut microbiota as well as on the plasma and fecal metabolomes upon exposure to the two antibiotics was performed. These plasma and fecal metabolites were then used to identify key biomarkers that are indicative of an altered gut microbiome resulting from the broad-spectrum activity of the two antibiotics.

In the previous chapters the rodents were orally exposed to drugs for 28 days. However, it was noted that the 28-day antibiotic exposure, may be longer than a real-life exposure regimen where antibiotic exposure duration is rather short, and thus may lead in the rat experiments to rather long-term or permanent effects on the gut microbiome of the host. Although post-antibiotic recovery of the gut microbiota has been vastly studied the restoration of the metabolite patterns post antibiotic cessation is rather unexplored. Hence, in **Chapter 4**, the ability of spontaneous restoration of the gut microbiota and metabolomes, one and two weeks after carbapenem antibiotic cessation, was studied. The results from this study will be indicative of if external or therapeutic intervention is needed to restore the gut and its metabolic functions post-antibiotic exposure.

In **Chapter 5** of the thesis, a different class of compounds, two non-caloric artificial sweeteners, were investigated for their effects on the microbiota and related metabolite patterns. The effects of the artificial sweeteners, acesulfame potassium and saccharin on the gut (fecal) bacterial composition and associated fecal and host plasma metabolomes was investigated in a 28-day rat study. Due to the growing human exposure to artificial sweeteners via the diet, it was of interest to characterize the effects of the two model sweeteners on the gut microbial population and related metabolomes.

Finally in **Chapter 6**, the key results from the previous chapters are highlighted and discussed along with future recommendations and perspectives with regard to rodent studies on effects on gut microbiota and related metabolism and translation of these key findings to humans.

References

1. Sender, R., S. Fuchs, and R. Milo, *Revised estimates for the number of human and bacteria cells in the body*. PLoS biology, 2016. **14**(8): p. e1002533.
2. Cresci, G.A. and E. Bawden, *Gut microbiome: what we do and don't know*. Nutrition in Clinical Practice, 2015. **30**(6): p. 734-746.
3. Jost, L., et al., *Partitioning diversity for conservation analyses*. Diversity and Distributions, 2010. **16**(1): p. 65-76.
4. *Structure, function and diversity of the healthy human microbiome*. nature, 2012. **486**(7402): p. 207-214.
5. Manichanh, C., et al., *Reshaping the gut microbiome with bacterial transplantation and antibiotic intake*. Genome research, 2010. **20**(10): p. 1411-1419.
6. Thursby, E. and N. Juge, *Introduction to the human gut microbiota*. Biochemical journal, 2017. **474**(11): p. 1823-1836.
7. Koppel, N., V. Maini Rekdal, and E.P. Balskus, *Chemical transformation of xenobiotics by the human gut microbiota*. Science, 2017. **356**(6344): p. eaag2770.
8. Agus, A., J. Planchais, and H. Sokol, *Gut microbiota regulation of tryptophan metabolism in health and disease*. Cell host & microbe, 2018. **23**(6): p. 716-724.
9. Clayton, T.A., et al., *Pharmacometabonomic identification of a significant host-microbiome metabolic interaction affecting human drug metabolism*. Proceedings of the National Academy of Sciences, 2009. **106**(34): p. 14728-14733.
10. Wilson, I.D. and J.K. Nicholson, *Gut microbiome interactions with drug metabolism, efficacy, and toxicity*. Translational Research, 2017. **179**: p. 204-222.
11. Forbes, J.D., G. Van Domselaar, and C.N. Bernstein, *The gut microbiota in immune-mediated inflammatory diseases*. Frontiers in microbiology, 2016. **7**: p. 1081.
12. Neis, E.P., C.H. Dejong, and S.S. Rensen, *The role of microbial amino acid metabolism in host metabolism*. Nutrients, 2015. **7**(4): p. 2930-2946.
13. Wolf, G., *Gut microbiota: a factor in energy regulation*. Nutrition reviews, 2006. **64**(1): p. 47-50.
14. Zhang, Y.-J., et al., *Impacts of gut bacteria on human health and diseases*. International journal of molecular sciences, 2015. **16**(4): p. 7493-7519.
15. Lecomte, V., et al., *Changes in gut microbiota in rats fed a high fat diet correlate with obesity-associated metabolic parameters*. PloS one, 2015. **10**(5): p. e0126931.
16. Behr, C., et al., *Gut microbiome-related metabolic changes in plasma of antibiotic-treated rats*. Arch Toxicol, 2017. **91**(10): p. 3439-3454.
17. Behr, C., et al., *Impact of lincosamides antibiotics on the composition of the rat gut microbiota and the metabolite profile of plasma and feces*. Toxicol Lett, 2018. **296**: p. 139-151.
18. Murali, A., et al., *Elucidating the Relations between Gut Bacterial Composition and the Plasma and Fecal Metabolomes of Antibiotic Treated Wistar Rats*. Microbiology Research, 2021. **12**(1): p. 82-122.
19. Behr, C., et al., *Microbiome-related metabolite changes in gut tissue, cecum content and feces of rats treated with antibiotics*. Toxicol Appl Pharmacol, 2018. **355**: p. 198-210.
20. Manichanh, C., et al., *Reshaping the gut microbiome with bacterial transplantation and antibiotic intake*. Genome Res, 2010. **20**(10): p. 1411-9.
21. Li, D., et al., *Microbial biogeography and core microbiota of the rat digestive tract*. Scientific reports, 2017. **7**(1): p. 1-16.
22. Lozupone, C.A., et al., *Diversity, stability and resilience of the human gut microbiota*. Nature, 2012. **489**(7415): p. 220-230.
23. Bidell, M.R., A.L. Hobbs, and T.P. Lodise, *Gut microbiome health and dysbiosis: A clinical primer*. Pharmacotherapy: The Journal of Human Pharmacology and Drug Therapy, 2022. **42**(11): p. 849-857.
24. Fredricks, D.N. *Microbial ecology of human skin in health and disease*. in *Journal of Investigative Dermatology Symposium Proceedings*. 2001. Elsevier.
25. Stephens, R.W., L. Arhire, and M. Covasa, *Gut microbiota: from microorganisms to metabolic organ influencing obesity*. Obesity, 2018. **26**(5): p. 801-809.

26. Stojanov, S., A. Berlec, and B. Štrukelj, *The influence of probiotics on the firmicutes/bacteroidetes ratio in the treatment of obesity and inflammatory bowel disease*. Microorganisms, 2020. **8**(11): p. 1715.
27. Magne, F., et al., *The firmicutes/bacteroidetes ratio: a relevant marker of gut dysbiosis in obese patients?* Nutrients, 2020. **12**(5): p. 1474.
28. Flint, H.J., *Obesity and the gut microbiota*. Journal of clinical gastroenterology, 2011. **45**: p. S128-S132.
29. Tilg, H., A.R. Moschen, and A. Kaser, *Obesity and the microbiota*. Gastroenterology, 2009. **136**(5): p. 1476-1483.
30. Musso, G., R. Gambino, and M. Cassader, *Gut microbiota as a regulator of energy homeostasis and ectopic fat deposition: mechanisms and implications for metabolic disorders*. Current opinion in lipidology, 2010. **21**(1): p. 76-83.
31. Kim, S., A. Covington, and E.G. Pamer, *The intestinal microbiota: antibiotics, colonization resistance, and enteric pathogens*. Immunological reviews, 2017. **279**(1): p. 90-105.
32. Noh, K., et al., *Role of intestinal microbiota in baicalin-induced drug interaction and its pharmacokinetics*. Molecules, 2016. **21**(3): p. 337.
33. Giambò, F., et al., *Toxicology and microbiota: How do pesticides influence gut microbiota? A review*. International Journal of Environmental Research and Public Health, 2021. **18**(11): p. 5510.
34. Tu, P., et al., *Gut microbiome toxicity: connecting the environment and gut microbiome-associated diseases*. Toxics, 2020. **8**(1): p. 19.
35. Collins, S.L. and A.D. Patterson, *The gut microbiome: an orchestrator of xenobiotic metabolism*. Acta Pharmaceutica Sinica B, 2020. **10**(1): p. 19-32.
36. Wos-Oxley, M.L., et al., *Comparative evaluation of establishing a human gut microbial community within rodent models*. Gut microbes, 2012. **3**(3): p. 234-249.
37. OECD, *Test No. 407: Repeated Dose 28-day Oral Toxicity Study in Rodents*. 2008.
38. Bäumlner, A.J. and V. Sperandio, *Interactions between the microbiota and pathogenic bacteria in the gut*. Nature, 2016. **535**(7610): p. 85-93.
39. Lin, M., et al., *Dynamic metabonomic and microbiological response of rats to lincomycin exposure: an integrated microbiology and metabonomics analysis*. RSC advances, 2015. **5**(80): p. 65415-65426.
40. Yarza, P., et al., *Uniting the classification of cultured and uncultured bacteria and archaea using 16S rRNA gene sequences*. Nature Reviews Microbiology, 2014. **12**(9): p. 635-645.
41. Janda, J.M. and S.L. Abbott, *16S rRNA gene sequencing for bacterial identification in the diagnostic laboratory: pluses, perils, and pitfalls*. Journal of clinical microbiology, 2007. **45**(9): p. 2761-2764.
42. Sperber, S., et al., *Metabolomics as read-across tool: An example with 3-aminopropanol and 2-aminoethanol*. Regulatory Toxicology and Pharmacology, 2019. **108**: p. 104442.
43. Kamp, H., et al., *Reproducibility and robustness of metabolome analysis in rat plasma of 28-day repeated dose toxicity studies*. Toxicology letters, 2012. **215**(2): p. 143-149.
44. Van Ravenzwaay, B., et al., *Metabolomics as read-across tool: A case study with phenoxy herbicides*. Regulatory Toxicology and Pharmacology, 2016. **81**: p. 288-304.
45. Van Ravenzwaay, B., et al., *The use of metabolomics in cancer research*. An Omics Perspective on Cancer Research, 2010: p. 141-166.
46. Van Ravenzwaay, B., et al., *The use of metabolomics for the discovery of new biomarkers of effect*. Toxicology letters, 2007. **172**(1-2): p. 21-28.
47. Mattes, W., et al., *Detection of hepatotoxicity potential with metabolite profiling (metabolomics) of rat plasma*. Toxicology letters, 2014. **230**(3): p. 467-478.
48. Ravenzwaay, B.V., et al., *The development of a database for metabolomics-Looking back on ten years of experience*. International Journal of Biotechnology, 2015. **14**(1): p. 47-68.
49. Roberts, M.S., et al., *Enterohepatic circulation: physiological, pharmacokinetic and clinical implications*. Clinical pharmacokinetics, 2002. **41**: p. 751-790.
50. Olsson, L.M., et al., *Dynamics of the normal gut microbiota: A longitudinal one-year population study in Sweden*. Cell Host & Microbe, 2022. **30**(5): p. 726-739. e3.

51. Ji, B.W., et al., *Macroecological dynamics of gut microbiota*. Nature microbiology, 2020. **5**(5): p. 768-775.
52. Cao, Y., et al., *Long-term use of antibiotics and risk of colorectal adenoma*. Gut, 2018. **67**(4): p. 672-678.
53. Yuan, J., et al., *Long-term use of antibiotics and risk of type 2 diabetes in women: a prospective cohort study*. International Journal of Epidemiology, 2020. **49**(5): p. 1572-1581.
54. Palacios, N., et al., *Long-Term Use of Antibiotics and Risk of Parkinson's Disease in the Nurses' Health Study*. Parkinson's Disease, 2020. **2020**.
55. Lavelle, A. and H. Sokol, *Gut microbiota-derived metabolites as key actors in inflammatory bowel disease*. Nature reviews Gastroenterology & hepatology, 2020. **17**(4): p. 223-237.
56. Macfarlane, G., et al., *Estimation of short-chain fatty acid production from protein by human intestinal bacteria based on branched-chain fatty acid measurements*. FEMS microbiology ecology, 1992. **10**(2): p. 81-88.
57. Mortensen, P.B. and M.R. Clausen, *Short-chain fatty acids in the human colon: relation to gastrointestinal health and disease*. Scandinavian Journal of gastroenterology, 1996. **31**(sup216): p. 132-148.
58. Shen, G., et al., *Gut microbiota-derived metabolites in the development of diseases*. Canadian Journal of Infectious Diseases and Medical Microbiology, 2021. **2021**.
59. Behr, C., et al., *Gut microbiome-related metabolic changes in plasma of antibiotic-treated rats*. Archives of Toxicology, 2017. **91**: p. 3439-3454.
60. Behr, C., et al., *Microbiome-related metabolite changes in gut tissue, cecum content and feces of rats treated with antibiotics*. Toxicology and Applied Pharmacology, 2018. **355**: p. 198-210.
61. Glorieux, G., T. Gryp, and A. Perna, *Gut-derived metabolites and their role in immune dysfunction in chronic kidney disease*. Toxins, 2020. **12**(4): p. 245.
62. Wikoff, W.R., et al., *Metabolomics analysis reveals large effects of gut microflora on mammalian blood metabolites*. Proceedings of the national academy of sciences, 2009. **106**(10): p. 3698-3703.
63. Keszthelyi, D., F. Troost, and A. Masclee, *Understanding the role of tryptophan and serotonin metabolism in gastrointestinal function*. Neurogastroenterology & Motility, 2009. **21**(12): p. 1239-1249.
64. Gao, J., et al., *Impact of the gut microbiota on intestinal immunity mediated by tryptophan metabolism*. Frontiers in cellular and infection microbiology, 2018. **8**: p. 13.
65. Murali, A., et al., *Connecting Gut Microbial Diversity with Plasma Metabolome and Fecal Bile Acid Changes Induced by the Antibiotics Tobramycin and Colistin Sulfate*. Chemical Research in Toxicology, 2023. **36**(4): p. 598-616.
66. Chiang, J.Y., *Regulation of bile acid synthesis*. Frontiers in Bioscience-Landmark, 1998. **3**(4): p. 176-193.
67. Cai, J.-S. and J.-H. Chen, *The mechanism of enterohepatic circulation in the formation of gallstone disease*. The Journal of membrane biology, 2014. **247**: p. 1067-1082.
68. Foley, M.H., et al., *Bile salt hydrolases: Gatekeepers of bile acid metabolism and host-microbiome crosstalk in the gastrointestinal tract*. PLoS pathogens, 2019. **15**(3): p. e1007581.
69. Saleem, M., et al., *Antimicrobial natural products: an update on future antibiotic drug candidates*. Natural product reports, 2010. **27**(2): p. 238-254.
70. Brogden, R., et al., *Tobramycin: a review of its antibacterial and pharmacokinetic properties and therapeutic use*. Drugs, 1976. **12**: p. 166-200.
71. Neu, H.C., *Tobramycin: an overview*. The Journal of infectious diseases, 1976: p. S3-S19.
72. Andrade, F.F., et al., *Colistin update on its mechanism of action and resistance, present and future challenges*. Microorganisms, 2020. **8**(11): p. 1716.
73. Rhouma, M., F. Beaudry, and A. Letellier, *Resistance to colistin: what is the fate for this antibiotic in pig production?* International journal of antimicrobial agents, 2016. **48**(2): p. 119-126.
74. Norrby, S.R., *Neurotoxicity of carbapenem antibacterials*. Drug safety, 1996. **15**(2): p. 87-90.
75. Moellering Jr, R.C., G.M. Eliopoulos, and D.E. Sentochnik, *The carbapenems: new broad spectrum β -lactam antibiotics*. Journal of Antimicrobial Chemotherapy, 1989. **24**(suppl_A): p. 1-7.

76. Aurilio, C., et al., *Mechanisms of action of carbapenem resistance*. *Antibiotics*, 2022. **11**(3): p. 421.
77. Lister, P.D., *Carbapenems in the USA: focus on doripenem*. *Expert Review of Anti-infective Therapy*, 2007. **5**(5): p. 793-809.
78. Raza, A., et al., *Oral meropenem for superbugs: challenges and opportunities*. *Drug Discovery Today*, 2021. **26**(2): p. 551-560.
79. Lustig, R.H., L.A. Schmidt, and C.D. Brindis, *The toxic truth about sugar*. *Nature*, 2012. **482**(7383): p. 27-29.
80. Sardesai, V.M. and T.H. Waldshan, *Natural and synthetic intense sweeteners*. *The Journal of Nutritional Biochemistry*, 1991. **2**(5): p. 236-244.
81. Edwards, C.H., et al., *The role of sugars and sweeteners in food, diet and health: Alternatives for the future*. *Trends in food science & technology*, 2016. **56**: p. 158-166.
82. Liu, C., et al., *Food Additives Associated with Gut Microbiota Alterations in Inflammatory Bowel Disease: Friends or Enemies?* *Nutrients*, 2022. **14**(15): p. 3049.
83. Rodriguez-Palacios, A., et al., *The artificial sweetener splenda promotes gut proteobacteria, dysbiosis, and myeloperoxidase reactivity in Crohn's disease-like ileitis*. *Inflammatory bowel diseases*, 2018. **24**(5): p. 1005-1020.
84. Raoul, P., et al., *Food additives, a key environmental factor in the development of IBD through gut dysbiosis*. *Microorganisms*, 2022. **10**(1): p. 167.
85. Shahriar, S., et al., *Aspartame, acesulfame K and sucralose-influence on the metabolism of Escherichia coli*. *Metabolism Open*, 2020. **8**: p. 100072.
86. Daly, K., A.C. Darby, and S.P. Shirazi-Beechey, *Low calorie sweeteners and gut microbiota*. *Physiology & behavior*, 2016. **164**: p. 494-500.
87. Touyz, L.Z., *Saccharin deemed "not hazardous" in United States and abroad*. *Current oncology*, 2011. **18**(5): p. 213-214.
88. Shankar, P., S. Ahuja, and K. Sriram, *Non-nutritive sweeteners: review and update*. *Nutrition*, 2013. **29**(11-12): p. 1293-1299.
89. Grembecka, M., *Natural sweeteners in a human diet*. *Roczniki Państwowego Zakładu Higieny*, 2015. **66**(3).





CHAPTER 2:

ELUCIDATING THE RELATIONS BETWEEN GUT BACTERIAL COMPOSITION AND THE PLASMA AND FECAL METABOLOMES OF ANTIBIOTIC TREATED WISTAR RATS

Aishwarya Murali, Varun Giri, Hunter James Cameron, Christina Behr, Saskia Sperber,
Hennicke Kamp, Tilmann Walk and Bennard van Ravenzwaay

Published in: MDPI MicrobiologyResearch12(2021),82–122.

Elucidating the Relations between Gut Bacterial Composition and the Plasma and Fecal Metabolomes of Antibiotic Treated Wistar Rats

Abstract: The gut microbiome is vital to the health and development of an organism, specifically in determining the host response to a chemical (drug) administration. To understand this, we investigated the effects of six antibiotic (AB) treatments (Streptomycin sulfate, Roxithromycin, Sparfloxacin, Vancomycin, Clindamycin and Lincomycin hydrochloride) and diet restriction (-20%) on the gut microbiota in 28-day oral toxicity studies on Wistar rats. The fecal microbiota was determined using 16S rDNA marker gene sequencing. AB-class specific alterations were observed in the bacterial composition, whereas restriction in diet caused no observable difference. These changes associated well with the changes in the LC–MS/MS- and GC–MS-based metabolome profiles, particularly of feces and to a lesser extent of plasma. Particularly strong and AB-specific metabolic alterations were observed for bile acids in both plasma and feces matrices. Although AB-group-specific plasma metabolome changes were observed, weaker associations between fecal and plasma metabolome suggest a profound barrier between them. Numerous correlations between the bacterial families and the fecal metabolites were established, providing a holistic overview of the gut microbial functionality. Strong correlations were observed between microbiota and bile acids, lipids and fatty acids, amino acids and related metabolites. These microbiome–metabolome correlations promote understanding of the functionality of the microbiome for its host.

Keywords: gut microbiome, metabolomics, antibiotics, repeated oral toxicity study, 16S gene sequencing, DADA2, correlation analysis, metabolic capacity

1. Introduction

The gut microbiome plays an essential role in host health and well-being by maintaining physiological homeostasis [1]. The human gastrointestinal tract has been known to possess more than 10^{14} microbial cells and hence over 100 times more genes than the human genome [2]. Bacterial cells are present in the human gut by 2–3 orders of magnitude more compared to the eukaryotes and archaea [3]. The gut flora is easily altered by several factors including host health, medication, environment, diet, age, host genetics, and immune system [4,5]. Specifically, host diet and antibiotic usage have important influences in altering the composition of the gut microbiome [6].

Bacteria carry out microbiome-associated reactions that have been well characterized including tyrosine and tryptophan metabolism, glycerol and mucin production, hydroxylation, glucuronidation and short-chain fatty acid (SCFA) metabolism [6,7]. Zimmermann et al., 2019 provided an outline of the drug-metabolizing activity of human gut bacteria and discovered that about 2/3 of the drugs are metabolized by at least one bacterial strain [4]. Maier et al., 2018 elucidated gut microbial compositional dysbiosis

influenced by non-antibiotic drugs [8]. Findings like these promote a better understanding of microbiome metabolism and metabolism-related microbiome–host interactions [6]. The gut bacteria work hand in hand with the host immune system development that in turn influences signaling pathways of multiple organs such as gastrointestinal tract (GI), liver, muscle, and brain. In addition to the production of metabolites that are advantageous for the host health and phenotype, gut bacteria also contribute to disease risks such as obesity, diabetes, colitis, neurodegenerative disorders and several other long-term health effects [9–12]. As species-specific gut microbiome contributions are highly likely, this research will help in identifying the modes of actions and human relevance.

Therefore, the understanding of microbial biotransformation is essential for the field of toxicology. While toxicity studies predominantly consider the role of the liver [13] for metabolism, gut-mediated microbiome metabolism is poorly characterized. The aim of this study was to investigate how families and species of the intestinal microbiome contribute to the status of natural components, referred to as metabolites, which are subsequently available for absorption from the intestinal tract. To investigate this, we determined microbiome communities as well as fecal and plasma metabolites. We introduced changes in the microbiome by the administration of several antibiotics and correlated the induced community changes with the changes in the fecal metabolome. Subsequently, the fecal metabolome changes were compared with the plasma metabolome. The correlation analysis now provides a connectivity map and shows how individual microbiome communities are responsible for the formation of fecal metabolites and how these are connected with the plasma metabolome.

Antibiotics are known to induce a gut compositional dysbiosis, making it possible to compare rat fecal and plasma metabolomes [14–17]. Targeted metabolite measurements of classes such as carbohydrates, amino acids, nucleic acids or fatty acids and their derivatives were used to identify specific metabolite patterns associated with the administration of different antibiotics [18].

We have used a standardized procedure to determine the metabolome of test substance since 2004. Metabolome data are uploaded in the MetaMap[®]Tox database to compare a given substance with the other metabolome profiles available in the database. The MetaMap[®]Tox or MMTox database comprises data for about 1000 compounds whose modes of action have been determined and is also used for statistical and visualization tools as described in van Ravenzwaay et al., 2016 [19]. It not only gives us the ability to determine the statistical significance of regulated metabolites but also allows the assessment of whether a specific metabolite value has ever been observed in control animals, providing a historical range of what is normal.

To expand the findings from the previous work of Behr et al. [14–16], we investigated the inter-omic correlations between the gut community and the fecal and plasma metabolomes. The standardized study protocol for the correlation analysis is shown in Figure 1. Gut microbial composition of Wistar rats was assessed by 16S rDNA gene sequencing of fecal samples. Subsequently, the fecal metabolome was analyzed and correlated with the microbiome community changes. Finally, we determine the plasma metabolomes of the antibiotic-treated rats to establish a correlation between the gut microbial changes

and both metabolome profiles. As treatment with compounds such as antibiotics frequently results in a reduction of food consumption at higher dose levels, we include in our studies a group of rats in which only the food supply was reduced to take into account possible effects of reduced food consumption.

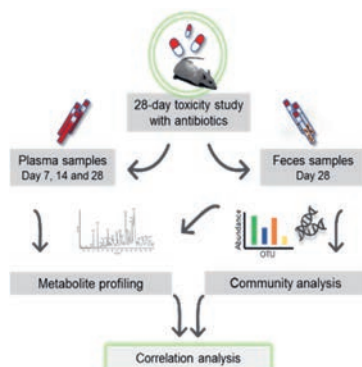


Figure 1. The schematic diagram shows the overall process of a 28-day oral toxicity study with plasma and feces sampling. Plasma sampling was conducted on days 7, 14, and 28 of the study and feces was sampled on the day of necropsy, day 28. Subsequently, plasma and feces samples were subjected to metabolomics and feces to 16S community analysis. With both omic datasets, correlation analyses were carried out.

2. Materials and Methods

2.1. Ethical Statement

The studies were approved by the BASF Animal Welfare Body, with the permission of the local authority, the Landesuntersuchungsamt Rheinland-Pfalz (approval number 23 177-07/G 13-3-016, approved on 10.02.2016). The studies were performed in an AAALAC-approved (Association for Assessment and Accreditation of Laboratory Animal Care International) laboratory in accordance with the German Animal Welfare Act and the effective European Council Directive.

2.2. Animals and Maintenance Conditions

Briefly, male and female Wistar rats (CrI:WI(Han)) were supplied by Charles River, Germany, and were 70 ± 1 days old at the beginning of the studies. The animals were single- and group-caged in the four studies reported in this publication. For the grouped caging conditions, the animals (5 rats per sex and cage in one group) were maintained in an air-conditioned room at a temperature of 20 to 24 °C, a relative humidity of 30 to 70%, and a 12 h light / 12 h dark cycle. Ground Kliba mouse/rat maintenance diet “GLP” was supplied by Provimi Kliba SA, Kaiseraugst, Switzerland. Diet and drinking water were available ad libitum (except 16–20 h before sampling) and regularly assayed for chemical contaminants and the presence of microorganisms.

2.3. Study Design

Four independent 28-day oral toxicity studies in Wistar rats were performed following the principles of the OECD 407 test guideline. Animal handling, treatment, and clinical examinations have been

described earlier [14,15,17]. All the animals were checked daily for any clinically abnormal signs and mortalities. Food consumption was determined on study days 6, 13 and 27. Additionally, body weights of all the animals were determined before the start of the administration period in order to randomize the animals and also on study days 6, 13 and 27. At the end of the treatment periods, the animals were sacrificed by decapitation under isoflurane anesthesia. These studies involved treatments with antibiotics belonging to five different classes (see Table 1). Furthermore, one group of animals was provided with a reduced amount of diet (approx. 20% less compared to ad libitum food intake) to observe their influence on gut dysbiosis and gut metabolic functions. Metabolite profiling was conducted on plasma, cecum and fecal samples, and microbiome profiling was conducted on the fecal samples.

2.4. Treatment of Animals with Antibiotics

Treatment groups involved 5 rats per sex and dose group. Dose levels of the antibiotics were selected such that the low dose (LD) and high dose (HD) would induce low yet reversible toxicity of the antibiotics. The antibiotics were gavaged daily using an appropriate vehicle for animals. The substances were administered in four separate studies (study 1: Vancomycin, Streptomycin, Roxithromycin; study 2: Sparfloxacin, Lincomycin; study 3: single caged restricted diet (-20%) fed study; study 4: Clindamycin study), each with a concurrent control group of 10 animals per sex, to allow for comparisons. Dose-levels, grouping of animals and form of preparation of the antibiotics are summarized in Table 1.

Table 1. Compounds used, dose levels, caging type and class of antibiotics. All compounds were administered orally by gavage.

Study Number	Treatment	Low Dose (mg/kg bw/day)	High Dose (mg/kg bw/day)	Caging	Form of Preparation	Class of Antibiotics
1-4	Control diet	-	-	Grouped (5)	-	-
1	Vancomycin	50	400	Grouped (5)	in ultra-pure water	Glycopeptides
1	Streptomycin sulfate	100	450	Grouped (5)	in water containing 0.5% CMC ^a	Aminoglycosides
1	Roxithromycin	200	600	Grouped (5)	in water containing 0.5% CMC ^a	Macrolides
2	Sparfloxacin	200	600	Grouped (5)	in water containing 0.5% CMC ^a	Fluoroquinolones
3	Restricted diet (-20%)	-	-	Single (1)	-	-
4	Clindamycin hydrochloride	200	600	Grouped (5)	in ultra-pure water	Lincosamides
4	Lincomycin hydrochloride	300	10000	Grouped (5)	in water containing 0.5% CMC ^a	Lincosamides

^acarboxymethyl cellulose: Tylose CB30000; Single caging = one rat per cage; kg bw = kilogram body weight

2.5. Sampling of Plasma, Cecum and Feces for Omics Profiling

Between 7:30 and 10:30 h, on study days 7, 14 and 28 blood samples were taken from the retro-bulbous sinus of all the rats under isoflurane anesthesia (1.0 mL K-EDTA blood) after overnight fasting. The

blood samples were centrifuged (10 °C, 20,000× g, 2 min), and the EDTA plasma was separated. The EDTA plasma samples were snap-frozen with liquid nitrogen gas to keep the samples devoid of oxygen and stored at -80 °C until metabolome profiling was performed. Cecum and feces samples were sampled during necropsy on day 28. Fecal samples were carefully removed from the rectum at the end of the study after the last administration of the test substances. The samples were collected in pre-cooled (dry-ice) vials, immediately snap-frozen in liquid nitrogen and stored at -80 °C until further profiling was performed. The blood plasma, cecum and fecal samples were used for metabolome analysis as standardized in Behr et al. 2017 [16]. The feces samples were additionally used for 16S bacterial profiling.

2.6. DNA Isolation and Bacterial 16S rDNA Gene Amplicon Sequencing

DNA was isolated from the fecal samples using InnuPREP stool DNA Kit (Analytik Jena GmbH, Jena, Thuringia, Germany) according to the manufacturer's instructions as published in Behr et al. 2018 [15]. Based on observations made during the process, the incubation temperature for the cells' lysis was lowered to 75 °C. DNA yield and integrity were assessed using a Nanodrop. Samples were sent to IMG[®] laboratories (Martinsried, Germany) for PCR, library preparation and sequencing. DNA was amplified using 16S V3-V4 primers (Bakt_341F :5'-CCTACGGGNGGCWGCAG-3' and Bakt_805r: 5'-GACTACHVGGGTATCTAATCC-3'). Sequencing was performed on the Illumina MiSeq[®] next-generation sequencing system (Illumina Inc., San Diego CA, USA). Signals were processed to fastq files, and the resulting 2 × 250 bp reads were demultiplexed using the MiSeq[®]-inherited MiSeq Control Software (MCS) v2.5.0.5.

2.7. Metabolome Profiling of Plasma, Cecum and Fecal Matrices

Blood plasma, cecum and fecal samples were used for mass-spectrometry based measurements of metabolites using GC-MS (gas chromatography-mass spectrometry) and LC-MS/MS [20]. First, removal of proteins from 60 µL of plasma samples was performed using 200 µL acetonitrile via precipitation reaction. The polar and non-polar fractions using water and a mixture of ethanol and dichloromethane (1:2, v/v). Five milligrams of feces was subjected to freeze-drying and grinding prior to extraction and extracted with a mixture of acetonitrile, water, ethanol and dichloromethane in a sample tube containing a 3 mm stainless steel ball using a Bead Ruptor (Omni International Inc., Kennesaw GA, USA). Additionally, dichloromethane was used for phase separation. Non-polar fraction was treated with methanol at acidic pH to form fatty acid methyl esters from free fatty acids as well as hydrolyzed complex lipids. Further, oxo-groups of the polar and non-polar fractions were converted to O-methyl-oximes with O-methyl-hydroxylamine hydrochloride and pyridine, followed by the addition of a silylating agent before analysis [15,17,21].

Both the fractions were re-prepared in appropriate solvent mixtures for LC-MS/MS analysis. LC analyses were performed by gradient elution on reverse-phase separation columns and mass

spectrometric detection was conducted with targeted and highly sensitive MRM (Multiple Reaction Monitoring) profiling in parallel to a full-screen analysis as described in patent WO2003073464 [21]. The acquisition in scan mode m/z ratio 15–600 for polar compounds and m/z ratio 40–600 for lipid compounds were applied for GC-MS analysis. MRM profiles for all the detected analytes were determined using standard solutions. The conditions applied for GC- and LC-MS are described as follows:

GC-MS conditions: CTC GC PAL, Agilent 6890 GC gas chromatograph, 5973 MSD mass spectrometer, gradient: 70 °C–340 °C, carrier gas: helium, acquisition in scan mode m/z 15–600 (polar compounds) / m/z 40–600 (lipid compounds) [15,17,21].

LC-MS conditions: Agilent 1100 HPLC System, AB Sciex API 4000 mass spectrometer, gradient elution for polar compounds with water/acetonitril/ammonium formate, gradient elution for lipid compounds with water/methanol/methyl tert-butyl ether/formic acid, MRM and Q3 Scan m/z 100–1000 [15,17,21].

Data for GC-MS and LC-MS/MS were normalized to the medians of reference samples that were obtained from pooled aliquots of all the samples in order to account for inter- and intra-instrumental biases. About 274 semi-quantitative metabolites were measured using the single peak signals in plasma samples according to methods optimized in patent WO2007012643A1 [15,17,21], which resulted in ratios/values that represented a relative change in the metabolites w.r.t control data. About 248 of these 274 detected metabolites were chemically identified, and 26 remain structurally unidentified. A total of 208 semi-quantitative metabolites were measured from feces samples, out of which 177 were chemically identified and 31 were structurally unidentified.

2.8. Targeted Bile Acid Profiling of Plasma and Fecal Matrices

Blood plasma and feces samples from the low-dose groups of controls and antibiotic-treated animals that were stored in –80 °C were used for bile acid profiling. Measurements of bile acids were performed using UHPLC-ESI-MS/MS consisting of a Waters Acquity UHPLC system coupled with an SCIEX 5500 Triple Quad™ LC-MS/MS system equipped with an ESI ion source. This facilitated successful measurements of 20 different bile acids. To enhance accuracy and precision of the data, the method provided seven calibration standards including a mixture of three isotope-labeled internal standards along with a quality control sample. Firstly, 5 mg of dried feces samples were extracted with 1 mL extraction solvent (ethanol (95%)/NaOH [0.1 N]) with an incubation of 30 min in an ultrasonic bath followed by a 10 min centrifugation step at 14,000 rpm, 4 °C [16,21]. The supernatant from the samples was removed and used for further analysis. Further, 10 µL of extracted feces/plasma samples were resuspended with 10 µL of internal standards mixture and added onto filter spots suspended in the wells of a 96-well filter plate (PALL Corporation, Port Washington NY, USA, AcroPrep™ PTFE 0.2 µm) fixed on top of a deep-well plate followed by extraction with 100 µL methanol by shaking at 600 rpm for 20 min on an Eppendorf ThermoMixer C (Eppendorf AG, Hamburg, Germany) as stated in Behr et

al. 2020. The elution step after extracting using methanol was performed by centrifugation at 5700 rpm for 5 min onto the deep-well plate, which was then detached from the 96-well filter plate. Sixty microliters of Milli-Q® water was added to the eluates by shaking briefly at 600 rpm for 5 min, after which the samples on the plate were analyzed by LC–MS/MS [16,21].

All the targeted isobaric bile acids were baseline-separated using ultrahigh-pressure liquid chromatography (UPLC) as described previously in Behr et al. 2020. UPLC systems were briefly used at a flow rate of 0.5–1 mL/min. Water with 0.01% formic acid and 10 mM ammonium acetate was mobile phase A, whereas mobile phase B was 30% (v/v) acetonitrile/methanol with 0.01% formic acid and 10 mM ammonium acetate [16]. The gradient program that was initially started at 35% B, was increased to 100% B in 3.5 min and then held at 100% B for 0.5 min, decreased to 35% B in 0.1 min, and then held at 35% B for 0.9 min, enabling a short runtime of 5 min. Chromatographic separation was performed using a reverse-phased UHPLC analytical column (Biocrates Life Sciences AG, Innsbruck, Austria) at 50 °C. Chromatographic performance was then enhanced using a SecurityGuard ULTRA Cartridge C28/ XB-C18 for 2.1 mm ID precolumn (Phenomenex Cat. No. AJ0- 8782). An injection volume of 5 µL was used. Mass spectrometric detection was accomplished with electrospray ionization in negative ion mode. Two MRM transitions were used for each target bile acid for semi-quantitative evaluation [16,21].

2.9. Statistics

The metabolic data were analyzed by univariate and multivariate statistical methods. The sex- and day-stratified heteroscedastic t-test (“Welch test”) was applied to compare metabolite levels of the different dose groups with respective controls for each matrix. For all the metabolites, changes were calculated as the ratio of the median of metabolite levels in individual rats in a treatment group to the median of metabolite levels in rats in a matched control group (time point, dose level and sex). These ratios are referred to as “relative abundance”. The computations were performed using the standardized routines setup in Java and Oracle database, and the relative abundances, *p*-values and *t*-values were collected as metabolic profiles and made available through MetaMap®Tox [19].

The Principal Component Analysis (PCA) and Hierarchical Clustering Analysis (HCA) were performed in R Statistical Software [22,23]. Prior to computing PCA and HCA, the data were transformed to a log scale, centered by subtracting the mean of the control group and scaled by the respective standard deviation for each metabolite. Missing data were imputed using the nearest neighbor method implemented in function `impute.knn` from the package `impute` [25]. The metabolites missing in more than 20% of samples, and subsequently, the animals missing more than 35% metabolites were removed from the analysis. The HCA was performed at the level of a treatment group based on the mean values of each metabolite within a specific dose and sex group.

2.10. Bioinformatics

The Divisive Amplicon Denoising Algorithm (DADA) treats every sequence uniquely without clustering them, which proves advantageous as the variability of as small as one nucleotide is considered [26]. DADA2 v1.10 package was used to process the sequencing data using a customized workflow [26]. A table of amplicon sequence variants (ASV) was obtained by denoising using a customized DADA2 v1.10 denoising workflow. The workflow includes quality control, primer removal, denoising, taxonomy assignments using RDP classifier and creation of a phylogenetic tree [27] (see Figure 2). Forward and reverse primers were trimmed from the raw reads using cutadapt [27]. As paired-end reads had to be used for further analysis, the reads or sequences were merged to about 415 bp length. Quality checking (QC) involved checking the read lengths and the quality of the joined reads. Taxonomy was assigned to ASV sequences using the Naïve Bayesian classifier implemented in DADA2 using the RDP database [28]. This resulted in the output in the form of a BIOM table with all the information regarding the sequences and abundances of ASVs and the assigned taxa information.

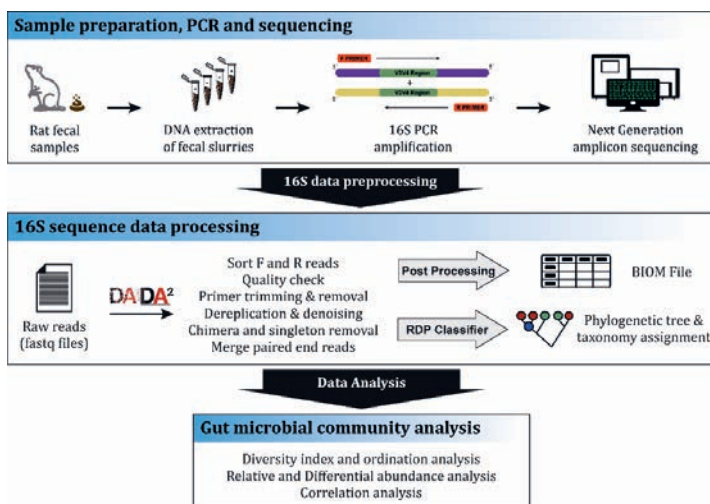


Figure 2. 16S community analysis workflow. The first step involved the preparation of fecal samples collected during necropsy (day 28) from the Wistar rats. Samples were subjected to DNA isolation, quantification and further 16S rDNA gene amplification by Polymer chain reaction (PCR) and sequencing report generation. The next step involved the data pre-processing where filtering, denoising and demultiplexing of the reads were conducted by DADA2 software and the final step was the bacterial community data analysis.

2.11. 16S Data Normalization, Diversity and Relative Abundances Analyses

The community analysis was conducted in R using RAM (Chen, Wen et al. “Package ‘RAM’” (2018)), and DESeq2 packages [29]. The raw data were checked for completeness, and empty rows were removed. The BIOM table contained 2,859,130 reads belonging to 31,023 ASVs from 198 samples. The raw reads were used for alpha diversity analysis using the group.diversity function in RAM package. As a part of data cleanup, ASVs or reads that did not have taxonomic assignment up to the family level were removed. Further, ASVs with non-zero counts in at least two samples were retained, and the others were removed, resulting in 2,496,649 reads belonging to 1946 ASVs. These filtered data were used for relative abundance analysis. Stacked bars were plotted using RAM package to determine

the relative bacterial abundances in the different antibiotic-treated rats. An additional stacked bar was plotted to estimate the group indicators, which indicate the core taxa that are specific to particular conditions. Parameters used for the group indicators are $A = 0.975$, $B = 0.975$, $\text{stat} = 0.975$, $p\text{-value} = 0.001$, where A refers to the probability that the animal belongs to a combination of conditions given that a taxonomic family is found and B refers to the probability of finding a bacterial family given that the animal belongs to a combination of treatment groups. Stat refers to the association between A and B.

Count normalization of the dataset and the differential abundance analysis was done using DESeq2 workflow (via Phyloseq) [30–32]. This procedure follows custom scripts from the DESeq2 package. The filtered and normalized data were used for beta diversity analysis and HCA. Principle Coordinate Analysis (PCoA) was carried out using phylogenetic (weighted UniFrac) and non-phylogenetic (Bray-Curtis) based distances.

For the DESeq2 model, study (experimental batch), sex and treatment (a composite variable of administered compound and dose) were used as independent variables, with an additional interaction term for sex and treatment. The \log_2 fold change values of bacterial family that are significantly present or absent in a particular treatment relative to the controls were estimated. An additional feature to include batch effects in DESeq2 was performed to include any minor study-dependent variabilities. The differential abundance analysis allowed us to visualize the significant changes in specific bacterial families in their abundances in different treatments with respect to the controls. This also allowed us to visualize differences between the two dose groups and sexes. These \log_2 fold change values were then used for final correlation analysis with the metabolome data.

2.12. Correlation Analysis

In order to enable the comparison of the metabolome data to the microbiome data, \log_2 fold changes were calculated for the two metabolome matrices. The fold change matrices were used to compute correlations between different metabolites and 16S bacterial families using R. Pearson correlation analysis was performed for fecal bacterial families with plasma and feces metabolomes, respectively. A separate targeted measurement was performed for the bile acids in the low-dose groups. A similar correlation analysis was conducted for these low-dose treatments for the bile acid metabolites. A correlation test was performed to determine statistical significance. Only metabolites and bacterial families that had correlations with $p < 0.05$ and absolute strength of correlation > 0.6 were retained.

3. Results

3.1. Clinical Signs

There were no mortalities in any of the treatment groups, except for one animal at the beginning of the study in the female group with Streptomycin treatment, which was not treatment-related. No clinical signs of toxicity were observed in any of the animals that received Lincomycin, Sparfloxacin,

Streptomycin and Vancomycin. Animals treated with Roxithromycin showed slight salivation immediately after administration. The group of female animals treated with Clindamycin showed relevant clinical signs including salivation and semi-closed eyelid (four animals), and one of the animals showed piloerection. Similarly, males treated with Clindamycin showed slight salivation (all animals), semi-closed eyelid (three animals) and, two of them were in poor condition. Except for salivation, these findings were only observed in the individual animals on 1–3 days of the administration period out of 28 days. Therefore, and in the absence of body weight effects, these observations were assessed as borderline effects indicative of marginal systemic toxicity of Clindamycin at 200 mg/kg body weight. Relative changes in body weight and food consumption noted upon administration of the test compounds are shown in Supplementary Table S1. Treated animals did not present any significant changes with respect to body weight when compared to the controls for both males and females.

3.2. Diversity Analysis

Shannon true diversity of the fecal microbiome of all the six antibiotic treatments and restricted-diet-fed rats was compared to controls for both dose groups and sexes (Figure 3). Shannon true diversity indicates the diversity of different bacterial taxa present in a specific treatment [33]. The larger the boxes in the boxplot, the higher is the variability between the individual samples of a specific group/condition. The dots falling outside the boxes are outliers. A clear reduction in the diversity in the samples of all the antibiotic treatments was noted. Control animals had higher inter-individual variability in both the sexes compared to antibiotic-treated animals. The higher the diversity, the higher the presence of different bacterial taxa, which is highest in the controls, followed by the restricted-diet-fed animals. Among the different antibiotic treatments tested, samples from Streptomycin-treated animals retained a relatively high diversity in bacterial taxa for both males and females compared to the other antibiotic-treated animals. Sparfloxacin and Vancomycin treated animals showed the least diversity in both the sexes. Overall, dose dependency was not very apparent and was quite marginal in both the sexes, with a possible exception of Streptomycin. Using the diversity information, the Shannon evenness boxplot was plotted (see Figure S1).

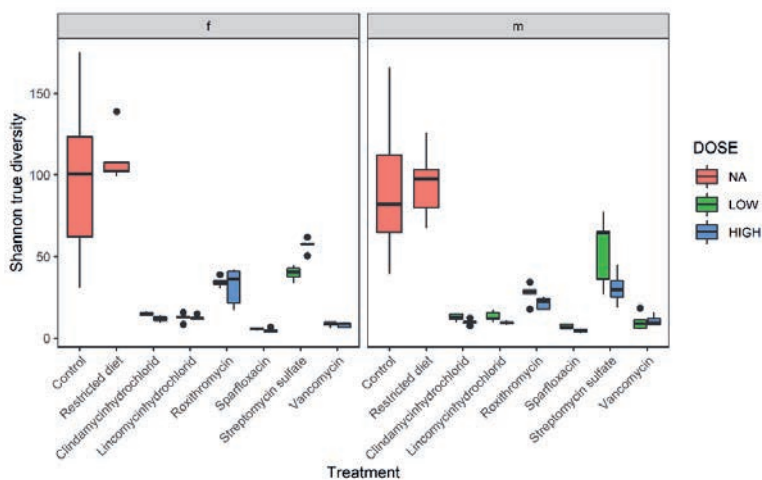


Figure 3. Shannon true diversity analysis of six antibiotic treatments, restricted-diet-fed and controls for both male and female Wistar rats. Boxplot shows the diversity analysis on the left for females (f) and on the right for males (m). The colors show different dose groups, where red refers to no dose applicable, blue box refers to high-dose and green refers to low-dose groups. The x-axis shows the different treatment groups, and y-axis shows Shannon diversity value; whiskers denote standard deviations, solid lines within the boxes indicate the group median and dots lying outside the boxes are outliers. A closer comparison of the treated groups and dose response is depicted in Supplementary Figure S9.

Consistent with the Shannon true diversity index, the Shannon evenness profiles of the antibiotics again showed a very marginal dose dependency for both sexes except for the Streptomycin treatments.

Following the alpha diversity analysis, a beta diversity analysis using two different distance matrices was conducted. One was a rank-based Principle Coordinate Analysis (PCoA) using a non-phylogenetic distance matrix called the Bray–Curtis distance. The second one was a phylogenetic-based distance matrix called Weighted UniFrac distances. Figure 4a depicts the non-phylogenetic distance-based rank PCoA analysis of the bacterial taxa present in different conditions. The PCoA was also used to observe any exclusive sex-based clustering. Six clear clusterings of the different treatments could be observed. We observed one cluster with controls, restricted-diet-fed and Streptomycin treated animals; a second with Roxithromycin, Sparfloxacin, Vancomycin; and two clusters formed by the lincosamides treated groups. In addition to the four clusters, two different yet closely located clusters of the two lincosamide treatments (Clindamycin and Lincomycin) were evident. Thus, the Streptomycin treatment showed the same results as in the diversity analysis; i.e., it appeared to be more similar to the controls than to any other antibiotic treatment.

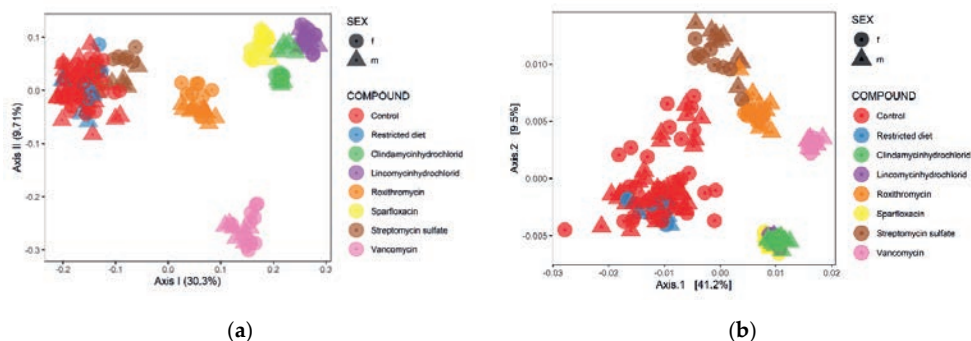


Figure 4. Principle Coordinate Analysis (PCoA) of bacterial families from different treatments. **(a)** The distance matrix used is Bray–Curtis, which is a rank-based clustering. **(b)** Principle Coordinate Analysis (PCoA) using weighted UniFrac distance matrix that is a phylogenetic-based distance that takes bacterial abundances into account.

Sex-dependent clustering could not be observed in any of the treatments, whereas a clear antibiotic class dependency was evident. Further, a phylogenetic distance-based beta diversity analysis demonstrated changes as shown in Figure 4b. Consistent with our previous Bray–Curtis-based PCoA analysis, the weighted UniFrac distance matrix produced six visible clusters. The samples from animals belonging to controls and restricted diet formed a cluster together in the phylogenetic distance-based matrix, similar to the Bray–Curtis distance matrix. Similarly, treatments of two lincosamides, Clindamycin and Lincomycin, clustered together and with Sparfloxacin treatments, whereas Streptomycin, Roxithromycin and Vancomycin treatment groups clustered separately from others. As this analysis involves phylogenetic associations between the bacterial taxa, the clusters at some points appear to converge with nearby associated clusters, showing homology in their relations. This also explains a large spread in the control and Streptomycin treatments and closeness of Sparfloxacin treatments to the lincosamides cluster.

3.3. Hierarchical Clustering Analysis

The hierarchical clustering of gut (fecal) bacterial families based on both sexes and dose groups is shown in Figure 5. Control data from all four selected studies have been combined. The hierarchical clustering showed clear antibiotic-specific clustering, consistent with what was observed in the beta diversity analysis. A heatmap was generated with hierarchical clustering (HC) of not only the different treatments (taking every single sample into account and not means or medians) or conditions but also the bacterial families. Potential co-occurrences of bacterial families are shown in Figure 5. As dose and sex did not contribute very much to the changes in the microbiome, they were combined for the analysis. Streptomycin treated animals clustered closely with controls, whereas Vancomycin-treated animals clustered the farthest from the control cluster. Restricted-diet-fed animals merged together with the control cluster, whereas five clear antibiotic-based clusters could be observed. Both lincosamides—Clindamycin and Lincomycin—clustered together, showing an antibiotic class-based effect.

The black bands on the right side of the figure represent the respective treatment that the bands correspond to. The bacterial families could be observed taking inter-individual variations into account. The presence or absence of some of these bacterial families like *Paenibacillaceae*, *Bacillaceae* and *Eubacteriaceae* also distinguish between the two lincosamides as they occur in Lincomycin- and not Clindamycin-treated animals. Families like *Anaeroplasmataceae* and *Deferribacteriaceae* were specific to only Vancomycin treatments compared to all the other treatment groups. Roxithromycin treatments shared some bacterial families including *Rikenellaceae* and *Eubacteriaceae* with Streptomycin treatments and controls. Sparfloxacin showed the highest abundances of specific families like *Bifidobacteriaceae* and *Coriobacteriaceae* families that could not be observed in such high abundances in any of the other treatment groups. Finally, the *Lachnospiraceae* family was prevalent in all the treatments and the controls except for Vancomycin-treated animals. Families like *Ruminococaceae* and *Erysipelotricaceae* were observed in all the treatment groups followed by *Lachnospiraceae* and *Verrucomicrobiaceae*, which were also present in all the treatment groups although varying in abundances. HC does not show any sex- or dose-based grouping, which means low dose (LD) selection was enough for the influencing alterations. Overall, the heatmap shows the clustering of not only the different treatments but also the 16S-analyses-based bacterial families.

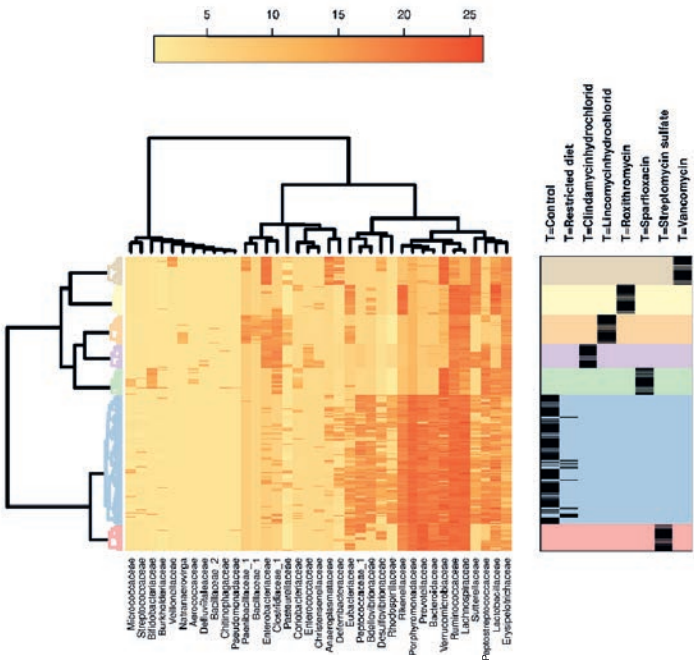


Figure 5. Hierarchical clustering analysis of 16S bacterial families in different treatments, dose groups and sexes. Heatmap showing occurrences of bacterial families in different antibiotic treatment groups, including hierarchical clustering of bacteria families and different treatments. Color coding on the right indicates the different treatment groups that correspond to the clustering analysis on the left. The black bands on the right show the samples from individual animals belonging to respective treatment groups. Dose groups and sexes showed very marginal differences; hence, they were not separated.

3.4. Relative Abundance Analysis

Relative abundance analysis is presented as a stacked bar graph (Supplementary Figure S3), where every color depicts one bacterial family. The inter-individual variability could be clearly observed in all the conditions. Antibiotic treatments portray occurrences of bacterial families significantly differently compared to the controls, with the exception of Streptomycin-treated animals, which is consistent with respect to diversity analyses, showing that the influence of Streptomycin on fecal microbiome communities is rather minor such that this group shows similar bacterial abundances as the restricted diet and control groups. Clindamycin- and Lincomycin-treated animals behaved fairly similarly with greater abundance of the *Ruminococcaceae* family than any other treatment group. Both the lincosamides showed the maximum abundance of *Firmicutes* phyla amongst all the other treatment groups. A very marginal dose- and sex-specific variation in the bacterial abundances could be observed. Roxithromycin showed a very high abundance of *Rikenellaceae* compared to any other treatment. Vancomycin-treated animals were observed to have the highest abundance of *Enterobacteriaceae*, which could only be seen in the two lincosamide treatment groups and likely in no other. Similar to Sparfloxacin, the Vancomycin treatment group showed more than 50% contribution of *Verrucomicrobiaceae* in the total abundance. *Enterobacteriaceae* family could be observed to be specific to Vancomycin and two lincosamide treatments (Supplementary Figure S3).

Group indicator analysis gives the relative abundances of the taxonomic groups, which are statistical indicators of the experimental conditions (different treatments, in our case). The families shown in Figure 6 show fidelity, specificity and association strength of 0.975. This means that core bacterial families that are specific to a condition or a combination of conditions have been shown here. Group indicators are derived from the likelihood of finding a specific bacterial family in a specific treatment. Figure 6 also shows clear inter-individual variability in the group indicator appearances. A very clear inter-individual variability can be observed in the stacked bar plot. The core bacterial families that have high contributions in a particular treatment group have a value of about 1 or closer. Antibiotic-specific core bacterial families can be observed. The animals in the Streptomycin treatment group showed group indicators highly similar to the controls and restricted diet-fed animals. However, unlike controls and Streptomycin groups, the restricted diet group of animals showed an increased abundance of the *Lactobacillaceae* family. This is consistent with the previous findings that caloric restriction promotes increased growth of *Lactobacillus* species in rat fecal microbiota [34]. *Verrucomicrobiaceae* was not a core bacterial family in Roxithromycin and lincosamide treatments compared to other treatment groups where they contributed as a core bacterial family. Clindamycin- and lincosamide-treated animals showed high contributions of *Enterobacteriaceae* followed by *Erysipeltrichaceae* families, demonstrating antibiotic-class-specific changes. Roxithromycin treatments possessed the highest abundance of the *Rikenellaceae* family, which could not be observed in any of the other treatments. Similarly, contributions of *Lachnospiraceae* family were observed in all the treatments except for

Vancomycin treatment. Overall, antibiotic-specific core bacterial families could be observed well from the analysis.

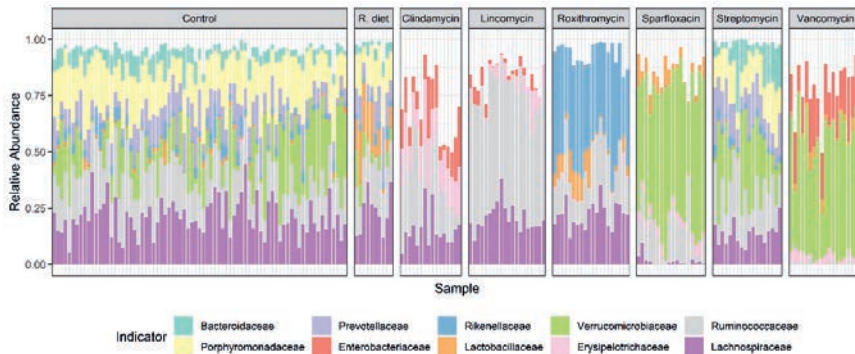


Figure 6. Stacked bar showing group indicators or core bacterial families that were detected in specific treatment groups, where R. diet refers to the restricted diet (~20%) group. Individual animal variability can be easily observed. Dose groups and sexes showed very marginal differences; hence, they were not separated. Antibiotic treatments clearly show class-dependent effects on the intestinal community composition. Compared to control, restricted diet and Streptomycin sulfate treatment groups, all the other antibiotics produced reduced/changed bacterial diversity and richness.

3.5. Differential Abundance Analysis

Differential abundance analysis was carried out using DESeq2 package, which is used to identify specific bacterial taxa (or families in our case) that are associated with specific treatments. This helps to understand more about specific bacterial families which are significantly abundant or rare in specific treatments compared to the controls. This provides more insight regarding the role of such specific bacterial taxa and eventually their influence in the metabolic activities of the different antibiotic-treated Wistar rats. Models were created for each treatment for each dose group and sex. This analysis was conducted in order to estimate the fold changes of significantly altered bacterial families in different treatments relative to the controls. This fold change information from DESeq2 analysis is further used for correlation analysis in order to compare with the fold changes of different metabolites in the three matrices. The results of this analysis are shown as scatter plots; see Supplementary Table S16, where each dot indicates individual read/amplicon sequence variant (ASV) belonging to a specific bacterial family.

Streptomycin LD treatments versus controls for both the sexes (females to the left and males on the right) can be used to observe the specific bacterial families, such as *Ruminococcaceae*, few ASVs that belong to this family of bacteria are present in almost 30 log₂FC, and others were very less in abundance compared to control animals. This is the reason why the log₂ fold change for most of the ASVs belonging to *Ruminococcaceae* family, as shown in Table S16, has a highly negative value when differential abundance analysis was conducted for female rats. *Eubacteriaceae* family could be observed to be present in very high abundance compared to controls in Streptomycin-treated female rats. Similarly, in males, many differentially abundant families could be observed similar to females.

Eubacteriaceae family could be observed to be present abundantly in males treated with Streptomycin compared to controls, and ASVs belonging to families like *Lachnospiraceae* and *Ruminococcaceae* were present in very high abundance and also low compared to controls. Other families including *Rikenellaceae*, *Sutterellaceae* and some others were present in lower abundance compared to controls for both sexes.

For the two different antibiotic treatments, only low-dose groups from both females and males have been depicted in the scatter plots; for the complete data of differential abundance scatter plots for all the LD treatments, see Supplementary Table S16. As differential abundance analysis for LD and HD only marginally differed, only the LD plots are shown in order to avoid overloading of redundant data. In Vancomycin LD treatments (see Table S16), not much difference could be observed between the males and females with respect to the differential abundance analysis, except for *Anaeroplasmataceae* family, in which it was observed in higher abundances in females than males. In both the sexes, *Enterobacteriaceae* and *Verrucomicrobiaceae* families were very high in abundance compared to control animals. Most of the other represented bacterial families were observed in reduced abundance compared to controls in both the sexes. These results showed how rarely or abundantly certain families are present when there is a lack of nourishment. The results from this analysis were consistent with what was observed in the heatmap of hierarchical clustering analysis.

3.6. Metabolome Data Analysis

3.6.1. Fecal Metabolome

A hierarchical clustering analysis was conducted for all the measured metabolites from the fecal samples of the controls and different treatments. The dendrogram in Figure 7a shows the clustering based on Euclidean distances of all the treatments and controls, based on sex and dose groups. Control groups from the four studies were combined into two, separating males and females. The clustering showed a very similar pattern as it was observed in the 16S clustering. Treatment-dependent clustering could be clearly observed. Controls and restricted-diet-fed animals had very similar fecal metabolome profiles, as they were observed to be closely clustered. Streptomycin- along with Roxithromycin-treated animals clustered the closest with each other and to controls compared to the other tested drugs. In Roxithromycin and Streptomycin treatment groups, a sex-based clustering could be observed in the dendrogram. Animals treated with the two lincosamides, Clindamycin and Lincomycin, clustered very closely but also had marginal differences between them. Clindamycin treatment group showed a dose-dependent clustering, which could not be observed for any of the other drugs. Closest to the lincosamides were samples from Sparfloxacin-treated animals. Vancomycin-treated samples showed the most distant clustering with respect to the controls. A Principal Component Analysis using the same data showed a very consistent observation (see Supplementary Figure S4). Similarly, HCA and PCA analysis of cecum metabolome data was carried out and can be found in the supplementary data (see Figures S5 and S6, respectively). Both the analyses result in similar and comparable clustering.

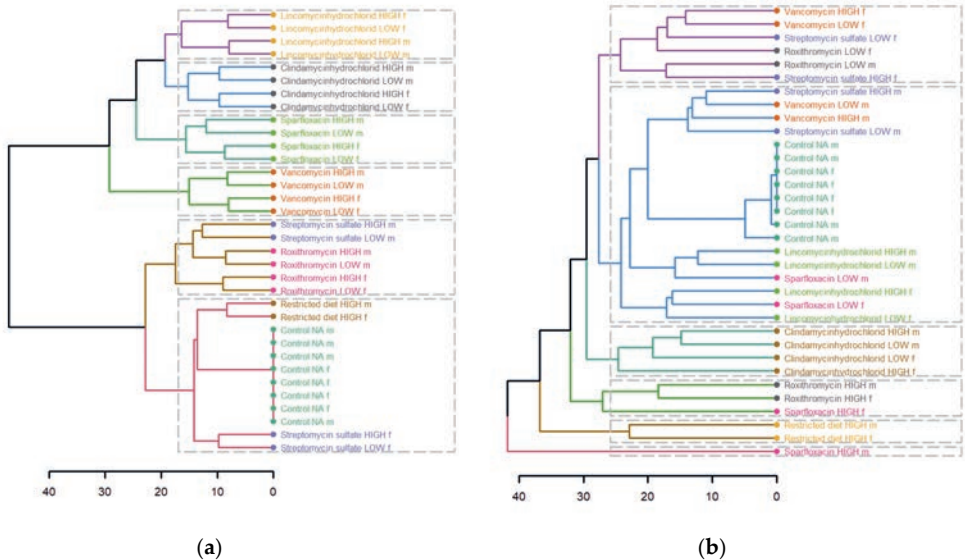


Figure 7. Dendrogram showing hierarchical clustering of (a) fecal and (b) plasma metabolites of different treatments, dose groups and sex. Euclidean distance was used, and different treatments are depicted, and different colors and dotted boxes show different clusters.

3.6.2. Plasma Metabolome

The dendrogram shown in Figure 7b shows the clustering of plasma metabolomes of controls, restricted-diet-fed and six antibiotic treatments. The clustering showed restricted-diet-fed samples to be very different from the controls, in sharp contrast to the observations made in the fecal or cecal metabolome (see Figure S5 for cecum metabolome HCA analysis) and microbiome clustering analysis. Sparfloxacin- and Roxithromycin-treated animals showed a dose-dependent clustering, which could not be observed in any of the other antibiotic treatments. Vancomycin treatment showed a big separation based on gender. Samples from animals treated with the two lincosamides, Clindamycin and Lincomycin, also showed a profound difference in their plasma metabolome profiles. Overall, the analysis showed far less treatment-based clustering than in the fecal and microbiome analysis. The exceptions being restricted diet feeding and the Clindamycin treatments, which formed neat clusters.

3.6.3. Controls vs. Restricted Diet in Plasma and Fecal Matrices

Restricted-diet-fed animals showed no significant differences compared to evaluate similarity. There was, however, a huge difference in the plasma metabolome, which makes it interesting to conduct an ordination analysis only using restricted diet and control data. When a PCA was prepared using the fecal metabolome data (see Figure 8a), the restricted diet treatments did not form a cluster different from the controls along Principle components (PCs) 1 and 2; however, they clearly separated along PCs 2 and 3.

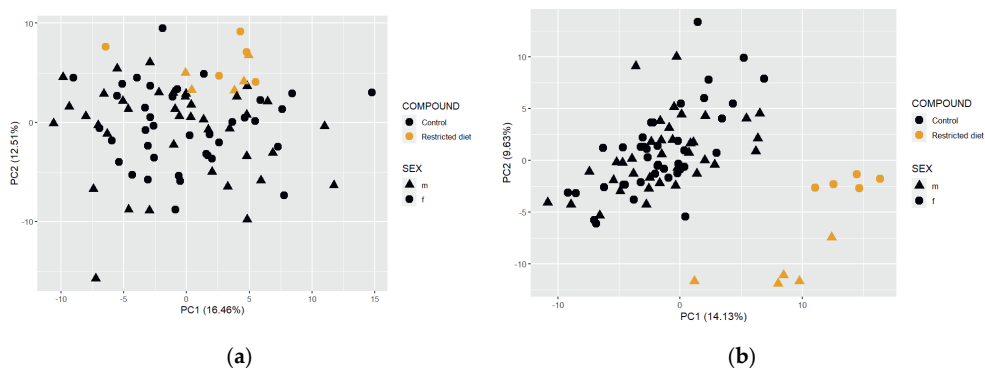


Figure 8. Principal component analysis (PCA) of restricted-diet-fed and controls from all the studies. **(a)** PCA using feces metabolome (left side); **(b)** plasma metabolome data (right side).

Further, when the same was done using a plasma metabolome data (see Figure 8b), a clear separation could be observed on the first principal component, between the controls and the restricted diet. This showed a clear influence of reduced nourishment on the plasma metabolome of the rats, which could not be observed in other matrices and in the gut bacterial community composition. This indication clearly means that the difference in the plasma metabolome of the 20% reduced diet does not come from the gut microbiome but the diet of the host itself.

Metabolome data from plasma, fecal and cecum could be compared from our results, and very marginal differences between fecal and cecum metabolome were observed, whereas the plasma metabolome differed significantly from the other two. The microbiome data showed very consistent clustering compared to feces and cecum metabolome profiles. The HCA analysis of microbiome data can be found in Supplementary Figure S2. The concordant findings prove the comparability of the two datasets. Restricted-diet animals had similar gut microbial composition and fecal and cecum metabolome profiles as controls but showed differences in the plasma metabolomes. Compared to all the antibiotics, samples from animals treated with Streptomycin showed the least differences in microbiome and fecal metabolome profiles compared to the controls, and those from the Vancomycin treated group showed the highest. The two lincosamides-treated animal groups showed a very marginal influence on both microbial composition and fecal metabolome, showing an antibiotic class-dependent effect. After Streptomycin, Roxithromycin treatment groups showed the highest similar influence of microbiome and fecal metabolome compared to the controls.

3.6.4. Comparison between Plasma, Feces and Cecum Metabolome Profiles

Cecum and fecal metabolomes were compared to observe the number of overlaps or contrasts between the different matrices. Pearson correlation was conducted to compare the different metabolome matrices to understand the similarities or differences between them (see Supplementary figure S8). A boxplot graph was prepared to analyze the Correlation coefficients of feces vs. cecum matrix, plasma vs. cecum and plasma versus feces metabolomes (Supplementary figure S8). The figure shows the highest correlations between feces and cecum metabolomes compared to others, with a correlation coefficient

value as high as 0.7 approximately. Whereas, cecum versus plasma matrix and feces versus plasma matrix were almost near 0, indicating the least comparability between plasma metabolome with both feces and cecum metabolomes. There were although some biomarker metabolites observed, that belonged to metabolites like indole-3-acetic acid and allantoin that showed highest correlations between the plasma and feces and cecum metabolome (see Supplementary Figure S8).

Cecum and feces metabolomes showed very high similarity. A diagonal line in the heat map shows the similarities between the metabolites that are in common between the two matrices. The straight line shows highly significant correlations between the cecal and fecal metabolites, proving the very slightly marginal difference between the two matrices. This result supports the concept of using feces as a matrix that can be obtained using non-invasive methods, and it also promotes a longitudinal study design (also known from Behr et al., 2018, comparing different gut tissue matrices). However, when plasma metabolome was compared with fecal and cecal metabolomes, very low correlations could be observed between plasma and the two matrices. Plasma metabolome appears to be an entirely different matrix compared to both feces and cecum based on its metabolite composition. With this, we hypothesize the potential reason could be that plasma metabolome comprises a crosstalk between the host and gut-mediated metabolites, as also known from Behr et al., 2018 [15]. Not only gut and host metabolites, but also co-metabolites could be found in plasma; hence, it would pose as an entirely different matrix compared to feces and cecum.

3.7. Correlation Analysis

Inter-omic Pearson Correlation was conducted to compare the log₂fold changes of significantly altered metabolites in all the three matrices compared to bacterial families, for all the treatments. The log₂fold change values were calculated for all the treatments relative to the controls using DEseq2. These fold change values for every treatment were compared between the metabolome and microbiome profiles. Some metabolites are present in multiple numbers due to their different types of mass spectrometry measurements (LC or GC). In all three matrices, it was observed that the majority of the bacterial families correlated strongly with the amino acids, lipids and related metabolite classes. Compared to plasma metabolome, feces metabolomes showed a higher number of correlations between the bacterial families and respective metabolites.

3.7.1. Feces Matrix

The correlation analysis between two omics datasets shows the relationship between the presence/absence of a particular gut bacterial family with the presence/absence of a specific fecal metabolite (see Figure 9). The complexity of changes, relative to the number of antibiotics employed, however, did not allow us to exactly identify individual metabolite–microbiome connections. For those fecal metabolites that we altered by the treatment the correlation analysis heat map does show how strong these are correlated (positively and/or negatively) with the gut bacterial families. Out of 39 annotated bacterial families, only 12 were found to possess the strongest correlations with feces

metabolite levels. The resulting strength of the correlation or the value of the correlation coefficient is governed by the cumulative relative changes of bacterial taxa/fecal metabolite in all the treatments with respect to controls. The stronger the correlations are (irrespective of the direction), the more chances are that they originate from all the treatments. A strongly positive correlation (red box) indicates that both the metabolite and bacterial family change in the same direction (either both are strongly upregulated or strongly downregulated), while the strongly negative (blue box) indicates an inverse correlation, meaning if the metabolite level increases, the fold change of the corresponding bacteria family must decrease and vice versa. To evaluate inter-treatment effects, one can go back to the DESeq2 data to refer to changes in the bacterial families in respective treatments and to metabolome profiles to refer to changes in different metabolite concentrations.

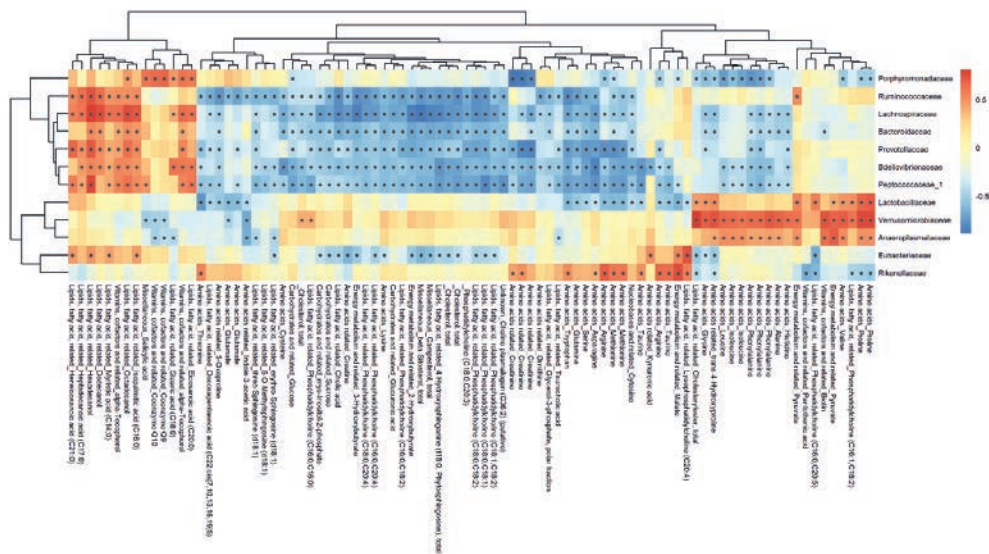


Figure 9. Pearson colorations of 16S bacterial families and corresponding fecal metabolite classes. The heatmap shows positive (red) and negative (blue) correlations between fecal metabolites and corresponding bacterial families. Metabolite classes have been indicated along with the metabolite names on the horizontal part of the figure. Black dots within the boxes indicate p -value < 0.05 calculated using cor.test.

Most of the amino acids such as arginine, histidine, alanine, valine, phenylalanine, glycine, asparagine, serine, glutamine, methionine and threonine show predominantly negative correlations with the bacterial families (Supplementary Figure S9). Only about 3-5 bacterial families from the list of 12 families positively correlate with these amino acids. Amino acids like glycine, valine and leucine are positively correlated with families *Verrucomicrobiaceae*, *Anaeroplasmataceae* and *Lactobacillaceae*, which belong to Verrucomicrobia, Tenericutes and Firmicutes phyla, respectively. *Lactobacillaceae*, *Verrucomicrobiaceae* and *Anaeroplasmataceae* form clusters of highly positive correlations with amino acids such as glycine, leucine, isoleucine, phenylalanine, alanine, valine and proline, suggesting common functions between these bacterial families.

Tryptophan, being one of the most important products from dietary source and endogenous bacterial metabolism, correlates negatively with a majority of bacterial families except for *Rikenellaceae* that correlates towards the positive direction in the feces matrix. Ornithine, which is well known to result from gut bacterial metabolism, also appears to have profoundly negative correlations with the gut bacterial families, with only 3-4 exceptions, including *Rikenellaceae*, *Porphyromonadaceae* and *Eubacteriaceae* (See Figure S9). Most metabolites involved in energy metabolism show few strong correlations, irrespective of the direction, whereas 2-hydroxybutyrate and 3-hydroxybutyrate have some strongly negative correlations with bacteria belonging to mostly Bacteroidetes followed by Firmicutes and Proteobacteria phyla. One of the several gut-microbiomes-associated biomarkers, indole-3-acetic acid, appears to have slightly weak correlations irrespective of the direction, with the majority of the bacterial families except for three bacterial families *Verrucomicrobiaceae*, *Anaeroplasmataceae* and *Ruminococcaceae*. Moreover, certain metabolites belonging to carbohydrates and related classes like lysine and glucuronic acid have mainly strong negative correlations, except for four bacterial taxa, namely, *Porphyromonadaceae*, *Rikenellaceae*, *Verrucomicrobiaceae* and *Anaeroplasmataceae* families (as shown in Figure 9).

Bacterial families *Verrucomicrobiaceae* and *Anaeroplasmataceae* have a very similar correlation, where they mostly positively correlate with the majority of fecal metabolites. Metabolites like hexadecanol, octadecanol and dodecanol that belong to complex fatty acids and lipids and related class have positive correlations with the majority of the bacterial families except for *Rikenellaceae*, for which the correlations are very weak. Clusters of positive correlations between specific bacterial families, including *Porphyromonadaceae*, *Ruminococcaceae*, *Lachnospiraceae*, *Bacteroidaceae*, *Prevotellaceae*, *Bdellovibrionaceae* and *Peptococcaceae*, could be observed with metabolites belonging to lipids, fatty acids and related classes, suggesting common functions between these bacterial families. Overall, most correlations between the intestinal bacteria and fecal metabolites belong to amino acids, lipids and fatty acids and energy metabolism-related metabolites.

A correlation analysis for 16S bacterial families and the bile acid pool from feces was carried out, and numerous correlations were observed irrespective of the direction (see Figure 10). Cholic acid, a primary bile acid, showed a negative correlation with the majority of bacterial families except for *Anaeroplasmataceae* and *Lactobacillaceae*, which belong to Tenericutes and Firmicutes phyla, respectively. *Ruminococcaceae* showed the strongest negative correlations with five taurine-conjugated bile acids, namely TCA, TMCA (both α and β), TCDCA and TUDCA. Two other taurine-conjugated bile acids, TDCA and TLCA, showed a completely different correlation in comparison, as they correlate positively with all the bacterial families listed except for two, *Lactobacillaceae* and *Peptostreptococcaceae*. Unconjugated secondary and tertiary bile acids that cluster the closest to each other, such as MCA (both α and β), HDCA, DCA and LCA, strongly and positively correlate with the majority of the 16S bacterial families except for *Anaeroplasmataceae*. A glycine conjugated bile acid GCA shows positive correlations only with the bacterial families *Lactobacillaceae*,

Peptostreptococcaceae and *Anaeroplasmataceae* compared to other bacterial families. Overall, four taurine-conjugated bile acids clustered together and show similar correlations with bacterial families, and unconjugated secondary and tertiary bile acids also clustered together and behaved similarly with respect to their correlations with bacterial families.

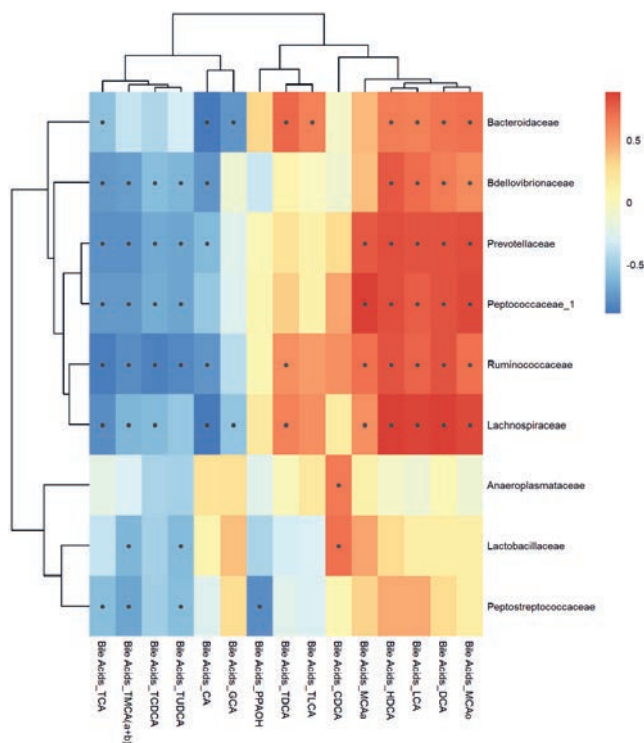


Figure 10. Inter-omic Pearson correlations between 16S bacterial taxa and bile acid metabolites measured from feces. Black dots within the boxes indicate p -value < 0.05 calculated using *cor.test*.

3.7.2. Plasma Matrix

Inter-omic correlations between the plasma metabolites and 16S bacterial families were less profound and not as many as between the fecal matrix and 16S bacterial families (see Figure 11). Out of 39 bacterial families, only 9 showed correlations with plasma metabolites. Similar to previous results, most of the correlated metabolites belonged to lipids and related classes, but also energy metabolites and amino acids and related metabolites. Lipids, fatty acids and derivatives like lysophosphatidylcholine, linolenic acid, and phosphatidylcholines strongly positively correlated with specifically the *Bdellovibrionaceae* family compared to all the other bacterial families (see Figure 11). Other metabolites like 3-hydroxyindole were mostly positively correlated with all of the nine bacterial families, including the strongest positive correlation with *Ruminococcaceae*. Creatine and creatinine strongly correlated in the negative direction particularly with four bacterial families, which are clustered very closely to each other in the dendrogram, namely *Ruminococcaceae*, *Bdellovibrionaceae*, *Lachnospiraceae* and *Peptostreptococcaceae*. Plasma metabolome does not only house gut-

microbiome-associated metabolites but a variety of host metabolites and co-metabolites as well. Plasma reflects a huge crosstalk of metabolites resulting from different sources (like nutrition, microbial metabolism); hence, it is obvious to attain very limited or only a handful of correlations between these metabolites and the gut bacterial families, compared to the feces. As observed in Figure 11, one of the key metabolites known to have an influence on the gut microbiome-mediated metabolism, Indole-3-acetic acid (IAA), is observed to have a few strong correlations. One of the strongest and negative correlations of IAA was with *Anaeroplasmataceae* family. Carbohydrates and related metabolites including hexoses produced mainly strong positive correlations with a majority of the bacterial families, except for *Rikenellaceae* (as shown in Figure 11).

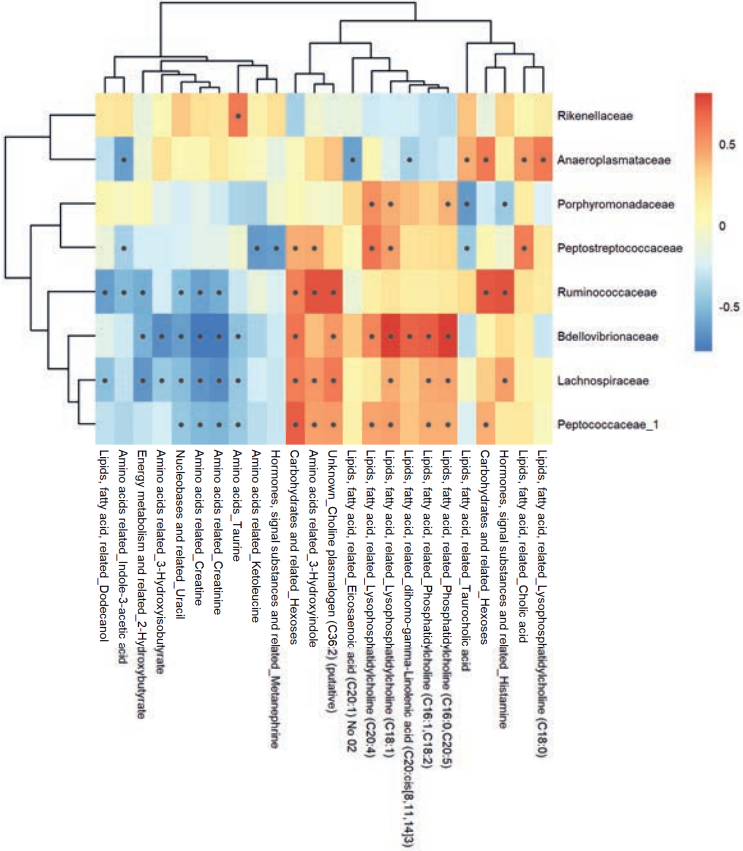


Figure 11. Pearson correlations of 16S bacterial families with plasma metabolite classes. The heatmap shows positive (red) and negative (blue) correlations between plasma metabolites and corresponding bacterial families. Metabolite classes have been indicated along with the metabolite names on the horizontal part of the figure. Black dots within the boxes indicate p -value < 0.05 calculated using cor.test.

In contrast to feces, most correlations observed between the plasma bile acids and 16S bacterial families are positively correlated, with a few exceptions (see Figure 12). Primary bile acids clustering close to each other, cholic acid and CDCA mostly produced positive correlations with all ten of the 16S bacteria families. Glycine-conjugated bile acids GCA, GCDCA and also GDCA show a very similar trend with

the majority of positive correlations with most 16S bacterial families with the difference in correlations with two bacterial families *Bacteroidaceae* and *Eubacteriaceae*. GCA and GCDCA showed negative correlations, while GDCA showed positive correlations with the two previously mentioned bacterial families. Among the taurine-conjugated secondary and tertiary bile acids, TLCA and TDCA showed a similar behavior in contrast to TCA and TMCA (both α and β). TLCA and TDCA showed positive correlations with all the ten bacteria taxa, while TCA and TMCA (both α and β) possessed the majority of negative correlations except for the *Eubacteriaceae* family. For unconjugated bile acids, although they formed separate clusters, MCA (both α and β), LCA and DCA showed comparable correlations with the bacterial associates. Additionally, other plasma biomarker metabolites such as 3-indoxylsulfate showed predominantly positive correlations, including the strongest positive correlations with the *Ruminococcaeae* family.

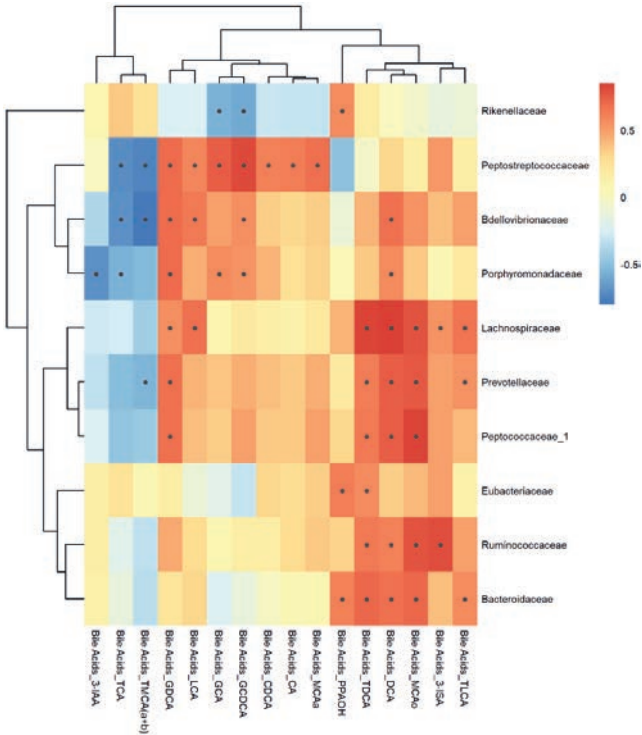


Figure 12. Correlation analysis using Pearson correlations between plasma bile acids and 16S bacterial families. Black dots within the boxes indicate p -value < 0.05 calculated using cor.test.

4. Discussion

The aim of this study was to understand the correlation between microbiome, fecal and plasma metabolomes. Our analysis now provides a connectivity map that shows how microbiome communities are responsible for the formation of fecal metabolites and how these are connected with the plasma metabolome.

4.1. Microbiome Analysis

Antibiotic class-specific effects on the gut bacterial composition in Wistar rats could be clearly and consistently observed in diversity and relative abundance analyses. The least effective antibiotic in changing microbiome communities was Streptomycin sulfate. This is not entirely surprising as Streptomycin has its primary antibiotic action on the aerobic microbiome, whereas most of the facultative anaerobes that dominate the gut are resistant to this antibiotic [17]. Treatment with Roxithromycin, affecting Gram-positive bacteria and some Gram-negative bacteria [17], produced the second least compositional changes in the gut microbiome. In contrast, Vancomycin produced profound changes in the gut microbiome, which is concordant to its broad bactericidal activity against Gram-positive organisms [17]. Animals treated with the lincosamide antibiotics Clindamycin and Lincomycin, showed very similar changes in bacterial communities, demonstrating a clear antibiotic class-dependent effect as they are selectively effective against staphylococci, streptococci and most anaerobic bacteria [36]. Dose-response was marginal for all antibiotics, with the exception of Streptomycin, indicating that the low doses were high enough to elicit gut dysbiosis. Sex-based differences at a family level were overall also marginal. However, it should be noted that at a species-level, at least in humans, sex-specific differences in microbiome communities have been described [36–38]. Dose-response was marginal for all antibiotics, with the exception of Streptomycin, indicating that the low doses were high enough to elicit gut dysbiosis. Sex-based differences at a family level were overall also marginal. However, it should be noted that at the species level, at least in humans, sex-specific differences in microbiome communities have been described [37,38]. The PCA analysis using phylogenetic distance clustering was in-line with the above-mentioned conclusions drawn from the Shannon index. Shannon diversity indices have two major components: the number of species present (or species richness) and their relative abundances (or species evenness). The latter showed that Vancomycin and Sparfloxacin treatments have the least even composition compared to all the others, irrespective of the dose groups and sex. Both antibiotics are known to have a broad-spectrum activity against Gram-negative and Gram-positive microorganisms [39]. This explains why we observed the least diverse and highly uneven (less dominant) bacterial taxa present in these two treatment groups. Relative abundance analysis showed on individual animal levels a clear inter-individual variability. From a birds-eye perspective, treatments can be readily identified as such; nevertheless, the samples from control animals possess such a recognizable variability of relative abundances of bacterial families that the sample size of any microbiome study needs to be considered. We therefore suggest that the control sample size of such studies should preferably involve at least 10 animals to account for variability. Evaluation of core bacterial taxa respective to the treatments showed that controls, restricted diet and, to a slightly lesser extent, Streptomycin sulfate treatment groups had high abundances of Firmicutes and Bacteroidetes phyla, which was also observed by Bao et al. in mice [40]. As Streptomycin sulfate is not effective against the majority of the gut microbiota, very similar relative

abundances of bacterial families in the treated and control groups can be expected, even in different species. The overall diversity of both the lincosamides-treated animal groups showed high abundances of Firmicutes and Proteobacteria, while Bacteroidetes levels were extremely reduced similar to what was seen in Behr et al. [15]. Most anaerobic bacteria that otherwise dominated the gut microbiota of control animals were wiped off by the two lincosamides. Roxithromycin showed the highest levels of Firmicutes and Bacteroidetes, as also shown by Zheng et al. [41]. Sparfloxacin treatments showed maximum abundances of Verrucomicrobia and Firmicutes phyla. Sparfloxacin, similarly to other quinolones and fluoroquinolones, kills bacteria, including Gram-positive and Gram-negative bacteria and other anaerobes; hence, the abundances of dominant species are reduced, whereas bacteria belonging to families *Verrucomicrobiaceae* and *Lactobacillaceae* increased compared to control animals. Finally, Vancomycin treatment groups showed the highest abundances of Verrucomicrobia and Proteobacteria phyla compared to all the other treatment groups, also wiping out the majority of the otherwise dominant bacteria in control animals. This antibiotic showed the maximum activity against the gut microbiota. Hierarchical clustering analysis based on the gut bacterial compositions showed that controls and restricted diet clustered together close to Streptomycin and most distant to Vancomycin. Vancomycin was observed to have the maximum dysbiosis compared to all the other antibiotic treatments. Both lincosamides clustered together but had minute differences in the abundances of families, e.g., *Enterococcaceae*, *Bacillaceae*, *Peptostreptococcaceae*, *Eubacteriaceae*. Roxithromycin and Sparfloxacin treatments clustered together with minor differences in the abundances of *Eubacteriaceae*, *Rikenellaceae*, *Clostridiaceae* and some others. Therefore, we observe antibiotic treatment-specific and class-specific gut composition alterations. Differential abundance analysis showed very minute dose-related effects and sex-dependent differences. The differential abundance results were comparable to the relative abundance stacked bar, where dominant/rare treatment-specific bacterial families could be observed, which is consistent with the hierarchical clustering analysis.

4.2. Metabolome Analysis

The dose levels of the antibiotics have been chosen as such as to have a significant influence on the gut microbiome, but not to lead to overt adverse effects in the treated animals. The absence of clinical signs of toxicity, effects on body weights and food consumption for most of the tested antibiotics makes it likely that systemic toxicity will not have played a role in the antibiotic treatments. Lincosamides, Roxithromycin and Sparfloxacin are known to be somewhat bioavailable [16], which could have had an influence on the plasma metabolome. At the very beginning of treatment, it might be possible that some clinical effects were noted for the high dose of clindamycin. However, after the first days of the study, the animals adapted to the treatment, and no more clinical signs were observed. To analyze a possible effect of systemic toxicity of the antibiotics on the plasma metabolome, they were administered at high- and low-dose levels to observe any dose-based response, the assumption being that the low and

high dose would result in similar effects on the microbiome—which it did—and that therefore additional high-dose-only-related changes in the plasma metabolome would be indicative for systemic or organ toxicity. The different metabolomes of the antibiotic-treated rats can be found in the Supplementary data (see Tables S2–S15). Plasma metabolome data did not show a profound treatment-based effect in the clustering, suggesting that the majority of the altered metabolites had a microbiome origin.

To understand the influence of restricted diet i.e., compromised nutrition on the metabolomes, PCA analyses were performed. Only the plasma metabolome showed a clear separation between controls and the reduced-diet group. This separation was not observed in the feces and cecum metabolomes and 16S bacterial community profile. This indicates that changes in the plasma metabolome induced by nutrition restrictions did not come from the gut microbial metabolism, but instead the host metabolism. Similar findings have been indicated in Zheng et al., who confirm that host-microbial co-metabolites in plasma were majorly changed due to caloric restrictions in humans [42].

Comparing the clustering of fecal metabolome with 16S microbiome clustering, we observed a similar grouping (refer to Figures 7a and S2), indicating that changes in the microbiome community are well correlated with the fecal metabolome profiles. This allows us to associate the 16S bacterial composition directly with the altered fecal metabolite levels to understand gut bacterial metabolism. Clustering analysis of cecum metabolome showed a bit more extensive antibiotic-treatment-specific clustering, but it was almost similar to the clustering of the fecal metabolome (see supplementary Figure S4).

The overlaps or differences between the correlation analysis of plasma, feces and cecum metabolome showed that cecum and fecal metabolome are highly correlated in line with the results of [43]. Thus, the feces metabolome is as informative as cecum and is a non-invasive method facilitating easy sampling procedures and longitudinal study designs. Further, when plasma metabolome was compared with feces and cecum metabolomes, almost no overlaps were observed, indicating that many of the fecal metabolites are not readily absorbed from the colon. These observations are in line with previous research [44,45],

We found indole-3-acetic acid to be a key biomarker metabolite (Supplementary Figure S8) [15–17]. This metabolite was observed to be significantly reduced in plasma, feces and cecum metabolomes of antibiotic-treated rats. Indole-3-acetic acid is produced either from bacterial indole production or from dietary tryptophan degradation by intestinal bacterial cells. The reduction of this key metabolite could be explained by a substantial loss of microorganisms, thereby reducing the ability to degrade tryptophan [15,17], and could potentially serve as a quantitative marker.

4.3. Correlation Analysis

Inter-omic correlation analysis between 16S bacterial families and both plasma and fecal metabolites were performed to elucidate the link between microbiome communities and fecal metabolites. We have approached the microbiome/metabolome correlation analysis from a holistic point of view,

demonstrating for most metabolites their correlation direction and strength. For a few selected metabolites, for which sufficient knowledge about their formation is available, we provide a more in-depth analysis. Firmicutes, specifically strains belonging to the *Clostridium* genus, are mainly known as amino-acid-fermenting bacteria, which is consistent with what we see in our feces microbiome–metabolome correlations.

4.3.1. Feces Metabolome-Microbiome

The majority of amino acids (see Figure 9) are upregulated in treatments that have more than 10-fold reduced *Prevotellaceae* levels in animals treated with lincosamides and Sparfloxacin antibiotics. Fluoroquinolones such as Sparfloxacin and lincosamides including Clindamycin are known to be active against this bacterial family [46,47]. Most gut bacteria are known to use amino acids as a preferred N-source. Arginine-to-ornithine conversion is also well studied in gut bacterial metabolism. In our correlation analysis, we see that levels of arginine are higher in Sparfloxacin treatment groups, and levels of ornithine are even higher in the feces of Sparfloxacin-treated animals. The Sparfloxacin treatment group has the highest abundance of *Peptostreptociccaeae* compared to controls and all the other treatments, which could indicate why the levels of ornithine in the feces of Sparfloxacin treated Wistar rats are significantly higher than in feces of all the others. We observed that amino acids such as glutamine, aspartate, lysine, valine (all branched-chain amino acid), threonine, serine and glycine were all significantly upregulated in all the treatments except for the restricted diet and Streptomycin treatment, indicating that reduced numbers of bacterial taxa are associated with reduced amino acid consumption. An overview of amino acid biosynthesis by gut microflora in humans and animals can be found in Dai et al. [48]. Three bacterial families, *Lactobacillaceae*, *Verrucomicrobiaceae* and *Anaeroplasmataceae*, form clusters of highly positive correlations with amino acids such as glycine, leucine, isoleucine, phenylalanine, alanine, valine and proline, suggesting common functions between these bacterial families.

Some of the amino acid fermentation products of gut bacteria include indole compounds such as tryptophan and organic acids such as lactate [48]. Tryptophan concentrations in all the treatments except for restricted diet and Streptomycin treatment groups were significantly increased. In particular, both lincosamide treatment groups (Clindamycin and Lincomycin) had very high levels of tryptophan in the feces, indicating that they reduced the bacterial taxa responsible for the conversion of tryptophan to indolic metabolites. It should be noted that *E. coli* strains belonging to the family *Enterobacteriaceae* are involved in the production of bacterial tryptophan and that these may also have been affected [49]. Kynurenic acid that results from tryptophan metabolism was significantly increased in the feces of Roxithromycin-, Streptomycin- and Vancomycin-treated animals. This indicates that the tryptophan was used by bacterial taxa occurring in these treatments. The Clindamycin treatment group had extremely high amounts of tryptophan; we also observed that kynurenic acid levels in the feces of these treatments also significantly increased compared to other treatments, but the levels were lower than

tryptophan levels. This shows that there must be bacterial transformation from tryptophan to kynurenic acid occurring in Clindamycin-treated animals, and that tryptophan production is much higher than the bacterial conversion of Tryptophan to Kynurenic acid, as shown by [50]. Glucuronic acid, which is also a product of tryptophan metabolism, was observed to be significantly increased in Sparfloxacin and Vancomycin treatment groups. In our correlation analysis, glucuronic acid had the strongest positive correlation with *Rikenellaceae*, *Verrucomicrobiaceae* and *Anaeroplasmataceae* families, which are highest in abundance in Sparfloxacin- and Vancomycin-treated animals. This could mean that these families play a specific role in the conversion of tryptophan to glucuronic acid. Pyruvate, an energy-related metabolite was significantly downregulated in the feces of all the treatments, whereas glucose levels were significantly upregulated in all the treatment groups except the restricted diet group, demonstrating that bacterial gluconeogenesis is altered by all the drugs.

A key metabolite of gut microbial metabolism is indole-3-acetic acid (IAA) [17]. The correlation analysis shows few weakly positive and many weakly negative correlations with the majority of bacterial families except *Verrucomicrobiaceae* and *Anaeroplasmataceae*, with strongly negative correlations. IAA levels in feces only significantly increased in Clindamycin treatment groups, whereas they were significantly lowered in all the other treatments. Bacterial IAA is known to be biosynthesized by Gram-negative and Gram-positive bacteria involving decarboxylation and deamination of tryptophan. Tryptophan-dependent pathways for IAA production include either indole-3-pyruvic acid (IPA) and indole-3-acetamide (IAM), or indole-3-acetonitrile (IAN) as important intermediates [51]. The fact that tryptophan levels were highly increased in the feces of animals treated with Lincomycin and Sparfloxacin, while IAA levels were significantly reduced, means that the conversion from tryptophan to IAA did not occur in these treatment groups. In the Clindamycin treatment groups, however, both tryptophan and IAA were increased in the feces, suggesting that there must be bacterial transformation directly from indole to IAA occurring in Clindamycin treatments unlike other treatments. Feces from Clindamycin-treated animals were observed to possess *Enterococcaceae* families in the highest abundance compared to all the other treatment groups, so it could be hypothesized that these families are responsible for the production of IAA from indole directly via a tryptophan-independent pathway.

Creatine and creatinine are both utilized by gut microbes for growth. Conversion of creatinine to creatine is not possible by mammalian metabolism, and creatinine is eliminated from the system. While bacteria belonging to Firmicutes and Proteobacteria phyla have been extensively studied to possess creatine degradation activity [50], creatinine levels in the feces were weakly correlated with almost all the bacterial families except *Porphyromonadaceae* and *Prevotellaceae*, which belong to Bacteroidetes phyla. Creatinine levels were highly significantly increased in the feces of all the treatment groups except for restricted diet and Streptomycin treatments, indicating that most of the facultative anaerobes dominating the gut of the animals belonging to these two treatment groups continue to utilize creatinine for further metabolism. Levels of creatine in the feces of lincosamides-and Vancomycin-treated animals

are not as high as creatinine, which means there is a conversion of creatinine to creatine occurring in these three treatment groups, but there is also accumulation of creatinine. This means that either there are other bacterial taxa that produce creatinine, or they do not carry out the conversion from creatinine to creatine in an efficient way. Relative abundances of *Porphyromonadaceae* and *Prevotellaceae* families are highest in restricted diet and Streptomycin treatment groups, where creatinine levels are not altered in the feces, suggesting that they may play a role in creatine metabolism. Metabolites that result from microbiome-mediated metabolism include lipids and lipoproteins, amino acids, glutamate, choline, acetate, butyrate and glycerol [52]. We also see similar results in our correlations analysis where bacterial taxa produced the strongest correlations with metabolites belonging to amino acids, lipids and fatty acids derivate classes in the feces. Clusters of positive correlations between specific bacterial families including *Porphyromonadaceae*, *Ruminococcaceae*, *Lachnospiraceae*, *Bacteroidaceae*, *Prevotellaceae*, *Bdellovibrionaceae* and *Peptococcaceae* could be observed with metabolites belonging to lipids, fatty acids and related classes, suggesting common functions between these bacterial families. All in all, the correlations showed most of the strongly correlated metabolites belonging to amino acids, lipids and related metabolites, in line with [53,54]. Our results on the role of gut bacteria in amino acid, complex lipids and fatty acid synthesis are similar to those published by Fujisaka et al. [45].

4.3.2. Plasma Metabolome-Microbiome

Although tryptophan levels in plasma were not altered significantly in any of the treatment groups, glucuronic acid resulting from tryptophan metabolism is significantly upregulated in most of the treatment groups, except the restricted diet, Vancomycin and Streptomycin treatment groups. In the correlation analysis, plasma tryptophan and glucuronic acid do not show any strong correlation with the gut bacterial families. This could mean that these metabolites could be from dietary sources and a result of host metabolism. Plasma creatine and creatinine clustered together in the correlation heatmap. Creatinine levels in all the treatment groups did not show a large alteration, but creatine showed significant downregulation only in the restricted diet group. As restricted-diet-fed animals did not have a large influence on the gut microbial dysbiosis, it could be concluded that this increase in creatine levels in plasma is related to host metabolism. The gut microbiome is extensively known to metabolize dietary tryptophan into indole, and its derivatives, such as indole-3-acetic acid (IAA) and indole-3-propionic acid (IPA)m which are also absorbed efficiently by the gut mucosa [55]. Plasma IAA was observed to be highly upregulated in the plasma of Vancomycin-treated animals. The *Verrucomicrobiaceae* family is highly abundant in this treatment group. This could potentially mean the higher abundance of this bacterial family contributed in the production of IAA, thereby increasing the levels, which is also described in Louis et al., where they identify specific colonic bacteria including *Verrucomicrobia* phyla that contribute to the production of propionate and butyrate in humans [56].

3-Indoxylsulfate (IS) in plasms was downregulated in the two lincosamides treatment groups and highly upregulated in the Roxithromycin treatment group. This could mean that in Roxithromycin treatment, the bacterial production of IS was higher due to the higher abundance of bacterial taxa such as *Eubacteriaceae*, which supports this conversion [57]. Tryptophanase activity of the gut bacteria is known to convert tryptophan to indole, which further gets absorbed in the gut and transformed to IS in the liver, which leads to an increase in plasma IS levels [58]. Overall, the 16S bacterial families were associated more with plasma metabolites belonging to amino acid classes, but also carbohydrates, energy metabolites and lipids, nucleic acids and related metabolites, which is consistent with what is observed in Fujisaka et al. [45]. 16S bacterial families showed high numbers of strong correlations (irrespective of the direction) with feces and cecum metabolites, whereas very limited correlations could be observed with plasma metabolites (see Figure 11).

4.4. Bile Acids

We conducted an extensive analysis for individual antibiotics on their influences on bile acid levels and tried to associate them with the responsible bacterial families. A standard workflow including the majority of the bile acid reactions combined is shown in Figure 13, where we can see which bile acids are produced in the liver and which ones are produced by the gut bacteria.

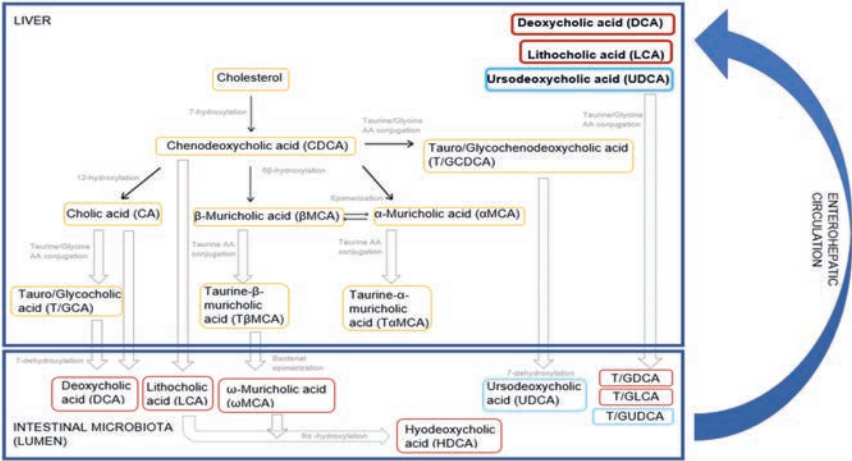


Figure 13. Host and gut microbiota-mediated bile acid metabolism in rodents. The schematic diagram shows yellow boxes for bile acids that are primarily synthesized in the liver, red boxes for secondary bile acids that are biotransformed from the primary bile acids by the gut microbiota and blue boxes for the tertiary bile acid that enters the enterohepatic circulation. Primary, secondary and tertiary bile acids are reabsorbed from the GI walls and re-enter the liver via enterohepatic circulation to stabilize the bile acid pool. This figure was made based on previous publications [59,60].

4.4.1. Clindamycin Hydrochloride Treatment

CDCA is the first metabolite that is produced from CYP enzyme-mediated hydroxylation activity of cholesterol in the liver. Following treatment with Clindamycin, CDCA levels are observed to be significantly downregulated in plasma and feces. This could mean an increased conversion of CDCA

to its conjugated forms or a reduced production due to reduced 7-hydroxylation activity. Conjugated primary bile acids such as TCDCA and GCDCA are formed from CDCA as a precursor. Rodents are known to preferentially conjugate in the liver using taurine (almost 90%) rather than Glycine [54], and our findings are in line with this knowledge. CA is formed from further hydroxylation of CDCA in the liver. CA levels were significantly upregulated in feces but downregulated in plasma. This could mean either that its precursor CDCA levels are reduced in plasma (as observed in Table 2) and hence that there is a significant downregulation of CA in plasma, or that CA could not be converted to DCA by the gut bacterial enzymes due to lack of gut microflora bioactivity. These two hypotheses are in line with our data that both CDCA and DCA levels were indeed reduced. This is also consistent with what we see in our data as TCDCA is highly upregulated in the feces compared to GCDCA, as would be expected from the preferential conjugation with taurine amino acids in rats. This also means that TCDCA is not deconjugated in the gut. Despite the profound increase in conjugated bile acids in the feces, in plasma, TCDCA levels are only marginally upregulated, whereas GCDCA are significantly downregulated. Consequently, reabsorption of both conjugated bile acids would appear to be very limited. Two of the other primary bile acids that result from hydroxylation of CDCA are MCA alpha and MCA beta. The feces and plasma levels of MCA (both alpha and beta) are significantly downregulated. The suggested hypothesis is that the conjugation step from MCA (alpha and beta) to taurine-conjugated TMCA (alpha and beta) must be higher in the clindamycin treatment group. This is very much in line with what we observe, as the TMCA (both alpha and beta) levels are highly significantly increased in feces, whereas in the plasma, the TMCA (alpha and beta) levels are only weakly upregulated. Taurine conjugate bile acids are known to be absorbed in the gut, providing an explanation for the increased levels of TMCA in plasma. Other taurine- and glycine-conjugated bile acids that are produced from CA are TCA and GCA. GCA is observed to be downregulated in both plasma and feces, whereas TCA is observed to be highly significantly upregulated in feces and downregulated in plasma. Upregulation of TCA in feces could correspond to more rapid conjugation of CA to TCA than to GCA and weak reabsorption of them from the small intestine.

Table 2. Fold changes of different bile acid levels going up (red boxes) and down (blue colored boxes) in the feces and plasma matrices of male and female Wistar rats of Clindamycin treatment (*p*-value depends on the shade of the colors, the darkest red is *p*-value <0.01, medium red is *p*-value <0.05; and the lightest shade of red is *p*-value <0.10 and similarly for blue coloring). F represents females, M represents males, 7 d, 14 d and 28 d denote blood sampling time points days 7, 14 and 28, respectively.

Metabolite Name	Analyte Name	Feces		Plasma					
		F	M	F 7d	F 14d	F 28d	M 7d	M 14d	M 28d
Cholate	CA	18.64	19.90	0.02	0.03	0.01	0.01	0.03	0.01
Chenodeoxycholate (chenodeoxycholic acid)	CDCA	0.30	0.08	0.02	0.03	0.04	0.02	0.10	0.02
Deoxycholate (deoxycholic acid)	DCA	0.00	0.00	0.35	0.00	0.01	0.10	0.36	0.01
Glycocholate, glycocholic acid	GCA	1.72	0.47	0.44	0.30	0.21	0.22	0.35	0.16

Glycochenodeoxycholate (glycochenodeoxycholic acid)	GCDCA	2.67	0.09	0.56	0.40	0.76	0.06	0.08	0.06
Glycodeoxycholate, -cholic acid	GDCA	0.58		0.04		0.07	0.01	0.01	0.02
Glycolithocholic acid	GLCA	0.52	0.44	0.54	0.26	0.68	0.12	0.79	0.36
Glycoursodeoxycholic acid	GDCA	2.82	2.25	0.11	1.03			0.97	0.30
Hyodeoxycholate, hyodeoxycholic acid	HDCA	0.00	0.00	0.01	0.01		0.00	0.01	0.00
Lithocholate, lithocholic acid	LCA	0.01	0.01	1.00			0.53	1.55	0.35
Muricholic acid (alpha)	MCAa	0.59	0.16	0.03	0.06	0.06	0.01	0.02	0.01
Muricholic acid (beta)	MCAb	2.36	0.87	0.11	0.25	0.39	0.15	0.31	0.39
Muricholic acid (omega)	MCAo	0.06	0.01	0.00	0.01	0.04	0.01	0.00	0.01
Taurocholate, taurocholic acid	TCA	47.42	90.80	1.34	1.01	1.63	4.68	2.94	4.56
Taurochenodeoxycholate	TCDCA	35.03	13.64	1.38	0.99	1.54	2.46	1.46	1.25
Taurodeoxycholate, -cholic acid	TDCA	0.25	0.15	0.02	0.01	0.01	0.01	0.01	0.05
Taurolithocholic acid	TLCA	0.15	0.34	0.04			0.04	0.19	0.14
Taurumuricholic acid (a+b)	TMCA(a+b)	155.83	192.72	1.96	1.41	2.38	4.97	2.57	3.99
Tauroursodeoxycholic acid	TUDCA	22.61	28.27	6.92			0.20	0.57	0.74
Ursodeoxycholate, Ursodeoxycholic acid, Ursodiol	UDCA	0.02	0.03	0.05	0.27	0.01	0.01	0.30	0.02

The most enigmatic data are the profound upregulation of CA in the feces and similarly profound downregulation in the plasma. This would strongly suggest that there is a lack of resorption of CA in the lower intestinal tract and in fact a loss of CA to the entire biological system.

Taurine-conjugated CA was reabsorbed; hence, we see an upregulation in the plasma. Secondary bile acids that result from bacterial deconjugation are namely DCA, LCA, MCAo and HDCA. In our data DCA, MCAo and HDCA levels show significant downregulation in both plasma and feces, again demonstrating impairment of bacterial deconjugation reactions. This is also in line with their precursor bile acids TCA and TMCA (both alpha and beta) levels being significantly upregulated in the feces. The tertiary bile acid UDCA produced from the downregulated secondary bile acid LCA is also reduced in both feces and plasma of this treatment group. The literature indicates that UDCA is produced from LCA in the intestine [61] or in the liver [62]. In our study, we see LCA levels reduced in the feces but unaffected in the plasma. Therefore, it would seem more likely that UDCA is produced in the gut rather than the liver. This could be because this metabolite gets reabsorbed into the liver and gets readily conjugated into its taurine form. This is in line with the TUDCA levels highly significantly upregulated in the feces. This proves the increased conjugation of the tertiary bile acid and lack of deconjugation in the gut. Other deconjugated secondary bile acids such as DCA and LCA can also be reabsorbed and enter into the liver for the conjugation reaction. Due to the impairment in the production of these secondary bile acids by the disturbed gut bacteria, the taurine/glycine-conjugated DCA and LCA also appear to be significantly downregulated in both plasma and feces. Taurine deconjugation is less likely to have happened according to our data. Glycine-conjugated bile acids look far less affected. This proves that Clindamycin-treated rats have overall impaired secondary bile acid production which is exactly what we expect after treating the animals with an antibiotic.

As Clindamycin is a member of the lincosamide group, it is no surprise that Lincomycin has a similar anti-biotic spectrum. Lincomycin-treated animals also show a clear impairment of secondary bile acid production due to perturbations in the gut flora. Both the antibiotics belong to the same class of antibiotics called Lincosamides, and they definitely show a similar influence on the bile acid profiles. The table of altered bile acid metabolites in the plasma and feces of lincomycin hydrochloride treatment group can be seen in the supplementary data (see Table S17). This altered bile acid levels in the feces and plasma of the two lincosamide treatment groups could be associated with the extreme downregulation of Firmicutes (including bacterial families such as *Lachnospiraceae*, *Peptococcaceae* and *Petptostreptococcaceae*), Bacteroidetes (including bacterial families such as *Prevotellaceae*, *Bacteroidaceae* and *Porphyromonadaceae*) and Proteobacteria (including bacterial families such as *Bdellovibrionaceae*, *Rhodospirillaceae*, *Desulfovibrionaceae*) compared to the control animals (see DESeq2 table S16). The reduction in levels of these previously mentioned bacteria may be related to the impairment of secondary bile acid production in those treatment groups.

4.4.2. Vancomycin Treatment

CDCA levels in the feces of Vancomycin treatment group do not appear to be significantly altered, whereas in the plasma, we observe a consistent downregulation of CDCA, as shown in Table 3. As we do not see a significant change in CDCA levels in the feces, it can be expected that metabolites such as TCDCA, GCDCA and MCA (both alpha and beta) should not be changed in the feces of this treatment group either. This is in line with what we see in our data. GCDCA, TCDCA and MCA (both alpha and beta) do not show significant changes in the feces of vancomycin-treated animals.

Table 3. Fold changes of different bile acid levels going up (red colored boxes) and down (blue boxes) in the feces and plasma matrices of male and female Wistar rats of Vancomycin treatment (p -value depends on the shade of the colors; the darkest red represents p -value <0.01 , medium red represents p -value <0.05 and the lightest shade of red represents p -value <0.10 , and similarly for blue). F represents females, M represents males, 7 d, 14 d and 28 d denote blood sampling time points days 7, 14 and 28, respectively.

Metabolite Name	Analyte Name	Feces		Plasma					
		F	M	F 7d	F 14d	F 28d	M 7d	M 14d	M 28d
Cholate	CA	19.45	38.66	0.18	0.60	0.14	0.10	0.13	0.13
Chenodeoxycholate (chenodeoxycholic acid)	CDCA	4.30	0.99	0.18	0.36	0.05	0.10	0.16	0.18
Deoxycholate (deoxycholic acid)	DCA	0.00	0.00	0.01	0.42	0.01	0.00	0.18	0.00
Glycocholate, glycocholic acid	GCA	2.67	1.45	0.46	1.54	0.73	0.39	0.36	0.18
Glycochenodeoxycholate (glycochenodeoxycholic acid)	GCDCA	1.01	1.54	0.39	0.87	0.64	0.30	0.27	0.42
Glycodeoxycholate, -cholic acid	GDCA	0.32	0.34	0.02	0.07	0.03	0.01	0.00	0.05
Glycolithocholic acid	GLCA	0.24	0.86	0.56	0.21	0.20	0.48	1.65	4.39
Glycoursodeoxycholic acid	GUDCA	1.44	1.44	1.65	1.18	3.31	0.43	16.34	10.13
Hyodeoxycholate, hyodeoxycholic acid	HDCA	0.00	0.00	0.01	0.01	0.00	0.00	0.00	0.00

Lithocholate, lithocholic acid	LCA	0.01	0.07	0.12	10.74	0.15	0.35	27.95	0.19
Muricholic acid (alpha)	MCAa	0.44	0.71	0.21	0.44	0.10	0.13	0.14	0.23
Muricholic acid (beta)	MCAb	0.50	0.53	0.54	1.01	1.35	0.17	0.18	0.38
Muricholic acid (omega)	MCAo	0.02	0.03	0.05	0.01	0.07	0.03	0.01	0.02
Taurocholate, taurocholic acid	TCA	4.18	7.39	2.04	6.99	3.83	2.47	2.71	2.62
Taurochenodeoxycholate	TCDCA	0.99	3.04	1.87	2.42	2.64	2.69	3.18	2.97
Taurodeoxycholate, -cholic acid	TDCA	0.16	0.09	0.01	0.02	0.01	0.01	0.01	0.01
Taurolithocholic acid	TLCA	0.42		0.03	0.04	0.03	0.12	0.18	1.58
Tauromuricholic acid (a+b)	TMCA(a+b)	2.86	3.89	3.10	4.02	3.59	1.93	2.71	3.11
Tauroursodeoxycholic acid	TUDCA	0.54	2.93	3.61	1.82		1.23		0.79
Ursodeoxycholate, Ursodeoxycholic acid, Ursodiol	UDCA			0.21	0.06	0.29	0.13	0.12	0.23

As with the lincosamide antibiotics, for Vancomycin, we also noted a profound increase in CA in the feces and a downregulation in the plasma, indicating that CA is not well resorbed from the lower intestinal tract. As DCA levels were very much reduced in the feces, this means that 7-alpha-dehydroxylation of CA was severely impaired, due to the change in the microbiome composition. We saw significant downregulation of DCA, a secondary bile acid, in both plasma and feces, again indicating impairment of bacterial deconjugation from TCA or GCA to DCA. Therefore, TCA as the preferred conjugated of CA was highly upregulated in both plasma and feces. Taurine-conjugated primary bile acids, including TCA, TMCA alpha and beta, are also highly upregulated in both plasma and feces, again in line with the lack of microbial deconjugation. As a consequence, secondary bile acids like DCA, LCA, MCAo and HDCA are downregulated in both plasma and feces. These secondary bile acids, including tertiary bile acid UDCA, can be reabsorbed in the gut and become re-conjugated with Taurine or Glycine AA. However, as their levels are reduced, the levels of G/TDCA and G/TLCA are also significantly downregulated in both plasma and feces. Taking into account the microbiome changes induced by Vancomycin, this could be related to the downregulation of many Bacteroidetes and Firmicutes phyla. Qualitatively, the overall changes in the bile acid levels induced by these antibiotics (vancomycin and lincosamides) are similar, but quantitatively, we see marginal differences.

4.4.3. Sparfloxacin Treatment

Many of the changes in BAs seen following Sparfloxacin-treated animals were similar to the ones described for the lincosamides and vancomycin groups (see Table 4). Again, profound changes were noted for CA in feces, DCA in feces and plasma and upregulation of particularly taurine-conjugated BAs in both feces and plasma.

Table 4. Fold changes of different bile acid levels going up (red boxes) and down (blue colored boxes) in the feces and plasma matrices of male and female Wistar rats of Sparfloxacin treatment (*p*-value depends on the shade of the colors; the darkest red represents *p*-value <0.01, medium red represents *p*-value <0.05 and the lightest shade of red represents *p*-value <0.10, and similarly for blue). F represents females, M represents males, 7 d, 14 d and 28 d denote blood sampling time points days 7, 14 and 28, respectively.

Metabolite Name	Analyte Name	Feces		Plasma					
		F	M	F 7d	F 14d	F 28d	M 7d	M 14d	M 28d
Cholate	CA	27.39	22.73	1.08	0.46	0.32	0.11	0.91	0.90
Chenodeoxycholate (chenodeoxycholic acid)	CDCA	0.52		0.32	0.17	0.37	0.04	0.28	0.94
Deoxycholate (deoxycholic acid)	DCA	0.01	0.00	0.09	0.02	0.08	0.01	0.18	0.03
Glycocholate, glycocholic acid	GCA	1.88	1.57	1.02	0.53	2.05	0.42	0.59	0.71
Glycochenodeoxycholate (glycochenodeoxycholic acid)	GCDCA	1.25	2.93	0.51	0.34	1.61	0.14	0.13	0.40
Glycodeoxycholate, -cholic acid	GDCA		2.70	0.08	0.25	0.51	0.02	0.01	0.12
Glycolithocholic acid	GLCA	8.22	1.33		0.90	0.71	0.24		1.93
Glycoursodeoxycholic acid	GUDCA	0.96	1.61					0.33	1.30
Hyodeoxycholate, hyodeoxycholic acid	HDCA	0.01	0.00	0.06	0.01		0.00	0.00	
Lithocholate, lithocholic acid	LCA	0.24	0.01	0.12	0.01	13.09	0.18	9.66	0.31
Muricholic acid (alpha)	MCAa	0.58	0.16	0.67	0.24	0.57	0.05	0.38	0.73
Muricholic acid (beta)	MCAb	0.33	0.37	1.46	1.21	0.31	0.25	1.87	1.10
Muricholic acid (omega)	MCAo	0.01	0.02	0.20	0.01	0.01	0.01	0.00	
Taurocholate, taurocholic acid	TCA	4.95	8.29	2.61	3.25	1.73	7.96	5.32	3.09
Taurochenodeoxycholate	TCDCA	2.29	4.99	1.21	1.44	1.77	3.85	3.63	2.08
Taurodeoxycholate, -cholic acid	TDCA	0.30	0.18	0.09	0.21	0.03	0.11	0.03	0.04
Taurolithocholic acid	TLCA	0.27	0.75		1.11	0.06	0.28	0.33	0.22
Tauromuricholic acid (a+b)	TMCA(a+b)	7.08	16.86	1.72	1.73	1.88	4.25	4.95	2.27
Tauroursodeoxycholic acid	TUDCA	2.12	9.35		10.27			7.76	1.82
Ursodeoxycholate, Ursodeoxycholic acid, Ursodiol	UDCA	0.25	0.01	0.36	0.56	0.23	0.13	1.20	1.17

The upregulation of CA in the feces, similar to the lincosamides and vancomycin, could be explained by a negative feedback mechanism associated with the high levels of conjugated bile acids, as a result of the reduced deconjugation steps. As indicated earlier, the reduction of CA in the plasma can be explained by a lack of reabsorption from the colon. GCDCA does not show any significant change in its levels in feces, although it is downregulated in plasma; TCDCA, on the other hand, is highly upregulated in both plasma and feces. This indicates a higher production of TCDCA than GCDCA, as also observed for the other antibiotic treatments; it also indicates that, due to interrupted bacterial deconjugation activity, these get accumulated in the feces. The Taurine-conjugated bile acids are reabsorbed from the gut and their elevated levels also result in increased plasma levels. MCA (both alpha and beta) show major downregulation in both plasma and feces, indicating that they are readily converted to their conjugated forms. The Taurine conjugate of MCA both alpha and beta (TMCA a+b) show high upregulation in both plasma and feces, confirming that the Taurine conjugation of MCA, both alpha and beta, is high in Sparfloxacin treatment groups. Secondary bile acids, including DCA, LCA, MCAo and HDCA, all show downregulation in both plasma and feces, indicating impairment in deconjugation by bacterial enzymes, thereby reducing their levels in both plasma and feces, which is consistent with UDCA a tertiary BA. In our data, G/TDCA, G/TLA and GUDCA show no change in their levels in both plasma and feces, whereas TUDCA shows upregulation in both plasma and feces,

indicating that whatever UDCA levels were sent to the liver were then readily reconjugated with Taurine, after which further deconjugation by the gut bacteria did not occur, leading to high levels in the feces. This is very similar to the lincosamide treatment group and can be linked to downregulation of Proteobacteria and Firmicutes phyla compared to controls.

4.4.4. Roxithromycin treatment

This roxithromycin treatment group showed very interesting results compared to all the antibiotics (see Table 5). CDCA levels in the plasma of the roxithromycin treatment group showed significant downregulation, whereas no significant changes in the feces were observed. This is consistent with what was observed in the other antibiotic treatment groups. CA is significantly downregulated in feces, an effect not observed in any of the other antibiotic treatment groups. Comparing this observation with the microbiome composition following roxithromycin treatment, it is noted that there is a unique upregulation of the *Rikenellaceae* in this group.

Table 5. Fold changes of different bile acid levels going up (red boxes) and down (blue colored boxes) in the feces and plasma matrices of male and female Wistar rats of Roxithromycin treatment (p -value depends on the shade of the colors.; the darkest red is p -value <0.01, medium red is p -value <0.05 and the lightest shade of red is p -value <0.10, and similarly for blue). F represents females, M represents males, 7 d, 14 d and 28 d denote blood sampling time points days 7, 14 and 28, respectively.

Metabolite Name	Analyte Name	Feces		Plasma					
		F	M	F 7d	F 14d	F 28d	M 7d	M 14d	M 28d
Cholate	CA	0.52	0.55	0.04	0.05	0.13	0.00	0.00	0.02
Chenodeoxycholate (chenodeoxycholic acid)	CDCA	0.90		0.02	0.06	0.08	0.02	0.01	0.05
Deoxycholate (deoxycholic acid)	DCA	0.49	0.70	0.75	0.58	0.86	0.15	0.11	0.20
Glycocholate, glycocholic acid	GCA	0.15	0.23	0.42	0.30	0.10	0.25	0.10	0.08
Glycochenodeoxycholate (glycochenodeoxycholic acid)	GCDCA	0.42	0.72	0.39	0.36	0.17	0.38	0.10	0.08
Glycodeoxycholate, -cholic acid	GDCA		0.49	0.51	0.37	0.07	0.14	0.05	0.07
Glycolithocholic acid	GLCA	0.41	1.63	0.28	0.27	0.49	0.33	0.93	0.66
Glycoursodeoxycholic acid	GUDCA	1.44		1.82	0.59	1.13	0.46	1.45	0.63
Hyodeoxycholate, hyodeoxycholic acid	HDCA	0.06	0.03	0.10	0.04	0.10	0.01	0.01	0.01
Lithocholate, lithocholic acid	LCA	0.23	0.35	0.71	0.46	0.72	0.64	6.52	0.50
Muricholic acid (alpha)	MCAa	0.73	0.62	0.22	0.19	0.11	0.08	0.02	0.05
Muricholic acid (beta)	MCAb	1.33	0.84	0.71	1.30	2.28	0.16	0.05	0.22
Muricholic acid (omega)	MCAo	0.77	0.60	1.19	0.60	1.47	0.74	0.36	0.42
Taurocholate, taurocholic acid	TCA	2.41	1.58	2.59	5.55	3.14	3.35	2.19	3.77
Taurochenodeoxycholate	TCDCA	1.42	1.54	1.69	1.48	1.84	2.07	2.02	2.28
Taurodeoxycholate, -cholic acid	TDCA	9.42	4.61	2.29	3.11	1.89	2.55	1.19	2.06
Taurolithocholic acid	TLCA	3.26	3.13	0.74	0.75	1.39	1.05	0.68	0.61
Tauromuricholic acid (a+b)	TMCA(a+b)	10.14	7.97	1.94	2.94	2.37	3.62	2.67	3.02
Tauroursodeoxycholic acid	TUDCA	3.42	2.20	9.03	1.23		1.24		0.55
Ursodeoxycholate, Ursodeoxycholic acid, Ursodiol	UDCA			0.11	0.06	0.53	0.03	0.05	0.01

The reduction of CA levels is in line with the reduced CDCA levels in plasma; however, as the precursor cholesterol was not affected (data not shown), a hypothesis could be that there is increased conjugation of CDCA. This is not at variance with the increased TCDCA levels in the plasma.

Other conjugated bile acids of CDCA, namely GCDCA and TCDCA, showed contrasting levels in plasma and feces. GCDCA was not significantly altered in feces but was downregulated in plasma, and TCDCA levels were highly upregulated in both plasma and feces. This again proves that taurine conjugation is higher than glycine conjugation and that taurine-conjugated BAs are readily reabsorbed in the gut. MCA, both alpha and beta, showed no alteration in the feces but downregulation in the plasma matrix of Roxithromycin antibiotic treatment group. This indicates that the hydroxylation reaction from CDCA to MCA alpha and beta and further conjugation of MCA alpha and beta to TMCA alpha and beta must be regulated in a way that it does not alter the levels of MCA alpha and beta. TMA alpha and beta are highly upregulated in both plasma and feces, indicating no further deconjugation of these metabolites, leading to an increase in their levels. Secondary bile acids such as LCA, DCA and HDCA were downregulated in both plasma and feces, showing the impairment in bacterial deconjugation in the gut due to antibiotic treatment. MCAo, on the other hand, which is also a secondary BA, did not show a significant change in feces and plasma. These secondary bile acids were reabsorbed from the gut, entered the enterohepatic circulation and were reconstituted with taurine or glycine. Glycine conjugated secondary BA, including GDCA, GLCA and GUDCA, showed significant downregulation in both plasma and feces, indicating a lack of deconjugation and impairment in their levels in the gut before being reconstituted in the liver. In contrast, taurine-conjugated secondary and tertiary BA, including TDCA, TLCA and TUDCA, showed an upregulation in feces and plasma of the Roxithromycin treatment group. Upregulation of TDCA and TLCA in the feces and plasma has not been observed in any of the other antibiotic groups. Taurine conjugation of primary as well as secondary BAs was increased by this antibiotic. This increased taurine conjugation could also be related to an altered FXR signaling pathway. Three BAs including CDCA, DCA and LCA reduce the 7-hydroxylase activity as a negative feedback via the FXR receptor. Even though CDCA, DCA and LCA were significantly low in both plasma and feces of antibiotic treatment groups, in this case, the 7-hydroxylase activity cannot be high. This would indicate that there were more factors playing a role in the maintenance of BA pool, and as we obviously disturbed them using antibiotics, these factors should be microbiome-derived. This could mean that further deconjugation of these taurine-conjugated secondary BAs are impaired, leading to an increase in their levels in feces and plasma.

Two major conclusions that can be derived analyzing the bile acid profiles of Roxithromycin treated animals are that, firstly, 7 α dehydroxylase activity of the gut bacterial species present in this treatment group must be high because CA levels are reduced in the feces and are metabolized to secondary bile acids. This could be associated with the highest abundances of *Rikenellaceae* family in this antibiotic treatment compared to controls and other treatments. Hence, these families of bacteria may be the primary source of 7 α dehydroxylase activity, which is otherwise absent in the other antibiotic treatment

groups. Secondly, we can assume that the taurine deconjugation is still impaired in this treatment group due to the higher accumulation of taurine-conjugated primary and secondary bile acids in both plasma and feces. This could be explained by the reduced abundances of bacterial families such as *Bacteroidaceae*, *Porphyromonadaceae* and *Prevotellaceae* in this antibiotic treatment, which might be responsible for the taurine amino acid deconjugation in the gut. Cholesterol levels in feces do not change significantly, meaning that bile acids somehow maintain the pool in such a way that the source cholesterol levels are not altered much.

4.4.5. Streptomycin Sulfate Treatment

Amongst all the other antibiotics, this treatment showed the least significantly altered bile acid levels, as shown in Table 6. CDCA levels are only marginally altered in both plasma and feces; hence, we only see marginal effects in GCDCA and TCDCA levels. This nevertheless shows very consistent increases in CA levels in feces and decreases in plasma, which is consistent with the other antibiotic treatments except Roxithromycin. Taurine and Glycine conjugates of CA, namely TCA and GCA, did not show a profound alteration in feces. This is unique amongst all of the antibiotic treatment groups. We note a moderate increase of TCA in the plasma, however. Overall, this suggests that deconjugation reactions are far less impaired by Streptomycin treatment. As this antibiotic causes only relatively moderate changes in the lower intestinal tract microbiome, it can be concluded that deconjugation reactions are occurring at this site. Moreover, further Streptomycin-specific changes have been observed in MCA alpha and beta levels. Unlike all the other antibiotics, these bile acids are significantly upregulated in both plasma and feces. We also see an upregulation in both alpha and beta TMCA levels in both plasma and feces. We can deduce that Streptomycin has a specific influence on hydroxylation of CDCA to produce MCA alpha and beta, because of which their levels are unusually increasing compared to all the other antibiotic treatments. Secondary bile acid DCA shows very marginal alteration, indicating that their production or bacterial deconjugation is not profoundly disturbed in the case of this antibiotic treatment group. However, other secondary bile acids such as LCA and HDCA show significant downregulation in both plasma and feces, indicating that this part of the bacterial transformation is impaired in Streptomycin, which is consistent with all other antibiotics. On the contrary, we see an upregulation in MCA-omega in both plasma and feces, which is again Streptomycin-specific. This indicates that Muricholic acid and related conjugates and deconjugated metabolites are altered by this antibiotic. We also see MCAo being reabsorbed in this antibiotic treatment, which was not observed in any of the other treatment groups. Taurine-conjugated secondary bile acids were not altered that much, but Glycine-conjugated ones were significantly downregulated. In these treatment groups, Taurine conjugation of reabsorbed secondary bile acids did not show a prominent influence whereas, a downregulation in Glycine conjugated secondary bile acids have been observed in both feces and plasma, which is consistent with what we have observed in other antibiotic treatments.

Table 6. Fold changes of different bile acid levels going up (red boxes) and down (blue boxes) in the feces and plasma matrices of male and female Wistar rats of Streptomycin sulfate treatment (*p*-value depends on the shade of the colors, the darkest red is *p*-value <0.01, medium red is *p* value <0.05 and the lightest shade of red is *p*-value <0.10, and similarly for blue). F represents females, M represents males, 7 d, 14 d and 28 d denote blood sampling time points days 7, 14 and 28, respectively.

Metabolite Name	Analyte Name	Feces		Plasma					
		F	M	F 7d	M 7d	F 14d	M 14d	F 28d	M 28d
Cholate	CA	8.33	3.68	0.49	0.97	0.14	0.71	0.01	0.24
Chenodeoxycholate (chenodeoxycholic acid)	CDCA	17.60	0.56	0.43	1.65	0.17	0.64	0.02	0.37
Deoxycholate (deoxycholic acid)	DCA	1.15	1.56	0.67	0.68	1.22	0.62	0.15	0.31
Glycocholate, glycocholic acid	GCA	1.14	0.29	3.56	0.72	0.58	1.53	0.35	0.26
Glycochenodeoxycholate (glycochenodeoxycholic acid)	GCDCA	0.61	0.70	1.28	0.93	0.98	0.41	0.10	0.31
Glycodeoxycholate, -cholic acid	GDCA	0.39	0.21	1.54	1.02	0.49	0.23	0.05	0.10
Glycolithocholic acid	GLCA	0.35	1.41	0.46	0.27	0.23	0.39	0.25	0.80
Glycoursodeoxycholic acid	GUDCA	0.89	0.50	1.65	0.61	1.00	1.06	1.24	0.89
Hyodeoxycholate, hyodeoxycholic acid	HDCA	0.20	0.04	0.18	0.25	0.34	0.03	0.01	0.03
Lithocholate, lithocholic acid	LCA	0.35	0.89	0.68	0.39	0.67	0.69	0.35	0.43
Muricholic acid (alpha)	MCAa	2.95	2.43	0.45	1.03	0.42	1.11	0.04	0.32
Muricholic acid (beta)	MCAb	1.07	2.79	1.89	1.81	0.77	1.89	0.53	0.87
Muricholic acid (omega)	MCAo	2.11	1.77	2.17	1.46	2.51	3.19	0.36	0.78
Taurocholate, taurocholic acid	TCA	2.07	1.13	1.73	2.97	2.05	4.50	3.28	2.67
Taurochenodeoxycholate	TCDCa	1.17	1.15	1.22	1.35	2.61	2.54	2.33	2.72
taurodeoxycholate, -cholic acid	TDCA	2.25	0.62	1.66	1.62	2.13	1.68	1.38	1.48
Tauroolithocholic acid	TLCA	0.60	1.68	1.11	0.83	1.05	0.66	0.38	0.47
Tauromuricholic acid (a+b)	TMCA(a+b)	1.86	1.79	1.60	2.44	2.59	3.01	2.64	2.64
Tauroursodeoxycholic acid	TUDCA	1.79	1.04	2.83			1.98		0.63
ursodeoxycholate, ursodeoxycholic acid, ursodiol	UDCA			1.65	0.16	0.20	1.60	0.17	0.39

5. Conclusions

The purpose of the study was to investigate if there are correlations between the microbiome, the fecal metabolome and the host's plasma metabolome. We have clearly demonstrated (1) a close connection between the microbiome and the fecal metabolome. We also noted that (2) the correlation between the fecal and plasma metabolome is much weaker. Moreover, (3) the best correlations between microbiome, fecal and plasma metabolome were obtained for bile acids. In addition, this study provides an extensive set of data for various antibiotic treatments on the gut microbiome and the fecal metabolome. However, the number of all possible combinations (the total of variables) between the microbiome and the metabolome by far exceeds the number of experiments with antibiotics. Therefore, in most cases, a perfect resolution (bacterial species to fecal metabolites) of these observed correlations is not (yet) possible. Overall, we see a huge impact of antibiotic treatments on bacterial deconjugation from primary to secondary and tertiary BA in both plasma and feces. Taurine conjugation is, relative to glycine conjugation, the preferred pathway in all antibiotic treatment groups. Taurine-conjugated primary BAs were readily reabsorbed in the gut and show elevated levels in the plasma. CA levels in the feces were profoundly increased in all treatment groups, except for Roxithromycin, and reduced in the plasma.

This is considered to be related to the loss of 7 α dehydroxylase activity and the lack of reabsorption of CA from the lower intestinal track. The reduced levels of CA in the Roxithromycin group are correlated with a unique increase of the *Rikenellaceae* family. All antibiotics resulted in increased levels of conjugated bile acids, indicating that they inhibit deconjugation reactions. Streptomycin, which induces the least feces microbiome/caecum changes, also causes only very minor accumulation of TMCA only. Bile acids make natural and xenobiotic compounds more bioavailable and hence increase absorption from the gut. An alteration of the bile acid pool is likely to lead to altered plasma concentrations of both endogenous metabolites as well as xenobiotics. Furthermore, bile acids themselves interact with nuclear receptors, such as FXR, PXR, CAR, VDR and TGR5, and alteration in the bile acid pool can be expected to have an effect on gene activation [16,21]. This may impact the cytochrome P450 expression and could interfere with drug detoxification mechanisms, finally leading to either a detoxification or toxification of a compound of interest. Furthermore, unconjugated BAs are in general important for controlling the microbial population and the integrity of the intestinal barrier function [16,21]. Regarding the points mentioned above, changes in the bile acid pool might have implications for affecting the intestinal microbiome itself, the gut-liver axis, the immune system and other systems of the body.

Each individual treatment group in this study elicited perturbations in the gut bacterial composition, as observed in the community analysis. Treatments showed a class-specific influence in the bacterial community composition. Clustering analysis of the fecal metabolome showed a virtual identical antibiotic-specific grouping as seen with the 16S microbiome analysis, (see Figure 7a and Supplementary Figure S2), demonstrating that these two matrixes are highly correlated. Plasma metabolome showed a rather different clustering, indicating that fecal metabolome changes are not well correlated with plasma metabolome changes. Dietary restriction did not induce gut dysbiosis and showed only marginal influences on the fecal metabolome. In contrast, rather explicit effects were seen on the plasma metabolome. Thus, the reduction of dietary nourishment (20% reduced diet) has only very limited effects in the intestinal tract (microbiome and fecal metabolome), whereas the plasma metabolome is profoundly different. Here, we also noted significant gender-specific changes or adaptations. The main purpose behind adding this group of animals fed with a restricted diet was to understand its possible effects on the microbiome and consequently on the metabolome, and it provided rather interesting findings.

Further, cecal and fecal metabolomes are highly comparable; therefore, in rats, fecal profiling should be preferred over cecum, as it is as informative and non-invasive. The strongest correlations obtained were between 16S bacterial families and fecal metabolites, that mainly belong to amino acids, lipids and related metabolite classes.

Key findings from this research work include the following. 1) Administration of different classes of antibiotics showed different compositional effects on the rat fecal microbiome, also showing a class-dependent effect. 2) Streptomycin sulfate and restricted diet showed the most comparable microbiota

compared to the rest of the treatments. 3) Compared to plasma metabolome, feces metabolome showed a clear antibiotic-treatment-specific separation, whereas restricted diet separated clearly in the clustering analysis of plasma metabolome, thereby highlighting the fact that dietary restriction changes the host metabolism without significantly altering the gut microbiota. 4) We conclude that the plasma metabolome responds entirely differently to antibiotic treatment compared to both feces and cecum metabolome, for which various correlations with the microbiome could be established. 5) We highlighted several metabolites like Indole derivatives and bile acids as being associated with the presence/absence of specific bacterial families. 6) We associated the accumulation of taurine conjugated bile acids and lack of secondary bile acid formation with antibiotic treatments. The least effective antibiotic was Streptomycin sulfate, which is in line with its antibiotic mode of action. The correlations obtained in this study act as a holistic collection for all the possible bacterial correlations with fecal/plasma metabolites, involving not only already known ones but also some novel or unexplored ones too. Many of these correlations just hint towards a potential relationship, since there are multiple bacterial strains involved in specific biological functions, so it is not just a simple one-to-one correlation, as currently analyzed. Further steps would involve direct network construction using a larger dataset that would explain the correlations in more detail, understanding further the inter-bacterial co-metabolic capacities, which would give a deeper insight into gut microbial metabolism. Understanding the underlying signaling cascades and the gene expression data would give us deeper knowledge about the gut microbiota and host-associated metabolism. An additional step in the future could be to have a use-case with the 16S, metabolome and metagenome data of different samples from animals treated with different substances that are known to perturb the gut microbiota and eventually their associated biological functions. The importance of advancing the field of microbiome-mediated metabolism and the formation of small molecules is not only of academic interest; most of the safety studies with biologically active ingredients and chemicals are done using the rat as the golden standard system. Differences in toxicity outcomes between humans and rats are frequently considered to be related to toxico-dynamic differences, particularly if liver metabolism in both species is assumed to be similar. However, the contribution of the gut microbiome to metabolism, and the potential species differences, have so far been largely ignored. Thus, a database containing the connection between bacterial composition and metabolic capacity for rats would need to be complemented by a similar connectivity for humans. It is of interest to note that despite the profound microbiome and fecal metabolome changes induced by the antibiotics, the effects on the plasma metabolome are rather limited. This, in combination with the mild or absent clinical signs of toxicity, would suggest that at least from a short-term perspective, even profound microbiome changes do not immediately affect its host's health. However, such microbiome changes may indeed interfere with the metabolic capacity of its host and could very well change, for instance, the intestinal metabolism of drugs when co-administered in a situation of microbiome dysbiosis. Overall, a combination of 16S bacterial community

analysis along with metabolome profiling could allow us to unravel the influence of antibiotics on the gut bacterial composition and metabolism.

Supplementary Materials: The following are available online at <https://www.mdpi.com/2036-7481/12/1/8/s1>, Figure S1: Shannon Evenness for all the treatments including both sexes and dose groups, Figure S2: Hierarchical clustering (HCA) analysis of 16S gene sequencing data, Figure S3: Relative abundance analysis of bacterial families for individual animals, Figure S4: Principle Component Analysis (PCA) of feces metabolites from different treatments, Figure S5: Dendrogram showing hierarchical clustering of cecum metabolites of different treatments, dose groups and sex, Figure S6: Principle Component Analysis (PCA) of cecum metabolites from different treatments, Figure S7: Principle Component Analysis (PCA) of plasma metabolites from different treatments, Figure S8: Boxplots comparing between different metabolome matrices, Figure S9: Shannon true diversity analysis of six antibiotic treatments focused for both male and female Wistar rats; Table S1: Relative changes in body weight and food consumption of male and female rats, Tables S2-S8: Top 25 (both directions) of plasma altered metabolites ($p < 0.1$) for both females and males respectively for restricted diet, Streptomycin sulfate, Roxithromycin, Sparfloxacin, Vancomycin, Clindamycin and Lincomycin hydrochloride respectively, Tables S9-S15: Feces altered metabolites ($p < 0.1$) for both females (left) and males (right) respectively for restricted diet, Streptomycin sulfate, Roxithromycin, Sparfloxacin, Vancomycin, Clindamycin and Lincomycin hydrochloride respectively, Table S16: The table below shows DESeq2 analysis results from the low dose (LD) groups of all the treatments, Table S17: : Fold changes of different bile acid levels in the feces and plasma matrices of male and female Wistar rats of Lincomycin hydrochloride treatment.

Author Contributions: A.M. is the main author who wrote this manuscript and conducted the data evaluation and discussion of the results obtained. V.G. also conducted the evaluation, mainly using statistics and visualization methods. H.J.C was solely responsible for the bioinformatics part of the work along with visualization of the data. C.B. also performed data evaluation and was the person responsible for conceptualization of the work. S.S. and H.K. were both responsible for data emulation and reviewing and for editing the manuscript draft. T.W. and his group were responsible for the analytics and measurements for methodology and data curation. B.v.R. performed the conceptualization of the project and reviewed the manuscript. He is the corresponding author and the supervisor of the work.

Funding: This research received no external funding.

Institutional Review Board Statement: The studies were approved by the BASF Animal Welfare Body, with the permission of the local authority, the Landesuntersuchungsamt Rheinland-Pfalz (approval number 23 177-07/G 13-3-016). The studies were performed in an AAALAC-approved

(Association for Assessment and Accreditation of Laboratory Animal Care International) laboratory in accordance with the German Animal Welfare Act and the effective European Council Directive.

Data Availability Statement: All data are stored under GLP or GLP-like archives at BASF SE, Ludwigshafen am Rhein, Germany. Metabolome data are stored in MetaMapTox database, BASF.

Acknowledgments: We cordially like to thank all the technical assistance from the animal facility technicians headed by Burkhard Flick, Irmgard Weber and the technicians from the lab of Clinical chemistry at BASF and analytics laboratories for their incredible work and support. This work was also intensively reviewed by Ivonne Rietjens and would like to thank her and the the University of Wageningen & Research for great interactive scientific discussions. We thank the discussion panel from the Metabolome team at the Experimental Toxicology Department in BASF and the group of BMS Berlin GmbH.

Conflicts of Interest: Authors declare no conflict of interest.

References

1. Li, D.; Chen, H.; Mao, B.; Yang, Q.; Zhao, J.; Gu, Z.; Zhang, H.; Chen, Y.Q.; Chen, W. Microbial Biogeography and Core Microbiota of the Rat Digestive Tract. *Sci. Rep.* **2017**, *7*, 45840, doi:10.1038/srep45840.
2. Gill, S.R.; Pop, M.; DeBoy, R.T.; Eckburg, P.B.; Turnbaugh, P.J.; Samuel, B.S.; Gordon, J.I.; Relman, D.A.; Fraser-Liggett, C.M.; Nelson, K.E. Metagenomic Analysis of the Human Distal Gut Microbiome. *Science* **2006**, *312*, 1355–1359, doi:10.1126/science.1124234.
3. Sender, R.; Fuchs, S.; Milo, R. Revised Estimates for the Number of Human and Bacteria Cells in the Body. *PLoS Biol.* **2016**, *14*, e1002533, doi:10.1371/journal.pbio.1002533.
4. Zimmermann, M.; Zimmermann-Kogadeeva, M.; Wegmann, R.; Goodman, A.L. Mapping human microbiome drug metabolism by gut bacteria and their genes. *Nat. Cell Biol.* **2019**, *570*, 462–467, doi:10.1038/s41586-019-1291-3.
5. Clarke, G.; Sandhu, K.V.; Griffin, B.T.; Dinan, T.G.; Cryan, J.F.; Hyland, N.P. Gut Reactions: Breaking Down Xenobiotic–Microbiome Interactions. *Pharmacol. Rev.* **2019**, *71*, 198–224, doi:10.1124/pr.118.015768.
6. ECETOC. *Microbiome Expert Workshop Report* (Porto, 8–9 July 2019); 2078-7219-036; ECETOC: Brussels, Belgium, 2020.
7. Bourassa, M.W.; Alim, I.; Bultman, S.J.; Ratan, R.R. Butyrate, neuroepigenetics and the gut microbiome: Can a high fiber diet improve brain health? *Neurosci. Lett.* **2016**, *625*, 56–63, doi:10.1016/j.neulet.2016.02.009.
8. Maier, L.; Pruteanu, M.; Kuhn, M.; Zeller, G.; Telzerow, A.; Anderson, E.E.; Brochado, A.R.; Fernandez, K.C.; Dose, H.; Mori, H.; et al. Extensive impact of non-antibiotic drugs on human gut bacteria. *Nat. Cell Biol.* **2018**, *555*, 623–628, doi:10.1038/nature25979.
9. Nicholson, J.K.; Holmes, E.; Kinross, J.; Burcelin, R.; Gibson, G.; Jia, W.; Pettersson, S. Host-Gut Microbiota Metabolic Interactions. *Science* **2012**, *336*, 1262–1267, doi:10.1126/science.1223813.
10. Zheng, H.; Chen, M.; Li, Y.; Wang, Y.; Wei, L.; Liao, Z.; Wang, M.; Ma, F.; Liao, Q.; Xie, Z. Modulation of Gut Microbiome Composition and Function in Experimental Colitis Treated with Sulfasalazine. *Front. Microbiol.* **2017**, *8*, 1703, doi:10.3389/fmicb.2017.01703.
11. Ghaisas, S.; Maher, J.; Kanthasamy, A. Gut microbiome in health and disease: Linking the microbiome–gut–brain axis and environmental factors in the pathogenesis of systemic and neurodegenerative diseases. *Pharmacol. Ther.* **2016**, *158*, 52–62, doi:10.1016/j.pharmthera.2015.11.012.
12. Ridaura, V.K.; Faith, J.J.; Rey, F.E.; Cheng, J.; Duncan, A.E.; Kau, A.L.; Griffin, N.W.; Lombard, V.; Henrissat, B.; Bain, J.R.; et al. Gut Microbiota from Twins Discordant for Obesity Modulate Metabolism in Mice. *Science* **2013**, *341*, 1241214, doi:10.1126/science.1241214.
13. Anders, M. Metabolism of drugs by the kidney. *Kidney Int.* **1980**, *18*, 636–647, doi:10.1038/ki.1980.181.
14. Behr, C.; Kamp, H.; Fabian, E.; Krennrich, G.; Mellert, W.; Peter, E.; Strauss, V.; Walk, T.; Rietjens, I.M.C.M.; Van Ravenzwaay, B. Gut microbiome-related metabolic changes in plasma of antibiotic-treated rats. *Arch. Toxicol.* **2017**, *91*, 3439–3454, doi:10.1007/s00204-017-1949-2.
15. Behr, C.; Ramirez-Hincapié, S.; Cameron, H.; Strauss, V.; Walk, T.; Herold, M.; Beekmann, K.; Rietjens, I.; Van Ravenzwaay, B. Impact of lincosamides antibiotics on the composition of the rat gut microbiota and the metabolite profile of plasma and feces. *Toxicol. Lett.* **2018**, *296*, 139–151, doi:10.1016/j.toxlet.2018.08.002.
16. Behr, C.; Slopianka, M.; Haake, V.; Strauss, V.; Sperber, S.; Kamp, H.; Walk, T.; Beekmann, K.; Rietjens, I.; Van Ravenzwaay, B. Analysis of metabolome changes in the bile acid pool in feces and plasma of antibiotic-treated rats. *Toxicol. Appl. Pharmacol.* **2019**, *363*, 79–87, doi:10.1016/j.taap.2018.11.012.
17. Behr, C.; Sperber, S.; Jiang, X.; Strauss, V.; Kamp, H.; Walk, T.; Herold, M.; Beekmann, K.; Rietjens, I.; van Ravenzwaay, B. Microbiome-related metabolite changes in gut tissue, cecum content and feces of rats treated with antibiotics. *Toxicol. Appl. Pharmacol.* **2018**, *355*, 198–210, doi:10.1016/j.taap.2018.06.028.
18. Van Ravenzwaay, B.; Herold, M.; Kamp, H.; Kapp, M.; Fabian, E.; Looser, R.; Krennrich, G.; Mellert, W.; Prokoudine, A.; Strauss, V.; et al. Metabolomics: A tool for early detection of toxicological effects and an opportunity for biology based grouping of chemicals—From QSAR to QBAR. *Mutat. Res. Toxicol. Environ. Mutagen.* **2012**, *746*, 144–150, doi:10.1016/j.mrgentox.2012.01.006.

19. van Ravenzwaay, B.; Sperber, S.; Lemke, O.; Fabian, E.; Faulhammer, F.; Kamp, H.; Mellert, W.; Strauss, V.; Strigun, A.; Peter, E.; et al. Metabolomics as read-across tool: A case study with phenoxy herbicides. *Regul. Toxicol. Pharmacol.* **2016**, *81*, 288–304, doi:10.1016/j.yrtph.2016.09.013.
20. Van Ravenzwaay, B.; Cunha, G.C.-P.; Leibold, E.; Looser, R.; Mellert, W.; Prokoudine, A.; Walk, T.; Wiemer, J. The use of metabolomics for the discovery of new biomarkers of effect. *Toxicol. Lett.* **2007**, *172*, 21–28, doi:10.1016/j.toxlet.2007.05.021.
21. De Bruijn, V.; Behr, C.; Sperber, S.; Walk, T.; Ternes, P.; Slopianka, M.; Haake, V.; Beekmann, K.; Van Ravenzwaay, B. Antibiotic-Induced Changes in Microbiome-Related Metabolites and Bile Acids in Rat Plasma. *Metabolites* **2020**, *10*, 242, doi:10.3390/metabo10060242.
22. R Core Team. *R: A Language and Environment for Statistical Computing*; R Core Team: Vienna, Austria, 2020.
23. RStudio Team. *RStudio: Integrated Development Environment for R*; RStudio: Boston, MA, USA, 2020.
24. Troyanskaya, O.G.; Cantor, M.; Sherlock, G.; Brown, P.O.; Hastie, T.; Tibshirani, R.; Botstein, D.; Altman, R.B. Missing value estimation methods for DNA microarrays. *Bioinformatics* **2001**, *17*, 520–525, doi:10.1093/bioinformatics/17.6.520.
25. Callahan, B.J.; McMurdie, P.J.; Rosen, M.J.; Han, A.W.; Johnson, A.J.A.; Holmes, S.P. DADA2: High-resolution sample inference from Illumina amplicon data. *Nat. Methods* **2016**, *13*, 581–583, doi:10.1038/nmeth.3869.
26. Martin, M. Cutadapt removes adapter sequences from high-throughput sequencing reads. *EMBnet J.* **2011**, *17*, 10–12, doi:10.14806/ej.17.1.200.
27. Cole, J.R.; Wang, Q.; Fish, J.A.; Chai, B.; McGarrell, D.M.; Sun, Y.; Brown, C.T.; Porras-Alfaro, A.; Kuske, C.R.; Tiedje, J.M. Ribosomal Database Project: Data and tools for high throughput rRNA analysis. *Nucleic Acids Res.* **2014**, *42*, D633–D642, doi:10.1093/nar/gkt1244.
28. Love, M.I.; Huber, W.; Anders, S. Moderated estimation of fold change and dispersion for RNA-seq data with DESeq2. *Genome Biol.* **2014**, *15*, 550, doi:10.1186/s13059-014-0550-8.
29. McMurdie, P.J.; Holmes, S. PHYLOSEQ: A Bioconductor Package for Handling and Analysis of High-Throughput Phylogenetic Sequence Data. *Biocomputing 2001* **2011**, 235–246, doi:10.1142/9789814366496_0023.
30. Paulson, J.N.; Stine, O.C.; Bravo, H.C.; Pop, M. Differential abundance analysis for microbial marker-gene surveys. *Nat. Methods* **2013**, *10*, 1200–1202, doi:10.1038/nmeth.2658.
31. Oksanen, J.; Blanchet, F.G.; Kindt, R.; Legendre, P.; Minchin, P.R., O'Hara, R. *Package 'Vegan'. Community Ecology Package, Version 2*; R Core Team: Vienna, Austria, 2013.
32. Liu, C.M.; Bs, K.S.; Nordstrom, L.; Dwan, M.G.; Moss, O.L.; Contente-Cuomo, T.L.; Keim, P.; Price, L.B.; Lane, A.P.; Bs, M.G.D.; et al. Medical therapy reduces microbiota diversity and evenness in surgically recalcitrant chronic rhinosinusitis. *Int. Forum Allergy Rhinol.* **2013**, *3*, 775–781, doi:10.1002/alar.21195.
33. Fraumene, C.; Manghina, V.; Cadoni, E.; Marongiu, F.; Abbondio, M.; Serra, M.; Palomba, A.; Tanca, A.; Laconi, E.; Uzzau, S. Caloric restriction promotes rapid expansion and long-lasting increase of *Lactobacillus* in the rat fecal microbiota. *Gut Microbes* **2017**, *9*, 104–114, doi:10.1080/19490976.2017.1371894.
34. Verdier, L.; Bertho, G.; Gharbi-Benarous, J.; Girault, J.-P. Lincomycin and clindamycin conformations. A fragment shared by macrolides, ketolides and lincosamides determined from TRNOE ribosome-bound conformations. *Bioorganic Med. Chem.* **2000**, *8*, 1225–1243, doi:10.1016/s0968-0896(00)00081-x.
35. Zhou, G.; An, Z.; Zhao, W.; Hong, Y.; Xin, H.; Ning, X.; Wang, J. Sex differences in outcomes after stroke among patients with low total cholesterol levels: A large hospital-based prospective study. *Biol. Sex Differ.* **2016**, *7*, 62, doi:10.1186/s13293-016-0109-3.
36. Kim, Y.S.; Unno, T.; Kim, B.-Y.; Park, M.-S. Sex Differences in Gut Microbiota. *World J. Men's Health* **2020**, *38*, 48–60, doi:10.5534/wjmh.190009.
37. Wishart, D.S. DrugBank: A comprehensive resource for in silico drug discovery and exploration. *Nucleic Acids Res.* **2006**, *34*, D668–D672, doi:10.1093/nar/gkj067.
38. Bao, H.-D.; Pang, M.-D.; Olaniran, A.; Zhang, X.-H.; Zhang, H.; Zhou, Y.; Sun, L.-C.; Schmidt, S.; Wang, R. Alterations in the diversity and composition of mice gut microbiota by lytic or temperate gut phage treatment. *Appl. Microbiol. Biotechnol.* **2018**, *102*, 10219–10230, doi:10.1007/s00253-018-9378-6.

39. Zhang, C.; Li, X.; Liu, L.; Gao, L.; Ou, S.; Luo, J.; Peng, X. Roxithromycin regulates intestinal microbiota and alters colonic epithelial gene expression. *Appl. Microbiol. Biotechnol.* **2018**, *102*, 9303–9316, doi:10.1007/s00253-018-9257-1.
40. Zheng, X.; Wang, S.; Jia, W. Calorie restriction and its impact on gut microbial composition and global metabolism. *Front. Med.* **2018**, *12*, 634–644, doi:10.1007/s11684-018-0670-8.
41. Zeng, H.; Grapov, D.; Jackson, M.L.; Fahrman, J.F.; Fiehn, O.; Combs, G.F. Integrating Multiple Analytical Datasets to Compare Metabolite Profiles of Mouse Colonic-Cecal Contents and Feces. *Metabolites* **2015**, *5*, 489–501, doi:10.3390/metabo5030489.
42. Nannes, C.E.; Waas, J.R.; Ling, N.; Nakagawa, S.; Banks, J.C.; Bell, D.G.; Bright, A.; Carey, P.W.; Chandler, J.; Hudson, Q.J.; et al. Comparing plasma and faecal measures of steroid hormones in Adelie penguins *Pygoscelis adeliae*. *J. Comp. Physiol. B* **2009**, *180*, 83–94, doi:10.1007/s00360-009-0390-0.
43. Fujisaka, S.; Avila-Pacheco, J.; Soto, M.; Kostic, A.; Dreyfuss, J.M.; Pan, H.; Ussar, S.; Altindis, E.; Li, N.; Bry, L.; et al. Diet, Genetics, and the Gut Microbiome Drive Dynamic Changes in Plasma Metabolites. *Cell Rep.* **2018**, *22*, 3072–3086, doi:10.1016/j.celrep.2018.02.060.
44. Goldstein, E.J.; Citron, D.M.; Gerardo, S.H.; Hudspeth, M.; Merriam, C.V. Comparative in vitro activities of DU-6859a, levofloxacin, ofloxacin, sparfloxacin, and ciprofloxacin against 387 aerobic and anaerobic bite wound isolates. *Antimicrob. Agents Chemother.* **1997**, *41*, 1193–1195, doi:10.1128/aac.41.5.1193.
45. Bahar, H.; Torun, M.M.; Demirci, M.; Kocazeybek, B. Antimicrobial Resistance and β -Lactamase Production of Clinical Isolates of *Prevotella* and *Porphyromonas* Species. *Chemotherapy* **2005**, *51*, 9–14, doi:10.1159/000084017.
46. Dai, Z.-L. Amino acid metabolism in intestinal bacteria: Links between gut ecology and host health. *Front. Biosci.* **2011**, *16*, 1768–1786, doi:10.2741/3820.
47. Alkhalaf, L.M.; Ryan, K.S. Biosynthetic Manipulation of Tryptophan in Bacteria: Pathways and Mechanisms. *Chem. Biol.* **2015**, *22*, 317–328, doi:10.1016/j.chembiol.2015.02.005.
48. Rikitake, K.; Oka, I.; Ando, M.; Yoshimoto, T.; Tsuru, D. Creatinine Amidohydrolase (Creatininase) from *Pseudomonas putida*: ePurification and Some Properties. *J. Biochem.* **1979**, *86*, 1109–1117, doi:10.1093/oxfordjournals.jbchem.a132605.
49. Idris, E.E.; Iglesias, D.J.; Talon, M.; Borriss, R. Tryptophan-Dependent Production of Indole-3-Acetic Acid (IAA) Affects Level of Plant Growth Promotion by *Bacillus amyloliquefaciens* FZB42. *Mol. Plant-Microbe Interact.* **2007**, *20*, 619–626, doi:10.1094/mpmi-20-6-0619.
50. Sanguinetti, E.; Collado, M.C.; Marrachelli, V.G.; Monleon, D.; Selma-Royo, M.; Pardo-Tendero, M.M.; Burchielli, S.; Iozzo, P. Microbiome-metabolome signatures in mice genetically prone to develop dementia, fed a normal or fatty diet. *Sci. Rep.* **2018**, *8*, 1–13, doi:10.1038/s41598-018-23261-1.
51. Apper, E.; Privet, L.; Taminiau, B.; Le Bourgot, C.; Svilar, L.; Martin, J.-C.; Diez, M. Relationships between Gut Microbiota, Metabolome, Body Weight, and Glucose Homeostasis of Obese Dogs Fed with Diets Differing in Prebiotic and Protein Content. *Microorganisms* **2020**, *8*, 513, doi:10.3390/microorganisms8040513.
52. Steinway, S.N.; Biggs, M.B.; Jr., T.P.L.; Papin, J.A.; Albert, R. Inference of Network Dynamics and Metabolic Interactions in the Gut Microbiome. *PLoS Comput. Biol.* **2015**, *11*, e1004338, doi:10.1371/journal.pcbi.1004338.
53. Zhao, Z.-H.; Xin, F.-Z.; Xue, Y.; Hu, Z.; Han, Y.; Ma, F.; Zhou, D.; Liu, X.-L.; Cui, A.; Liu, Z.; et al. Indole-3-propionic acid inhibits gut dysbiosis and endotoxin leakage to attenuate steatohepatitis in rats. *Exp. Mol. Med.* **2019**, *51*, 1–14, doi:10.1038/s12276-019-0304-5.
54. Louis, P.; Flint, H.J. Formation of propionate and butyrate by the human colonic microbiota. *Environ. Microbiol.* **2017**, *19*, 29–41, doi:10.1111/1462-2920.13589.
55. Jazani, N.H.; Savoj, J.; Lustgarten, M.; Lau, W.L.; Vaziri, N.D. Impact of Gut Dysbiosis on Neurohormonal Pathways in Chronic Kidney Disease. *Diseases* **2019**, *7*, 21, doi:10.3390/diseases7010021.
56. Zheng, X.; Xie, G.; Zhao, A.; Zhao, L.; Yao, C.; Chiu, N.H.L.; Zhou, Z.; Bao, Y.; Jia, W.; Nicholson, J.K.; et al. The Footprints of Gut Microbial–Mammalian Co-Metabolism. *J. Proteome Res.* **2011**, *10*, 5512–5522, doi:10.1021/pr2007945.
57. Wahlström, A.; Sayin, S.I.; Marschall, H.-U.; Bäckhed, F. Intestinal Crosstalk between Bile Acids and Microbiota and Its Impact on Host Metabolism. *Cell Metab.* **2016**, *24*, 41–50, doi:10.1016/j.cmet.2016.05.005.

58. Martin, F.J.; Dumas, M.; Wang, Y.; Legido-Quigley, C.; Yap, I.K.S.; Tang, H.; Zirah, S.; Murphy, G.M.; Cloarec, O.; Lindon, J.C.; et al. A top-down systems biology view of microbiome-mammalian metabolic interactions in a mouse model. *Mol. Syst. Biol.* **2007**, *3*, 112, doi:10.1038/msb4100153.
59. Di Ciaula, A.; Garruti, G.; Baccetto, R.L.; Molina-Molina, E.; Bonfrate, L.; Wang, D.Q.-H.; Portincasa, P. Bile Acid Physiology. *Ann. Hepatol.* **2017**, *16*, S4–S14, doi:10.5604/01.3001.0010.5493.
60. Li, J.; Dawson, P.A. Animal models to study bile acid metabolism. *Biochim. Biophys. Acta (BBA)-Mol. Basis Dis.* **2019**, *1865*, 895–911, doi:10.1016/j.bbadis.2018.05.011.





CHAPTER 3:

CONNECTING GUT MICROBIAL DIVERSITY WITH PLASMA METABOLOME AND FECAL BILE ACID CHANGES INDUCED BY THE ANTIBIOTICS TOBRAMYCIN AND COLISTIN SULFATE

Aishwarya Murali, Varun Giri, Franziska Maria Zickgraf, Philipp Ternes, Hunter James Cameron, Saskia Sperber, Volker Haake, Peter Driemert, Hennicke Kamp, Dorothee Funk-Weyer, Shana J. Sturla, Ivonne M.C.M. Rietjens, Bennard van Ravenzwaay

Published in: *Chemical Research in Toxicology* 36 (2023), 598–616

Connecting gut microbial diversity with plasma metabolome and fecal bile acid changes induced by the antibiotics tobramycin and colistin sulfate

1. Abstract

The diversity of microbial species in the gut has a strong influence on health and development of the host. Further, there are indications that the variation in expression of gut bacterial metabolic enzymes is less diverse than the taxonomic profile, underlying the importance of microbiome functionality, particularly from a toxicological perspective. To address these relationships, the gut bacterial composition of Wistar rats was altered by a 28-day oral treatment with the antibiotics tobramycin or colistin sulfate. On the basis of 16S marker gene sequencing data, tobramycin was found to cause a strong reduction in the diversity and relative abundance of the microbiome, whereas colistin sulfate had only a marginal impact. Associated plasma and fecal metabolomes were characterized by targeted mass spectrometry-based profiling. The fecal metabolome of tobramycin-treated animals had a high number of significant alterations in metabolite levels compared to controls, particularly in amino acids, lipids, bile acids, carbohydrates and energy metabolites. The accumulation of primary bile acids and significant reduction of secondary bile acids in the feces indicated that the microbial alterations induced by tobramycin inhibit bacterial deconjugation reactions. The plasma metabolome showed less, but still many alterations in the same metabolite groups, including reductions in indole derivatives and hippuric acid, and furthermore, despite marginal effects of colistin sulfate treatment, there were nonetheless also systemic alterations in bile acids. Aside from these treatment-based differences, we also uncovered inter-individual differences particularly centering on the loss of *Verrucomicrobiaceae* in the microbiome, but with no apparent associated metabolite alterations. Finally, by comparing the dataset from this study with metabolome alterations in the MetaMapTox® database, key metabolite alterations were identified as plasma biomarkers indicative of altered gut microbiomes resulting from a wide activity spectrum of antibiotics.

2. Keywords

Metabolomics, gut microbiome, tobramycin, colistin sulfate, 16S data analysis, repeated dose oral study

3. Introduction

Gut microbiota are vital to host metabolism and consequently for host health and disease¹. Bacteria in the gastrointestinal tract (GIT) outnumber eukaryotes and archaea by 2–3 orders of magnitude, and they produce thousands of metabolites that influence host homeostasis and health². The bacterial composition of the GIT, as determined by 16S amplicon sequencing, is altered in various diseases such as colon cancer, ulcerative colitis, Crohn's disease, Alzheimer's disease, obesity, and diabetes^{3, 4, 5}. Moreover, the microbiome appears to be required for producing 71% of fecal and 15% of blood metabolites, as supported by comparative metabolomes of colonized vs germ-free (GF) animals⁶.

Finally, when examining the fecal metabolomes of twins, Zierer *et al.*, 2018 demonstrated only a modest influence of host genetics on metabolome characteristics⁵.

The gut microbiota is intrinsically highly variable and can be altered by environmental factors, such as diet and use of antibiotics^{7, 8}. Animal and human studies have also revealed that antibiotics are associated with health risks such as diarrhea, colitis, cholestasis, various other gastrointestinal disorders and multiple other off-target effects^{9 10 11}. Further, prolonged exposures of humans and animals to some broad-spectrum antibiotics are also known to induce organ-specific toxicity such as nephrotoxicity, ototoxicity and others^{12 13}. Apart from that, extensive use of antibiotics in humans and/or food-producing animals also lead to acquired resistance^{14 15}.

The intestinal microbiota performs several essential functions including fermentation of indigestible food components, synthesis of important vitamins, amino acids, secondary (2°) bile acids and short-chain fatty acids (SCFAs), elimination of toxic compounds, regulation of the immune system, production of mucosal L-ornithine, and many others^{7, 16}. Furthermore, gut bacteria produce 2° bile acid (BA) metabolites from primary (1°) BAs via bacterial deconjugation and dehydroxylation reactions¹⁷. It is important to define, therefore, how diet and drug-induced alterations in gut microbiota can lead to functional outcomes via altered metabolites and the physiological processes they regulate.

The metabolic capabilities of gut microbes are a basis of the functional crosstalk between the gut microbiota and the host and can be addressed by large scale quantification of dynamic changes in microbial metabolites as an informative complement to community profiling (or taxonomics) analysis. Thus, about 250 blood plasma and about 600 fecal metabolites can be measured via targeted metabolomics analysis of in non-invasive biospecimens such as urine and feces, as well as i.e. blood, cecum content, or gut sections of the intestines of experimental animals¹⁸⁻²⁰. Analytes include amino acids, bile acids, carbohydrates, lipids, vitamins, hormones, energy metabolites, nucleobases and their derivatives. Thus, while metabolomics data reveal a functional basis for host phenotypes⁵ it is not possible to well predict how shifts in gut microbial diversity translate to altered metabolite profiles.

Several factors can perturb the gut microbiota, such as the use of antibiotics²¹, and they are well known to functionally alter the gut microbiota²². Antibiotics are broadly classified on the basis of their activity spectrum or mode of action. For example, aminoglycosides are broad spectrum antibiotics active against Gram-negative bacteria, including *Enterobacteriaceae*, *Escherichia coli*, *Klebsiella pneumoniae*, *Pseudomonas aeruginosa* and many others. In addition to Gram-negatives, aminoglycosides are also active against some Gram-positive bacteria such as *Staphylococcus* spp., including methicillin-resistant (MRSA) and vancomycin-resistant strains, *Streptococcus* spp., and *Mycobacterium* spp.²³. They are generally not absorbed from the gut and function by inhibiting protein synthesis by binding 16S rRNA near the A site of the 30S ribosomal subunit, and also bind to bacterial membranes, such as lipopolysaccharides and phospholipids within the outer membrane of Gram-negative bacteria and to

teichoic acid and phospholipids within the cell membrane of Gram-positive bacteria²⁴. Tobramycin, an aminoglycoside derived from the actinomycete *Streptomyces tenebrarius*, has poor bioavailability with 90% being eliminated and only about 10% becoming systemically bioavailable²⁵. Colistin sulfate is a polymyxin antibiotic that penetrates into and disrupts the bacterial cell membrane through a detergent-like mechanism. The bioavailability of colistin is very low as it was very poorly absorbed after oral administration according to the summary report published on colistin by the Committee for veterinary medicinal products. Low bioavailability of the administered antibiotics is important because if antibiotics are absorbed from the gut, they have a strong influence on host metabolism and, consequently, the metabolomes^{20, 26, 27}.

To better understand the relationship between shifts in gut microbiota families and the consequent effects on metabolite profiles either in the fecal metabolome or in systemic circulation, we used the aminoglycoside antibiotic tobramycin, and the Polymyxin E antibiotic colistin sulfate to perturb the gut composition of male and female Wistar rats in a 28-day oral study. Microbial alterations were characterized by quantitative taxonomic 16S profiling of the fecal microbiome. To connect changes in the microbiome with changes in the fecal and plasma metabolome^{28, 29}. Blood plasma was sampled on days 7, 14 and 28 of the study and feces were sampled on day 28 of the study and profiled by targeted LC-MS/MS-based metabolomics. Alterations in several metabolite classes, including amino acids, carbohydrates, fatty acids, bile acids, energy metabolites and their derivatives, were measured following treatment with a high versus low dose of each drug.

4. Materials and methods

The 28-day oral study with Wistar rats was carried out based on the OECD 407 Principles of Good Laboratory Practice and the GLP provisions of the German Chemicals Act.

4.1. Ethical statement

The animal study was performed in an AAALAC-approved (Association for Assessment and Accreditation of Laboratory Animal Care International) laboratory in compliance with the German Animal Welfare Act and the effective European Council Directive. The study was approved by the BASF Animal Welfare Body, with the permission of the local authority, the Landesuntersuchungsamt Koblenz, Germany (approval number 23 177-07/G 18-3-098).

4.2 Animals and maintenance conditions

Male and female Wistar rats (CrI:WI(Han)) of the age group 70 ± 1 days were supplied by Charles River, Germany, before the beginning of the planned study. The rats (5 per sex and cage, per treatment group) were acclimatized for a week, in an air-conditioned room at a temperature of 20–24 °C, a relative humidity level of 30–70%, and a 12 h light / 12 h dark cycle. The lights were turned off from 6 PM to 6 AM and the animals were sacrificed on day 28 of the study between 7AM to 9AM. Ground Kliba

mouse/rat maintenance diet “GLP” by Provimi Kliba SA, Kaiseraugst, Switzerland, was supplied for the feeding throughout the course of the study. Diet and drinking water were available *ad libitum* (except 16–20 hours before sampling. In order to reduce any variation based on the diet consumption and as a standard procedure used in clinical chemistry and metabolomics, the animals were fasted overnight before the sample collection. Diet and drinking water were regularly assessed for chemical contaminants and the presence of microorganisms.

4.3 Treatment of animals with drugs

Tobramycin or colistin sulfate were administered daily by gavage to five rats per treatment group per sex (see Figure 1). The selected doses of the antibiotics were such that they were expected to induce gut dysbiosis. The high doses were selected to be as high as possible without inducing systemic toxicity and the low doses were ten times lower than the high doses^{30 31, 32 32}. The high dose was never above 1,000 mg/kg bw as this is the limit dose for oral administration according to OECD guidelines. Because there were no indications in the literature of toxicity, tobramycin was prepared in deionized water for oral administration at doses of 100 mg/kg body weight/day and 1000 mg/kg body weight/day respectively. For colistin sulfate, literature indicated that, oral administration in Wistar rats with 1000 mg/kg bw/day dose, resulted in significant changes in organ weights and hence a No-observed-effect level (NOEL) was established to be 200 mg/kg bw, furthermore, in a 90-day rat day, an oral dose of up to 60 mg/kg bw/d of colistin had no adverse effects. Whereas, in Sprague-Dawley rats, significant changes in organ weights were observed at a dose of 120 mg/kg bw/day and hence a NOEL was established at 40 mg/kg bw/day³³. Hence, in our study a high dose of colistin sulfate of 100 mg/kg bw/day and a ten times lower low dose of 10 mg/kg bw/day, were selected. An antibiotic suspension (10 ml/kg bw/day) was administered to five rats per treatment group per dose group for each sex, with a concurrent control group of 10 animals per sex.

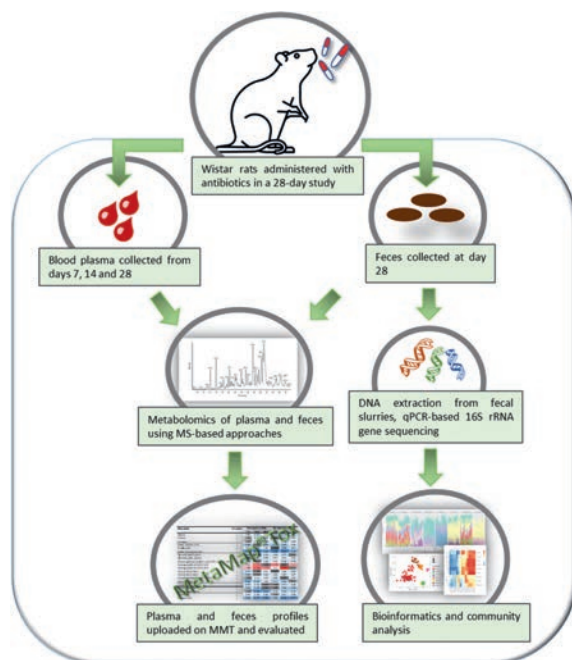


Figure 1: Schematic representation of the study design for plasma and fecal metabolite profiling and the corresponding 16S bacterial community analysis of 28-day orally administered antibiotic-treated male and female Wistar rats. MMT refers to the in-house database MetaMapTox® that consists of toxicity data of more than 1000 different compounds and is extensively used for metabolome data analyses.

4.4 Clinical examination

All the animals were checked daily for any signs of clinical signs, abnormal macroscopic findings, and mortalities. Standard operating procedures as described in the Organization for Economic Co-operation and Development (OECD) 407 guidelines were used for all clinical- and pathological examinations. Parameters including food consumption and body weights were determined before the start of the treatment administration period, in order to randomize the animals, and further on the study days 6, 13 and 27. Food consumption was measured by weighing the food at the start of the experiment and after 24h, and by calculating the difference between the weights of the rats before and after the 24 h period.

4.5 Blood and fecal sampling for metabolite profiling

On days 7, 14 and 28, after a fasting period of 16-20 hours, blood samples were collected between 7:30AM and 10:30AM from the retro-orbital sinus of all the rats (including controls and all treatment groups) under isoflurane anesthesia (1.0 ml K-EDTA blood). Blood samples were subjected to centrifugation (10 °C, 2000 x g, 10 min) and the EDTA plasma was separated. These EDTA plasma samples were then snap-frozen with N₂ and stored at -80 °C until metabolite profiling was performed. Feces were carefully retrieved from the rectum after gentle massaging, and when no feces were present, samples were then scraped from the colon during necropsy on day 28 after a fasting period of 16-20

hours. The samples were collected in pre-cooled (dry-ice) vials, snap-frozen in liquid nitrogen and stored at -80°C until further processing for fecal dry weight measurements, DNA isolation, 16S gene PCR amplification and sequencing.

4.6 DNA extraction and 16S rRNA amplicon sequencing

Dry weights of stored fecal samples from all controls and antibiotic-treated rats were measured, transferred to labeled pre-cooled (dry-ice) DNA/RNA Shield-Lysis collection tubes (BIOZOL Diagnostica Vertrieb GmbH, Eching, Germany) avoiding excess thawing of the frozen fecal pellets. Fecal slurries kept on dry ice and their measured weight details were sent to IMG^M® laboratories (Martinsried, Germany) for DNA isolation, amplicon-based 16S rRNA gene sequencing plus an additional qPCR assay for bacterial gDNA load quantification using an Illumina MiSeq sequencing platform. DNA isolation from the fecal slurries was conducted using the QIAamp Fast DNA Stool Mini Kit (Qiagen) followed by quantification with Qubit (ThermoFisher). In brief, 1 μl of each sample was used to determine the dsDNA concentration ($\text{ng}/\mu\text{l}$) in comparison to a given standard provided with the kit. The DNA concentration was determined by creating a linear trend line and applying the mathematical equation of linear regression by IMG^M® laboratories. DNA was amplified using universal primer pair 341F/805R of the V3-V4 region of the 16S gene. An aliquot of each final PCR product including the positive and negative controls was run on a 2% agarose gel (Midori Green-stained) to analyze the quality of the generated amplicons and to evaluate the expected amplicon size. Next Generation Sequencing (NGS) was performed on the Illumina MiSeq® next generation sequencing system (Illumina Inc.) resulting in 250bp paired end reads with a minimum of 10,000 reads per sample. An additional bacterial DNA quantification analysis was carried out by amplification using qRT-PCR analysis by the VII7 System. The produced raw data were processed, de-multiplexed and went to QC for final report generation. The final report was then used for further bioinformatic analyses.

4.7 Metabolite profiling of plasma and feces matrices

Mass spectrometry-based metabolite profiling of blood plasma was performed by extracting metabolites from 60 μl rat plasma by adding 1500 μl extraction buffer (methanol, dichloromethane, water and toluene (93:47:16,5:1, v/v) buffered with ammonium acetate) using a ball mill (Bead Ruptor Biolab). Internal standards were added to the extraction mixture. After centrifugation, ($15294 \times g$, 10min, 12°C) a 100 μl aliquot of the extract was subjected to LC-MS/MS. Thus, 2.5 μl of the extract were injected each for reversed-phase and hydrophilic interaction liquid chromatography (ZIC - HILIC, 2.1 x 10mm, 3.5 μm , Supelco) followed by MS/MS detection (AB Sciex QTrap 6500+) using the positive and negative ionization mode. For reverse-phase high performance liquid chromatography (RP-HPLC, Ascentis Express C18, 5cm x 2.1mm, 2,7 μm Supelco), gradient elution was performed with water/methanol/0.1 M ammonium formate (1:1:0.02 w/w) and methyl-tert-butylether/2-

propanol/methanol/0.1M ammonium formate (2:1:0.5:0.035 w/w) with 0.5% (w%) formic acid (0 min-100% A, 0.5 min 75% A, 5.9 min 10% A, 600 µl/min). HILIC gradient elution was performed with (C) acetonitrile/water (99:1, v/v) and 0.2 (v%) acetic acid and (D) 0.007 M ammonium acetate with 0.2 (v%) acetic acid (0_min 100% C, 5 min 10% C, 600 µl/min).

A second aliquot of the extract was mixed with water (3,75:1, v/v) resulting in a phase separation. The polar (upper phase, 400 µl) and lipid (lower phase, 90 µl) were used for GC analysis. Both phases were analyzed with gas chromatography-mass spectrometry (GC7890-5975 MSD, Agilent Technologies) after derivatization as described in Green *et al.*³⁴. Briefly, the non-polar fraction was treated with methanol under acidic conditions (that is, 1mol/l HCl) to produce fatty acid methyl esters that were derived from both free fatty acids and hydrolysed complex lipids. The polar and non-polar fractions were further derivatized with *O*-methyl-hydroxylamine hydrochloride to convert oxo-groups to *O*-methyloximes, and subsequently with a silylating agent (N-methyl-N-(trimethylsilyl) trifluoroacetamide). For GC analysis, 0.5 µl of the derivatized phase-separated extract were used each for analysis of the polar and lipid fractions. BAs analysis approach was based on a kit from Biocrates³⁵.

All samples were analyzed once in a randomized analytical sequence design to avoid artificial results with respect to analytical shifts. For GC-MS and LC-MS/MS profiling, data were normalized to the median of reference samples which were derived from a pool formed from aliquots of all samples to account for inter- and intra-instrumental variation. In plasma, 272 semiquantitative metabolites could be analyzed using the single peak signal of the respective metabolite and a normalization strategy according to the patent WO2007012643A1³⁶ resulting in ratio values representing the metabolite changes in treated versus control animals³⁷. Of these 272 metabolites, the chemical structures of 246 were identified and 26 remained unknown.

Similarly, the stored fecal samples were subjected to a freeze-drying process. The product temperature and the vapor pressure at the beginning of the freeze-drying process were -40 °C and 0.120 mbar respectively changing to +30 °C and 0.01 mbar for a total running time of 42 h. About 10 mg of freeze-dried rat feces were used from the controls and different antibiotic-treated animals for extraction with 1400 µl of a mixture of methanol and dichloromethane (2:1, v/v) with formic acid (0.6 v%) including a stainless-steel ball for homogenization with a ball mill (Bead Ruptor Biolab). After centrifugation (15294 × g for 10 min @12°C, an aliquot of the extract was subjected to LC-MS/MS analysis as described above for the plasma metabolite analyses. As with the GC-MS method applied for plasma samples, 750 µl of the polar (upper phase) and 90 µl of lipid (lower phase) were used for GC analysis. The same LC-MS/MS method used to analyze fecal samples was used for plasma matrix. In feces, 632 semiquantitative metabolites could be analyzed, of which the chemical structures of 348 were identified and 284 were unknown.

4.8 16S data processing

A standardized in-house 16S marker gene sequencing data processing using DADA2 algorithm was used as described previously in Murali *et al.*, 2021²⁸. The customized workflow involved data quality control (QC), primer removal, denoising, taxonomy assignments using the RDP classifier and creation of a phylogenetic tree. Forward and reverse primers were trimmed from the raw reads using cutadapt software. As paired-end reads were to be used for further analysis, the reads were merged to about 415 bp length. The QC step involved checking the read lengths and the quality of the joined reads. Taxonomy was assigned to the individual Amplicon Sequence Variants (ASVs) using the Naïve Bayesian classifier implemented in DADA2 with the RDP database. This resulted in the output of a BIOM table with all the information regarding the sequences and abundances of ASVs and the assigned taxa information²⁸.

4.9 Statistical analysis of microbiome data

Post-processing of the 16S marker gene data was performed for bacterial community analysis in R software using the RAM and Phyloseq packages³⁸, as described previously in Murali *et al.*, 2021²⁸. The processed data were checked for completeness, and empty rows were removed. The BIOM table contained 501535 reads belonging to 26552 ASVs from 57 samples. The raw reads were used for alpha diversity analysis using the group.diversity function in the RAM package. As a part of data clean-up, amplicon sequence variants (ASVs) or reads that did not have taxonomic assignment up to the family level were removed. Further, ASVs with non-zero counts in at least two samples were retained, and the others were removed, resulting in 436521 reads belonging to 970 ASVs. These filtered data were used for relative abundance analysis. Stacked bars were plotted using RAM package to determine the relative bacterial abundances in the different antibiotic-treated rats. Count normalization of the dataset was done to the sum of counts per sample. The filtered and normalized data were used for beta diversity analysis. Principle Coordinate Analysis (PCoA) was carried out using Bray-Curtis distances²⁸. Differential abundance analysis was performed on the filtered ASV counts using the R package DESeq2³⁹. PCoA plots with Hotelling's ellipses were drawn with the ggplot::stats_ellipse function with default settings modified from Fox *et al.*, 2011⁴⁰.

4.10 Statistical analysis of metabolome data

Analysis of the metabolite data was performed by uni- and multivariate statistical methods. A sex and day-stratified heteroscedastic t-test (Welch test) was applied to compare the levels of different metabolites from different doses of antibiotics relative to controls for both plasma and feces matrices. Relative fold changes for all the metabolites were calculated as the ratio of the medians of metabolite levels in individual animals per treatment group to the medians of metabolite levels in individual corresponding control animals (for each sampling time point, dose level and sex). These ratios are referred to as relative fold change levels. Computational work was conducted using standardized scripts.

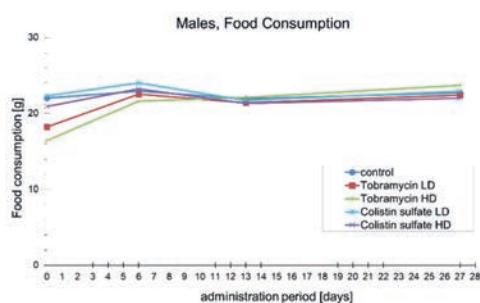
Finally, the relative fold change values, p- and t-values of metabolites were uploaded as metabolite profiles and made available on the in-house database MetaMapTox® (or MMT)⁴¹⁻⁴³. For the multivariate analysis of these profiles, the data were log-transformed, centered, and scaled by unit variance for each metabolite and then used for Principal Component Analysis (PCA). Any missing data present were imputed using the nearest neighbor method implemented in function `impute.knn` from the R package `impute`²⁸. PCA analysis was performed in R Statistical software²⁸. Treatment related effects were evaluated on MMT using the standardized procedure of comparing resulting metabolite levels of different antibiotics against the control group⁴².

5. Results

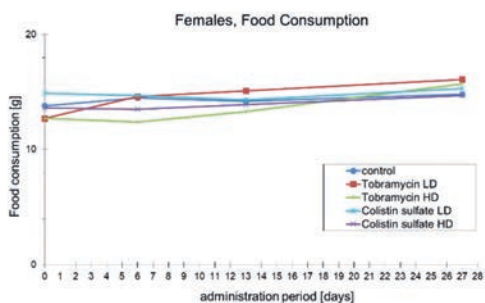
5.1 Body weight and food consumption is not largely altered by tobramycin or colistin sulfate

Tobramycin was orally administered at doses of 100 mg/kg body weight/day (LD) and 1000 mg/kg body weight/day (HD) and the doses selected for colistin sulfate for oral administration was 10 mg/kg body weight/day (LD) and 100 mg/kg body/day weight (HD) respectively. No mortalities were noted in any of the treatment groups. The male animals which received the HD of tobramycin showed clinical toxicity, that is, soft feces, whereas no clinical signs of toxicity were observed for the animals treated with colistin sulfate. All animals treated with tobramycin HD showed also a discoloration in the kidneys at necropsy. Body weight development and food consumption were not affected by any treatment except for the tobramycin HD group in which a reduced BW gain (not significant) of male rats at day 13 was observed (Figure 2, Table S1).

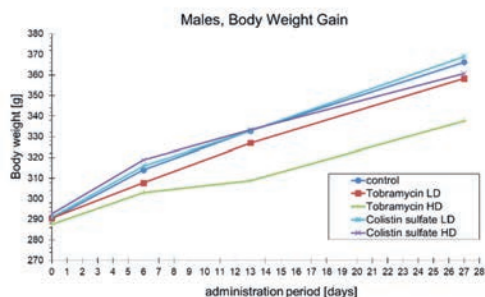
(A)



(B)



(C)



(D)

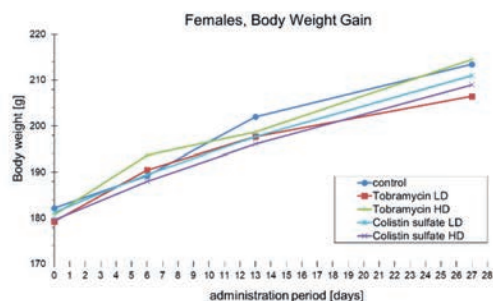


Figure 2: Plots representing food consumption (in grams) and body weight (in grams) of the controls and different antibiotics treatment groups on days 0, 6, 13 and 27, in male (A, C) and female (B, D) animals, respectively. Changes in body weight and food consumption could be compared with control group and baseline values at day 0. The differences were not statistically significant. LD means low dose and HD means high dose groups.

5.2 Tobramycin, but not colistin sulfate, induces large shifts in bacterial communities

Shannon true diversity of the fecal microbiota of samples from the different antibiotic treatments was compared to controls for both dose groups and sexes (see Figure 3). Shannon true diversity indicates the diversity of different bacterial taxa present in a specific treatment, as a key index reflecting the species richness of a particular ecosystem²⁸. The alpha diversity in the control groups in both male and female rats were similar. However, a reduction in the variability in the samples of the tobramycin groups was noted, except for the LD group in female animals. Dose-dependent differences were marginal and less apparent in the colistin- vs tobramycin-treated animals.

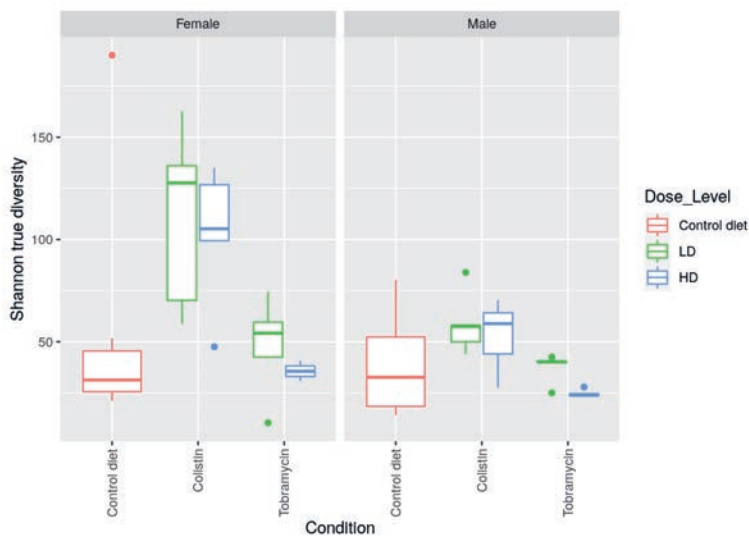


Figure 3: Shannon true diversity analysis of tobramycin and colistin sulfate treatments for both male and female Wistar rats. The colors show different dose groups, where blue refers to the high (HD), green to the low dose (LD) and red refers to the control diet group.

Having established alterations in the microbial communities of the individual samples by alpha diversity analysis, we probed the diversity changes from one environment (treatment) to another by beta diversity analysis using a rank-based Principal Coordinate Analysis (PCoA) using a non-phylogenetic distance matrix called Bray-Curtis distance. By comparing the non-phylogenetic distance-based rank PCoA analyses of the bacterial taxa present in samples from controls and antibiotic treatments, we observed a clear separation of the tobramycin treatment group from control (Figure 4). While the colistin group separated in a dose-dependent manner from the control cluster on Principal component 1 (PC1), the separation was weak compared to the tobramycin treatment. These observations are consistent with the broad-spectrum activity of tobramycin. PCoA plots with Hotelling ellipses for both males and females separately show a clear separation between the groups (see Figure S5).

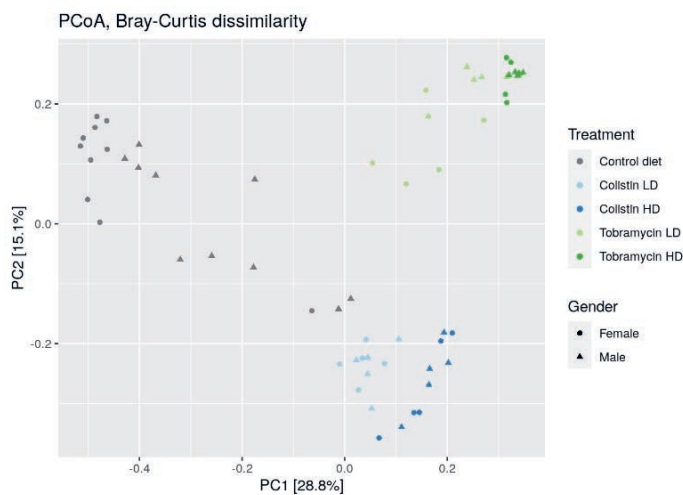


Figure 4: Principal Coordinate Analysis (PCoA) of bacterial families from controls and different antibiotic treatments using Rank-based clustering with Bray–Curtis distance matrix. Dark grey points indicate samples from controls, while samples from tobramycin high (HD) and low (LD) dose groups are indicated in dark and light green, respectively and those from colistin HD and LD are indicated in dark and light blue colors, respectively, where dots represent samples from female rats and triangles from males.

By relative abundance analysis, we analyzed the distribution of major microbial taxa in each community and identified variations for both antibiotic treatments (Figure 5). For tobramycin, consistent with the alpha diversity analysis, the bacterial families were significantly different than controls whereby *Lachnospiraceae*, *Porphyromonadaceae*, *Prevotellaceae*, *Bacteroidaceae* and *Erysipelotrichaceae* were present in all cases, and females treated with LD tobramycin exceptionally included also *Ruminococcaceae*. To understand in more detail the specific bacterial taxa associated with the treatment that were either significantly abundant or rare, we also performed a differential abundance analysis using the DESeq2 package. As evident from Log2FC (log2 fold change) values for bacterial families (Figures 6A and 6B), there were clear changes in specific bacterial families after tobramycin treatment. These were consistent for both dose levels and were characterized by a substantial reduction in

Anaeroplasmataceae and *Peptococcaceae* and an increase in *Prevotellaceae* and *Erysipelotrichaceae*. Slight reductions in *Ruminococceae* and *Rikenellaceae* could also be observed in samples from both the dose groups of tobramycin-treated male and female rats.

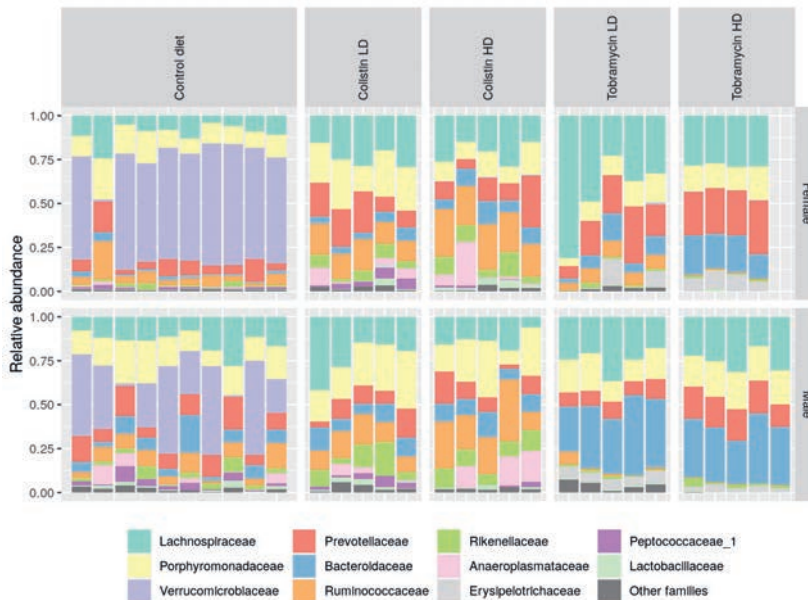


Figure 5: Relative abundance stack bar plot of bacterial families that were detected in samples from controls and all antibiotic treatment groups. Inter-individual variability in the 16S bacterial abundances can be easily observed. Clear antibiotic-specific effects were observed on the intestinal community composition. Most individual control animals had higher levels of *Verrucomicrobiaceae* family, whereas these were absent in one female and two male control animals out a total of twenty control animals. LD means low dose and HD means high dose groups.

For colistin, results were similar to controls, however there was a pronounced exception: Most individual control animals had higher levels of *Verrucomicrobiaceae* family bacteria, whereas these were absent in the colistin treatment groups. *Verrucomicrobiaceae* were also absent in one female and two male control animals out a total of twenty control animals. Furthermore, relative abundance analysis of a much larger sample size with data that was not used in this publication (Figure S1) suggests highly irregular and unexplainable occurrences of *Verrucomicrobiaceae* families in certain fecal samples from controls and antibiotic-treated animals. In the differential abundance analysis (Figure 6A), this consistent treatment-associated reduction of the *Verrucomicrobiaceae* family was pronounced, with an almost 2.3-fold (or ca. 60%) reduction on average. Notably for the tobramycin-treated animals, there also was a significant reduction in the *Verrucomicrobiaceae* family however this significant reduction was in addition to several reductions in the abundances of other previously mentioned bacterial families. Finally, in contrast to males, samples from females treated with HD or LD colistin had slightly increased numbers of *Anaeroplasmataceae*. Overall, the alterations in abundances of specific families of bacteria

were antibiotic-specific, influenced to some extent by drug concentrations and sex, and the *Verrucomicrobiaceae* was particularly sensitive to both drugs, but with large interindividual variability.

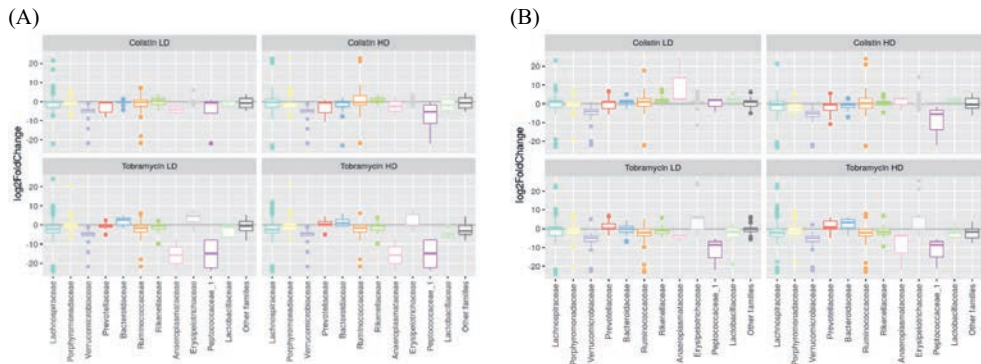


Figure 6: Differential abundances in dominant bacterial families in the low (LD) and high (HD) dose groups of tobramycin and colistin sulfate antibiotic treatments relative to controls in males (A) and females (B). Differential abundance analysis using log₂FC (log₂ fold change) values of bacterial families in samples from male and female rats of specific treatments relative to controls was performed

5.3 Tobramycin strongly alters fecal metabolomes

Given the significant changes observed by 16S compositional analysis of fecal samples for tobramycin but not colistin, we anticipated that metabolite profiles in the feces of tobramycin-treated animals would be extensive. Indeed, PCA plots of the fecal metabolome profiles of controls and antibiotic-treated groups indicated a strong separation of the tobramycin group from both control and colistin clusters for both sexes (Figures 7A and 7B). The PCAs provide a bird's eye perspective of the effects of the two antibiotics on fecal metabolomes for both dose levels and in both sexes. Clear effects of tobramycin were observed in the fecal metabolome. However, regarding colistin, the data points of the fecal metabolome overlap with the controls, indicative of a substantial similarity.

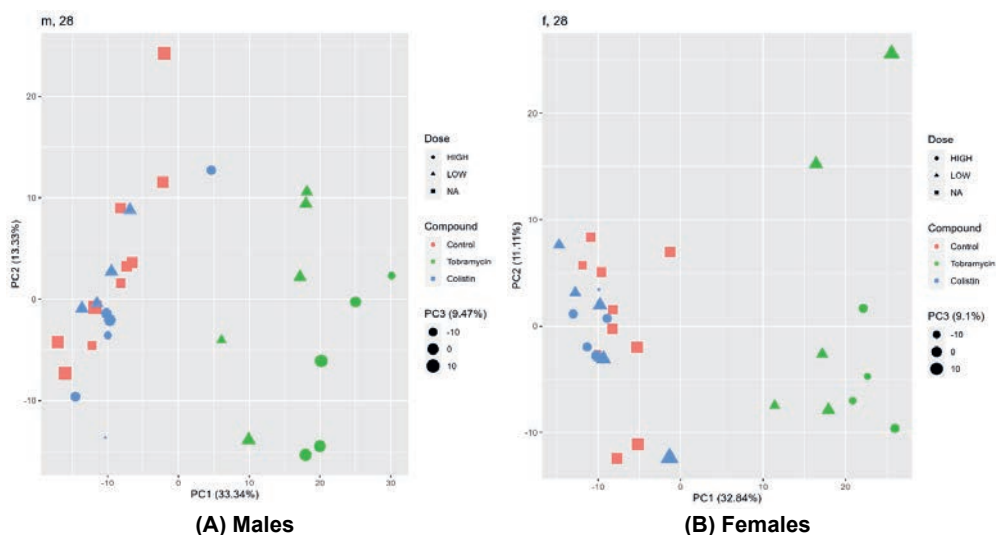


Figure 7: Principal component analysis (PCA) of the fecal metabolome profiles of controls and antibiotic treatments. PCA for male Wistar rats at day 28 of the study (A) and for females (B). The data points are sized by the PC3 value. PCAs were plotted with the feces metabolome data of controls (in red), colistin treatment (in blue) and tobramycin treatment (in green). The low dose groups of both the antibiotics are indicated by triangles and high dose groups by circles.

Out of 621 different fecal metabolites measured in the samples from control and antibiotic-treated groups at day 28 of the study, about 350 metabolites significantly changed upon tobramycin HD treatment in both sexes. This included metabolites predominantly belonging to amino acids and related class. Specific metabolites like taurine, succinate and creatinine show strong increase in tobramycin-treatment group compared to controls in both sexes (see Supplementary table S2).

5.4 Tobramycin causes significant changes in the fecal metabolites specifically the bile acids

Given the sheer amount of metabolite changes and because the effect of bile acid class was observed to be the strongest, here we focused on important metabolites strongly associated with the microbiome-related bile acids (BAs). However, we observed not only many BAs being changed following tobramycin treatment - 16 of 22 BAs in feces of tobramycin HD were significantly increased or decreased for the tobramycin-treated females of both dose groups (p value < 0.05). For the male rats treated with HD tobramycin, of 22 BAs measured from the feces, about 14 were significantly changed, irrespectively of the direction of change at p value < 0.05 (see Table 1B). Fecal 1° BAs including CA, CDCA, α - and β -MCA were significantly increased in both sexes (Table 1A and 1B). Further, an increase in the taurine conjugated 1° BAs could be seen whereas glycine conjugated 1° BA, GCA, were significantly decreased. On the other hand, 2° BAs including conjugated 2° BAs were consistently decreased in the feces of tobramycin-treated females. Further, the 2° BAs including the conjugated 2° BAs are consistently decreased in the feces of tobramycin treated animals in both sexes. Overall, the

fecal metabolome of tobramycin-treated animals appeared to have strongly and significantly changed compared to the control group, which included significant changes in the BAs.

Table 1: Tobramycin-induced bile acid metabolite level fold changes in feces of (A) female (f) and (B) male (m) Wistar rats.

(A)

		Tobramycin HD ^c	Tobramycin LD ^c
Metabolite	Class	f28	f28
α-Muricholic Acid (αMCA)	1° BA ^a	2.39	2.90
β-Muricholic Acid (βMCA)	1° BA	6.01	9.30
Chenodeoxycholic acid (CDCA)	1° BA	9.60	6.60
Cholic acid (CA)	1° BA	92.87	9.75
Glycocholic acid (GCA)	Glycine conjugated 1° BA	0.30	0.75
Tauro-β-muricholic Acid (TβMCA)	Taurine conjugated 1° BA	12.18	21.03
Taurochenodeoxycholate (TCDCA)	Taurine conjugated 1° BA	2.14	2.00
Taurocholic acid sodium salt (TCA)	Taurine conjugated 1° BA	6.12	4.15
Deoxycholic acid (DCA)	2° BA ^b	0.00	1.14
Hyodeoxycholic acid (HDCA)	2° BA	0.00	0.03
isoLCA	2° BA	0.02	0.38
Lithocholic acid (LCA)	2° BA	0.00	0.31
ω-Muricholic Acid (ωMCA)	2° BA	0.05	0.52
Glycolithocholic Acid (GLCA)	Glycine conjugated 2° BA	0.07	0.24
Taurodeoxycholate (TDCA)	Taurine conjugated 2° BA	0.14	24.07
Tauroolithocholic Acid (TLCA)	Taurine conjugated 2° BA	0.06	5.16
Cholesterol, total	Complex lipids, fatty acids and related	4.15	4.02

(B)

		Tobramycin HD ^a	Tobramycin LD ^a
Metabolite	Class	m28	m28
Cholic acid	1° BA	87.02	3.91
Chenodeoxycholic acid	1° BA	12.41	3.88
Taurocholic acid sodium salt	Taurine conjugated 1° BA	6.28	2.42
Tauro-β-muricholic Acid	Taurine conjugated 1° BA	4.39	11.88
Taurochenodeoxycholate	Taurine conjugated 1° BA	2.43	1.80
Deoxycholic acid	2° BA	0.00	1.24
Lithocholic acid	2° BA	0.00	0.56
Hyodeoxycholic acid	2° BA	0.00	0.02
ω-Muricholic Acid	2° BA	0.05	0.20
isoLCA	2° BA	0.02	0.41
Glycolithocholic Acid	Glycine conjugated 2° BA	0.27	0.63
Glycodeoxycholate	Glycine conjugated 2° BA	0.08	0.43
Tauroolithocholic Acid	Taurine conjugated 2° BA	0.19	12.09
Taurodeoxycholate	Taurine conjugated 2° BA	0.04	19.86
Cholesterol, total	Complex lipids, fatty acids and related	4.13	4.57

^a Wistar rats (N=5 per group) treated with tobramycin (100 (LD) and 1000 (HD) mg/kg bw/day) for 28 days (f28 or m28). Statistically significant changes (Welch-t-test; p value < 0.05) are shown in bold numbers where red boxes mean an increase in the respective fecal bile acids.

5.5 Colistin sulfate induces only marginal changes in the fecal metabolites including bile acids

Out of 621 fecal metabolites measured, the metabolite patterns of the colistin HD treated female, but not male, animals revealed significant changes in only about 10% of the metabolites, including amino acids, lipids, bile acids and related, compared to the control group. (see Table S3 for complete list). Amongst BAs, there were only three significant changes (Table 2, p value < 0.05) and the magnitude of change was minor compared to the tobramycin treatment group. Finally, there were not many altered fecal metabolites upon colistin treatment, which is consistent with the PCA analysis, and the notion that this antibiotic has a minimal effect on the fecal metabolome.

Table 2: Colistin sulfate-induced few bile acid metabolite level fold changes in feces of female (f) Wistar rats.

Metabolite	Class	Colistin HD ^a	Colistin LD ^a
		f28	f28
α-Muricholic Acid	1° BA	2.38	2.30
ω-Muricholic Acid	2° BA	2.37	2.37
Hyodeoxycholic acid	2° BA	0.18	0.46

^a Female Wistar rats (N=5 per group) treated with tobramycin (100 (LD) and 1000 (HD) mg/kg bw/day) for 28 days (f28). Statistically significant changes (Welch-t-test; p value < 0.05) are shown in bold numbers where red boxes mean an increase in the respective fecal bile acids.

5.6 Plasma metabolome analyses show clear effects of tobramycin treatment

To understand potential systemic influences of drug-induced microbiome shifts, plasma metabolome profiles were characterized using the same method as for the fecal metabolomes. Moreover, we could expand the evaluation to include temporal dynamics by sampling blood on days 7, 14 and 28 of the study. Thus, on analyzing the PCA plots of the plasma metabolome profiles (including plasma bile acids) of controls and antibiotic-treated groups (Figure 8A), we observed a strong separation of the tobramycin group in PC2 vs. PC3 from controls and colistin, however, this took time to develop and was evident at day 28 (Figures 8A and 8B) but not days 7 or 14 (Figure S4). The separation of the tobramycin group in PC1 vs. PC2 was not as clear as in PC2 vs. PC3, and for the colistin sulfate group there was simply nothing separated out (Figure S3). Therefore, consistent with the fecal metabolome data, tobramycin has a uniquely strong functional influence, compared to colistin, on the plasma metabolome.

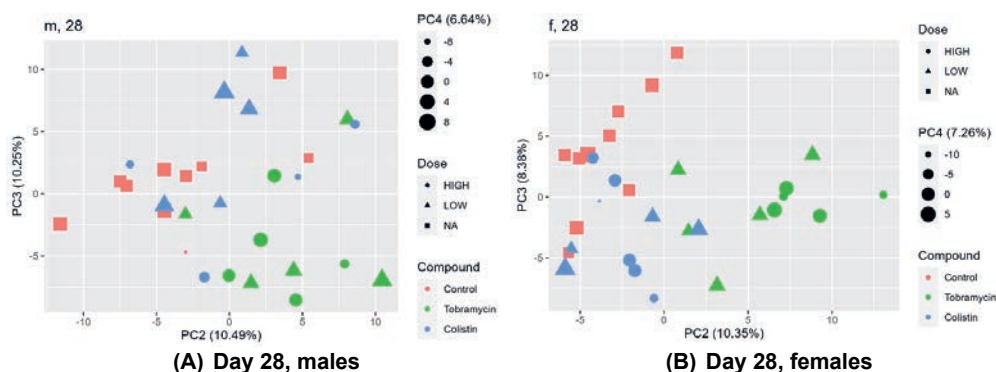


Figure 8: Principal component analysis (PCA) of the blood plasma metabolome profiles of controls and antibiotic treatments. The figure includes PCAs for samples from male Wistar rats (A) at day 28 of the study and PCAs for samples from female Wistar rats (B) at day 28 of the study. Principal component 2 (PC2) vs PC3 is shown here. The sample points are sized by the PC3 value. PCAs were plotted with the blood plasma metabolome data of controls (in red), colistin treatment (in blue) and tobramycin treatment (in green). The low dose groups of both the antibiotics are indicated by triangles and high dose groups by circles.

5.7 Tobramycin causes significant changes in the plasma metabolites including the key gut microbiome biomarkers and bile acids

Following the observation by PCA analysis of diverse plasma metabolite alterations in both tobramycin treatment groups, a more in-depth analysis of the most significantly changed (p value < 0.05) plasma metabolites including amino acids, carbohydrates, fatty acids, BAs and their derivatives was conducted (Tables 3(A) and (B)). Indole derivatives (indole-3-acetic acid, indole-3-propionic acid and 3-indoxylsulfate) and hippuric acid were significantly reduced by HD tobramycin (Table S5). These were established as key metabolites associated with a gut-dysbiosis in a previous study of lincosamide antibiotics administration, where the levels of these plasma metabolites were strongly and significantly reduced when compared to the samples from control animals in both sexes and dose groups²⁷. A higher number of different classes of plasma metabolites was changed in the tobramycin HD group of male rats than females. In males, too, a significant regulation in the key metabolites including indole-3-propionic acid and hippuric acid was noted (see Supplementary table S6).

Table 3: Tobramycin-induced blood plasma bile acid level fold changes of (A) female (f) and (B) male (m) Wistar rats.

(A)

Metabolite	Class	Tobramycin HD ^a			Tobramycin LD ^a		
		f7	f14	f28	f7	f14	f28
Glycocholic acid	Glycine conjugated 1° BA	0.91	0.34	0.35	1.35	0.32	0.62
Glycochenodeoxycholic acid	Glycine conjugated 1° BA	1.64	0.20	0.38	3.12	0.14	0.35
Tauro-β-muricholic Acid	Taurine conjugated 1° BA	2.60	1.77	1.62	1.16	1.42	1.20
Deoxycholic acid	2° BA	0.01	0.00	0.00	0.31	0.43	0.15
Lithocholic acid	2° BA	0.03	0.02	0.02	0.18	0.31	0.04
Hyodeoxycholic acid	2° BA	0.06	0.00	0.00	0.03	0.02	0.01

ω-Muricholic Acid	2° BA	0.21	0.01	0.00	0.39	0.16	0.16
isoLCA	2° BA	0.27	0.20	0.20	0.42	0.42	0.11
Glycolithocholic Acid	Glycine conjugated 2° BA	0.14	0.07	0.08	0.16	0.17	0.33
Glycodeoxycholate	Glycine conjugated 2° BA	0.06	0.03	0.04	1.12	0.30	0.20
Glycoursodeoxycholic Acid	Glycine conjugated 2° BA	2.37	0.71	1.94	3.08	1.35	1.32
Taurolithocholic Acid	Taurine conjugated 2° BA	0.01	0.02	0.01	0.18	0.19	0.23
Tauroursodeoxycholic Acid	Taurine conjugated 2° BA	1.74	14.18	9.57	1.49	5.09	2.12
Taurodeoxycholate	Taurine conjugated 2° BA	0.00	0.00	0.00	0.48	1.13	0.39

(B)

Metabolite	Class	Tobramycin HD ^a			Tobramycin LD ^a		
		m7	m14	m28	m7	m14	m28
α-Muricholic Acid	1° BA	0.19	0.13	0.30	0.42	0.47	0.12
Deoxycholic acid	2° BA	0.00	0.00	0.00	0.12	0.11	0.43
Lithocholic acid	2° BA	0.01	0.10	0.08	0.11	0.08	0.3
Hyodeoxycholic acid	2° BA	0.01	0.00	0.00	0.01	0.00	0.01
ω-Muricholic Acid	2° BA	0.15	0.03	0.00	0.08	0.01	0.03
isoLCA	2° BA	0.03	0.10	0.53	0.03	0.28	0.49
Glycodeoxycholate	Glycine conjugated 2° BA	0.00	0.00	0.00	0.31	0.19	0.09
Taurolithocholic Acid	Taurine conjugated 2° BA	0.01	0.02	0.08	0.03	0.06	0.42
Taurodeoxycholate	Taurine conjugated 2° BA	0.00	0.01	0.00	0.14	0.28	1.31

^a Metabolite fold changes in plasma bile acids of Wistar rats (N=5 per group) dosed with tobramycin (100 (LD) and 1000 (HD) mg/kg bw/day) for 7, 14 and 28 days (f7, f14 and f28 or m7, m14 and m28). Statistically significant changes (Welch-t-test; p-value < 0.05) are shown in bold numbers where red boxes mean an increase and yellow boxes mean a reduction in the respective plasma bile acids

Out of 22 BAs measured from the blood plasma of tobramycin HD treated female rats, 14 were significantly changed relative to controls (see Table 3A). A HD-specific response on the BAs could be observed in tobramycin-treated female rats, which showed a significant reduction in the 2° BAs including DCA, LCA, ωMCA reducing them to very low levels. A significant increase in taurine-conjugated primary BA including TBMCA could be observed. Glycine-conjugated 1° and 2° BAs also showed a significant reduction in the HD group in females. Overall, an accumulation of taurine-conjugated 1° BAs and a significant reduction in 2° BAs could be observed in the blood plasma of tobramycin-treated female rats.

Out of 22 measured plasma BAs from samples from tobramycin HD treated male rats, 9 showed significant alteration compared to controls (see Table 3B). Consistent to females, a significant reduction in the 2° BAs and conjugated 2° BAs including DCA, LCA, ωMCA and their conjugated forms could be observed. Additionally, taurine conjugated BAs are also significantly decreased, including TLCA and TDCA in males. However, unlike females, males did not have any significant changes in the plasma glycine conjugated BAs, except for GDCA, which is observed to be significantly decreased in tobramycin HD group in males. Overall, these changes in the plasma BAs showed a clear dose-response relationship.

5.8 Colistin sulfate induces only marginal changes in the plasma metabolites including bile acids

By in-depth analysis of significantly changed plasma metabolites resulting from treatment with colistin, amino acids, carbohydrates, fatty acids and related metabolites were evident for LD and HD treated animals, but nonetheless, the number of altered metabolites was lower in blood plasma than had been observed for the corresponding fecal metabolomes. The list of significantly changed metabolites also included one of the known key metabolites that are associated with an altered microbiota – Indole-3-acetic acid – that was observed to be significantly decreased compared to controls. Unlike tobramycin, not many (~ 10% significantly changed metabolites at p value < 0.05) plasma metabolites are strongly altered in the colistin-treated females (Table S7). 7 out of 22 measured plasma BAs from colistin HD treated female rats were significantly changed relative to controls (see Table 4A). A clear dose-dependent effect could be observed as in the LD group only one BA was changed at a single time point. The altered BAs exhibited significant reduction in the 7 and 14 colistin HD groups but at day 28, the effect was insignificant, except for Hyodeoxycholic acid, the most sensitive BA. Overall, the effect of this antibiotic on BA metabolism in female animals is weak compared to tobramycin and minimal antibiotic effects could be observed on the typical gut associated BA metabolites in females.

Table 4: Colistin-induced plasma bile acid level fold changes of (A) female (f) and (B) male (m) Wistar rats.

(A)

Metabolite	Class	Colistin HD ^a			Colistin LD ^a		
		f7	f14	f28	f7	f14	f28
α-Muricholic Acid	1° BA	0.27	0.19	1.17	0.39	0.91	1.37
Taurocholic acid sodium salt	Taurine conjugated 1° BA	2.33	2.09	1.23	0.82	1.09	0.93
Hyodeoxycholic acid	2° BA	0.20	0.04	0.14	0.33	0.45	0.53
Taurodeoxycholate	Taurine conjugated 2° BA	2.53	1.98	1.14	1.04	1.15	1.34

(B)

Metabolite	Class	Colistin HD ^a			Colistin LD ^a		
		m7	m14	m28	m7	m14	m28
ω-Muricholic Acid	2° BA	0.10	0.20	0.71	0.24	0.16	0.83

^a Metabolite fold changes in plasma bile acids of Wistar rats (N=5 per group) dosed with colistin (10 (LD) and 100 (HD) mg/kg bw/day) for 7, 14 and 28 days (f7, f14 and f28 or m7, m14 and m28). Statistically significant changes (Welch-t-test; p-value < 0.05) are shown in bold numbers where red boxes mean an increase and yellow boxes mean a reduction in the respective plasma bile acids.

On the other hand, the majority of the significantly changed metabolites in HD colistin-treated males belong to amino acids, carbohydrates, energy metabolism and related classes. None of the previously established key metabolites associated with antibiotic treatment were altered in the colistin-treated males unlike females (see Supplementary Table S8). In males treated with colistin HD, out of 22 measured plasma bile acids, only 1 BA, ωMCA (see Table 4B), was found to be significantly reduced

on days 7 and 14 of both doses, whereas the effect was not significant at day 28. Overall, only minimal effects on the BAs, if any, were observed in the colistin groups in both sexes.

5.9 Comparative analysis of fecal and plasma metabolome profiles

By comparing plasma vs fecal metabolome data, it was evident that for the fecal metabolome, there were strong metabolite alterations induced by especially tobramycin treatment, including a dose-response relationship (HD > 55% of all measured metabolites were significantly changed, LD ca. 38%, Table 5), but that these alterations were highly dampened in the plasma metabolome (Table 5). Moreover, despite the profound difference between in fecal metabolite profiles arising from tobramycin vs. colistin treatment, the plasma metabolites from both were quantitatively almost the same. The similarity in plasma metabolomes suggests that some systemic metabolic effects may arise independent of the microbiome.

Table 5: Percentages of total number of significantly changed metabolites in plasma (light blue) and feces (light orange) resulting from tobramycin treatment at (A) high (HD) or (B) low dose (LD) and from colistin treatment at (C) HD or (D) LD respectively.

(A)	Tobramycin HD, males*				Tobramycin HD, females*			
	Plasma			Feces	Plasma			Feces
	7d	14d	28d	28d	7d	14d	28d	28d
% of total sig. changed metabolites	16.55	27.03	15.2	55.95	21.28	22.63	13.85	58.04
(B)	Tobramycin LD, males*				Tobramycin LD, females*			
	Plasma			Feces	Plasma			Feces
	7d	14d	28d	28d	7d	14d	28d	28d
% of total sig. changed metabolites	13.85	15.54	9.12	39.71	16.89	14.53	13.18	37.14
(C)	Colistin sulfate HD, males*				Colistin sulfate HD, females*			
	Plasma			Feces	Plasma			Feces
	7d	14d	28d	28d	7d	14d	28d	28d
% of total sig. changed metabolites	17.9	19.26	7.43	9.65	9.46	15.2	10.13	10.29
(c)	Colistin sulfate LD, males*				Colistin sulfate LD, females*			
	Plasma			Feces	Plasma			Feces
	7d	14d	28d	28d	7d	14d	28d	28d
% of total sig. changed metabolites	16.22	10.13	5.74	10.93	12.5	9.46	8.45	10.29

*p value < 0.05

6 Discussion

We investigated how tobramycin and colistin sulfate, two antibiotics of different classes, alter the intestinal (fecal) microbiota community composition and how these changes are associated with changes in the fecal and plasma metabolomes of male and female Wistar rats in a 28-day oral study. Major findings of our research include the following: (1) Tobramycin altered gut composition and strongly reduced bacterial diversity. (2) Tobramycin significantly changed the fecal metabolome,

particularly the BAs, indicating reduced bacterial deconjugation and dehydroxylation reactions which potentially are a result of bacterial dysbiosis induced by the antibiotic. (3) Colistin had comparatively less influence on the gut composition, without clear changes in bacterial diversity. (4) Colistin had minimal effects on the fecal metabolome, suggesting no change in the gut. And (5) additionally, tobramycin, but not colistin, altered levels of plasma biomarkers known to be connected to microbiome shifts, such as hippuric acid and indole derivatives.

6.1 Microbiome analysis

The tobramycin-treated groups stood out from the colistin-treated groups in terms of alpha and beta diversity, demonstrating a reduction in the 16S bacterial diversity and indicating that the LD of tobramycin was already enough to substantively perturb the gut microbiota of male and female Wistar rats. All investigated phyla, except for families belonging to phyla Firmicutes (*Lachnospiraceae* and *Erysipelotrichaceae*) and Bacteroidetes (*Prevotellaceae* and *Bacteroidaceae*), were reduced by tobramycin, consistent with its broad-spectrum anti-bacterial activity against various Gram-negative and some Gram-positive bacteria²³. With colistin, on the other hand, there was higher bacterial diversity particularly in females. The increase is consistent with a previous report by Guo et al., who also observed higher diversity in the microbiota communities of samples from 30-day old piglets fed with basic diet supplemented with 20 g colistin sulfate per day. These data suggest colistin may induce expression of antibiotic resistance genes⁴⁴. Interestingly, only in one specific family was reduced by colistin, namely the *Verrucomicrobiaceae*. Moreover, Bray-Curtis based beta diversity analysis confirmed that the changes were related to this reduction of the *Verrucomicrobiaceae*. However, there was also *Verrucomicrobiaceae* family in selected control animals, suggesting potential high inter-individual differences, which has been reported previously also for rabbits⁴⁵. Finally, when *Verrucomicrobiaceae* was excluded from the relative abundance and alpha diversity analyses, it was apparent that for both classifiers, bacterial families in the samples from controls and colistin were similar, but the tobramycin groups were different (Figure 9).

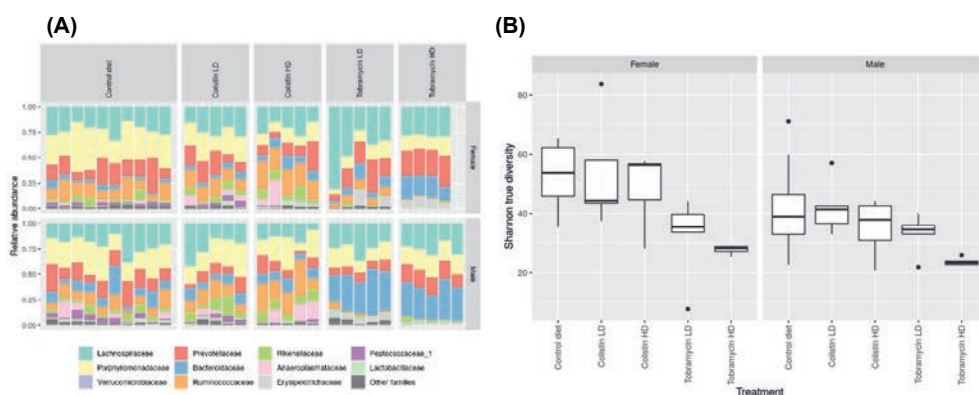


Figure 9: Stacked bar plot showing relative abundances of bacterial families excluding *Verrucomicrobiaceae* (A) and Alpha diversity plot (B) of samples from controls and all antibiotic groups. Tobramycin-specific effects were observed on the intestinal community composition. LD means low dose and HD means high dose groups.

6.2 Metabolome Analysis

6.2.1 Tobramycin treatment

The substantial effects of tobramycin on the gut composition are well reflected in fecal metabolome profiles, such that of 621 measured fecal metabolites, for the HD, about 56% and 58% of metabolites were significantly changed, and for the LD about 40% and 37% were changed for male or female rats, respectively, relative to control. Amongst these, we evaluated bile acids in detail as they have a well-known strong association with intestinal bacteria and well-characterized transformation relationships (Figure 10). Thus, 1° BAs (cholic acid, CA and chenodeoxycholic acid, CDCA) are synthesized in the liver from cholesterol and are conjugated with either taurine (T) or glycine (G), thereby gaining their amphiphilic properties, before they are further secreted into the bile and finally into the small intestine to promote lipid absorption^{46, 47}. BAs (about > 95%) are actively reabsorbed in the ileum while a minority manages to escape reabsorption, reaching the colon followed by excretion⁴⁷. When reaching the intestine, 1° BAs are further metabolized by unique microbial enzymes to unconjugated forms, 2° and 3° BAs acids (such as deoxycholate (DCA), tauro- and glycodeoxycholate (GDCA, TDCA), ω-muricholate (ω-MCA), hyodeoxycholate (HDCA), ursodeoxycholate (UDCA), tauro- and glyoursodeoxycholic acid (TUDCA, GUDCA), lithocholate (LCA), tauro- and glycolithocholic acid (TLCA, GLCA))^{47, 48}. Bacterial bile salt hydrolase (BSH) enzymes modify BAs by cleaving the peptide linkage between the amino acid (T or G) and the 1° bile acids. Furthermore, certain microbes, predominantly anaerobes, possess a 7α-dehydroxylation activity to further convert 1° BAs into 2° BAs. The BAs can enter the enterohepatic circulation via active or passive transport, are recycled and re-conjugated in the liver, and then re-excreted into the bile and the intestine^{28, 47, 48}.

In all tobramycin-induced fecal metabolomes, 1° BAs, such as CA and TCA, as well as taurine- and glycine-conjugated 1° BAs increased. On the other hand, tobramycin induced a consistent strong reduction in 2° BAs, specifically DCA, HDCA and LCA. Together, these effects are consistent with a lack of utilization of 1° BA to produce 2° or 3° BAs. Additionally, gut bacteria are known to deconjugate taurine- or glycine-conjugated 1° BAs and further dehydroxylate them to produce 2° BAs. This inhibitory effect was also observed *in vitro*⁴⁹, supporting that tobramycin significantly reduced those bacteria responsible for these reactions. Taurine- and glycine-conjugated 2° BAs are also reduced in the feces of both the sexes, demonstrating the attenuation of 2° BAs conjugation with taurine or glycine amino acid. The accumulation of taurine conjugated 1° BAs in the fecal samples of tobramycin-treated male and female rats shows that the deconjugation of these taurine-conjugated 1° BAs is reduced in these treatment groups. Moreover, the profound increase in TCA appears to be related not only to reduced deconjugation but is also associated with reduced passage through the intestinal wall mediated by downregulation of genes coding for bile acid transporters⁴⁹. Finally, the 1° BA fecal accumulation appears to be a robust characteristic response of microbiome disruptions, as it has been observed also for other antibiotics, such as clindamycin, lincomycin, and vancomycin^{27, 37} and this has been seen in other situations such as in disease states like cancer, lupus, non-alcoholic fatty liver disease, cirrhosis and many others⁵⁰.

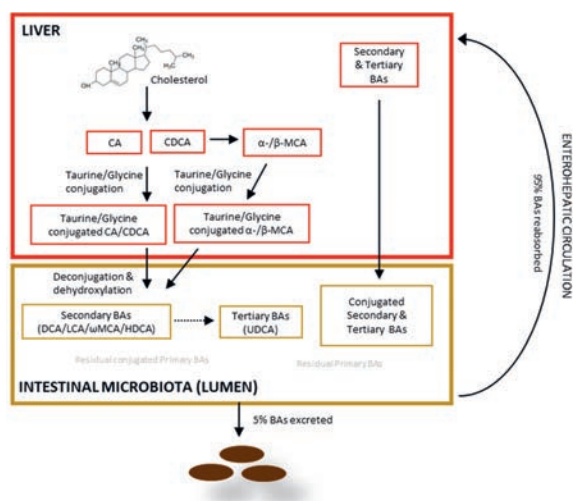


Figure 10: Host and gut microbiota-mediated bile acid metabolism in rodents. The schematic diagram shows red boxes for bile acids that are primarily synthesized in the liver and/or enter into the liver via the enterohepatic circulation (portal vein), brown boxes for 2° BAs that are produced from the 1° BAs by the gut microbiota and 3° BAs, and other residual bile acids enter the ileum. 95% of these conjugated and/or unconjugated 1°, 2° and 3° BAs are reabsorbed from the GI walls and re-enter the liver via enterohepatic circulation to stabilize the bile acid pool. Figure adapted from Murali et al. 2021²⁸.

Given the strong effects of tobramycin on fecal 16S composition metabolic functions, it was interesting to find by ordination analysis of changes in the blood plasma metabolites that previously established

plasma metabolites known to be associated with perturbations in the gut microbiome were altered, but that the fold-change levels were moderate. Thus, hippuric acids and indole derivatives (incl. indole-3-acetic acid, indole-3-propionic acids and 3-indoxylsulfate) and glycerol were significantly reduced in both sexes, however, these fold-changes were lower than observed previously for vancomycin and lincosamide antibiotic treatments^{20, 28, 48}. Other important metabolites, such as plasma bile acids, also showed concordant findings between fecal and plasma metabolomes, including significant reductions in 2° BAs (DCA, LCA and HDCA were all very low in the HD tobramycin groups). These observations are consistent with reduced levels of these 2° BAs result from reduced deconjugation by gut bacteria. Finally, glycine- and taurine-conjugated 2° BAs were likewise significantly reduced in the plasma of the tobramycin groups. Thus, tobramycin is not only changing the fecal 16S composition but also the fecal metabolome and subsequently, the plasma metabolome, hereby indicating a strong influence on the gut metabolic functionality. The major mechanism observed was the disturbance in the enterohepatic circulation of the BAs via reduced production of 2° BA and higher accumulation of the conjugated 1° BAs. This is in line with already observed findings of other antibiotics belonging to aminoglycosides, fluoroquinolones and lincosamides^{28, 37}.

The MetaMapTox® or MMT database was used to compare the plasma metabolome profile of tobramycin with all other compounds in the database, following the standard protocol as published by van Ravenzwaay et al.^{19, 51, 52}. The database consists of metabolite profiles of several thousand compounds including more than thousand chemical entities indicative for toxicological modes of action. The top matches (applying the 95th percentile cut-off) included other antibiotics belonging to classes including aminoglycosides and carbapenems (Table S4). Based on these analyses, a threshold value of 0.40 of Pearson's correlation coefficient for male animals and 0.50 for female animals displays approximately the 95th percentile of all correlation coefficients obtained by the profile comparison^{41, 52}. In males, the plasma metabolome profile of the tobramycin HD treatment correlated strongly with that of other aminoglycosides antibiotics and with that in females treated with antibiotics belonging to the carbapenems. The results indicate that antibiotics, even if they have a different mode of action, form a specific and selective group of compounds with respect to their effects on the plasma metabolome. The lesser the absorption of these antibiotics in the gut, the lesser is their impact on the host plasma metabolomes. In specific, the host plasma metabolite profile is dependent on the bactericidal/-static efficacy spectrum of the antibiotic, its bioavailability, and consequently its potential systemic effect. We also used the MMT database to compare the plasma metabolome of HD tobramycin-treated animals with more than 110 pre-defined patterns for toxicity including various types of liver and kidney toxicity, but found no association^{19, 41, 42, 53}. The ability of the metabolomics in combination with the MMT database to detect various forms of liver toxicity has shown by^{54, 55}, and for the kidney by⁵⁶. Additionally, no clinical observations were seen in any of the tobramycin treated groups. For the tobramycin HD group, plasma creatinine levels were also overall not relevantly altered (data not

shown), indicating a lack of potential kidney-associated toxicity. The fact that consistent changes in plasma metabolite patterns emerged amongst the antibiotics, suggests plasma metabolome profiling as a strategy to identify and characterize substances that may have gut microbiome-altering properties.

6.2.2 Colistin sulfate treatment

Taking into account the marginal effects of colistin on the microbiome composition, and the absence of an effect on the fecal metabolome, it appears that this antibiotic does not alter the gut microbiome functionality at the doses assessed. This is likely related to an intrinsically reduced activity of colistin rather than attributable to differences in the doses of the drug since the LD level of tobramycin (100 mg/kg bw/day) induced more changes than the HD level of colistin (100 mg/kg bw/day). Additionally, when the fecal metabolome profiles of samples from controls with and without high abundances of *Verrucomicrobiaceae* family were compared, they were similar, suggesting that the presence or absence of this family is on one hand highly variable, but neither influences metabolism. The lack of effects on the plasma metabolome may be a result of the low oral bioavailability of colistin and the fact that it only targets Gram negative bacteria, whereas broad-spectrum antibiotics like tobramycin, vancomycin and lincomycin, elicited strong responses in the plasma metabolome^{26,27,33}. Nonetheless, indole-3-acetic acid was reduced in male rats, but very little, and no changes were seen in female rats, which has been observed previously for other broad-spectrum antibiotics^{26,28,48}. The generally less pronounced effects of colistin, relative to tobramycin, are likely to be related to an intrinsically reduced potential of this antibiotic and not due to differences in dose levels. This conclusion is based on the fact that the LD level of tobramycin (100 mg/kg bw/day) induced more changes than the HD level of colistin (100 mg/kg bw/day), reflecting effects of the same dose level.

6.3 Microbiome-Metabolome correlation analyses

As the current knowledge regarding microbial bile acid transformations and related capabilities of the gut bacterial species is limited, the results of this study extend the list of bacterial families known to perform bile acid transformations. The reduced abundances of *Prevotellaceae* and *Anaeroplasmataceae* bacterial families (see Figure 6) in the tobramycin LD and HD groups, along with the significant reduction in the bacterial deconjugation and dehydroxylation reactions suggest that they are not involved in biotransformation of 1° to 2° BAs. On the other hand, an increase in bacterial families including *Erysipelotrichaceae* and *Peptococcaceae* potentially indicates their lack of bacterial deconjugation and dehydroxylation reactions. Weakly reduced *Rikenellaceae* and *Ruminococcaceae* bacterial families in the tobramycin groups suggests a potential bile acid transformation activity of these families. Most strains with potential bile acid-transforming capabilities were found in the Bacteroidetes and Firmicutes phyla. This relationship is in line with the observations of Lee et al. 2020 and Lucas et al. 2021^{3,57}. A Pearson-based correlation analysis may be performed between these changed bacterial families and the respective plasma or feces metabolites in order to associate specific or set of microbes

with their metabolic functions (Supplementary figures S7 & S8). However, there are a few limitations of such an analysis, including low sample size in our study, lack of high resolution 16S sequencing data, which restricts us to use bacterial family level taxonomic classification instead of species or strain level and lastly a correlation analysis may not necessarily mean causality so these correlations can not be directly interpreted but they rather should be taken as a hint of a potential relationship.

The *Verrucomicrobiaceae* family was reduced in a few samples from controls and in all antibiotic treatment groups. We identified the bacterial species that belong to the *Verrucomicrobiaceae* family in fecal samples from the control group and observed that more than 75% were from a single species, *Akkermansia muciniphila*. A relative abundance bar plot of this analysis is included in the Supplementary data (see Figure S2). As there were two male and one female control animal which did not show any *Verrucomicrobiaceae* in the relative abundance analysis (see figure 5), we compared the fecal metabolome of these particular control animals with the other controls, in which the *Verrucomicrobiaceae* played a dominant role, and they had similar metabolite profile to the rest of the controls. This finding suggests that the *Verrucomicrobiaceae*, and in particular *Akkermansia muciniphila*, do not contribute much to the measured metabolites. This conclusion is confirmed by the observation that the overall fecal metabolome of the colistin-treated animals, which lacked *Verrucomicrobiaceae*, was also rather similar to controls. Ganesh et al. 2013 demonstrated *Akkermansia muciniphila* to be a mucin-degrading commensal bacteria that dominates the human intestine in early-life and is not harmful to the host⁵⁸. The capacity to degrade mucin by *Akkermansia muciniphila* seems to not influence metabolic outputs measured herein. Furthermore, variable fluctuations in the abundances of the *Verrucomicrobiaceae* bacterial family require further investigation to understand the potential relevance. Another aspect of combined microbiome and metabolome research would be to investigate resilience and reversibility following discontinuation of antibiotic treatment.

6.4 Comparative analysis of tobramycin and previously published antibiotics

Tobramycin, an aminoglycoside antibiotic used in the present study, induced prominent changes in the feces and plasma BA pool as well as key plasma biomarkers. To evaluate similarities between the modes of action of Tobramycin and other classes of antibiotics including lincosamides (clindamycin, lincomycin), macrolide (roxithromycin), glycopeptide (vancomycin) and fluoroquinolone (sparfloxacin), the feces and plasma metabolomes changes at p value < 0.05 were compared and analyzed^{20, 28, 48}. In the plasma metabolome indole-3-acetic acid and hippuric acid are remarkable as they are reduced in most of the AB classes. Consistent to tobramycin, a clear reduction of IAA was observed in HD groups of streptomycin sulfate, vancomycin and Sparfloxacin and a significant reduction in HA was observed in HD groups of streptomycin, roxithromycin, clindamycin and vancomycin respectively of both male and female Wistar rats. As none of the mentioned antibiotics

other than streptomycin belongs to the same class of antibiotics as tobramycin, this confirmed these plasma metabolites as essential biomarkers associated with altered gut microbiota.

Further similarities between tobramycin and the other previously tested antibiotics were found in the regulation of the BA pool. Profound accumulation of CA (except in roxithromycin treatment) and other taurine conjugated 1° BAs, especially TCA, was observed consistently in the feces of all the antibiotic-treated rats except for streptomycin sulfate. It should be noted that streptomycin was reported to have an overall minimal effect on the fecal bacterial composition. Compared to the rest of the antibiotics, tobramycin shows the highest accumulation of fecal CA, which indicates a strongly reduced gut bacterial capability of converting CAs to 2° BAs as well as a reduced conjugation activity of CA in the liver. In contrast, several unconjugated and glycine conjugated BAs were significantly reduced in the blood plasma of all antibiotic treatments where slight sex-specific differences was observed as the effects were even more pronounced in the females of tobramycin treatment. 2° BAs including DCA, LCA, ωMCA, HDCA and their conjugates were significantly reduced in both plasma and feces of male and female animals of all antibiotic treatments, due to loss of potential gut bacteria that transform 1° to 2° BAs by bacterial deconjugation and dehydroxylation reactions. In conclusion, antibiotics possessing different activity spectra against gut bacteria, including lincosamides, macrolides, fluoroquinolones, glycopeptides and aminoglycosides lead to consistent impairment of deconjugation and dehydroxylation reactions, indicating a strong deregulation in the host BA pool, an altered BA reuptake via the enterohepatic circulation and that this impairment in microbiome function can be diagnosed via analysis of plasma metabolites.

6.5 Limitations and suggestions for further research

Even though the 28-day antibiotic administration period in this study is longer than the typical 5-day treatment of humans, no adverse effects on the health of the rats were observed. It cannot be excluded however, that humans may respond differently and that consequences for human health may become apparent despite the absence of effects on rats. Xiao et al 2018 highlighted that the administration of gentamycin and vancomycin, significantly decreased the intestinal microbiota diversity and subsequently altered the BA composition in mice⁵⁹. Alterations in BA composition were described to contribute to cholestasis in paediatric intestinal failure patients by regulating FXR signalling. Li et al 2017 demonstrated that six different antibiotics inhibited the bile salt export pump (BSEP) resulting in hepatic bile acid accumulation and liver injury⁶⁰. They also indicated that antibiotic associated gut perturbations disturb bile acid homeostasis. This may lead to drug-induced liver injury in both humans and rodents. Furthermore, Edwards et al 1988 indicated that antibiotics such as fluoroquinolones hinder drug clearance by inhibiting their metabolism⁶¹. Hence, it is not unlikely that changed metabolic capacity, in particular changes related to deconjugation reactions, may alter bioavailability of drugs

with potentially significant consequences for human health, if drugs and antibiotics are taken simultaneously.

One of the limitations of this study was a lack of feces sampling at days 7 and 14 which would have extended the possibilities for a direct comparison with the plasma metabolome data beyond 28-day time point. Multiple sampling points for feces and metabolome can be included in future studies. Additionally, in this study, microbiota data were limited to family-level assignments and a dataset with a much higher resolution, genus- or species-level assignments would be even more informative. Any adverse or toxicological outcomes of the metabolome changes and their consequences for host health either with or without co-administration with other drugs is not known. To address this, further studies, need to be performed⁴⁹. Further, taking into account the observed variations in control animals, the establishment of a baseline analysis of the inter-individual variability in the intestinal microbiota is highly recommended to understand if changes are within biological variation or not. To establish pertinent correlations between particular micro-organisms and metabolites, the number of antibiotics in the present study was too low to account for the number of variables (gut microbiome as well as the number of fecal and plasma metabolites) was too small to derive correlations which would pass a statistical test. An extensive correlation analysis of the microbial and metabolomic changes with a far greater number of compounds is part of the goal of the CEFIC LRI ELUMICA project.

7 Conclusions

We highlight the following key observations: 1) Changes in the gut microbiota induced by tobramycin treatment are linked to changes in fecal BAs and particularly a reduction of deconjugation reactions. 2) Indole-3-acetic acid, indole-3-propionic acid, 3-indoxylsulfate and hippuric acid are plasma biomarkers for gut microbiome dysbiosis. 3) The effects of tobramycin on the metabolome aligned well with previously published studies on other antibiotics. 4) Colistin, only showed a marginal effect on gut bacterial composition and fecal metabolome but did elicit changes in some BAs in the plasma, suggesting a potential systemic effect. The use of antibiotics with different modes of action is vital to deduce the potential functions of intestinal bacteria on bile acid metabolism. Further studies are needed to better understand the importance of fluctuations in the abundances of the *Verrucomicrobiaceae* bacterial family. Another aspect of combined microbiome and metabolome research would be to investigate resilience and reversibility following discontinuation of antibiotic treatment.

8 Declaration of conflicting interests

The authors declare that there are no conflicts of interest.

9 Acknowledgments

We cordially would like to thank all the technical assistance from the animal facility technicians including Mr. Gunter Rank and the rest of the team, headed by Burkhard Flick as well as Irmgard Weber

and the technicians from the lab of clinical chemistry at BASF SE, Ludwigshafen as well as the analytical support provided by BASF Metabolome Solutions, Berlin. We would also like to thank our master thesis student Livia Borggreffe for the extensive literature research on gut bacterial bile acid metabolism. Furthermore, we thank the discussion panel from the ELUMICA science monitoring team, and our project partners Nina Zhang from Wageningen University and Research and Shuhuan Zhai and Dr. Katherine Hurley from ETH Zurich for extensive scientific discussions. Also, a big thanks to the Metabolome team at the Experimental Toxicology Department in BASF and the group of BMS Berlin GmbH. This research received an external funding from the Long-range Research Initiative (LRI), which is an initiative from the European Chemical Industry Council. Our research is extensively reviewed by an External Science Advisory Panel from Cefic-LRI.

10 Supporting Information

The Supporting Information is available free of charge at <https://pubs.acs.org/doi/10.1021/acs.chemrestox.2c00316>. Stacked bar plots of all sampling time points as well as showing relative abundances of one specific taxon, Akkermancia muciniphila, belonging to the Verrucomicrobiaceae; PC2 vs PC3 Principle Component Analysis plots of plasma metabolome profiles of samples from all antibiotic groups; changes in body weights and food consumption of animals belonging to all antibiotic classes relative to control group; feces and plasma metabolome profiles of tobramycin and colistin treatment groups for males and females; Top treatment correlations of the plasma metabolome of samples from day 28 of tobramycin HD treatment for both sexes.

References

- (1) Nicholson, J. K.; Holmes, E.; Kinross, J.; Burcelin, R.; Gibson, G.; Jia, W.; Pettersson, S. Host-gut microbiota metabolic interactions. *Science* **2012**, *336* (6086), 1262-1267. DOI: 10.1126/science.1223813. Kinross, J. M.; Darzi, A. W.; Nicholson, J. K. Gut microbiome-host interactions in health and disease. *Genome medicine* **2011**, *3* (3), 1-12. Holmes, E.; Li, J. V.; Athanasiou, T.; Ashrafian, H.; Nicholson, J. K. Understanding the role of gut microbiome–host metabolic signal disruption in health and disease. *Trends in microbiology* **2011**, *19* (7), 349-359.
- (2) Zheng, X.; Xie, G.; Zhao, A.; Zhao, L.; Yao, C.; Chiu, N. H.; Zhou, Z.; Bao, Y.; Jia, W.; Nicholson, J. K.; et al. The footprints of gut microbial-mammalian co-metabolism. *J Proteome Res* **2011**, *10* (12), 5512-5522. DOI: 10.1021/pr2007945.
- (3) Lee, Y.; Lee, H.-Y. Revisiting the bacterial phylum composition in metabolic diseases focused on host energy metabolism. *Diabetes & Metabolism Journal* **2020**, *44* (5), 658-667.
- (4) Liyana, A. Z.; Appannah, G.; Sham, S. Y. Z.; Fazliana, M.; Nor, N. S. M.; Ambak, R.; Samad, A. A.; Dahlan, N. Y.; Aris, T. Effectiveness of a community-based intervention for weight loss on cardiometabolic risk factors among overweight and obese women in a low socio-economic urban community: findings of the MyBFF@home. *BMC Womens Health* **2018**, *18* (Suppl 1), 126. DOI: 10.1186/s12905-018-0593-1. Ghaisas, S.; Maher, J.; Kanthasamy, A. Gut microbiome in health and disease: Linking the microbiome-gut-brain axis and environmental factors in the pathogenesis of systemic and neurodegenerative diseases. *Pharmacol Ther* **2016**, *158*, 52-62. DOI: 10.1016/j.pharmthera.2015.11.012.
- (5) Zierer, J.; Jackson, M. A.; Kastenmuller, G.; Mangino, M.; Long, T.; Telenti, A.; Mohnhey, R. P.; Small, K. S.; Bell, J. T.; Steves, C. J.; et al. The fecal metabolome as a functional readout of the gut microbiome. *Nat Genet* **2018**, *50* (6), 790-795. DOI: 10.1038/s41588-018-0135-7.
- (6) Visconti, A.; Le Roy, C. I.; Rosa, F.; Rossi, N.; Martin, T. C.; Mohnhey, R. P.; Li, W.; de Rinaldis, E.; Bell, J. T.; Venter, J. C. Interplay between the human gut microbiome and host metabolism. *Nature communications* **2019**, *10* (1), 1-10.
- (7) Clarke, G.; Sandhu, K. V.; Griffin, B. T.; Dinan, T. G.; Cryan, J. F.; Hyland, N. P. Gut Reactions: Breaking Down Xenobiotic-Microbiome Interactions. *Pharmacol Rev* **2019**, *71* (2), 198-224. DOI: 10.1124/pr.118.015768.
- (8) Gill, S. R.; Pop, M.; Deboy, R. T.; Eckburg, P. B.; Turnbaugh, P. J.; Samuel, B. S.; Gordon, J. I.; Relman, D. A.; Fraser-Liggett, C. M.; Nelson, K. E. Metagenomic analysis of the human distal gut microbiome. *Science* **2006**, *312* (5778), 1355-1359. DOI: 10.1126/science.1124234. Koppel, N.; Maini Rekdal, V.; Balskus, E. P. Chemical transformation of xenobiotics by the human gut microbiota. *Science* **2017**, *356* (6344). DOI: 10.1126/science.aag2770.
- (9) Mogg, G.; Keighley, M.; Burdon, D.; Alexander-Williams, J.; Youngs, D.; Johnson, M.; Bentley, S.; George, R. Antibiotic-associated colitis—a review of 66 cases. *British Journal of Surgery* **1979**, *66* (10), 738-742.
- (10) Davies, M. H.; Harrison, R. F.; Elias, E.; Hubscher, S. G. Antibiotic-associated acute vanishing bile duct syndrome: a pattern associated with severe, prolonged, intrahepatic cholestasis. *J Hepatol* **1994**, *20* (1), 112-116. DOI: 10.1016/s0168-8278(05)80476-3 From NLM Medline.
- (11) Bartlett, J. G. Antibiotic-associated diarrhea. *Clin Infect Dis* **1992**, *15* (4), 573-581. DOI: 10.1093/clind/15.4.573 From NLM Medline.
- (12) Matz, G.; Rybak, L.; Roland, P. S.; Hannley, M.; Friedman, R.; Manolidis, S.; Stewart, M. G.; Weber, P.; Owens, F. Ototoxicity of ototopical antibiotic drops in humans. *Otolaryngology--Head and Neck Surgery* **2004**, *130* (3_suppl), S79-S82.
- (13) Tulkens, P. M. Nephrotoxicity of aminoglycoside antibiotics. *Toxicology letters* **1989**, *46* (1-3), 107-123.
- (14) Singer, R. S.; Finch, R.; Wegener, H. C.; Bywater, R.; Walters, J.; Lipsitch, M. Antibiotic resistance—the interplay between antibiotic use in animals and human beings. *The Lancet infectious diseases* **2003**, *3* (1), 47-51.
- (15) Smith, D. L.; Harris, A. D.; Johnson, J. A.; Silbergeld, E. K.; Morris Jr, J. G. Animal antibiotic use has an early but important impact on the emergence of antibiotic resistance in human commensal bacteria. *Proceedings of the National Academy of Sciences* **2002**, *99* (9), 6434-6439.

- (16) Zimmermann, M.; Zimmermann-Kogadeeva, M.; Wegmann, R.; Goodman, A. L. Mapping human microbiome drug metabolism by gut bacteria and their genes. *Nature* **2019**, *570* (7762), 462-467. DOI: 10.1038/s41586-019-1291-3. Heintz-Buschart, A.; Wilmes, P. Human gut microbiome: function matters. *Trends in microbiology* **2018**, *26* (7), 563-574. Qi, H.; Li, Y.; Yun, H.; Zhang, T.; Huang, Y.; Zhou, J.; Yan, H.; Wei, J.; Liu, Y.; Zhang, Z. Lactobacillus maintains healthy gut mucosa by producing L-Ornithine. *Communications biology* **2019**, *2* (1), 1-14. Zhang, J.; Empl, M. T.; Schwab, C.; Fekry, M. I.; Engels, C.; Schneider, M.; Lacroix, C.; Steinberg, P.; Sturla, S. J. Gut microbial transformation of the dietary imidazoquinoxaline mutagen MelQx reduces its cytotoxic and mutagenic potency. *Toxicological Sciences* **2017**, *159* (1), 266-276.
- (17) Swann, J. R.; Want, E. J.; Geier, F. M.; Spagou, K.; Wilson, I. D.; Sidaway, J. E.; Nicholson, J. K.; Holmes, E. Systemic gut microbial modulation of bile acid metabolism in host tissue compartments. *Proc Natl Acad Sci U S A* **2011**, *108 Suppl 1*, 4523-4530. DOI: 10.1073/pnas.1006734107. Claus, S. P.; Ellero, S. L.; Berger, B.; Krause, L.; Bruttin, A.; Molina, J.; Paris, A.; Want, E. J.; de Waziers, I.; Cloarec, O.; et al. Colonization-induced host-gut microbial metabolic interaction. *mBio* **2011**, *2* (2), e00271-00210. DOI: 10.1128/mBio.00271-10.
- (18) van Ravenzwaay, B.; Brunborg, G.; Kleinjans, J.; Galay Burgos, M.; Vrijhof, H. Use of 'omics to elucidate mechanism of action and integration of 'omics in a systems biology concept. *Mutat Res* **2012**, *746* (2), 95-96. DOI: 10.1016/j.mrgentox.2012.04.004.
- (19) van Ravenzwaay, B.; Herold, M.; Kamp, H.; Kapp, M. D.; Fabian, E.; Looser, R.; Krennrich, G.; Mellert, W.; Prokoudine, A.; Strauss, V.; et al. Metabolomics: a tool for early detection of toxicological effects and an opportunity for biology based grouping of chemicals—from QSAR to QBAR. *Mutat Res* **2012**, *746* (2), 144-150. DOI: 10.1016/j.mrgentox.2012.01.006.
- (20) Behr, C.; Kamp, H.; Fabian, E.; Krennrich, G.; Mellert, W.; Peter, E.; Strauss, V.; Walk, T.; Rietjens, I.; van Ravenzwaay, B. Gut microbiome-related metabolic changes in plasma of antibiotic-treated rats. *Arch Toxicol* **2017**, *91* (10), 3439-3454. DOI: 10.1007/s00204-017-1949-2.
- (21) Lange, K.; Buerger, M.; Stallmach, A.; Bruns, T. Effects of antibiotics on gut microbiota. *Digestive Diseases* **2016**, *34* (3), 260-268. Ianiro, G.; Tilg, H.; Gasbarrini, A. Antibiotics as deep modulators of gut microbiota: between good and evil. *Gut* **2016**, *65* (11), 1906-1915.
- (22) Ferrer, M.; Mendez-Garcia, C.; Rojo, D.; Barbas, C.; Moya, A. Antibiotic use and microbiome function. *Biochem Pharmacol* **2017**, *134*, 114-126. DOI: 10.1016/j.bcp.2016.09.007. Schwartz, D. J.; Langdon, A. E.; Dantas, G. Understanding the impact of antibiotic perturbation on the human microbiome. *Genome Med* **2020**, *12* (1), 82. DOI: 10.1186/s13073-020-00782-x.
- (23) Serio, A. W.; Keepers, T.; Andrews, L.; Krause, K. M. Aminoglycoside revival: review of a historically important class of antimicrobials undergoing rejuvenation. *EcoSal Plus* **2018**, *8* (1).
- (24) Sullivan, M. D.; Edlund, M. J.; Fan, M. Y.; Devries, A.; Brennan Braden, J.; Martin, B. C. Risks for possible and probable opioid misuse among recipients of chronic opioid therapy in commercial and medicaid insurance plans: The TROUP Study. *Pain* **2010**, *150* (2), 332-339. DOI: 10.1016/j.pain.2010.05.020.
- (25) Cooney, G.; Lum, B.; Tomaselli, M.; Fiel, S. Absolute bioavailability and absorption characteristics of aerosolized tobramycin in adults with cystic fibrosis. *The Journal of Clinical Pharmacology* **1994**, *34* (3), 255-259.
- (26) Behr, C.; Sperber, S.; Jiang, X.; Strauss, V.; Kamp, H.; Walk, T.; Herold, M.; Beekmann, K.; Rietjens, I.; van Ravenzwaay, B. Microbiome-related metabolite changes in gut tissue, cecum content and feces of rats treated with antibiotics. *Toxicol Appl Pharmacol* **2018**, *355*, 198-210. DOI: 10.1016/j.taap.2018.06.028.
- (27) Behr, C.; Ramirez-Hincapie, S.; Cameron, H. J.; Strauss, V.; Walk, T.; Herold, M.; Beekmann, K.; Rietjens, I.; van Ravenzwaay, B. Impact of lincosamides antibiotics on the composition of the rat gut microbiota and the metabolite profile of plasma and feces. *Toxicol Lett* **2018**, *296*, 139-151. DOI: 10.1016/j.toxlet.2018.08.002.
- (28) Murali, A.; Giri, V.; Cameron, H. J.; Behr, C.; Sperber, S.; Kamp, H.; Walk, T.; van Ravenzwaay, B. Elucidating the Relations between Gut Bacterial Composition and the Plasma and Fecal Metabolomes of Antibiotic Treated Wistar Rats. *Microbiology Research* **2021**, *12* (1), 82-122.
- (29) Murali, A.; Giri, V.; Cameron, H. J.; Sperber, S.; Zickgraf, F. M.; Haake, V.; Driemert, P.; Walk, T.; Kamp, H.; Rietjens, I. M. Investigating the gut microbiome and metabolome following treatment

with artificial sweeteners acesulfame potassium and saccharin in young adult Wistar rats. *Food and Chemical Toxicology* **2022**, 113123.

(30) Mulder, J. G.; Wiersma, W. E.; Welling, G. W.; van der Waaij, D. Low dose oral tobramycin treatment for selective decontamination of the digestive tract: a study in human volunteers. *Journal of Antimicrobial Chemotherapy* **1984**, *13* (5), 495-504. DOI: 10.1093/jac/13.5.495 (accessed 12/1/2022).

(31) Prazma, J.; Postma, D. S.; Pecorak, J. B.; Fischer, N. D. Ototoxicity of tobramycin sulfate. *Laryngoscope* **1976**, *86* (2), 259-268. DOI: 10.1288/00005537-197602000-00022 From NLM Medline.

(32) Rogier, R.; Evans-Marin, H.; Manasson, J.; van der Kraan, P. M.; Walgreen, B.; Helsen, M. M.; van den Bersselaar, L. A.; van de Loo, F. A.; Van Lent, P. L.; Abramson, S. B. Alteration of the intestinal microbiome characterizes preclinical inflammatory arthritis in mice and its modulation attenuates established arthritis. *Scientific reports* **2017**, *7* (1), 1-12.

(33) Products, T. E. A. f. t. E. o. M. *COMMITTEE FOR VETERINARY MEDICINAL PRODUCTS - COLISTIN SUMMARY REPORT*. 2002. https://www.ema.europa.eu/en/documents/mrl-report/colistin-summary-report-1-committee-veterinary-medicinal-products_en.pdf (accessed).

(34) Green, J. M.; Owen, M. D. Herbicide-resistant crops: utilities and limitations for herbicide-resistant weed management. *J Agric Food Chem* **2011**, *59* (11), 5819-5829. DOI: 10.1021/jf101286h.

(35) Marksteiner, J.; Blasko, I.; Kemmler, G.; Koal, T.; Humpel, C. Bile acid quantification of 20 plasma metabolites identifies lithocholic acid as a putative biomarker in Alzheimer's disease. *Metabolomics* **2018**, *14* (1), 1. DOI: 10.1007/s11306-017-1297-5.

(36) Walk, T. B.; Looser, R.; Bethan, B.; Herold, M. M.; Kamlage, B.; Schmitz, O.; Wiemer, J. C.; Prokoudine, A.; van Ravenzwaay, B.; Mellert, W. System and method for analyzing a sample using chromatography coupled mass spectrometry. Google Patents: 2011.

(37) de Bruijn, V.; Behr, C.; Sperber, S.; Walk, T.; Ternes, P.; Slopianka, M.; Haake, V.; Beekmann, K.; van Ravenzwaay, B. Antibiotic-Induced Changes in Microbiome-Related Metabolites and Bile Acids in Rat Plasma. *Metabolites* **2020**, *10* (6). DOI: 10.3390/metabo10060242.

(38) McMurdie, P. J.; Holmes, S. phyloseq: an R package for reproducible interactive analysis and graphics of microbiome census data. *PLoS one* **2013**, *8* (4), e61217. McMurdie, P. J.; Holmes, S. Phyloseq: a bioconductor package for handling and analysis of high-throughput phylogenetic sequence data. *Pac Symp Biocomput* **2012**, 235-246.

(39) Love, M. I.; Huber, W.; Anders, S. Moderated estimation of fold change and dispersion for RNA-seq data with DESeq2. *Genome Biol* **2014**, *15* (12), 550. DOI: 10.1186/s13059-014-0550-8.

(40) Fox, J.; Weisberg, S. Multivariate linear models in R. *An R Companion to Applied Regression*. Los Angeles: Thousand Oaks **2011**.

(41) Sperber, S.; Wahl, M.; Berger, F.; Kamp, H.; Lemke, O.; Starck, V.; Walk, T.; Spitzer, M.; Ravenzwaay, B. V. Metabolomics as read-across tool: An example with 3-aminopropanol and 2-aminoethanol. *Regul Toxicol Pharmacol* **2019**, *108*, 104442. DOI: 10.1016/j.yrtph.2019.104442.

(42) van Ravenzwaay, B.; Sperber, S.; Lemke, O.; Fabian, E.; Faulhammer, F.; Kamp, H.; Mellert, W.; Strauss, V.; Strigun, A.; Peter, E.; et al. Metabolomics as read-across tool: A case study with phenoxy herbicides. *Regul Toxicol Pharmacol* **2016**, *81*, 288-304. DOI: 10.1016/j.yrtph.2016.09.013.

(43) van Ravenzwaay, B.; Cunha, G. C.; Leibold, E.; Looser, R.; Mellert, W.; Prokoudine, A.; Walk, T.; Wiemer, J. The use of metabolomics for the discovery of new biomarkers of effect. *Toxicol Lett* **2007**, *172* (1-2), 21-28. DOI: 10.1016/j.toxlet.2007.05.021.

(44) Guo, L.; Zhang, D.; Fu, S.; Zhang, J.; Zhang, X.; He, J.; Peng, C.; Zhang, Y.; Qiu, Y.; Ye, C. Metagenomic sequencing analysis of the effects of colistin sulfate on the pig gut microbiome. *Frontiers in Veterinary Science* **2021**, *8*, 676.

(45) Eshar, D.; Weese, J. S. Molecular analysis of the microbiota in hard feces from healthy rabbits (*Oryctolagus cuniculus*) medicated with long term oral meloxicam. *BMC veterinary research* **2014**, *10* (1), 1-9.

(46) Sagar, N. M.; Cree, I. A.; Covington, J. A.; Arasaradnam, R. P. The interplay of the gut microbiome, bile acids, and volatile organic compounds. *Gastroenterol Res Pract* **2015**, *2015*, 398585. DOI: 10.1155/2015/398585. Zhang, Y.; Limaye, P. B.; Renaud, H. J.; Klaassen, C. D. Effect of various antibiotics on modulation of intestinal microbiota and bile acid profile in mice. *Toxicol Appl Pharmacol* **2014**, *277* (2), 138-145. DOI: 10.1016/j.taap.2014.03.009. Wahlstrom, A.; Sayin, S. I.; Marschall, H. U.; Backhed, F. Intestinal Crosstalk between Bile Acids and Microbiota and Its Impact on Host Metabolism. *Cell Metab* **2016**, *24* (1), 41-50. DOI: 10.1016/j.cmet.2016.05.005.

- (47) Enhsen, A.; Kramer, W.; Wess, G. Bile acids in drug discovery. *Drug Discovery Today* **1998**, *3* (9), 409-418.
- (48) Behr, C.; Slopianka, M.; Haake, V.; Strauss, V.; Sperber, S.; Kamp, H.; Walk, T.; Beekmann, K.; Rietjens, I.; van Ravenzwaay, B. Analysis of metabolome changes in the bile acid pool in feces and plasma of antibiotic-treated rats. *Toxicol Appl Pharmacol* **2019**, *363*, 79-87. DOI: 10.1016/j.taap.2018.11.012.
- (49) Zhang, N.; Wang, J.; Bakker, W.; Zheng, W.; Baccaro, M.; Murali, A.; van Ravenzwaay, B.; Rietjens, I. In vitro models to detect in vivo bile acid changes induced by antibiotics. *Arch Toxicol* **2022**. DOI: 10.1007/s00204-022-03373-4.
- (50) Telleria, O.; Alboniga, O. E.; Clos-Garcia, M.; Nafria-Jimenez, B.; Cubiella, J.; Bujanda, L.; Falcón-Pérez, J. M. A Comprehensive Metabolomics Analysis of Fecal Samples from Advanced Adenoma and Colorectal Cancer Patients. *Metabolites* **2022**, *12* (6), 550. He, J.; Chan, T.; Hong, X.; Zheng, F.; Zhu, C.; Yin, L.; Dai, W.; Tang, D.; Liu, D.; Dai, Y. Microbiome and metabolome analyses reveal the disruption of lipid metabolism in systemic lupus erythematosus. *Frontiers in immunology* **2020**, *11*, 1703. Wahlström, A.; Sayin, S. I.; Marschall, H.-U.; Bäckhed, F. Intestinal crosstalk between bile acids and microbiota and its impact on host metabolism. *Cell metabolism* **2016**, *24* (1), 41-50.
- (51) van Ravenzwaay, B. Initiatives to decrease redundancy in animal testing of pesticides. *ALTEX* **2010**, *27* (3), 112-114.
- (52) Ravenzwaay, B. V.; Kamp, H.; Montoya-Parra, G. A.; Strauss, V.; Fabian, E.; Mellert, W.; Krennrich, G.; Walk, T.; Peter, E.; Looser, R. The development of a database for metabolomics-looking back on ten years of experience. *International Journal of Biotechnology* **2015**, *14* (1), 47-68.
- (53) Kamp, H.; Strauss, V.; Wiemer, J.; Leibold, E.; Walk, T.; Mellert, W.; Looser, R.; Prokoudine, A.; Fabian, E.; Krennrich, G.; et al. Reproducibility and robustness of metabolome analysis in rat plasma of 28-day repeated dose toxicity studies. *Toxicol Lett* **2012**, *215* (2), 143-149. DOI: 10.1016/j.toxlet.2012.09.015.
- (54) Kamp, H.; Fabian, E.; Groeters, S.; Herold, M.; Krennrich, G.; Looser, R.; Mattes, W.; Mellert, W.; Prokoudine, A.; Ruiz-Noppinger, P. Application of in vivo metabolomics to preclinical/toxicological studies: case study on phenytoin-induced systemic toxicity. *Bioanalysis* **2012**, *4* (18), 2291-2301.
- (55) Mattes, W.; Davis, K.; Fabian, E.; Greenhaw, J.; Herold, M.; Looser, R.; Mellert, W.; Groeters, S.; Marxfeld, H.; Moeller, N. Detection of hepatotoxicity potential with metabolite profiling (metabolomics) of rat plasma. *Toxicology letters* **2014**, *230* (3), 467-478.
- (56) Mattes, W.; Kamp, H.; Fabian, E.; Herold, M.; Krennrich, G.; Looser, R.; Mellert, W.; Prokoudine, A.; Strauss, V.; van Ravenzwaay, B. Prediction of clinically relevant safety signals of nephrotoxicity through plasma metabolite profiling. *BioMed research international* **2013**, *2013*.
- (57) Lucas, L.; Barrett, K.; Kerby, R.; Zhang, Q.; Cattaneo, L.; Stevenson, D.; Rey, F.; Amador-Noguez, D. Dominant Bacterial Phyla from the Human Gut Show Widespread Ability To Transform and Conjugate Bile Acids. *Msystems* **2021**, *6* (4), e00805-00821.
- (58) Ganesh, B. P.; Klopffleisch, R.; Loh, G.; Blaut, M. Commensal Akkermansia muciniphila exacerbates gut inflammation in Salmonella Typhimurium-infected gnotobiotic mice. *PLoS one* **2013**, *8* (9), e74963. Hooper, L. V.; Gordon, J. I. Commensal host-bacterial relationships in the gut. *Science* **2001**, *292* (5519), 1115-1118.
- (59) Xiao, Y.; Zhou, K.; Lu, Y.; Yan, W.; Cai, W.; Wang, Y. Administration of antibiotics contributes to cholestasis in pediatric patients with intestinal failure via the alteration of FXR signaling. *Exp Mol Med* **2018**, *50* (12), 1-14. DOI: 10.1038/s12276-018-0181-3 From NLM Medline.
- (60) Li, Y.; Hafey, M. J.; Duong, H.; Evers, R.; Cheon, K.; Holder, D. J.; Galijatovic-Idrizbegovic, A.; Sistare, F. D.; Glaab, W. E. Antibiotic-Induced Elevations of Plasma Bile Acids in Rats Independent of Bsep Inhibition. *Toxicological Sciences* **2017**, *157* (1), 30-40. DOI: 10.1093/toxsci/kfx015 (accessed 12/1/2022).
- (61) Edwards, D. J.; Bowles, S. K.; Svensson, C. K.; Rybak, M. J. Inhibition of drug metabolism by quinolone antibiotics. *Clin Pharmacokinet* **1988**, *15* (3), 194-204. DOI: 10.2165/00003088-198815030-00004 From NLM Medline.





CHAPTER 4:

GUT MICROBIOTA AS WELL AS METABOLOMES OF WISTAR RATS RECOVER WITHIN TWO WEEKS AFTER DORIPENEM ANTIBIOTIC TREATMENT

Aishwarya Murali, Franziska Maria Zickgraf, Philipp Ternes, Varun Giri, Hunter James Cameron, Saskia Sperber, Volker Haake, Peter Driemert, Hennicke Kamp, Dorothee Funk Weyer, Shana J. Sturla, Ivonne M. G. M. Rietjens and Bennard van Ravenzwaay

Published in: MDPI Microorganisms 11 (2023), 533

Gut Microbiota as well as Metabolomes of Wistar Rats Recover within Two Weeks after Doripenem Antibiotic Treatment

Abstract: An understanding of the changes in gut microbiome composition and its associated metabolic functions is important to assess the potential implications thereof on host health. Thus, to elucidate the connection between the gut microbiome and the fecal and plasma metabolomes, two poorly bioavailable carbapenem antibiotics (doripenem and meropenem), were administered in a 28-day oral study to male and female Wistar rats. Additionally, the recovery of the gut microbiome and metabolomes in doripenem-exposed rats were studied one and two weeks after antibiotic treatment (i.e., doripenem-recovery groups). The 16S bacterial community analysis revealed an altered microbial population in all antibiotic treatments and a recovery of bacterial diversity in the doripenem-recovery groups. A similar pattern was observed in the fecal metabolomes of treated animals. In the recovery group, particularly after one week, an over-compensation was observed in fecal metabolites, as they were significantly changed in the opposite direction compared to previously changed metabolites upon 28 days of antibiotic exposure. Key plasma metabolites known to be diagnostic of antibiotic-induced microbial shifts, including indole derivatives, hippuric acid, and bile acids were also affected by the two carbapenems. Moreover, a unique increase in the levels of indole-3-acetic acid in plasma following meropenem treatment was observed. As was observed for the fecal metabolome, an overcompensation of plasma metabolites was observed in the recovery group. The data from this study provides insights into the connectivity of the microbiome and fecal and plasma metabolomes and demonstrates restoration post-antibiotic treatment not only for the microbiome but also for the metabolomes. The importance of overcompensation reactions for health needs further studies.

Keywords: metabolomics; gut microbiome; carbapenems; gut microbiota and metabolome recovery; repeated dose oral study

1. Introduction

The human gut harbors thousands of different species of bacteria, fungi, archaea, and viruses, where bacteria exceed eukaryotes and archaea by 2–3 orders of magnitude, forming a complex community known as the gut microbiota [1, 2]. While intestinal microbiota performs several vital metabolic functions crucial to the host [3, 4], its composition is highly variable and susceptible to dysbiosis, which results from pressures such as diet, immune function, environmental chemical exposures, and the use of drugs. Furthermore, microbial dysbiosis is associated with human diseases such as Crohn’s disease, colon cancer, diabetes, allergies, Alzheimer’s and Parkinson’s disease, depression, and stroke [5-7]. Moreover, the ability of the gut microbiota to (bio)transform molecules is relevant for pharmacology and toxicology [8].

Antibiotics, in particular, are known to compositionally as well as functionally (metabolism-wise) affect the gut microbiota [9, 10]. This makes antibiotics ideal compounds to induce a temporary shift in the gut composition and to determine the changes in metabolic output. In previous studies, we have shown how different classes of antibiotics, including aminoglycosides, fluoroquinolones, lincosamides, and polymyxin E, induce selective changes in the gut microbiome of experimental animals and how these are reflected by antibiotic class-specific changes in the fecal and plasma metabolomes [1, 11-13]. Several antibiotics belonging to classes including aminoglycosides, fluoroquinolones, lincosamides, and polymyxin E have been studied to understand their effects on the gut microbiota composition as well as the related metabolic outputs [1, 14, 15].

Two antibiotics belonging to the carbapenem class have been selected for the present study as this class has not been investigated before. Both meropenem and doripenem are broad-spectrum carbapenem antibiotics that are active against Gram-positive and Gram-negative bacteria, and these antibiotics have poor oral bioavailability from the gastrointestinal tract [16-18]. To selectively identify metabolome changes in the plasma because of changes in the microbiome, antibiotics with low bioavailability are preferred to avoid plasma metabolome changes related to the potential systemic toxicity of the antibiotics. Several clinical trials have previously demonstrated that carbapenems have low oral bioavailability and hence must be administered intravenously because they cannot cross gastrointestinal membranes readily [17, 19]. The shift in the gut microbiota composition induced by antibiotics can be determined using 16S marker gene sequencing of fecal samples and the corresponding changes in metabolites can be assessed using metabolomics. Highly sensitive mass spectrometry-based (MS) techniques allow for the detection of a broad range of metabolites, such as amino acids, bile acids, carbohydrates, lipids, vitamins, energy metabolites, hormones, and their derivatives. In the current study, we have used an optimized procedure to determine the fecal and plasma metabolome upon antibiotic-induced microbiome changes.

Currently, the existing knowledge on the ability of the gut bacterial communities to spontaneously recover after antibiotic treatment is stopped is not very well defined [20, 21]. In both humans and mice, Suez et al., 2018 observed faster spontaneous recovery of the indigenous stool/mucosal microbiome when administering a probiotic. Legrand et al., 2020, also observed strain-specific recovery of the human gastrointestinal tract after antibiotic treatment is stopped [21, 22]. It is important to not only understand this recovery pattern of gut bacterial strains following antibiotic treatment but also to characterize the associated metabolite recoveries as they may be an important factor for long-term host health. Understanding the restoration abilities of intestinal and metabolic homeostasis are necessary to be understood in the context of dysbiosis resulting from broad-spectrum antibiotics, as it lays the groundwork for potential strategies that could reduce the long-term adverse effects of antibiotic treatment on the gut health [23, 24]. Furthermore, there is a lack of knowledge in the direction of metabolite recovery, and the consequences of microbiome recovery on fecal and plasma metabolomes are also not known, hence they are essential to be understood.

In previously published works, the antibiotic classes aminoglycosides, fluoroquinolones, lincosamides, and macrolides and their effects on the gut microbiome were studied [1, 11, 12, 15]. Here, we expand the previous work by investigating the effects of the carbapenem class. The main objective of this study is to understand the contribution of gut bacterial communities to metabolite production by addressing large-scale quantification of dynamic changes in microbial metabolites as a functional component to community profiling (or taxonomics) analysis. Antibiotics were selected to induce a shift in the gut composition and functions, and the criteria for selection included their ability to induce perturbation in the gut microbiota, low or no systemic bioavailability, and a low/no systemic toxicity. The latter two points were important to avoid systemic toxicity influencing the plasma metabolome profiles.

We assessed perturbations in the gut composition by orally administering meropenem trihydrate and doripenem hydrate to young adult male and female rats in a 28-day study and its consequences on fecal and plasma metabolomes. Young adult Wistar rats have been selected for this study because rodent models are widely used in the assessment of chemical safety assessments for humans and have significantly contributed to delineating correlations between the intestinal microbiome and associated diseases [25]. Finally, we characterized the capacity of the microbiome and its associated plasma and fecal metabolomes to spontaneously recovery after one or two weeks following the cessation of doripenem exposure. These findings show that not only the gut microbiota but also the metabolomes can be restored post-antibiotic treatment, evidencing the interconnection between the gut microbiome and metabolome.

2. Materials and Methods

A 28-day oral study using Wistar rats with two further weeks of recovery for the doripenem-exposed animals was carried out based on the OECD 407 guidelines under the principles of Good Laboratory Practice of the German Chemicals Act.

2.1. Ethics Statement

This animal study was performed in an AAALAC-approved (Association for Assessment and Accreditation of Laboratory Animal Care International) laboratory in compliance with the German Animal Welfare Act and the effective European Council Directive. This study was approved by the BASF Animal Welfare Body, with the permission of the local authority, the Landesuntersuchungsamt Koblenz, Germany (approval number 23 177-07/G 18-3-098) [13].

2.2. Animals and Maintenance Conditions

Wistar rats of both sexes (CrI:WI(Han)) of the age group 70 ± 1 days were purchased from Charles River, Germany, prior to the start of the planned study. The handling of the animals, acclimatization, conditions of the animal test facility, and other related information regarding the study have been presented and published by Murali et al., 2022 [13].

2.3. Treatment of Animals with Drugs

In this study, five rats per treatment group per sex were exposed (orally, with gavage) to the two antibiotics (meropenem trihydrate and doripenem hydrate) on a daily basis (see Table 1 and Figure 1). Meropenem was prepared for oral administration by resuspending it in deionized water at doses of 100 mg/kg body weight/day and 300 mg/kg body weight/day. Doripenem was also prepared in deionized water for oral administration at doses of 100 mg/kg body weight/day and 1000 mg/kg body/day weight. Antibiotic dose levels were selected, based on the available literature, to alter the targeted microbiome population without causing systemic toxicity. An antibiotic suspension of 10 mL/kg bw/day was administered orally to five rats per treatment group per dose group per sex each with a corresponding control group of ten rats per sex, to allow direct comparisons.

Table 1. Compounds used, dose levels, and form of preparation. All compounds were administered orally using gavage.

Treatment	Low Dose (mg/kg bw/d ^a)	High Dose (mg/kg bw/d ^a)
Meropenem trihydrate	100	300
Doripenem hydrate	100	1000

^a mg/kg bw/d means milligrams per kilogram body weight of rat per day

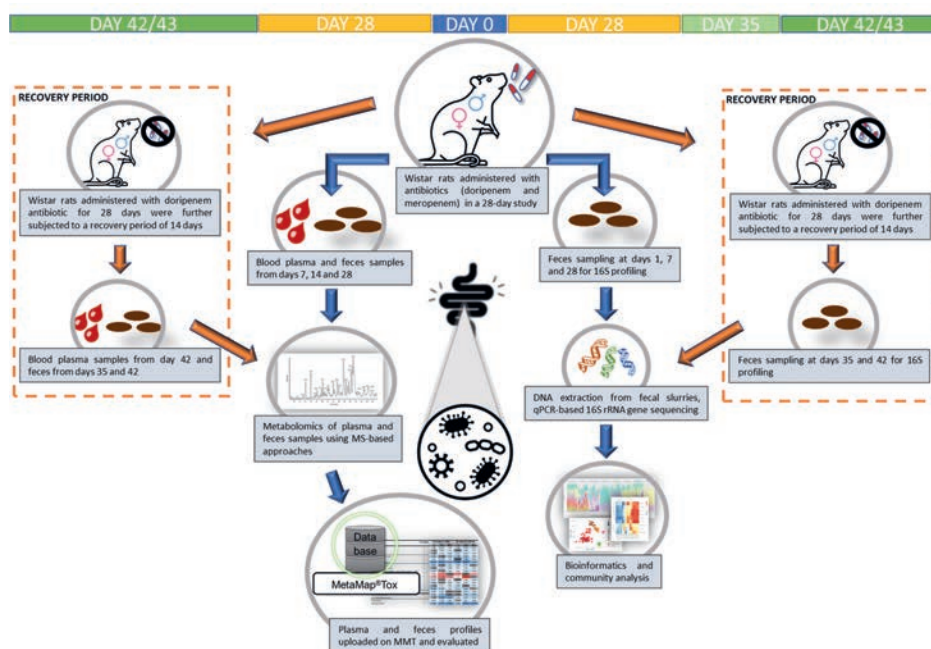


Figure 1. Schematic representation of the study design for plasma and fecal metabolome analyses and the corresponding gut (fecal) 16S bacterial profiling in a 28-day oral gavage study using meropenem- and doripenem- (administered at high and low doses) treated male and female young adult Wistar rats. Note: For doripenem, an additional one- and two-week recovery period, as indicated by the orange dashed boxes, was included to analyze the reversibility. The top row indicates sampling timeline.

2.4. Clinical Examination

All the animals were checked daily for any signs of clinical toxicity, abnormal macroscopic findings, and mortalities. Standard operating procedures following the Organization for Economic Co-operation and Development (OECD) 407 guidelines were used for all clinical and pathological examinations. Details related to regular examinations have been followed based on our previous publication, Murali et al., 2022 [13].

2.5. Blood and Fecal Sampling for Metabolite Profiling

On days 7, 14, and 28, and additionally on days 42/43 for the doripenem groups only, after a fasting period of 16–20 h, collection of blood samples was performed between 7:30 and 10:30 h from the retro-orbital sinus of all the rats (including controls and all treatment groups) under isoflurane anesthesia (1.0 mL K-EDTA blood). After centrifugation (10 °C, 20,000× g, 2 min), EDTA plasma was separated from the collected blood samples. After snap-freezing the EDTA plasma samples with N₂, they were stored at 80 °C for metabolite profiling. Following gentle massaging of the rectum, feces were collected from rats exposed to different antibiotic exposures on days 7, 14, and 28; from the doripenem-recovery group, feces were collected from females on days 35 and 42 and from males on day 43. Following 16–20 h of fasting, if no feces samples could be obtained, then the samples were simply taken by scraping from the rat colons on the day of necropsy, i.e., on days 28 and 42/43. Pre-cooled (dry ice) vials were filled with these samples, which were then snap-frozen in liquid N₂ and stored at 80 °C until processing for fecal dry weight measurements, and further to perform DNA isolation and 16S gene PCR amplification and sequencing.

2.6. DNA Isolation and 16S Marker Gene Sequencing

Dry weights of stored fecal samples collected on days 1, 7, 28, 35, and 42/43 from all controls and antibiotic-treated rats were measured and then transferred to labeled pre-cooled (dry-ice) DNA/RNA Shield-Lysis collection tubes (BIOZOL Diagnostica Vertrieb GmbH, Eching, Germany) avoiding excess thawing of the frozen fecal pellets. The processing of fecal slurries for further DNA isolation, quantification, sequencing, and the final report produced was based on the process previously published by Murali et al., 2022 [13].

2.7. Metabolomics of Plasma and Feces Matrices and Statistical Analysis

Mass spectrometry-based metabolite profiling of blood plasma and feces samples collected from the controls, antibiotic-treated, and recovery groups was performed according to the protocol published previously by Murali et al., 2022 [13, 26, 27].

In plasma, 272 semiquantitative metabolites were analyzed using the single peak signal of the respective metabolite and a normalization strategy according to the patent [28] resulting in fold change ratios representing the metabolite changes in treated versus control animals [1]. Of these 306 metabolites, the chemical structures of 280 were identified and 26 remained unknown. In feces, 632 semiquantitative

metabolites could be analyzed, out of which the chemical structures of 348 were identified and 284 were unknown.

Furthermore, statistical analysis of the metabolome data of plasma and feces matrices, as well as the uploading of these data into our in-house database MetaMapTox[®] (or MMT), followed by a PCA analysis were performed following the protocol published by Murali et al., 2022 [1, 12, 13, 29].

2.8. The 16S Data Processing and Statistical Analysis of the Data

The data processing pipeline used was an in-house standardized algorithm using DADA2 for 16S marker gene data as published in Murali et al., 2022 [12]. The customized workflow and further steps including a quality check (QC) followed by taxonomic assignments were conducted based on the previous publication by Murali et al., 2022 [13]. The overall methods used followed the publication by Murali et al., 2022.

Furthermore, post-processing of the 16S data was performed using different packages, as presented in Murali et al., [12]. The entire raw data used for the study consisted of 5,027,882 reads belonging to 5533 taxa from a total of 251 samples. Reads with non-zero counts on at least two samples were retained, and the rest were removed as a part of the cleaning up of the raw data, which resulted in 4,429,863 reads belonging to 2053 taxa from a total of 251 samples. Furthermore, reads that were not assigned to a minimum of the family level of taxonomy were removed, resulting in 4,429,863 reads belonging to 2053 taxa from 251 samples. Further analysis including diversity, relative, and differential abundance analyses following the protocol published by Murali et al., 2022 [13, 30].

3. Results

3.1. No Visible Signs of Toxicity or Change in the Body Weight or Food Consumption after Administering Carbapenems

After administering meropenem and doripenem to male and female rats for 28 days, there were no mortalities nor signs of clinical toxicity, except for one male rat (no. 55) receiving doripenem LD. This animal developed a lower jaw lesion and lost body weight; therefore, it was excluded from the study on day 7. All sampled feces had a normal consistency. Food consumption and body weight values of male (A,C) and female (B,D) animals from the two antibiotic treatment groups relative to the control animals, respectively, have been presented (Figure 2). During the 28-day study, both control and antibiotic-treated animals maintained roughly the same body weights and food consumption rates. Animals belonging to the group that was administered doripenem and then allowed a recovery period without daily antibiotic administration for a period of two weeks, i.e., the doripenem-recovery group, also consumed a similar amount of food and gained a similar amount of weight as the control animals.

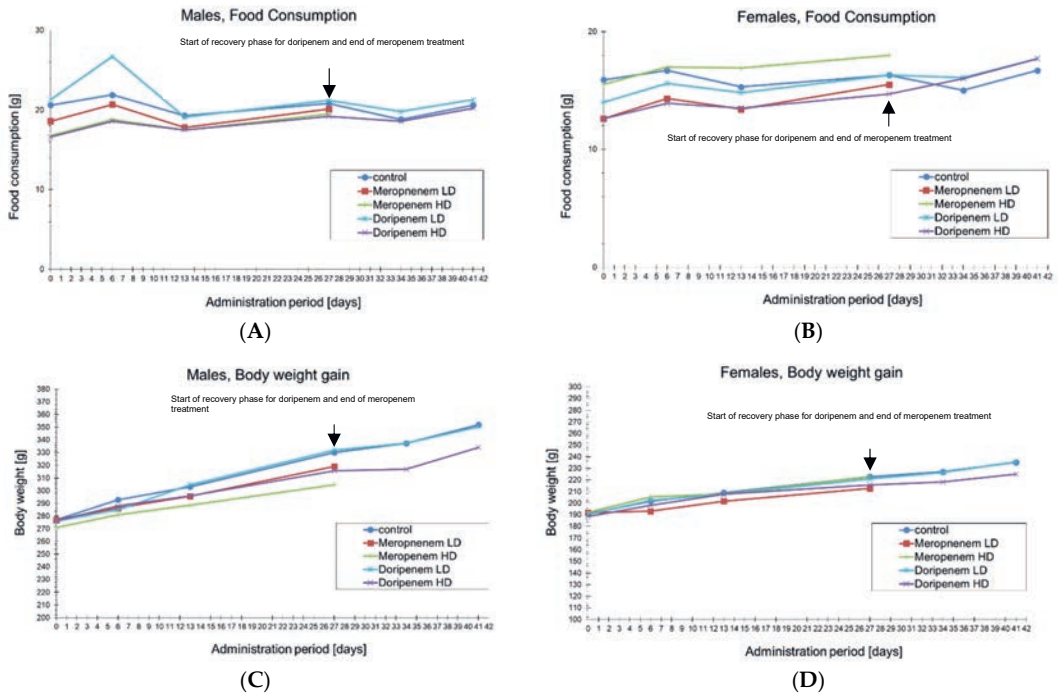


Figure 2. Line plots representing food consumption (in grams) and body weight (in grams), in male (A,C) and female (B,D) animals, respectively, compared to the controls and different antibiotics treatment groups on days 0, 6, 13, and 27 and additionally on days 35 and 42/43 for the doripenem-recovery groups. The end of meropenem treatment and the start of doripenem-recovery groups have been highlighted with black arrows. Changes in body weight and food consumption were compared between control and treated groups and showed no significant differences (p -value < 0.05).

3.2. Bacterial Diversity Was Reduced by Carbapenem Treatment and Returned to Control Levels in the Doripenem-Recovery Group

Alpha diversity, representing the diversity of bacterial taxa present in a specific condition or treatment group, was evaluated using the Shannon true diversity algorithm (Figure 3). The size of the boxes in the plot represents the variability between the samples from individual animals of a specific group. The higher the diversity, the greater the presence of different bacterial taxa. The increase in alpha diversity of microbiota from fecal samples collected from day 1 of the study to day 42/43 in both sexes demonstrated a greater presence of differential taxa over the course of the study. As anticipated, compared to the microbiota from the controls, the alpha diversity of the microbiota from animals belonging to all the antibiotic groups from days 1 to 28 shows a clear reduction. There was no clear dose-dependent effect concerning the two dose levels of the antibiotics. Furthermore, after the animals administered with doripenem were allowed a drug-free recovery period of one or two weeks, there was a corresponding increase in alpha diversity to a level similar to that in the control animals for both sexes (Figure 3).

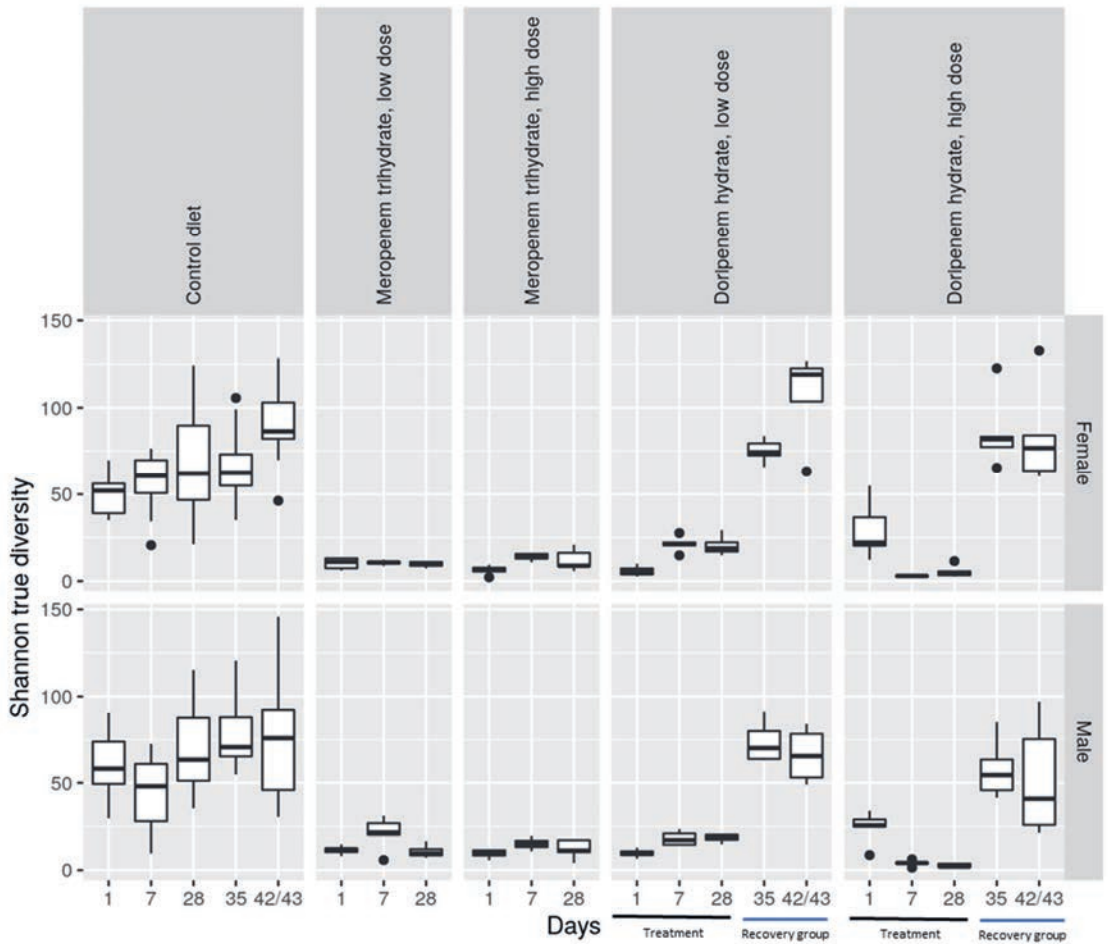


Figure 3. Shannon true diversity analysis of the antibiotic treatments, meropenem, doripenem, and controls for both male and female Wistar rats. The top row shows data for females (f) and the bottom row shows data for males (m). Doripenem treatment time points (days 1, 7, and 28) and recovery time points (days 35 and 42/43) are indicated with black and blue lines, respectively, on the x-axis. Whiskers denote standard deviations, and solid lines within the boxes indicate the group medians. The dots falling outside the boxes demonstrate the most extreme values.

To compare the diversity between different ecosystems, as might be present in the different treatment groups, a rank-based Principal Coordinate Analysis (PCoA) was carried out using a non-phylogenetic Bray-Curtis distance matrix. The results of this analysis were consistent with observations for alpha diversity, including the emergence of treatment-specific clusters (Figure 4), irrespective of the dose of the two antibiotics. Overall, at least three distinct clusters were apparent in the PCoA plot for males and females. All control microbiota from all time points clustered together, whereas day 1 microbiota from animals treated with antibiotics formed a separate cluster. The days 7 and 28 microbiota from animals treated with antibiotics clustered together and separated both from controls and day 1 treated animals for both sexes. These observations have several implications: (1) Doripenem and meropenem have similar effects on bacterial taxa, confirming their common mode of action. (2) Beta diversity

composition on day 1 is different from days 7 and 28, suggesting that the treatment effects had not yet emerged on day 1. (3) A fourth cluster was observed, which was more distinct in females, that consisted of day 1 microbiota from the doripenem HD group and indicated a possible dose-response one day after the administration of doripenem HD. Upon prolonged exposure, this dose-dependency could no longer be observed. (4) Finally, microbiota from control animals on days 35 and 42/43 clustered together with the doripenem-recovery groups one and two weeks after the cessation of doripenem treatment.

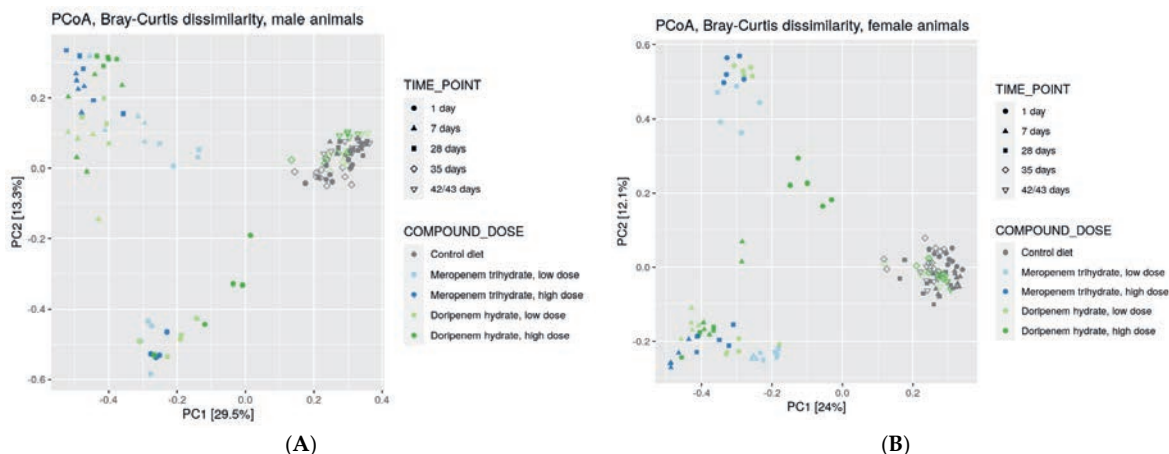


Figure 4. Principal Coordinate Analysis (PCoA) of bacterial families from controls, meropenem, and doripenem antibiotic-treated rats at different time points. Rank-based clustering with Bray-Curtis distance matrix of samples from (A) males and (B) females are presented.

3.3. Reduced Relative Bacterial Abundances Following Carbapenem Treatment is Reversible

Having established a general comparison of bacterial diversity between the control and different treatment groups, the relative abundances of different dominant bacterial families were evaluated (Figure 5). This revealed a profound inter-individual variability in relative levels of different bacterial families in all treatment and control groups. Bacterial abundance was reduced after day 1 treatment with both meropenem and doripenem and increased on days 7 and 28. Bacterial families including *Lactobacillaceae*, *Porphyromonadaceae*, and *Prevotellaceae* showed a strong depletion in microbiota from days 7 and 28 for all carbapenem treatment groups. For day 1 microbiota from the meropenem LD group, the start of a dysbiosis in the bacterial communities was observed in both sexes, whereas on days 7 and 28, the microbiota of the females reached a new and stable gut composition, whereas this took longer for males. Furthermore, the day 1 doripenem LD microbiota also exhibited an intermediate dysbiosis, whereas an altered but stable bacterial composition was observed on days 7 and 28 for both sexes. Such a transition or intermediate composition of the gut microbiome was not observed for the animals administered high doses of carbapenems.

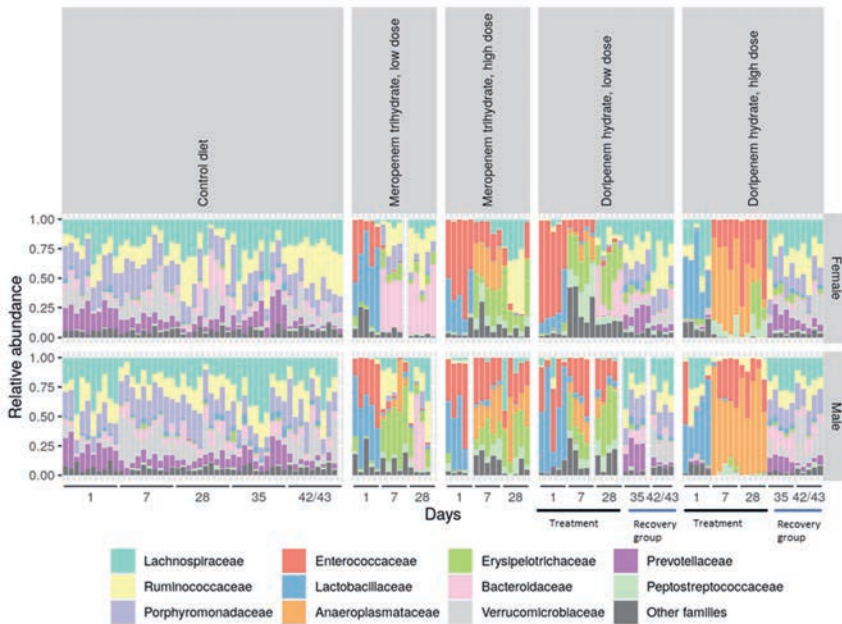


Figure 5. Stacked bar diagram showing relative abundances of the detected bacterial families in the different experimental groups. Inter-individual variability in the composition can be observed. Dose groups and sexes showed significant differences specifically in samples from days 1, 7, and 28 relative to the controls. Antibiotic-specific effects were observed on the intestinal community composition. For the doripenem group, treatment time points, i.e., days 1, 7, and 28, and recovery time points, i.e., 35 and 42/43, are highlighted with black and blue lines on the x-axis, respectively.

In the doripenem-recovery groups, bacterial abundances were comparable to the microbiota from the control group, whereas the microbiota on day 35 (one week after the stop of doripenem treatment) still showed minor differences. This observation was more pronounced in female animals (Figure 6). Overall, the analysis suggested that the bacterial abundances in microbiota after one and two weeks of the cessation of doripenem treatment in male rats may completely recover to have a 16S composition comparable to the control group. The doripenem-recovery groups also indicated a recovery two weeks after doripenem treatment was stopped in female animals.

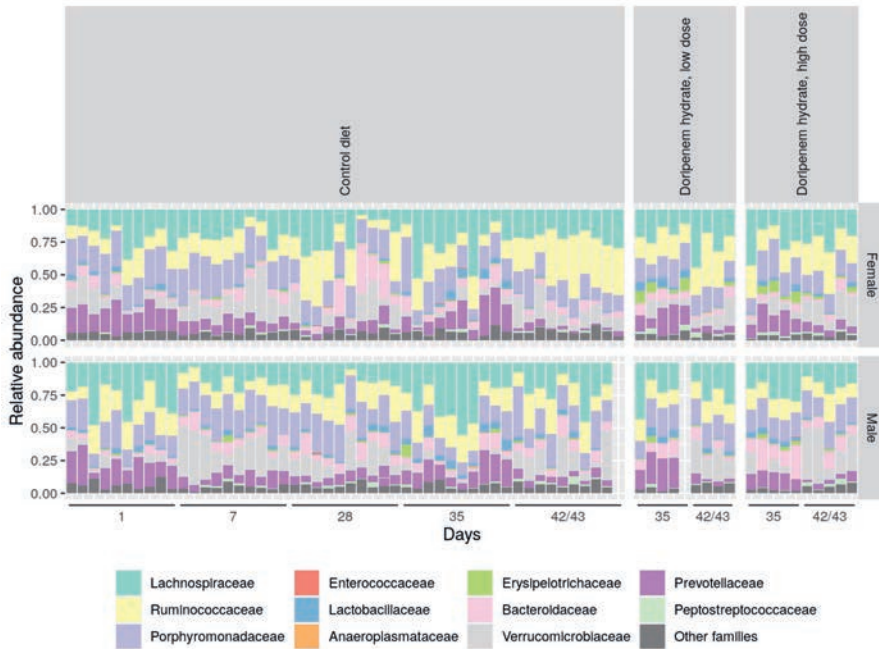


Figure 6. Stacked bar diagram showing relative abundances of bacterial families that were detected in the controls and doripenem-recovery groups. An indication of the recovery of abundant bacterial families one and two weeks post-doripenem treatment was observed and resulted in abundances comparable to the controls.

3.4. Differential Abundance Analyses Confirmed Spontaneous Recovery Post-Doripenem Cessation

Differential abundance analysis using the DESeq2 package was performed to identify whether increases or decreases in specific bacterial families were associated with specific treatment groups compared to the controls. The differential abundance analyses of both meropenem- and doripenem-treated microbiota on days 1, 7, and 28 of the study from both male and female animals can be found in the Supplementary Materials (Figure S2). The differential analyses confirmed an absence of differences compared to controls for the male rats given a recovery period, i.e., days 35 and 43 of the study (Figure 7A,B, respectively). These results indicated recovery of the previously altered bacterial families including *Lactobacillaceae*, *Porphyromonadaceae*, and *Prevotellaceae*, to their original or baseline levels after one week for males and persisting two weeks post-doripenem cessation. On the other hand, for females, after one-week post-doripenem cessation, there were still a few changes in bacterial families, including *Enterococcaceae* and *Aneroplasmataceae*, which both recovered fully two weeks post-doripenem cessation.

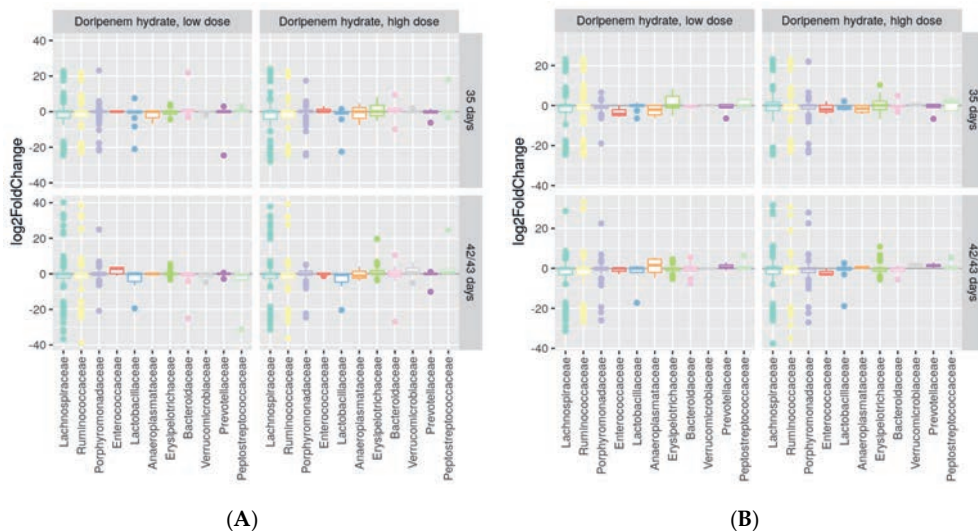


Figure 7. Differential abundances in dominant bacterial families one and two weeks post-doripenem-treated samples from the low- (LD) and high- (HD) dose groups relative to the controls for males (A) and females (B). Differential abundance analysis was performed using log₂FC (log₂ fold change) values.

3.5. Fecal Metabolomes Are Altered by Carbapenems and Spontaneously Recover after Doripenem Treatment Is Stopped

Principal Component Analysis or PCA plots of fecal metabolome data from days 7, 14, and 28 (Figure 8) indicated a clear separation between the controls and the antibiotic-treated animals in PC1. In the doripenem HD females, a further separation (separating in PC2) could be observed particularly for fecal metabolomes on days 14 and 28. The metabolome profiles of feces from the doripenem-recovery groups clustered together with the controls indicating full recovery of the fecal metabolome within one week after the cessation of treatment. This observation is in line with the conclusions from the 16S community analyses, specifically for the male rats where a full recovery was observed one week after doripenem cessation.

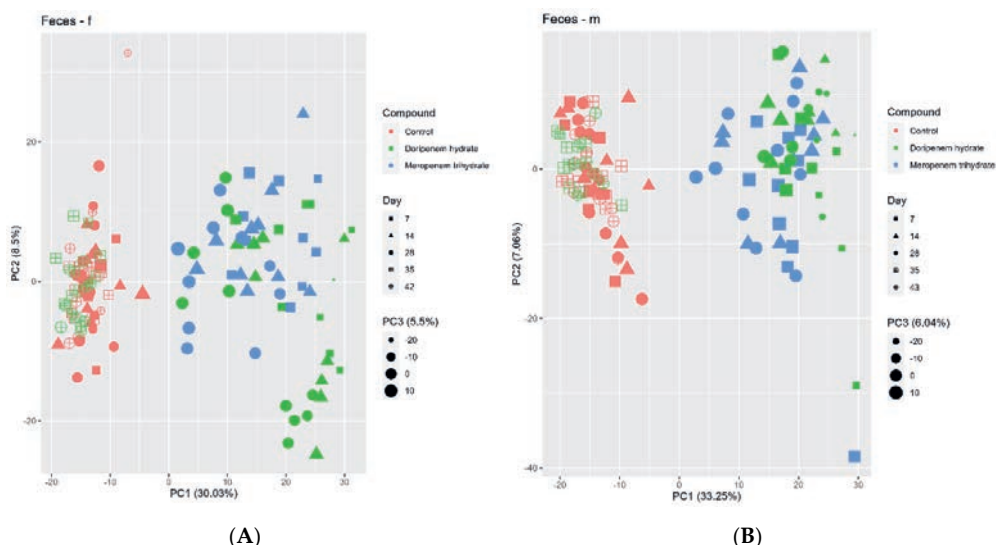


Figure 8. Principal component analysis (PCA) of the fecal metabolome profiles of controls (red), meropenem- (blue), and doripenem- (green) treated rats. PCA for fecal metabolome profiles of (A) female and (B) male Wistar rats on days 7, 14, and 28 of the study and days 35 and 42/43 for the doripenem-recovery group. The data points are sized by the PC3 value. Different shapes of the data points represent respective sampling time points. Dose group-specific effects were marginal, so the groups were not separated based on the dose levels.

3.5.1. Meropenem Trihydrate Treatment alters Fecal Bile Acids

The analysis of 620 different metabolites in feces revealed significant alterations upon antibiotic treatment. Of these, approx. 300 were significantly altered by the meropenem HD treatment in both sexes. The complete list of significantly changed fecal metabolites in meropenem-treated male and female animals is presented in the Supplementary Materials (Tables S1 and S2), where, for females in particular, the majority of the significantly changed fecal metabolites were amino acids, bile acids (BAs), lipids, energy metabolites, vitamins, and related metabolite classes. The list of significantly changed BAs in meropenem-treated female rats is presented in Table 2 using the HD group as reference for change against the controls. Of the 22 measured BAs, 11 were significantly changed compared to the control group, including the secondary (2°) BAs, deoxycholic acid (DCA), lithocholic acid (LCA), ω -muricholic acid (ω MCA), hyodeoxycholic acid (HDCA), and isoLCA. These 2° BAs were significantly reduced in the fecal metabolomes from almost all the sampling time points from both the meropenem LD and HD treatment groups. Several taurine-conjugated primary (1°) and 2° BAs were significantly increased; particularly, TCA (taurocholic acid sodium salt and taurocholic acid-3-sulfate) (TCA) was strongly and significantly increased in fecal metabolomes from all the time points from both the meropenem LD and HD treatment groups.

Table 2. Meropenem-induced BA fold changes in feces of female (f) Wistar rats (N = 5 per group) dosed with 100 (LD) and 300 (HD) mg/kg bw/day observed on days 7, 14, and 28 (f7, f14, and f28). Statistically significant changes (Welch *t*-test; *p*-value < 0.05) are shown where red boxes mean a significant increase, yellow boxes mean a significant decrease, and white boxes indicate an insignificant change in the respective fecal BAs.

Metabolite	Class	Meropenem Trihydrate HD			Meropenem Trihydrate LD		
		f7	f14	f28	f7	f14	f28
Deoxycholic acid	2° BA *	0.01	0.01	0.06	0.09	0.16	0.17
Cholic acid	1° BA *	10.78	9.57	7.33	17.48	1.14	0.91
Lithocholic acid	2° BA	0.02	0.03	0.02	0.08	0.15	0.15
Taurocholic acid sodium salt	Taurine-conjugated 1° BA	4.70	2.04	3.85	3.41	1.87	1.14
Taurolithocholic Acid	Taurine-conjugated 2° BA	0.04	0.12	0.15	0.41	0.61	0.78
Taurocholic Acid 3-sulfate	Taurine-conjugated 1° BA	185.39	197.22	280.09	40.98	81.49	6.10
Tauro- β -muricholic Acid	Taurine-conjugated 1° BA	3.51	2.01	3.42	2.14	1.30	1.10
Taurochenodeoxycholate	Taurine-conjugated 1° BA	2.08	1.43	2.60	1.71	1.56	1.17
Hyodeoxycholic acid	2° BA	0.01	0.01	0.01	0.02	0.01	0.04
o-Muricholic Acid	2° BA	0.19	0.04	0.03	0.60	0.12	0.13
isoLCA	2° BA	0.01	0.01	0.01	0.08	0.28	0.31

* 1° BA means primary bile acids, and 2° BA means secondary bile acids.

In males, almost 300 fecal metabolites were significantly changed, the majority of which belonged to amino acids, BAs, lipids, carbohydrates, energy metabolites, nucleobases, vitamins, and their derivatives. Similar to females, 11 out of the 22 measured fecal bile acids were observed to be significantly altered at a *p*-value < 0.05 (Table 3). In males, a significant reduction was observed in the 2° BAs, including DCA, LCA, ω MCA, HDCA, and isoLCA in both the meropenem LD and HD groups compared to the controls. A significant increase was observed in a few 1° BAs including CA, α -muricholic acid (α TMCA), and β -muricholic (β MCA) and also in some of the taurine-conjugated 1° BAs such as TCA and tauro- β -muricholic acid (T β MCA) on almost all sampling time points in both the meropenem LD and HD treatment groups.

Table 3. Meropenem-induced BA fold changes in feces of male Wistar rats (N = 5 per group) dosed with 100 (LD) and 300 (HD) mg/kg bw/day observed on days 7, 14, and 28 (m7, m14, and m28). Statistically significant changes (Welch *t*-test; *p*-value < 0.05) are shown where red boxes mean an increase, yellow boxes mean a significant decrease, and white boxes indicate an insignificant change in the respective fecal BAs.

Metabolite	Class	Meropenem Trihydrate HD			Meropenem Trihydrate LD		
		m7	m14	m28	m7	m14	m28
Deoxycholic acid	2° BA	0.01	0.01	0.00	0.20	0.21	0.24
Cholic acid	1° BA	13.78	22.75	33.78	4.61	5.80	7.61
Lithocholic acid	2° BA	0.02	0.03	0.02	0.13	0.10	0.08
Taurocholic acid sodium salt	Taurine-conjugated 1° BA	4.49	110.41	12.63	8.93	19.40	0.33
Taurocholic Acid 3-sulfate	Taurine-conjugated 1° BA	15.24	921.65	113.19	83.21	759.51	0.13
Tauro- β -muricholic Acid	Taurine-conjugated 1° BA	3.50	26.50	12.70	10.01	12.34	2.03
a-Muricholic Acid	1° BA	23.88	2.53	2.28	18.70	5.85	2.13
b-Muricholic Acid	1° BA	8.16	2.43	2.13	5.03	1.73	3.48
Hyodeoxycholic acid	2° BA	0.02	0.00	0.00	0.01	0.00	0.01
o-Muricholic Acid	2° BA	0.35	0.05	0.05	0.14	0.15	0.07
isoLCA	2° BA	0.01	0.01	0.01	0.14	0.19	0.14

Overall, the fecal metabolome of the meropenem-treated rats appeared to have strongly and significantly changed compared to the control group, which included significant changes in the BAs.

3.5.2. Doripenem Hydrate Treatment Significantly Alters Fecal BA Metabolites, Which Recover after the Cessation of Treatment

About 620 metabolites were measured in the fecal samples from the doripenem-treated Wistar rats, out of which about 350 fecal metabolites were significantly changed at a p -value < 0.05 in all groups. The majority of these fecal metabolites belong to amino acids, BAs, lipids, carbohydrates, nucleobases, vitamins, and their related classes. The complete list of fold changes in fecal metabolites is presented in the Supplementary Materials (Tables S3 and S4). Out of the 22 measured fecal BAs, 14 were significantly altered at a p -value < 0.05 in the HD-treated female rats (Table 4). This consisted of significantly reduced 2° BAs such as DCA, LCA, HDCA, ωMCA, and isoLCA. Consistently, taurine-conjugated 1° BAs including TCA, TβMCA, and taurochenodeoxycholate (TCDCA) were all significantly increased in fecal metabolomes from almost all time points, which was more prominent in the HD-treated females. Some taurine and glycine-conjugated 2° BAs such as tauroolithocholic acid (TLCA), taurodeoxycholate (TDCA), glycolithocholic acid (GLCA), and glycodeoxycholate (GDCA) were observed to be significantly reduced in both the LD and HD treatment groups.

In the female doripenem-recovery group, recovery of the formerly significantly changed fecal BAs could be observed, specifically in the LD recovery group (Table 4). However, a few of the BAs that were significantly decreased during the doripenem treatment period, i.e., LCA, isoLCA TCA, GLCA, and TCA, were still significantly altered after the recovery period and were actually increased. Likewise, there were examples in the opposite direction, i.e., some BAs that were significantly increase during the treatment period were significantly reduced compared to the controls after the recovery period. This overcompensation effect observed for the fecal metabolomes may relate to a possible metabolic feedback mechanism.

Table 4. Doripenem-induced BA fold changes in feces of female Wistar rats (N = 5 per group) dosed with 100 (LD) and 1000 (HD) mg/kg bw/day observed on days 7, 14, and 28 (f7, f14, and f28) and on days 35 and 42 (f35 and f42) for the recovery group. Statistically significant changes (Welch t -test; p -value < 0.05) are shown where red boxes mean an increase, yellow boxes mean a significant decrease, and white boxes indicate an insignificant change in the respective fecal BAs.

Metabolite	Class	Doripenem HD			Doripenem HD Recovery		Doripenem LD			Doripenem LD Recovery	
		f7	f14	f28	f35	f42	f7	f14	f28	f35	f42
Deoxycholic acid	2° BA	0	0	0	0.85	0.5	0.01	0	0.03	1.04	0.68
Cholic acid	1° BA	3.44	2.81	5.6	1.15	1.08	15.5	15.76	15.61	1.23	0.88
Lithocholic acid	2° BA	0.01	0.01	0.01	2.23	1.13	0.02	0.01	0.03	1.68	1.11
Taurocholic acid sodium salt	Taurine-conjugated 1° BA	8.1	6.65	5.78	0.09	0.37	3.83	2.12	2.46	0.28	0.85
Glycolithocholic Acid	Glycine-conjugated 2° BA	0.2	0.13	0.06	6.89	5.76	0.56	0.09	0.29	5.39	0.63
Taurolithocholic Acid	Taurine-conjugated 2° BA	0.03	0.02	0.01	0.9	2.66	0.2	0.03	0.4	1.25	0.89
Taurocholic Acid 3-sulfate	Taurine-conjugated 1° BA	395.06	302.06	28.52	1.03	0.91	139.94	156.93	16.82	2.13	1.32

Tauro-b-muricholic Acid	Taurine-conjugated 1° BA	6.8	4.47	2.27	0.39	0.82	2.02	1.59	1.73	0.82	0.85
Taurochenodeoxycholate	Taurine-conjugated 1° BA	1.65	1.94	1.95	0.92	0.86	1.63	1.18	1.87	0.98	0.77
Taurodeoxycholate	Taurine-conjugated 2° BA	0.54	0.46	0.49	0.66	0.64	0.55	0.48	0.46	0.66	0.69
Glycodeoxycholate	Glycine-conjugated 2° BA	0.46	0.33	0.35	1.48	1.28	0.45	0.26	0.39	1.05	0.93
Hyodeoxycholic acid	2° BA	0	0	0	6.9	3	0.03	0	0.01	1.82	0.49
o-Muricholic Acid	2° BA	0.01	0	0.01	0.74	0.08	0.28	0.08	0.08	1.3	1.25
isoLCA	2° BA	0	0	0.01	3.18	1.5	0.01	0	0.02	1.63	1.2

The doripenem-treated male rats showed significant changes in about 320 fecal metabolites at a p -value < 0.05 . The majority of these metabolites belonged to amino acids, BAs, carbohydrates, lipids, energy metabolites, nucleobases, vitamins, and their derivatives. The list of significantly changed fecal BAs in samples from the doripenem LD- and HD-treated males and from the doripenem-recovery group relative to the controls at a p -value < 0.05 is presented in Table 5. A total of nine significantly changed BAs were observed in males which includes 2° BAs such as DCA, LCA, HDCA, ωMCA, and isoLCA, consistent with females treated with the doripenem antibiotic. Compared to females, a lower number of changes in the conjugated 1° and 2° BAs were observed in males. The 1° BA, CA, and a few taurine-conjugated 1° BAs including TCA and TβMCA were significantly increased in the doripenem LD- and HD-treated male rats compared to the controls. Other than in females, the fecal metabolome of the doripenem-recovery males showed a virtually full recovery on day 43. The observed statistically significant decrease in isoLCA is of questionable nature as such an effect was not seen on day 35 (Table 5). In addition, in the doripenem HD day 35 recovery group, two fecal BAs, HDCA and ωMCA, were significantly changed.

Table 5. Doripenem-induced BA fold changes in feces of male Wistar rats (N = 5 per group) dosed with 100 (LD) and 1000 (HD) mg/kg bw/day observed on days 7, 14, 28 (m7, m14 and m28) and on days 35 and 42 (m35 and m43) for the doripenem-recovery group. Statistically significant changes (Welch t -test; p -value < 0.05) are shown where red boxes mean an increase, yellow boxes mean a significant decrease, and white boxes indicate an insignificant change in the respective fecal BAs.

Metabolite	Class	Doripenem HD			Doripenem HD Recovery		Doripenem LD			Doripenem LD Recovery	
		m7	m14	m28	m35	m43	m7	m14	m28	m35	m43
Deoxycholic acid	2° BA	0.01	0	0.01	0.77	1.15	0.01	0	0	0.91	0.78
Cholic acid	1° BA	14.31	26.92	5.47	0.98	0.87	15.34	20.97	14.38	1	0.47
Lithocholic acid	2° BA	0.02	0.02	0.02	1.09	1.07	0.02	0.02	0.02	1.07	0.74
Taurocholic acid sodium salt	Taurine-conjugated 1° BA	16.62	73.02	11.51	0.5	0.2	6.14	15.13	4.85	0.76	0.38
Taurocholic Acid 3-sulfate	Taurine-conjugated 1° BA	142.02	1738.7	129.59	2.24	0.37	20.83	85.11	43.38	1.52	0.12
Tauro-b-muricholic Acid	Taurine-conjugated 1° BA	20.19	148.81	40.8	0.7	0.67	4.03	6.14	2.65	0.64	0.45
Hyodeoxycholic acid	2° BA	0.01	0	0.01	0.23	0.84	0.01	0	0.01	0.58	0.45
o-Muricholic Acid	2° BA	0.08	0	0	2	1.32	0.14	0.03	0.02	1.05	0.6
isoLCA	2° BA	0.01	0	0	0.78	0.89	0	0	0.01	0.96	0.55

3.6. Plasma Metabolome Analysis Also Shows Some Effects of Both Carbapenems on Key Plasma Metabolites and Plasma Bile Acid Levels Followed by a Recovery in the Doripenem-Recovery Group

The plasma metabolome profiles of the controls and antibiotic treatment groups were analyzed using PCA (Figure 9). Although the separation between the different treatments and controls was not very strong, the plasma metabolome of the control group formed a separate cluster. For males, a good separation between both the treatments and controls (in PC2) can be observed. In addition, there is also some form of separation between the doripenem and meropenem treatment groups (PC1 / PC2). For females, a separation of both treatments from the controls can be seen (in PC2) with, however, a few exceptions (all related to meropenem). For both sexes overall, the doripenem groups are better separated from the controls indicating a possible stronger effect of doripenem on the plasma metabolome profiles of the male and female Wistar rats. There is no clear separation on PC1 for both treatments. The samples from the doripenem-recovery group (i.e., on day 42/43 of the study) clustered together with the controls, which is consistent with the results of the 16S community analysis and fecal metabolome analysis, indicating recovery from the treatment-related changes.

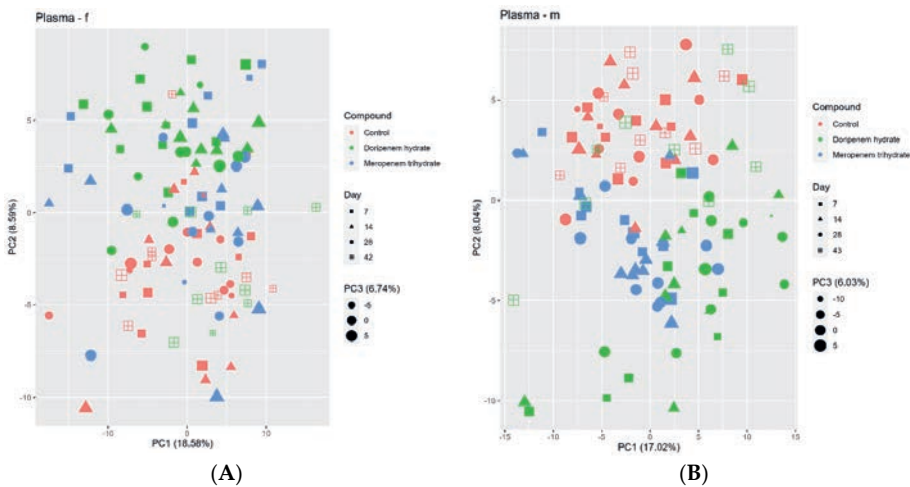


Figure 9. Principal component analysis (PCA) of the blood plasma metabolome profiles of controls (red), meropenem- (blue), and doripenem- (green) treated rats. PCA for plasma metabolome profiles of (A) female and (B) male Wistar rats on days 7, 14, and 28 of the study and on day 42/43 for the doripenem-recovery group. The data points are sized by the PC3 value. Different shapes of the data points represent respective sampling time points. Dose group-specific effects were marginal, so the groups were not separated based on the dose levels.

3.6.1. Meropenem Trihydrate Treatment Alters Key Plasma Biomarkers of Microbiota Alterations

An in-depth analysis of individual plasma metabolites, including BAs that were significantly altered in the meropenem group (p -value < 0.05), was performed. Of 294 measured blood plasma metabolites, 27 were significantly altered in the meropenem HD treatment groups in females and 25 in males (Tables 6 and 7). These were determined by comparing the HD group with the controls and subsequently

analyzing the values of these metabolites for the LD. Most of these altered metabolites belonged to amino acids, BAs, carbohydrates, energy metabolites, hormones, and their derivatives.

Table 6. Meropenem-induced plasma metabolite fold changes in female (f) Wistar rats (N = 5 per group) dosed with 100 (LD) and 300 (HD) mg/kg bw/day observed on 7, 14, and 28 days (f7, f14, and f28). Statistically significant changes (Welch *t*-test; *p*-value < 0.05) are shown where red boxes mean a significant increase in the respective plasma metabolites and yellow boxes mean a significant reduction compared to control levels.

Metabolite	Class	Meropenem Trihydrate HD			Meropenem Trihydrate LD		
		f7	f14	f28	f7	f14	f28
Threonine	Amino acids	0.87	0.80	0.84	0.93	0.99	1.05
Glycine	Amino acids	0.92	0.89	0.87	0.86	0.87	0.97
Threonine	Amino acids	0.83	0.82	0.84	0.99	0.94	1.03
Cysteine	Amino acids	0.85	1.03	0.93	0.92	1.11	1.08
3-Hydroxyindole	Amino acids-related	0.11	0.10	0.24	0.86	0.45	0.97
Indole-3-acetic acid	Amino acids-related	5.60	4.82	5.66	1.68	2.44	1.94
3-Indoxylsulfate	Amino acids-related	0.10	0.15	0.27	0.87	0.59	1.10
Deoxyribonucleic acids, total	Carbohydrates and related	0.81	0.93	1.06	0.79	0.91	0.73
Xylitol	Carbohydrates and related	1.64	1.52	1.54	0.84	0.76	1.41
3-Hydroxybutyrate	Energy metabolism and related	1.30	1.23	0.97	1.13	1.04	0.96
3-Hydroxybutyrate	Energy metabolism and related	1.41	1.32	1.15	1.29	1.12	1.02
3-Methoxytyrosine	Hormones, signal substances and related	1.43	1.44	1.44	1.18	1.20	1.24
17-Hydroxypregnenolone	Hormones, signal substances and related	0.02	0.01	0.03	0.02	0.03	0.02
Hippuric acid	Miscellaneous	0.24	0.24	0.43	0.48	0.53	0.99
Cytosine	Nucleobases and related	0.78	0.77	1.08	0.76	0.78	0.78

Table 7. Meropenem-induced plasma BA fold changes in female (f) Wistar rats (N = 5 per group) dosed with 100 (LD) and 300 (HD) mg/kg bw/day observed on 7, 14, and 28 days (f7, f14, and f28). Statistically significant changes (Welch *t*-test; *p*-value < 0.05) are shown where red boxes mean a significant increase in the respective plasma BAs and yellow boxes mean a significant reduction compared to control levels.

Metabolite	Class	Meropenem Trihydrate HD			Meropenem Trihydrate LD		
		f7	f14	f28	f7	f14	f28
Deoxycholic acid	2° BA	0.04	0.04	0.24	0.49	0.82	1.03
Lithocholic acid	2° BA	0.01	0.02	0.05	1.04	0.72	1.82
Taurolithocholic Acid	Taurine-conjugated 2° BA	0.01	0.03	0.07	0.07	0.19	0.26
Tauroursodeoxycholic Acid	Taurine-conjugated 2° BA	3.49	1.83	6.66	5.30	2.14	8.83
Taurodeoxycholate	Taurine-conjugated 2° BA	0.00	0.00	0.04	0.08	0.14	0.32
Glycocholic acid	Glycine-conjugated 1° BA	4.30	1.82	5.16	2.28	3.68	3.61
Glycochenodeoxycholic acid	Glycine-conjugated 1° BA	8.51	2.62	13.20	10.69	16.07	12.32
Glycodeoxycholate	Glycine-conjugated 2° BA	0.05	0.14	0.39	0.57	2.94	3.19
Glycoursodeoxycholic acid	Glycine-conjugated 2° BA	22.25	11.61	35.10	10.72	32.78	24.98
Hyodeoxycholic acid	2° BA	0.03	0.03	0.03	0.14	0.05	0.18
o-Muricholic Acid	2° BA	0.20	0.16	0.29	0.88	0.23	1.21
isoLCA	2° BA	0.06	0.48	0.34	0.07	0.35	0.72

In the plasma metabolomes of female animals, some of the gut microbiome-associated key plasma biomarkers, as determined in previous studies, were observed to be significantly changed [11, 14, 15]. These biomarkers include indole-3-acetic acid (IAA), 3-indoxylsulfate (3IS), hippuric acid (HA), and 3-hydroxybutyrate. In particular, 3IS and HA were significantly reduced in the meropenem HD- and

LD-treated females, especially in plasma metabolomes on days 7 and 14. IAA showed a slight yet significant increase in the meropenem treatment groups at almost all sampling time points, while 3-hydroxybutyrate showed only a significant increase in plasma metabolomes on days 7 and 14 in the meropenem HD treatment group relative to the controls. Other essential gut microbiome-associated metabolites, such as BAs, were significantly changed in the meropenem treatment group relative to the controls. Overall, a stronger effect on plasma metabolites was seen in the HD group. The list of 12 significantly altered plasma BAs out of the 22 measured BAs in the meropenem-treated females is listed in Table 6.

The 2° BAs including DCA, LCA, HDCA, ωMCA, and isoLCA were all significantly reduced specifically in all the samples from the meropenem HD-treated females. Taurine-conjugated 2° BAs including TLCA and TDCA were significantly reduced, whereas tauroursodeoxycholic acid (TUDCA) was significantly increased in the treated females. Unlike feces, plasma did not show any significant changes in TCA. Three of the four glycine-conjugated 1° and 2° plasma BAs were increased and one was decreased, none of which were changed in the feces of the treated females.

As indicated earlier, for males treated with meropenem, 25 out of the 294 measured plasma metabolites were significantly altered. The majority of these plasma metabolites belonged to amino acids, BAs, lipids, energy metabolites, hormones, and relative classes (Tables 8 and 9). In males, three of the plasma key metabolites were significantly changed, including 3IS, IAA, and HA, where HA and 3IS were reduced and IAA was increased in the meropenem-treated males compared to the controls. However, none of the other key biomarkers appeared on the list. In addition, 14 out of the 22 measured plasma BAs were significantly changed in the meropenem-treated males (Table 9). For males, a dose–response relationship was also noted.

Table 8. Meropenem-induced plasma metabolite fold changes in male (m) Wistar rats (N = 5 per group) dosed with 100 (LD) and 300 (HD) mg/kg bw/day observed on 7, 14, and 28 days (m7, m14, and m28). Statistically significant changes (Welch *t*-test; *p*-value < 0.05) are shown where red boxes mean a significant increase in the respective plasma metabolites and yellow boxes mean a significant reduction compared to control levels.

Metabolite	Class	Meropenem trihydrate HD			Meropenem trihydrate LD		
		m7	m14	m28	m7	m14	m28
Threonine	Amino acids	0.86	0.82	0.75	0.90	1.04	0.97
Threonine	Amino acids	0.93	0.78	0.75	0.89	0.98	0.92
Methionine	Amino acids	0.97	0.88	0.88	1.02	0.98	1.05
3-Indoxylsulfate	Amino acids-related	0.11	0.11	0.09	0.74	0.63	0.46
Indole-3-acetic acid	Amino acids-related	3.02	6.51	9.41	5.03	4.17	6.45
3-Hydroxyindole	Amino acids-related	0.12	0.11	0.14	1.07	0.64	0.48
Lysophosphatidylcholine (C18:2)	Complex lipids, fatty acids and related	1.07	0.96	1.14	0.97	0.96	1.17
Citrate	Energy metabolism and related	1.09	1.17	1.17	1.04	1.11	1.28
Cortisol	Hormones, signal substances and related	3.36	2.72	4.95	1.43	1.69	2.21
Corticosterone	Hormones, signal substances and related	2.68	1.64	1.65	2.90	2.15	2.34

18-Hydroxy-11-deoxycorticosterone	Hormones, signal substances and related	2.16	1.52	1.27	2.44	2.61	2.40
Hippuric acid	Miscellaneous	0.52	0.33	0.53	0.27	0.41	0.32

Consistent with the observations for females, the 2° BAs including DCA, LCA, HDCA, ωMCA, and isoLCA were all significantly reduced specifically in the plasma metabolomes on days 7 and 14 for the meropenem HD- and day 28 for the meropenem LD-treated males. Several taurine-conjugated 1° (TCA, TβMCA, and TCDCA) and 2° plasma BAs (TCA, TDCA, and TUDCA), and one glycine-conjugated 2° BA, GDCA, were significantly changed specifically in males treated with meropenem HD relative to the controls. TLCA, TDCA, and GDCA were significantly reduced specifically in the plasma metabolomes on days 7 and 28 of the meropenem HD-treated males compared to the controls, whereas TβMCA and TCDCA were significantly increased at all time points for the meropenem HD-treated males. Compared to females, marginal changes were observed in the plasma BAs in the meropenem LD- and HD-treated males at all sampling time points.

Table 9. Meropenem-induced blood plasma BA fold changes in male (m) Wistar rats. Metabolite fold changes in plasma BAs of male Wistar rats (N = 5 per group) dosed with meropenem (100 (LD) and 300 (HD) mg/kg bw/day) observed on 7, 14, and 28 days (m7, m14, and m28). Statistically significant changes (Welch *t*-test; *p*-value < 0.05) are shown where red boxes mean a significant increase in the respective plasma BAs and yellow boxes mean a significant reduction compared to control levels.

Metabolite	Class	Meropenem Trihydrate HD			Meropenem Trihydrate LD		
		m7	m14	m28	m7	m14	m28
Ursodeoxycholic acid	2° BA	1.54	8.42	3.22	2.41	4.27	2.23
Deoxycholic acid	2° BA	0.01	NA	0.02	0.46	1.84	0.29
Lithocholic acid	2° BA	0.02	0.14	0.02	0.14	0.59	0.07
Taurolithocholic Acid	Taurine-conjugated 2° BA	0.05	0.08	0.08	0.16	0.16	0.31
Taurocholic Acid 3-sulfate	Taurine-conjugated 1° BA	0.22	1.10	0.31	0.65	0.30	0.34
Tauro- <i>b</i> -muricholic Acid	Taurine-conjugated 1° BA	1.73	4.06	1.96	0.95	1.03	1.10
Tauroursodeoxycholic Acid	Taurine-conjugated 2° BA	1.25	7.42	5.90	1.44	1.18	0.63
<i>b</i> -Muricholic Acid	1° BA	1.45	3.56	2.23	1.51	1.65	1.88
Taurochenodeoxycholate	Taurine-conjugated 1° BA	2.42	3.53	2.05	1.17	0.68	1.22
Taurodeoxycholate	Taurine-conjugated 2° BA	0.02	0.00	0.03	0.10	0.21	0.10
Glycodeoxycholate	Glycine-conjugated 2° BA	0.01	NA	0.01	0.64	3.02	0.09
Hyodeoxycholic acid	2° BA	0.01	0.03	0.01	0.03	0.01	0.00
<i>o</i> -Muricholic Acid	2° BA	0.11	1.23	0.07	0.12	0.14	0.09
isoLCA	2° BA	0.26	2.59	0.12	0.29	0.44	0.35

3.6.2. Doripenem Hydrate Treatment Significantly Alters Plasma Metabolites during Treatment and the Metabolites Recover after Doripenem Administration is Stopped

Significant changes (*p* < 0.05) in plasma metabolites of doripenem-treated animals were observed on days 7, 14, and 28 of treatment (Tables 10 and 11). Among the several measured metabolites, the majority of the significantly changed ones belonged to amino acids, BAs, carbohydrates, lipids, energy metabolites, signal substances, nucleobases, and their derivatives. These also included key plasma biomarkers associated with the perturbed gut microbiota, that have been previously reported. Among

the known plasma biomarkers, indole-3-propionic acid (IPA), 3IS, and HA were observed to be significantly reduced in plasma metabolomes from days 7, 14, and 28 [11, 14, 15].

Plasma metabolites on day 42 doripenem-recovery group in females (two weeks of no exposure), recovered after the doripenem administration was stopped. Although the metabolites from the LD group recovered fully, in the HD group, there were two metabolites that were not fully recovered. Two further metabolites, HA and TCA, were changed in the opposite direction in the HD group two-weeks post-doripenem cessation as compared to the doripenem-treated HD groups.

Table 10. Doripenem-induced plasma metabolite fold changes in female (f) Wistar rats (N = 5 per group) dosed with 100 (LD) and 1000 (HD) mg/kg bw/day observed on days 7, 14, and 28 (f7, f14, and f28) and on day 42 (f42) from the doripenem-recovery group. Statistically significant changes (Welch *t*-test; *p*-value < 0.05) are shown where red boxes mean a significant increase, yellow boxes mean a significant decrease, and white boxes indicate an insignificant change in the respective plasma metabolites compared to control group.

Metabolite	Class	Doripenem				Doripenem			
		HD			Recovery	LD			Recovery
		f7	f14	f28	f42	f7	f14	f28	f42
Tyrosine	Amino acids	1.11	0.79	0.75	0.84	0.83	0.83	0.97	1.12
Threonine	Amino acids	0.83	0.77	0.80	1.06	0.92	0.90	0.90	1.02
Tyrosine	Amino acids	0.88	0.82	0.80	0.84	0.86	0.86	0.95	0.98
trans-4-Hydroxyproline	Amino acids-related	0.90	0.81	0.89	1.07	1.11	0.93	0.93	1.14
3-Hydroxyindole	Amino acids-related	0.09	0.09	0.06	0.79	0.31	0.55	0.63	0.72
Ketoleucine	Amino acids-related	0.67	0.76	0.71	0.79	0.81	0.74	0.88	0.96
Indole-3-propionic acid	Amino acids-related	0.85	0.87	0.66	0.77	1.74	0.93	0.93	0.90
3-Indoxylsulfate	Amino acids-related	0.06	0.04	0.03	0.96	0.24	0.37	0.66	0.93
Deoxyribonucleic acids, total	Carbohydrates and related	0.76	0.92	0.72	0.99	0.79	0.80	0.78	0.91
Ceramide (d18:1,C24:1)	Complex lipids, fatty acids and related	0.80	0.71	0.74	1.27	1.20	1.29	1.37	1.06
Ceramide (d18:1,C24:0)	Complex lipids, fatty acids and related	0.73	0.68	0.62	1.25	1.02	1.25	1.19	1.09
Citrate	Energy metabolism and related	1.09	1.26	1.26	1.09	1.05	1.10	1.12	0.98
2-Hydroxybutyrate	Energy metabolism and related	1.55	1.60	2.09	1.17	1.37	1.52	1.14	0.73
3-Methoxytyrosine	Hormones, signal substances and related	1.10	1.22	1.2	1.26	1.38	1.41	1.05	1.10
17-Hydroxypregnenolone	Hormones, signal substances and related	0.01	0.01	0.02	0.83	0.01	0.04	0.53	1.25
beta-Sitosterol, total	Miscellaneous	0.62	0.74	0.74	1.12	1.01	1.07	0.80	1.13
Hippuric acid	Miscellaneous	0.23	0.25	0.48	1.58	0.39	0.32	0.52	1.00
Cytosine	Nucleobases and related	0.86	0.77	0.71	0.88	0.89	0.64	0.83	0.75
Allantoin	Nucleobases and related	0.75	0.89	0.86	1.01	0.73	0.82	1.01	0.97
Cholesterol, total		0.84	0.99	0.69	1.32	1.04	1.30	0.83	1.15

Of the 22 measured plasma BAs in the HD doripenem-treated female rats, 12 were significantly altered at a *p* < 0.05 (Table 11). The 2° BAs including DCA, HDCA, ωMCA, and isoLCA were significantly changed at all time points. The list also consisted mostly of the taurine-conjugated 1° and 2° BAs, including significant increases in TCA, TβMCA, and TCDCA and a reduction in TLCA, TUDCA, and TDCA in the HD-treated female animals. Plasma BAs in the **doripenem-recovery group** also recovered. As also noted in the females, a few BAs in the males, i.e., GLCA, TLCA, HDCA, and

isoLCA, were increased in the HD-recovery group, while they were reduced during the treatment phase. In the LD group, only GLCA showed this overcompensation, whereas all other BAs in the LD-recovery group were not significantly different from the controls. This dose-response observation confirmed that this overcompensation is a real effect.

Table 11. Doripenem-induced plasma BA fold changes in female (f) Wistar rats (N = 5 per group) dosed with 100 (LD) and 1000 (HD) mg/kg bw/day observed on days 7, 14, and 28 (f7, f14, and f28) and on day 42 (f42) for the doripenem-recovery group. Statistically significant changes (Welch *t*-test; *p*-value < 0.05) are shown where red boxes mean a significant increase, yellow boxes mean a significant decrease, and white boxes indicate an insignificant change in the respective plasma BAs compared to control groups.

Metabolite	Class	Doripenem							
		Doripenem HD			Doripenem HD Recovery		Doripenem LD		
		f7	f14	f28	f42	f7	f14	f28	f42
Deoxycholic acid	2° BA	0.02	0.02	0.03	3.41	0.02	0.06	0.32	2.57
Taurocholic acid sodium salt	Taurine-conjugated 1° BA	0.99	3.46	1.88	0.44	0.68	0.66	0.76	0.49
Glycolithocholic Acid	Glycine-conjugated 2° BA	0.11	0.12	0.33	9.27	0.04	0.37	1.26	13.31
Taurolithocholic Acid	Taurine-conjugated 2° BA	0.01	0.01	0.04	3.43	0.01	0.03	0.18	1.32
Taurocholic Acid 3-sulfate	Taurine-conjugated 1° BA	1.68	2.09	2.41	0.98	1.26	1.83	2.24	1.62
Tauro-b-muricholic Acid	Taurine-conjugated 1° BA	1.24	6.05	2.74	0.78	1.48	1.52	1.22	1.21
Tauroursodeoxycholic Acid	Taurine-conjugated 2° BA	14.68	7.45	17.31	3.88	5.43	2.66	11.53	0.97
Taurochenodeoxycholate	Taurine-conjugated 1° BA	1.29	2.94	1.91	1.30	1.38	1.33	1.28	1.12
Taurodeoxycholate	Taurine-conjugated 2° BA	0.00	0.00	0.01	0.65	0.00	0.00	0.05	0.68
Hyodeoxycholic acid	2° BA	0.02	0.01	0.01	19.38	0.05	0.01	0.02	2.55
o-Muricholic Acid	2° BA	0.11	0.08	0.14	0.66	0.16	0.13	0.45	1.98
isoLCA	2° BA	0.08	0.27	0.23	3.90	0.07	0.10	0.13	3.06

In the HD males, 40 out of the 294 measured plasma metabolites were significantly changed in samples on days 7, 14, and 28 (Table 12). These included metabolites belonging to amino acids, BAs, carbohydrates, lipids, energy metabolites, signal substances, nucleobases, vitamins, and their derivatives and a dose-response was observed. Furthermore, among the significantly changed plasma metabolites, some of the key biomarkers including 3IS and HA were observed to be reduced at all time points in the doripenem HD males. Plasma metabolites on day 42 from the doripenem-LD recovery males showed complete recovery without any over-compensation. In the doripenem-HD recovery group, 3 metabolites did not fully recover (tyrosine, glucose, and xylitol), whereas two other metabolites, 3-hydroxyindole and HA, showed an over-compensation as they were significantly changed in the opposite direction (i.e., were increased in the recovery group, while decreased under treatment).

Table 12. Doripenem-induced plasma metabolite fold changes in male (m) Wistar rats (N = 5 per group) dosed with 100 (LD) and 1000 (HD) mg/kg bw/day observed on days 7, 14, and 28 (m7, m14, and m28) and on day 42 (m42) for the doripenem-recovery group. Statistically significant changes (Welch *t*-test; *p*-value < 0.05) are shown where red boxes mean a significant increase, yellow boxes mean a significant decrease, and white boxes indicate an insignificant change in the respective plasma metabolites compared to control group.

	Doripenem HD	Doripenem		Doripenem LD	Doripenem LD
		HD	LD		
		Recovery	Recovery		Recovery

Metabolite	Class	m7	m14	m28	m43	m7	m14	m28	m43
Tyrosine	Amino acids	0.71	0.95	0.8	0.86	0.83	1.07	0.82	0.93
Alanine	Amino acids	0.76	0.9	1	0.90	0.9	0.86	0.96	0.96
Glycine	Amino acids	0.87	0.94	0.81	1.00	0.89	0.82	0.77	0.97
Threonine	Amino acids	0.77	0.99	0.81	1.05	0.84	0.83	0.78	0.89
Tyrosine	Amino acids	0.75	0.77	0.76	0.97	0.83	1	0.92	0.94
3-Hydroxyindole	Amino acids-related	0.12	0.08	0.1	1.40	0.2	0.59	0.58	1.18
3-Hydroxyisobutyrate	Amino acids-related	0.99	0.83	0.72	0.95	0.86	0.92	0.76	1.12
Ketoleucine	Amino acids-related	0.67	0.68	0.86	0.80	0.84	0.82	0.9	0.74
3-Indoxylsulfate	Amino acids-related	0.2	0.05	0.18	1.08	0.18	0.73	0.48	0.88
Deoxyribonucleic acids, total	Carbohydrates and related	0.85	0.8	0.8	1.01	1.09	0.88	0.9	1.06
Glucose	Carbohydrates and related	0.68	0.59	0.68	0.68	0.91	0.72	0.81	1.06
Xylitol	Carbohydrates and related	0.69	0.4	0.69	0.60	0.93	0.62	0.52	1.03
Taurocholic acid	Complex lipids, fatty acids and related	4.45	6.15	4.22	0.51	1.67	1.41	0.95	1.41
Docosapentaenoic acid (C22: cis [7,10,13,16,19]5)	Complex lipids, fatty acids and related	0.86	0.65	0.58	1.13	0.8	0.67	0.64	0.49
Lysophosphatidylcholine (C20:4)	Complex lipids, fatty acids and related	0.94	0.77	0.84	1.13	0.95	0.9	0.85	0.84
Pyruvate	Energy metabolism and related	1.5	2.23	1.25	1.17	2.03	2.18	1.27	1.53
Pyruvate	Energy metabolism and related	1.52	2.26	1.06	1.43	2.49	2.87	1.32	1.62
Lactate	Energy metabolism and related	0.59	0.8	0.74	0.97	0.83	0.99	0.91	1.01
3-Phosphoglycerate (3-PGA)	Energy metabolism and related	0.43	0.27	0.72	0.83	0.56	0.35	0.92	0.94
Pregnenolone	Hormones, signal substances and related	0.52	0.49	0.38	0.77	1.04	0.89	1.04	0.78
Hippuric acid	Miscellaneous	0.31	0.31	0.46	1.67	0.38	0.42	0.32	0.99
Uric acid	Nucleobases and related	0.8	0.81	0.91	0.83	0.8	0.75	0.94	0.94
Cytosine	Nucleobases and related	0.78	0.81	0.85	0.97	1.03	0.93	0.95	1.06
Uric acid	Nucleobases and related	0.71	0.59	0.76	0.74	0.72	0.72	0.89	0.88
Threonic acid	Vitamins, cofactors and related	0.5	0.58	0.71	0.84	0.68	0.68	0.84	1.11
Phosphatidylcholine (C18:0,C20:3)		0.85	0.72	0.64	1.28	0.78	0.64	0.7	0.79

Seventeen out of the twenty-two measured plasma BAs were significantly altered in the doripenem-treated males ($p < 0.05$). The list consisted of several 2° Bas, including ursodeoxycholic acid (UDCA), DCA, HDCA, and ω MCA, that are observed to be significantly reduced specifically in the HD-treated males (Table 13). Three 1° BAs, CA, chenodeoxycholic acid (CDCA), and α -muricholic acid (α MCA), were significantly reduced in the HD group. Additionally, many conjugated BAs including taurine- and glycine-conjugated 1° and 2° BAs were also significantly altered in the doripenem-treated males, specifically in the HD group.

Table 13. Doripenem-induced plasma BA fold changes in male (m) Wistar rats (N = 5 per group) dosed with 100 (LD) and 1000 (HD) mg/kg bw/day observed on days 7, 14, and 28 (m7, m14, and m28) and on day 42 (m42) for the doripenem-recovery group. Statistically significant changes (Welch *t*-test; p -value < 0.05) are shown where red boxes mean a significant increase, yellow boxes mean a significant decrease, and white boxes indicate an insignificant change in the respective plasma metabolites compared to the control group in the respective plasma BAs.

Metabolite	Class	Doripenem				Doripenem			
		HD		HD Recovery	LD		LD Recovery		
		m7	m14	m28	m43	m7	m14	m28	m43
Ursodeoxycholic acid	2° BA	0.09	0.38	0.18	0.55	1.11	5.52	2.15	0.13
Deoxycholic acid	2° BA	0	0	0.01	1.28	0.01	0.02	0.01	0.32

Cholic acid	1° BA	0.03	0.06	0.03	1.13	0.77	1.5	0.6	0.09
Chenodeoxycholic acid	1° BA	0.05	0.05	0.05	0.91	0.55	1.12	0.56	3.64
Taurocholic acid sodium salt	Taurine-conjugated 1° BA	3.6	3.71	4.27	0.68	2.27	0.86	0.83	1.41
Glycolithocholic Acid	Glycine-conjugated 2° BA	0.08	0.24	0.23	0.69	0.2	0.24	0.12	0.21
Taurolithocholic Acid	Taurine-conjugated 2° BA	0.06	0.1	0.21	1.16	0.06	0.06	0.07	0.69
Tauro-b-muricholic Acid	Taurine-conjugated 1° BA	4.21	4.48	4.86	0.90	2.46	1.4	1.19	1.39
Tauroursodeoxycholic Acid	Taurine-conjugated 2° BA	5.01	2.21	4.79	0.85	1.71	1.38	1.66	0.99
a-Muricholic Acid	1° BA	0.05	0.07	0.04	2.08	0.52	2.79	0.95	0.29
Taurochenodeoxycholate	Taurine-conjugated 1° BA	3.13	3.6	3.24	0.63	2.47	1.1	1.26	0.94
Taurodeoxycholate	Taurine-conjugated 2° BA	0.02	0.02	0.03	1.39	0.02	0.02	0.02	1.15
Glycocholic acid	Glycine-conjugated 1° BA	0.37	0.16	0.31	1.63	0.65	0.74	0.72	0.28
Glycochenodeoxycholic acid	Glycine-conjugated 1° BA	0.32	0.12	0.2	0.78	0.62	0.76	0.55	0.41
Glycodeoxycholate	Glycine-conjugated 2° BA	0	0	NA	0.45	0	0	0	0.30
Hyodeoxycholic acid	2° BA	0.04	0	0	0.48	0.01	0.01	0	0.72
o-Muricholic Acid	2° BA	0.14	0.02	0.01	0.81	0.11	0.28	0.08	0.54

Taurine-conjugated 1° BAs, TCA, TβCA, and TCDCA, were significantly increased whereas taurine-conjugated 2° BAs including TLCA, TUDCA, and TDCA were significantly decreased in the HD treatment group. Glycine-conjugated 1° BAs including glycocholic acid (GCA) and glycochenodeoxycholic acid (GCDCA) and 2° BAs, GLCA and GDCA, also were all observed to be significantly reduced, indicating a sex-specific response as these were not affected in this pattern in females. BA plasma levels in both doripenem-LD and -HD males recovered completely on day 42.

3.7. Comparative Analysis of the Metabolome Suggests Stronger Effects of Carbapenem Antibiotics on Feces Than Plasma Metabolomes

There was a stronger effect of the antibiotic treatments on the fecal metabolites (35–59% significantly changed metabolites at p -value < 0.05) compared to plasma (only 10–21%) (Table 14). Upon comparing the percentage changes in the plasma and fecal metabolomes in the doripenem-recovery groups to previously changed levels upon doripenem treatment, it can be concluded that the recovery of altered metabolites was faster in males than in females. Additionally, it was noted that the feces metabolome recovered faster than the plasma, as more than 50% of the previously changed fecal metabolites reversed back to normal control values on day 42/43 (two weeks after no exposure to the antibiotic). Furthermore, with the false discovery rate at a p -value of 0.05 being 5%, the plasma metabolomes of the doripenem-HD recovery males and the doripenem-LD recovery females also suggested complete recovery. Comparing the percentages of significantly altered plasma and feces metabolites in the meropenem-treated animals, the number of changes in the fecal metabolomes was about 4–5 times higher than that in the plasma. This observation is similar in both the carbapenem treatment groups and in both sexes, indicating consistent antibiotic-class based effects on the metabolomes, and both antibiotics show a similar strength (Table 14C,D).

Table 14. Percentages of the total number of significantly changed plasma (in light blue) and fecal (in light orange) metabolites at a p -value < 0.05 for the (A) HD and (B) LD groups of doripenem treatment plus the doripenem-recovery group and (C) HD and (D) LD groups of meropenem treatment in both sexes, respectively.

		Doripenem HD, males								Doripenem HD, females									
(A)	% of total sig. changed metabolites	Plasma			Feces			Plasma			Feces			Plasma			Feces		
		7d	14d	28d	7d	14d	28d	7d	14d	28d	7d	14d	28d	7d	14d	28d	7d	14d	28d
		20.2	16.8	19.7	47.7	48.5	49.0	18	14.95	19.59	12.16	18.9	18.58	58.54	54.5	54.5	24.76	22.5	
				7.43	5	5	4					2							
		Doripenem LD, males								Doripenem LD, females									
(B)	% of total sig. changed metabolites	Plasma			Feces			Plasma			Feces			Plasma			Feces		
		7d	14d	28d	7d	14d	28d	7d	14d	28d	7d	14d	28d	7d	14d	28d	7d	14d	28d
		14.8	14.1	15.6	42.7	46.7	40.3	12.06	6.27	16.89	14.86	10.8	7.78	54.66	49.03	36.65	18	12.54	
				18.92	6	8	5					1							
		Meropenem HD, males						Meropenem HD, females											
(C)	% of total sig. changed metabolites	Plasma			Feces			Plasma			Feces								
		7d	14d	28d	7d	14d	28d	7d	14d	28d	7d	14d	28d						
		10.54	11.9	14.97	44.69	50.48	47.27	15.31	10.2	13.6	56.91	43.25	42.93						
		Meropenem LD, males						Meropenem LD, females											
(D)	% of total sig. changed metabolites	Plasma			Feces			Plasma			Feces								
		7d	14d	28d	7d	14d	28d	7d	14d	28d	7d	14d	28d						
		6.8	7.82	12.24	46.46	34.73	32.96	9.86	12.24	8.5	49.36	45.18	31.51						

4. Discussion

We investigated how two carbapenem antibiotics, meropenem trihydrate and doripenem hydrate, alter the gut (fecal) microbiota composition and the derived plasma and fecal metabolites of male and female Wistar rats, as well as the recovery of these parameters one and two weeks after ending the administration of doripenem (Figure 10). The major findings of this research include the following: 1. Meropenem and doripenem induced significant changes in the gut (fecal) microbiota composition with antibiotic-specific changes. 2. There were significant changes in the fecal metabolic profiles, particularly including alterations in BA levels. 3. Additionally, there were significant changes in the levels of plasma metabolites previously identified as key markers of microbiota shifts, as well as BAs. 4. When animals were allowed a period of recovery following doripenem treatment, the changes in the 16S bacterial composition as well as fecal metabolites reversed after 2 two weeks. 5. A few plasma metabolites in the doripenem-HD recovery group showed incomplete recovery or overcompensation.

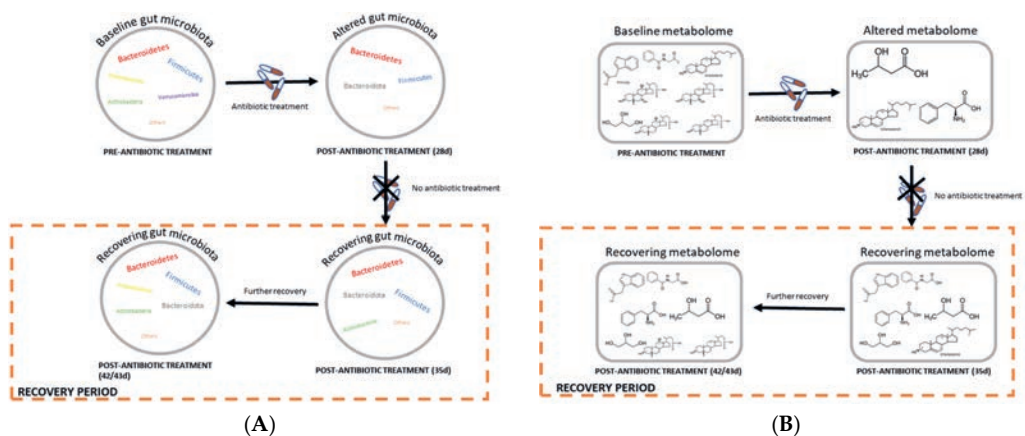


Figure 10. Schematic diagrams of the recovery processes of (A) gut or fecal microbiota and (B) plasma and feces metabolomes before and after doripenem antibiotic treatments. Baseline state indicates the original or ‘normal’ state of the gut microbiota or metabolomes prior to antibiotic administration, which becomes altered upon 28 days of antibiotic administration. Further, post-antibiotic treatment, a recovery or overcompensation takes place where the gut bacteria as well as the host metabolomes try to return to the ‘normal’ state.

4.1. Microbiome Analysis

The effects of the two carbapenem treatments on the gut microbiome composition was different from other antibiotic classes, i.e., aminoglycosides, lincosamides, and fluoroquinolones, analyzed by Behr et al., 2017 and 2018, de Bruijn et al., 2020, and Murali et al., 2021. As carbapenems exhibit a broad spectrum of antimicrobial activity against Gram-negative and Gram-positive bacteria, treatment groups consistently showed a reduced bacterial Shannon true diversity. Overall, in the control groups, the bacterial Shannon true or alpha diversity gradually increases with time from day 1 until day 42/43 of the study. This is consistent to Hoffmann et al., 2017, who also observed a higher Shannon diversity in older mice compared to younger ones [31]. The beta diversity analysis shows that samples of both treatment groups cluster together, with day 1 samples clearly separated from the rest of the sampling time points. This could be because of a yet incomplete elimination of less susceptible bacteria, with a subsequent further reduction in diversity at later time points which appears to be complete on day 7. Furthermore, the changes in 16S bacterial compositions on days 7 and 28 in the carbapenem groups were sex specific. A similar observation was noted in previously published studies using aminoglycosides, fluoroquinolones, lincosamides, and polymyxin E antibiotics. The factors responsible for these albeit subtle differences are still not very well established [12, 13, 32]. A few publications have highlighted potential reasons including the differences in hormone dynamics, host genetics, body mass index as some of the factors [33, 34]. Overall, however, compared to the sex specific differences observed in rats, the species strain and environmental conditions of the animals have a more significant influence on its gut microbiota composition.

In the doripenem hydrate recovery group, the diversity analysis showed rapid recovery. The alpha diversity following one week of stopping the exposure in the doripenem-recovery LD and HD groups were comparable to the corresponding controls. Interestingly, in females of the doripenem-recovery LD

group on day 42, the bacterial diversity appeared to be slightly higher than in the corresponding control group.

An inter-individual variability could be observed in the relative abundance analysis, particularly in the *Verrucomicrobiaceae*, as seen in previous investigations, where this high variability in *Verrucomicrobiaceae* in the control animals was already noted. To assess the long-term variability in controls, further studies would be helpful and needed to attain a historic range of the bacterial families for a better interpretation of results (similar to historical control data in clinical or histopathology). Consistent with the diversity analysis, the relative abundance analysis also showed a distinct bacterial composition on day 1 of the antibiotic treatment groups compared to the rest of the sampling time points. The meropenem and doripenem HD groups showed a more pronounced reduction in bacterial diversity than the LD group in both sexes, resulting in increased relative abundances of *Enterococcaceae*, *Anaeroplasmataceae*, *Erysipelotrichaceae*, and *Peptostreptococcaceae* compared to the controls indicating that these are highly likely to be resistant to carbapenem antibiotics. In both the meropenem and doripenem LD groups, the bacterial abundances changed with the time of exposure to the respective antibiotics, which indicates that the bacteria that are resistant to the activity of the respective antibiotics start to colonize and fill niches that are made available by the selected antibiotic, and hence, on day 1, this overgrowth with the above mentioned four strains was less evident than the succeeding sampling time points [35]. Furthermore, samples from recovery time points, that is, one and two weeks after the doripenem treatment was stopped, showed comparable bacterial abundances (observed in both relative and differential abundance analyses) as controls, which again demonstrates that the gut microbiota repopulation one week after antibiotic exposure was stopped. Similar observations were noted upon the cessation of other antibiotics such as ciprofloxacin and vancomycin in humans where gut bacterial communities began to return to their initial state after one and two weeks post-antibiotic cessation, respectively [36, 37].

4.2. Metabolome Analysis

4.2.1. Both Carbapenems Altered Gut-Derived BAs and Plasma Biomarkers

The PCA analysis of the fecal metabolome showed a strong effect of meropenem. From the 620 measured fecal metabolites, as many as 47% and 43% metabolites were significant in the HD males and females, while in the LD groups, these values were 33% and 32%, respectively. Fecal 1° BAs including taurine-conjugated 1° BAs significantly increased in fecal metabolomes from all the time points (days 7, 14, and 28) of all the meropenem groups. Strong increases in CA suggest the lack of utilization of the 1° BAs for further bacterial dehydroxylation reactions to produce corresponding 2° or 3° BAs. The accumulation of taurine-conjugated 1° BAs, specifically TCAs, also indicates reduced deconjugation activity of the remaining intestinal bacterial communities. This observation is in line with the antibiotics from other classes, such as the lincosamide antibiotics (clindamycin and lincomycin) and vancomycin [11, 12, 15]. Furthermore, TCA was observed to be actively transported from the intestine,

and it was shown that TCA uptake is increased in the ileal epithelium of Germ-free rats [38]. Therefore, although meropenem trihydrate, vancomycin, lincomycin, and clindamycin are antibiotics with a different spectrum of activity, their interference with bacterial BA metabolism appears to be rather similar.

Strong reductions in 2° BAs, specifically in DCA, HDCA, ωMCA, and LCA, were observed in the meropenem treatment groups. This substantial reduction in these 2° BAs confirms the lack of an ability to convert 1° BAs into 2° BAs by gut bacteria. Gut bacteria are known to deconjugate the taurine- or glycine-conjugated 1° BAs and further dehydroxylate them to produce respective 2° BAs. The majority of gut bacteria are anaerobes, and mainly anaerobic bacteria possess a 7α- dehydroxylation activity to convert 1° BAs into 2° BAs [39]. Consequently, it can be assumed that meropenem trihydrate significantly reduced those essential gut (or fecal) bacteria that are responsible for these reactions. The PCA analyses of the plasma metabolome showed only some alterations compared to the controls. Among the 294 measured plasma metabolites, only about 15% and 13% were significantly changed in the samples from day 28 of meropenem HD-treated males and females, respectively. In the LD group, these values were 12% and 8.5% in male and female rats, respectively. These values are above the false discovery rate but far less compared to the changes in the fecal metabolites.

Some of the previously established plasma biomarkers that are known to be associated with perturbations in the gut microbiome include HA, indole derivatives (incl. IAA, IPA, and 3-indoxylsulfate), and glycerol [11]. From these, a significant reduction in 3-IS and HA was observed in both sexes of the meropenem treatment groups, confirming their usefulness as general indicators of disturbed gut microbiome composition and metabolic functionality. Surprisingly, one of the indole derivatives, IAA, which was previously found to be significantly reduced during treatments with antibiotics belonging to the aminoglycosides, lincosamides, and fluoroquinolones classes [11, 12, 32, 40], was significantly increased in the meropenem treatment group, specifically in the HD group (Table S5). This observation suggests a meropenem-specific effect on this specific plasma key metabolite in both sexes. A potential cause of this significant increase of this otherwise reduced plasma biomarker could be the loss of essential gut bacteria that normally utilize these metabolites.

Plasma BAs at all sampling time points showed significant alterations compared to the controls, including significant reductions in 2° BAs. Plasma 2° BAs including DCA, LCA, HDC, ωMCA, and isoLCA were all very low in the HD meropenem groups, indicating either reduced deconjugation reactions by gut bacteria consistent with the fecal BAs or a reduced conversion of deconjugated 1° into 2° BAs. Similarly, almost all the conjugated 2° BAs were also significantly reduced in the plasma of the meropenem groups. Thus, meropenem is observed to not only alter the fecal 16S composition but also consequently the fecal metabolome and the plasma metabolome, hereby indicating a potential influence on gut metabolic functionality. This is in line with previous observations from other antibiotics belonging to aminoglycosides, fluoroquinolones, and lincosamides, as published by de Bruijn et al., 2020 and Murali et al., 2021 [1, 12]. Finally, to evaluate the observed effects of meropenem

on the different metabolites including BAs as a potential systemic effect, we investigated if any form of liver toxicity could have been involved. We used the MetaMapTox database to compare the plasma metabolome of meropenem HD-treated animals with the pre-defined patterns for liver toxicity, as previously published [41-43]. This comparison did not indicate any association with liver toxicity. Similar to meropenem, samples from rats treated with doripenem had significantly altered fecal metabolites consequent to the changes in the gut 16S composition. The PCA analysis showed strong changes in the treatment groups in both sexes. From the 620 measured fecal metabolites, about 50% and 54.5% were significantly changed in the HD-treated male and female rats, respectively, and about 40% and 37% in the LD, respectively.

The 1° BAs and several conjugated 1° BAs were significantly increased in feces samples from all the animals treated with doripenem, specifically in the HD group. Amongst these, TCA was strongly increased in the feces of these samples in both sexes. Such high accumulation of 1° as well as conjugated 1° BAs indicates a reduction in gut bacteria that have the ability to perform the conversion of 1° as well as conjugated 1° BAs into their respective 2° and 3° forms via dehydroxylation and deconjugation reactions, as discussed previously for meropenem. Furthermore, 2° BAs including DCA, LCA, HDCA, ωMCA, and isoLCA were significantly reduced in all the samples from the doripenem treatment group relative to the controls, confirming the lack of bacterial deconjugation and 7α-dehydroxylation activities. Furthermore, conjugated 2° BAs were also consistently reduced. This could be the result of the reduction in gut bacteria possessing special enzymes necessary for deconjugation, which also explains that further conjugation of these 2° BAs in the liver is highly unlikely to take place. Unique bacterial enzymes called the bile salt hydrolases (BSH) are known to transform 1° into 2° BAs by cleaving the peptide linkage between the amino acid and the primary bile acid. Moreover, and in contrast to males, females treated with the doripenem antibiotic showed a significant decrease in glycine-conjugated 2° BAs, GLCA, and GDCA, highlighting the sex-specific effects of the antibiotic on these fecal BAs.

Similar to meropenem, far fewer changes in the plasma metabolome were observed for the doripenem treatment. Amongst the 294 measured blood plasma metabolites, about 20% and 19% were significantly changed in HD-treated male and female rats, respectively, and about 15% and 11% in the LD groups, respectively. Key plasma biomarkers including 3IS and HA were consistently reduced in all treatment groups. In females, IPA was significantly reduced in all the plasma metabolomes from the doripenem HD treatment. Significant reduction in these biomarkers is known to be associated with gut-dysbiosis based on the observations published by Behr et al., 2018, where a temporary shift in the gut microbiota was induced as well as the associated fecal metabolites using antibiotic of different classes including aminoglycosides, lincosamides, and fluoroquinolones [11, 14, 15]. This observation is similar to that of the meropenem treatment, strongly indicating a carbapenem class-specific response.

Several conjugated 1° BAs were significantly increased in the plasma of the doripenem treatment group in both sexes. This substantiates the observation in the fecal metabolome upon the antibiotic treatment

and indicates impairment of bacterial deconjugation activity and further accumulation of these conjugated BAs in the system. In males, additionally, 1° BAs, CA, and CDCA as well as some of the glycine-conjugated 1° BA were significantly reduced specifically in the HD group. Reduced levels of CDCA in the plasma of the HD group males in the absence of any significant change in CDCA in the feces suggests a possible increase in the conjugation activity of CDCA to TCDCA. This reduction in CA and CDCA in the plasma of antibiotic-treated rats is not unique as it was also observed upon roxithromycin treatment [12, 32, 40]. Furthermore, a significant reduction in 2° BAs including DCA, HDCA, and ωMCA could be consistently observed in all HD treatment groups. The 2° BAs isoLCA and UDCA were significantly reduced in females and males treated with doripenem HD, respectively. This decrease suggests an impairment in the bacterial dehydroxylation and deconjugation activity. In line with this observation, conjugated 2° BAs were also significantly reduced indicating the lack of 2° BAs to further undergo conjugation reaction in the liver.

4.2.2. Doripenem Hydrate Showed Indication of Recovery of Significantly Changed Metabolites 2-Weeks Post Doripenem Cessation

In females, the fecal metabolome from one-week post-doripenem high-dose cessation still showed significant changes in almost 57% of the previously changed BAs. The majority of these BAs changed in the opposite direction compared to the antibiotic-treated group. Similarly, in the LD group, fecal doripenem recovery metabolome from one-week post-antibiotic cessation (day 35) still showed significant changes in 36% of the previously changed BAs, out of which the majority of the changes were in the opposite direction. These observations suggest that a mechanism of overcompensation occurred in the fecal metabolome one week after doripenem treatment was stopped. This could be a potential feedback mechanism of the body in order to attain metabolic homeostasis one-week post-doripenem cessation. This can be further observed in the fecal metabolome from two-weeks post-doripenem cessation, as the changes in these samples are lower than on day 35, therefore, suggesting advancement towards full recovery. In males, the recovery seems to be faster than in females. This observation again indicates subtle differences between the sexes extending beyond the microbiome to the associated metabolites. During antibiotic administration, the effects on the fecal BA levels was also stronger in females, and this may explain why recovery in females was slower than in males.

The recovery of the plasma metabolome was analyzed with samples from two-weeks post-doripenem cessation. There was full recovery of the plasma metabolome of the LD group for males and females. For one metabolite (HA) there was overcompensation in the HD group females, i.e., the direction of change was reversed in the doripenem-recovery groups compared to control group. Interestingly, there were four bile acids for which an overcompensation was noted. In the HD group males, two metabolites (3-hydroxyindol and HA) were still increased despite the two weeks of recovery time, whereas none of the BAs were significantly changed two weeks after doripenem treatment was stopped in both LD and HD males. Similarly, for the HD group females, a longer duration than two weeks would ideally be

needed for a full recovery. In males, there were three metabolites, tyrosine, glucose, and xylitol, and two metabolites in females, citrate and 3-methoxytyrosine, which had not fully recovered. These metabolites that remained significantly altered two-weeks post-doripenem antibiotic cessation could either mean that they need more time to go back to their normal or baseline state or that they could be potential markers of disturbance, which may help provide therapeutic targets for microbiota recovery following antibiotic treatment [44]. Further, in contrast to females, all bile acids had returned to levels comparable to controls.

4.3. Associations between the Changes in Gut Microbiota and Associated Metabolites

Based on our observations, we hypothesize possible functions of gut bacteria, specifically with respect to BA metabolism. Several published studies on the species that have 7 α -dehydroxylating activity (resulting in secondary bile acids) have focused on *Clostridium* sp., *Bifidobacterium* sp., *Bacteroides* sp., and *Bifidobacterium* sp. [45], whereas many other dominant facultative anaerobes of the intestinal bacteria have been less explored regarding their abilities to perform dehydroxylation and deconjugation reactions. Our research indicated other bacterial families also to be involved in BA pool regulation. Drastic reduction in two specific bacterial families, *Bacteroidaceae* and *Prevotellaceae* (belonging to Proteobacteria and Bacteroidetes phyla, respectively), were observed in all antibiotic treatment groups compared to controls for both sexes. As a significant reduction in the 2° BAs (in both plasma and feces) was also found in these antibiotic treatment groups, this suggests a role of these two bacterial families, which are normally rather abundant, in bacterial deconjugation and dehydroxylation reactions transforming 1° into 2° BAs. Moreover, increases in the relative abundances of the *Enterococcaceae* family were consistently observed in both the meropenem and doripenem treatment groups suggesting that they do not contribute to BA-related metabolism. Other rather weakly reduced bacterial families in the meropenem LD and HD treatment groups were observed to be *Lachnospiraceae*, *Ruminococcaceae*, and *Porphyromonadaceae* in both sexes of antibiotic treatments, also indicating a potential bile acid transformation activity of the two families [39]. Overall, all these changed bacterial families recovered to levels comparable to the controls in microbiota from one and two weeks after doripenem treatment was stopped, which was also consequently observed in the metabolomes (both blood plasma and feces), further validating these associations between the altered gut microbiota and its associated metabolites (specifically, BAs).

5. Conclusions

In this 28-day oral feeding study on Wister rats, we observed that broad spectrum carbapenem antibiotics induced significant changes in the gut microbiota and related fecal metabolome profiles, specifically concerning the BA pool. Additionally, there was an efficient recovery and reconstitution in the 16S bacterial composition as well as in fecal metabolites following alterations induced by doripenem. In plasma metabolomes, however, specifically for animals administered doripenem HD, the

recovery was slower and there were indications of overcompensation of several metabolites that either were overly increased or decreased from their perturbation levels during the treatment itself, suggesting an ongoing recovery process. The plasma metabolites were consistent with changes in metabolites previously established as key biomarkers of microbiota shifts including BAs, but a unique observation was that one of the key metabolites, indole-acetic acid (IAA), increased following meropenem treatment but not doripenem or any other antibiotics tested under the same experimental conditions. While further studies are needed to understand whether there are any adverse or toxicological consequences to host health due to the measured changes in the metabolites, and how this might be influenced by co-administration with other drugs, the results suggest a relatively efficient recovery of the gut bacterial communities as well as their associated metabolic/functional output. The effective spontaneous recovery suggests that there may be little need for therapeutic interventions for restoration of the microbiome. Furthermore, due to apparent inter-species differences in the gut microbiota composition between rodents and humans, these results may not be directly applied or translated to human beings. This study also challenges the use/requirement for probiotics to restore gut communities. Whether overcompensated metabolites will return to their normal state, although likely, would require an extension beyond two weeks after antibiotic cessation.

Supplementary Materials: The following supporting information can be downloaded at: <https://www.mdpi.com/article/10.3390/microorganisms11020533/s1>, Figure S1: Principal Coordinate Analysis (PCoA) of bacterial families from controls, meropenem, and doripenem antibiotic-treated rats; Figure S2: Differential abundances of dominant bacterial families in carbapenem-treated samples; Table S1: Meropenem-induced feces metabolite fold changes in female Wistar rats; Table S2: Meropenem-induced feces metabolite fold changes in male Wistar rats; Table S3: Doripenem-induced feces metabolite fold changes in female Wistar rats; Table S4: Doripenem-induced feces metabolite fold changes in male Wistar rats; Table S5: Summarized table indicating the trend of significant alterations in plasma biomarkers.

Author Contributions: Writing—original draft preparation, formal analysis and investigation, A.M.; conceptualization, B.v.R., F.M.Z., H.K., and S.S.; methodology, B.v.R., F.M.Z., V.H., and P.D.; software and visualization, A.M., V.G., P.T., and H.J.C.; validation and data curation, V.G. and P.T.; Resources, B.v.R.; writing—review and editing, B.v.R., I.M.R., F.M.Z., S.J.S., and D.F.W.; supervision, B.v.R., I.M.R., and F.M.Z.; project administration, H.K. and F.M.Z.; funding acquisition, B.v.R. All authors have read and agreed to the published version of the manuscript.

Funding: This research was funded by the Long-Range Research Initiative of the European Chemical Industry Council, grant number Cefic-C7.

Data Availability Statement: All data are stored under GLP or GLP-like archives at BASF SE, Ludwigshafen am Rhein, Germany. Metabolome data are stored in MetaMapTox database, BASF.

Acknowledgments: We kindly thank all the technical assistants at the animal facility laboratory including Gunter Rank and Anne Wittke as well as Irmgard Weber and the technicians from the lab of Clinical Chemistry at BASF SE, Ludwigshafen, for the assistance in sample acquisition and storage. We further extend our gratitude to the analytical support provided by BASF Metabolome Solutions GmbH, Berlin. Furthermore, we thank the discussion panel from the ELUMICA monitoring team, and our project partners Nina Zhang from Wageningen University and Research and Shuhuan Zhai from ETH Zurich for extensive scientific discussions. Our research has been funded and extensively reviewed by an External Science Advisory Panel (Funding Committee) from Cefic-LRI (Grant number: Cefic-C7).

Conflicts of Interest: The authors declare no conflict of interest.

References

1. de Bruijn, V., et al., Antibiotic-induced changes in microbiome-related metabolites and bile acids in rat plasma. *Metabolites*, 2020. **10**(6): p. 242.
2. Visconti, A., et al., Interplay between the human gut microbiome and host metabolism. *Nature communications*, 2019. **10**(1): p. 1-10.
3. Jost, L., et al., Partitioning diversity for conservation analyses. *Diversity and Distributions*, 2010. **16**(1): p. 65-76.
4. Human Microbiome Project, C., Structure, function and diversity of the healthy human microbiome. *Nature*, 2012. **486**(7402): p. 207-14.
5. Carding, S., et al., Dysbiosis of the gut microbiota in disease. *Microbial ecology in health and disease*, 2015. **26**(1): p. 26191.
6. Schippa, S. and M.P. Conte, Dysbiotic events in gut microbiota: impact on human health. *Nutrients*, 2014. **6**(12): p. 5786-5805.
7. Martinez, K.B., V. Leone, and E.B. Chang, Western diets, gut dysbiosis, and metabolic diseases: Are they linked? *Gut microbes*, 2017. **8**(2): p. 130-142.
8. Sousa, T., et al., The gastrointestinal microbiota as a site for the biotransformation of drugs. *International journal of pharmaceutics*, 2008. **363**(1-2): p. 1-25.
9. Mikkelsen, K.H., et al., Effect of antibiotics on gut microbiota, gut hormones and glucose metabolism. *PloS one*, 2015. **10**(11): p. e0142352.
10. Mu, C. and W. Zhu, Antibiotic effects on gut microbiota, metabolism, and beyond. *Applied microbiology and biotechnology*, 2019. **103**(23): p. 9277-9285.
11. Behr, C., et al., Gut microbiome-related metabolic changes in plasma of antibiotic-treated rats. *Arch Toxicol*, 2017. **91**(10): p. 3439-3454.
12. Murali, A., et al., Elucidating the Relations between Gut Bacterial Composition and the Plasma and Fecal Metabolomes of Antibiotic Treated Wistar Rats. *Microbiology Research*, 2021. **12**(1): p. 82-122.
13. Murali, A., et al., Investigating the gut microbiome and metabolome following treatment with artificial sweeteners acesulfame potassium and saccharin in young adult Wistar rats. *Food and Chemical Toxicology*, 2022. **165**: p. 113123.
14. Behr, C., et al., Microbiome-related metabolite changes in gut tissue, cecum content and feces of rats treated with antibiotics. *Toxicol Appl Pharmacol*, 2018. **355**: p. 198-210.
15. Behr, C., et al., Impact of lincosamides antibiotics on the composition of the rat gut microbiota and the metabolite profile of plasma and feces. *Toxicol Lett*, 2018. **296**: p. 139-151.
16. Baldwin, C.M., K.A. Lyseng-Williamson, and S.J. Keam, Meropenem. *Drugs*, 2008. **68**(6): p. 803-838.
17. Raza, A., et al., Oral meropenem for superbugs: challenges and opportunities. *Drug Discovery Today*, 2021. **26**(2): p. 551-560.
18. Lister, P.D., Carbapenems in the USA: focus on doripenem. *Expert Review of Anti-infective Therapy*, 2007. **5**(5): p. 793-809.
19. El-Gamal, M.I., et al., Recent updates of carbapenem antibiotics. *European journal of medicinal chemistry*, 2017. **131**: p. 185-195.
20. Ng, K.M., et al., Recovery of the gut microbiota after antibiotics depends on host diet, community context, and environmental reservoirs. *Cell host & microbe*, 2019. **26**(5): p. 650-665. e4.
21. Legrand, T.P., et al., Antibiotic-induced alterations and repopulation dynamics of yellowtail kingfish microbiota. *Animal microbiome*, 2020. **2**(1): p. 1-16.
22. Suez, J., et al., Post-antibiotic gut mucosal microbiome reconstitution is impaired by probiotics and improved by autologous FMT. *Cell*, 2018. **174**(6): p. 1406-1423. e16.
23. Raymond, F., et al., Partial recovery of microbiomes after antibiotic treatment. *Gut Microbes*, 2016. **7**(5): p. 428-434.
24. Chng, K.R., et al., Metagenome-wide association analysis identifies microbial determinants of post-antibiotic ecological recovery in the gut. *Nature ecology & evolution*, 2020. **4**(9): p. 1256-1267.
25. Li, D., et al., Microbial biogeography and core microbiota of the rat digestive tract. *Scientific reports*, 2017. **7**(1): p. 1-16.

26. Green, J.M. and M.D. Owen, Herbicide-resistant crops: utilities and limitations for herbicide-resistant weed management. *J Agric Food Chem*, 2011. **59**(11): p. 5819-29.
27. Marksteiner, J., et al., Bile acid quantification of 20 plasma metabolites identifies lithocholic acid as a putative biomarker in Alzheimer's disease. *Metabolomics*, 2018. **14**(1): p. 1.
28. Walk, T.B., et al., System and method for analyzing a sample using chromatography coupled mass spectrometry. 2011, Google Patents.
29. van Ravenzwaay, B., et al., Metabolomics as read-across tool: A case study with phenoxy herbicides. *Regul Toxicol Pharmacol*, 2016. **81**: p. 288-304.
30. Love, M.I., W. Huber, and S. Anders, Moderated estimation of fold change and dispersion for RNA-seq data with DESeq2. *Genome Biol*, 2014. **15**(12): p. 550.
31. Hoffman, J.D., et al., Age drives distortion of brain metabolic, vascular and cognitive functions, and the gut microbiome. *Frontiers in Aging Neuroscience*, 2017. **9**: p. 298.
32. Behr, C., et al., Analysis of metabolome changes in the bile acid pool in feces and plasma of antibiotic-treated rats. *Toxicology and Applied Pharmacology*, 2019. **363**: p. 79-87.
33. Org, E., et al., Sex differences and hormonal effects on gut microbiota composition in mice. *Gut microbes*, 2016. **7**(4): p. 313-322.
34. Kim, N., Sex difference of gut microbiota. *Sex/gender-specific medicine in the gastrointestinal diseases*, 2022: p. 363-377.
35. Bengtsson-Palme, J. and D.J. Larsson, Concentrations of antibiotics predicted to select for resistant bacteria: proposed limits for environmental regulation. *Environment international*, 2016. **86**: p. 140-149.
36. Isaac, S., et al., Short-and long-term effects of oral vancomycin on the human intestinal microbiota. *Journal of Antimicrobial Chemotherapy*, 2016. **72**(1): p. 128-136.
37. Dethlefsen, L. and D.A. Relman, Incomplete recovery and individualized responses of the human distal gut microbiota to repeated antibiotic perturbation. *Proceedings of the National Academy of Sciences*, 2011. **108**(supplement_1): p. 4554-4561.
38. Riottot, M. and E. Sacquet, Increase in the ileal absorption rate of sodium taurocholate in germ-free or conventional rats given an amylo maize-starch diet. *British journal of nutrition*, 1985. **53**(2): p. 307-310.
39. Ridlon, J.M., D.-J. Kang, and P.B. Hylemon, Bile salt biotransformations by human intestinal bacteria. *Journal of lipid research*, 2006. **47**(2): p. 241-259.
40. Behr, C., et al., Analysis of metabolome changes in the bile acid pool in feces and plasma of antibiotic-treated rats. *Toxicol Appl Pharmacol*, 2019. **363**: p. 79-87.
41. Mattes, W., et al., Detection of hepatotoxicity potential with metabolite profiling (metabolomics) of rat plasma. *Toxicol Lett*, 2014. **230**(3): p. 467-78.
42. Ramirez, T., et al., Prediction of liver toxicity and mode of action using metabolomics in vitro in HepG2 cells. *Arch Toxicol*, 2018. **92**(2): p. 893-906.
43. Keller, J., et al., Added value of plasma metabolomics to describe maternal effects in rat maternal and prenatal toxicity studies. *Toxicol Lett*, 2019. **301**: p. 42-52.
44. Nobel, Y.R., et al., Metabolic and metagenomic outcomes from early-life pulsed antibiotic treatment. *Nature communications*, 2015. **6**(1): p. 1-15.
45. Guzior, D.V. and R.A. Quinn, microbial transformations of human bile acids. *Microbiome*, 2021. **9**(1): p. 1-13.

Disclaimer/Publisher's Note: The statements, opinions and data contained in all publications are solely those of the individual author(s) and contributor(s) and not of MDPI and/or the editor(s). MDPI and/or the editor(s) disclaim responsibility for any injury to people or property resulting from any ideas, methods, instructions or products referred to in the content.





CHAPTER 5:

INVESTIGATING THE GUT MICROBIOME AND METABOLOME FOLLOWING TREATMENT WITH ARTIFICIAL SWEETENERS ACESULFAME POTASSIUM AND SACCHARIN IN YOUNG ADULT WISTAR RATS

Aishwarya Murali, Varun Giri, Hunter James Cameron, Saskia Sperber, Franziska Maria Zickgraf, Volker Haake, Peter Driemert, Tilmann Walk, Hennieke Kamp, Ivonne MCM Rietjens and Bennard van Ravenzwaay

Published in: Food and Chemical Toxicology 165 (2022), 113123

Investigating the gut microbiome and metabolome following treatment with artificial sweeteners acesulfame potassium and saccharin in young adult Wistar rats

Abstract

To elucidate if artificial sweeteners modify fecal bacterial composition and the fecal and plasma metabolomes, Wistar rats from both sexes were treated for 28 days with acesulfame potassium (40 and 120 mg/kg body weight) and saccharin (20 and 100 mg/kg body weight). Targeted MS-based metabolome profiling (plasma and feces) and fecal 16S gene sequencing were conducted. Both sweeteners exhibited only minor effects on the fecal metabolome and microbiota. Saccharin treatment significantly altered amino acids, lipids, energy metabolism and specifically, bile acids in the plasma metabolome. Additionally, sex-specific differences were observed for conjugated primary and secondary bile acids. Acesulfame potassium treated male rats showed larger alterations in glycine conjugated primary and secondary bile-acids than females. Other changes in the plasma metabolome were more profound for saccharin than acesulfame potassium, for both sexes. Changes in conjugated bile-acids in plasma, which are often associated with microbiome changes, and the absence of similarly large changes in microbiota suggest an adaptative change of the latter, rather than toxicity. Further studies with a high resolution 16S sequencing data and/or metagenomics approach, with particular emphasis on bile acids, will be required to explore the mechanisms driving this metabolic outcome of saccharin in Wistar rats.

Keywords

Metabolomics, repeated dose toxicity, gut microbiota, artificial sweeteners, metabolite profiles, 16S rRNA gene sequencing

1. Introduction

The interplay between gut microbiota and host metabolism has gained a lot of attention in the recent decades [1-3]. Gut microbiome is profoundly involved in host metabolism and plays a vital role in host physiology. It is known to influence not only host well-being but also the health risks such as glucose tolerance, obesity, hyperinsulinemia, cardiovascular disease, and other ailments [4-6]. Apart from host development and well-being, it is regarded as an important component in the fields of toxicology, pharmacology, neurology, and others [7]. The significance of the co-evolving intestinal microbes on host health and disease is well studied [8-10] but the underlying biological mechanisms remain vastly unclear [7, 11, 12]. While Next-Generation Sequencing (NGS) technologies have been extensively used for a better understanding of gut microorganisms as well as their associations with the host health, integrated omics approaches help further unravel the complex host-microbiome interactions [13]. Metabolic profiles of various matrices, such as urine, blood, feces, gut tissues, etc., are used to study the metabolic functions of the gut microbiota, the host, and the crosstalk between the two [1, 2]. Changes

in blood and fecal metabolites have been predominately investigated to understand this interplay. Blood metabolome, besides including host metabolites, is also known to reflect metabolites that largely result from gut microbes-host co-metabolism whereas the fecal metabolome is known to directly compliment the 16S sequencing-based approaches with a functional readout of the gut microbiome [14].

Using the metabolome profiles of different compounds (including antibiotics, drugs, agro- and industrial-chemicals, etc.), treatment-specific metabolic patterns have been established over the last 15 years at BASF SE – Germany and stored in a database called MetaMap®Tox (MMT). This database consists of metabolite profiles from several different matrices of more than 1000 different treatments. MMT has been used for the identification and prediction of toxicological modes of action of new test compounds [7, 12, 15-18]. In previous studies, metabolic profiling of several different classes of antibiotics has been performed using different matrices including blood plasma, cecum content, feces and gut tissue sections (ileum, jejunum, duodenum). Several key gut microbiota-associated metabolites or biomarkers including indole-derivates (indole-3-acetic acid, indole-3-propionic acid, hippuric acid, 3-indoxylsulfate), glycerol and bile acids have been identified in blood plasma and feces matrices on administering antibiotics in two different dose levels to male and female Wistar rats [12, 19, 20]. The clear comparability between microbiome composition and fecal metabolome indicates that feces can be used as a non-invasive, yet informative matrix compared to cecum content or gut tissue, promoting a longitudinal study design [7, 19, 20].

There are some reports indicating an effect of artificial sweeteners (AS) on gut microbiome and subsequent changes in host well-being, which include glucose tolerance, obesity, hyperinsulinemia and cardiovascular disease [4-6]. The association between microbiome and host health has become general knowledge and the potential detrimental effects of sugar consumption has increased the exposure to these sweeteners. Therefore, the aim of our study was to investigate the effects of AS on the gut microbiota and its association with fecal and plasma metabolomes of Wistar rats. Acesulfame potassium and saccharin are both US Food and Drug Administration approved low-caloric artificial sweeteners [5, 21]. Acesulfame potassium has not been associated with any toxicity and saccharin is also considered as safe. The carcinogenic effect of saccharin was downgraded from possible carcinogen to not classifiable as a carcinogen to humans in 1998. The acceptable daily intake (ADI) is 5 mg/kg body weight for saccharin [22, 23] and 15 mg/kg body weight for acesulfame potassium [23, 24]. Changes to the gut microbial composition upon administration of the substances have been earlier studied [6], but the interplay with the host has not been investigated for an effect on fecal or plasma metabolomes. To investigate this, the aim of the present study was to characterize the effects of these two model artificial sweeteners on the gut microbiota and the fecal and plasma metabolomes of Wistar rats.

Here we report the results of a 28-day oral toxicity study to quantify the potential effects of different doses of acesulfame potassium and saccharin on the gut bacterial composition and metabolomes of male

and female Wistar rats. Targeted MS-based metabolome profiling of plasma and feces and community analysis via Illumina-based 16S marker gene sequencing of feces were conducted. With the evaluation of changes in the fecal microbiota and blood and feces metabolomes, a comprehensive understanding of how gut microbial changes upon treatment with the artificial sweeteners influences its metabolic functions and consequently its influence on the host was gained.

2. Materials and methods

A 28-day oral toxicity study was carried out in compliance with the OECD 407 Principles of Good Laboratory Practice and the GLP provisions of the German Chemicals Act.

2.1 Ethical statement

The animal study was performed in an AAALAC-approved (Association for Assessment and Accreditation of Laboratory Animal Care International) laboratory in accordance with the German Animal Welfare Act and the effective European Council Directive. This study was approved by the local authorizing agency for animal experiments (Landesuntersuchungsamt Rheinland-Pfalz, Koblenz, Germany) on 14 January 2019, as referenced by the approval number 23 177-07/G 18-3-098. For the study design, reference was made to the official OECD guideline 407, which requires the use of 5 animals per sex and dose group.

2.2 Animals and maintenance conditions

Male and female Wistar rats (CrI:WI(Han)) of the age group 70 ± 1 days, were supplied by Charles River, Germany, before the beginning of the planned study. The rats (5 per sex and cage per treatment group) were acclimatized for a week, in an air-conditioned room at a temperature of 20–24 °C, a relative humidity level of 30–70%, and a 12 h light / 12 h dark cycle. The lights were turned off from 6PM to 6AM and the animals were sacrificed on day 28 of the study between 7AM to 9AM. Ground Kliba mouse/rat maintenance diet “GLP” by Provimi Kliba SA, Kaiseraugst, Switzerland, was supplied for the feeding throughout the course of the study. Diet and drinking water were available *ad libitum* (except 16–20 hours before sampling. In order to reduce any variation based on the diet consumption and as a standard procedure used in clinical chemistry and metabolomics, the animals were fasted overnight before the sample collection. Diet and drinking water were regularly assessed for chemical contaminants and the presence of microorganisms.

2.3 Treatment of animals with compounds

The artificial sweeteners, acesulfame potassium and saccharin were administered daily by gavage to five rats per treatment group per sex (see Table 1 and Figure 1). Acesulfame potassium was prepared in deionized water for oral administration at dose levels of 40 mg/kg body weight/day and 120 mg/kg body weight/day, respectively. These dose levels selected were 2.5 and 8 times higher than the ADI for

acesulfame potassium. Similarly, saccharin was prepared in a 0.5% carboxymethyl cellulose (CMC) suspension at dose levels of 20 mg/kg body weight/day and 100 mg/kg body/day weight, respectively. The dose levels selected were 4 and 20 times higher than the ADI for saccharin. The dose levels for both the sweeteners, low dose (LD) and high dose (HD) were set based on previous literature data [22-24]. 10 mL/kg bw/day of the sweeteners were administered from the prepared concentrations to five rats per treatment group per dose group per sex each with a concurrent control group of 10 animals per sex, to allow comparisons. All the animals were checked daily for any clinically abnormal signs and mortalities. Food consumption was determined on study days 6, 13 and 27. Additionally, body weights of all the animals were determined before the start of the administration period in order to randomize the animals and also on study days 6, 13 and 27. At the end of the treatment periods, the animals were sacrificed by decapitation under isoflurane anesthesia.

Table 1: Treatments, dose levels and form of preparation of the treatments. All treatments were administered orally by gavage.

Treatment	Low dose (mg/kg bw/d ^a)	High Dose (mg/kg bw/d ^a)	Form of preparation
Acesulfame potassium	40	120	In deionized water
Saccharin	20	100	In 0,5% CMC ^b

^amg/kg body weight/day, ^bcarboxymethyl cellulose

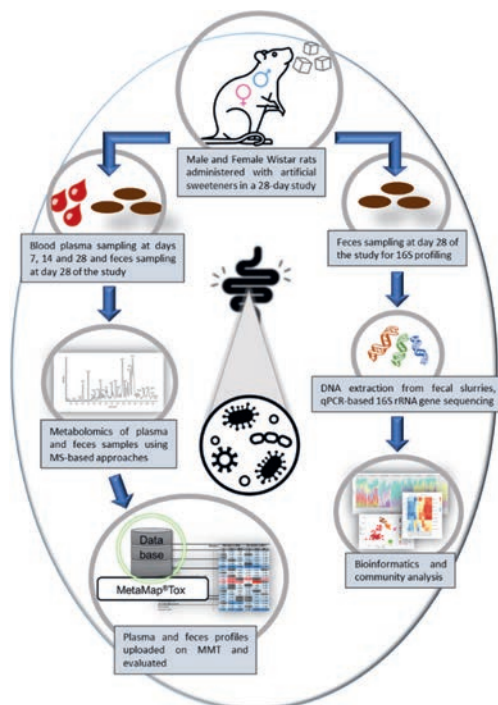


Figure 1: Schematic presentation of the study design for plasma and fecal metabolite profiling and the corresponding 16S bacterial community analysis of 28-day orally gavaged artificial sweetener-treated male and female Wistar rats.

2.4 Blood and feces sampling for metabolite profiling

On days 7, 14 and 28, after a fasting period of 16-20 hours, blood samples were collected between 7:30 and 10:30 h from the retro-orbital sinus of all the rats (including controls and both treatment groups) under isoflurane anesthesia (1.0 ml K-EDTA blood). The collected blood samples were subjected to centrifugation (10 °C, 20,000 x g, 2 min) and the EDTA plasma was separated. These EDTA plasma samples were then snap-frozen into liquid N₂ and stored at -80 °C until the metabolite profiling was performed. Feces were carefully sampled by removing them from the rectum after gentle massaging, and when no feces were present, samples were then scraped from the colon during necropsy on day 28 after a fasting period of 16-20 hours. The samples were collected in pre-cooled (dry-ice) vials, snap-frozen in liquid nitrogen and stored at -80 °C until further processing for fecal dry weight measurements, DNA isolation, 16S gene PCR amplification and sequencing.

2.5 Clinical examination

All the animals were checked regularly for any abnormal macroscopic findings and mortalities. Standard operating procedures as described in the Organization for Economic Co-operation and Development (OECD) 407 guidelines were used for all clinical- and pathological examinations. Parameters such as food consumption and body weights were determined before the start of the treatment administration period in order to randomize the animals and on the study days 6, 13 and 27. Food consumption was measured by weighing the fixed amount of food and re-weighing after 24h and by calculating the difference between the weights of the rats before and after the 24h period. At the end of the study period, on day 28, animals were decapitated under isoflurane anesthesia. Metabolite profiling of blood plasma and feces as well as fecal 16S rRNA gene sequencing and further community analysis were performed for samples from all controls and sweetener-treated animals.

2.6 DNA extraction and 16S rRNA amplicon sequencing

Dry weights of stored rectum fecal samples from all controls and artificial sweetener-treated rats were measured, transferred to labeled pre-cooled (dry-ice) DNA/RNA Shield-Lysis collection tubes (BIOZOL Diagnostica Vertrieb GmbH, Eching, Germany) avoiding excess thawing of the frozen fecal pellets. Fecal slurry samples on dry ice and their measured weight details were sent to IMG^M laboratories (Martinsried, Germany) for DNA isolation, amplicon-based 16S rRNA gene sequencing plus an additional qPCR assay for bacterial gDNA load quantification using Illumina MiSeq sequencing platform. DNA isolation from the fecal slurries was conducted using QIAamp Fast DNA Stool Mini Kit (Qiagen) followed by quantification with Qubit (ThermoFisher In brief, 1 µl of each sample was used to determine dsDNA concentration (ng/µl) in comparison to a given standard provided with the kit. The DNA concentration was determined by creating a linear trend line and applying the mathematical equation of linear regression by IMG^M laboratories. DNA was amplified using universal primer pair 341F/805R of V3-V4 region of the 16S gene. An aliquot of each final PCR product

including the positive and negative controls was run on a 2% agarose gel (Midori Green-stained) to analyze the quality of the generated amplicons and to evaluate the expected amplicon size. Next Generation sequencing (NGS) was performed on the Illumina MiSeq® next generation sequencing system (Illumina Inc.) resulting in 250bp paired end reads with a minimum of 10,000 reads per sample. An additional bacterial DNA quantification analysis was carried out by amplification using qRT-PCR analysis by VII7 System. The produced raw data were processed, de-multiplexed and went to QC for final report generation. The final report was then used for further bioinformatics analysis.

2.7 Metabolite profiling of plasma and feces matrices

Mass spectrometry-based metabolite profiling of blood plasma and feces matrices was performed according to a standardized protocol described below.

Targeted metabolites were measured from 60 µl rat plasma extracted by adding 1500 µl extraction buffer (methanol, dichloromethane, water and toluene (93:47:16,5:1, v/v) buffered with ammonium acetate) using a ball mill (Bead Ruptor Biolab). Internal standards were added to the extraction mixture to enhance reproducible analysis. After centrifugation, (12000 rpm 10min@ 12°C) a 100 µl aliquot of the extract was subjected to LC-MS/MS. Here, 2.5 µl of the extract were injected each for reversed-phase and hydrophilic interaction liquid chromatography (ZIC - HILIC, 2.1 x 10mm, 3.5 µm, Supelco) followed by MS/MS detection (AB Sciex QTrap 6500+) using the positive and negative ionization mode. For reverse-phase high performance liquid chromatography (RP-HPLC, Ascentis Express C18, 5cm x 2.1mm, 2,7µm Supelco), gradient elution was performed with water/methanol/0.1 M ammonium formate (1:1:0.02 w/w) and methyl-tert-butylether/2-propanol/methanol/0.1M ammonium formate (2:1:0.5:0.035 w/w) with 0.5% (w/v) formic acid (0 min-100% A, 0.5 min 75% A, 5.9 min 10% A, 600 µl/min). HILIC gradient elution was performed with (C) acetonitrile/water (99:1, v/v) and 0.2 (v/v) acetic acid and (D) 0.007 M ammonium acetate with 0.2 (v/v) acetic acid (0_min 100% C, 5 min 10% C, 600 µl/min).

A second 1200 µl aliquot of the extract was mixed with water (3,75:1, v/v) resulting in a phase separation. 400 µl of the polar (upper phase) and 90 µl of lipid (lower phase) were taken for GC analysis. Both phases were analyzed with gas chromatography-mass spectrometry (GC7890-5975 MSD, Agilent Technologies) after derivatization as described in Grossmann *et al.* [25]. Briefly, the non-polar fraction was treated with methanol under acidic conditions to produce fatty acid methyl esters that were derived from both free fatty acids and hydrolyzed complex lipids. The polar and non-polar fractions were further derivatized with O-methyl-hydroxylamine hydrochloride to convert oxo-groups to O-methyloximes, and subsequently with a silylating agent (N-methyl-N-(trimethylsilyl) trifluoroacetamide). For GC analysis, 0.5 µl of the derivatized phase-separated extract were used each for analysis of the polar and lipid fractions. Bile acids analysis approach was based on a kit from Biocrates [26].

All of the samples were analyzed once in a randomized analytical sequence design to avoid artificial results with respect to analytical shifts. For GC-MS and LC-MS/MS profiling, data were normalized to the median of reference samples which were derived from a pool formed from aliquots of all samples to account for inter- and intra-instrumental variation. In plasma, 272 semiquantitative metabolites could be analyzed using the single peak signal of the respective metabolite and a normalization strategy according to the patent WO2007012643A1[27] resulting in ratio values representing the metabolite change in treated versus control animals [13]. Of those 272 metabolites, 246 are chemically identified and 26 are structurally unknown.

Similarly, the stored fecal samples were subjected to a freeze-drying process for further measurements. The product temperature and the vapor pressure at the beginning of the freeze-drying process were -40°C and 0.120 mbar respectively changing to +30°C and 0.01 mbar for a total running time of 42 h. About 10 mg of freeze-dried rat feces were used from the controls and different sweetener-treated animals for extraction with 1400 µl of a mixture of methanol and dichloromethane (2:1, v/v) with formic acid (0.6 v%) including a stainless-steel ball for homogenization with a ball mill (Bead Ruptor Biolab). After centrifugation (12000 rpm 10 min @12°C, an aliquot of the extract was subjected to LC-MS/MS analysis as described above.

In accordance to the GC-MS method applied for plasma samples, 750 µl of the polar (upper phase) and 90 µl of lipid (lower phase) were taken for GC analysis. Furthermore, the method applied for fecal samples was the same method as used for plasma matrix. In feces, 632 semiquantitative metabolites could be analyzed, of which 348 are chemically identified and 284 are structurally unknown.

2.8 Statistics

Analysis of the metabolite data was performed by uni- and multivariate statistical methods. A sex and day-stratified heteroscedastic t-test (Welch test) was applied to compare the levels of different metabolites from different doses of sweeteners relative to controls for both plasma and feces matrices. Relative fold changes for all the metabolites were calculated as the ratio of the medians of metabolite levels in individual animals per treatment group to the medians of metabolite levels in individual corresponding control animals (for each sampling time point, dose level and sex). These ratios are referred to as relative fold change levels. Computational work was conducted using standardized scripts. Finally, the relative fold change values, p- and t-values of metabolites were uploaded as metabolite profiles and made available on the in-house database MetaMapTox® (or MMT) [15, 17, 28]. For the multivariate analysis of these profiles, the data were log-transformed, centered, and scaled by unit variance for each metabolite and then used for Principal Component Analysis (PCA). Any missing data present were imputed using the nearest neighbor method implemented in function `impute.knn` from the R package `impute` [7]. PCA analysis was performed in R Statistical software [7]. Treatment related

effects were evaluated on MMT using the standardized procedure of comparing resulting metabolite levels of different treatments against the control group [17].

2.9 Bioinformatics

A standardized in-house 16S marker gene data processing using DADA2 algorithm was used as presented in Murali *et al.*, 2021 [7]. The customized workflow involves data quality control (QC), primer removal, denoising, taxonomy assignments using the RDP classifier and creation of a phylogenetic tree. Forward and reverse primers were trimmed from the raw reads using cutadapt software. As paired-end reads were to be used for further analysis, the reads were merged to about 415 bp length. The QC step involved checking the read lengths and the quality of the joined reads. Taxonomy was assigned to the individual Amplicon Sequence Variants (ASVs) using the Naïve Bayesian classifier implemented in DADA2 with the RDP database. This resulted in the output of a BIOM table with all the information regarding the sequences and abundances of ASVs and the assigned taxa information [7].

2.10 16S data handling and analysis

Post-processing of the 16S marker gene data was performed for bacterial community analysis in R software using RAM package library, as published in Murali *et al.*, 2021 [7]. The processed data were checked for completeness, and empty rows were removed. The BIOM table contained 501535 reads belonging to 26552 ASVs from 57 samples. The raw reads were used for alpha diversity analysis using the `group.diversity` function in the RAM package. As a part of data cleanup, ASVs or reads that did not have taxonomic assignment up to the family level were removed. Further, ASVs with non-zero counts in at least two samples were retained, and the others were removed, resulting in 436521 reads belonging to 970 ASVs. These filtered data were used for relative abundance analysis. Stacked bars were plotted using RAM package to determine the relative bacterial abundances in the different artificial sweetener-treated rats. Count normalization of the dataset was done based on the qPCR values. The filtered and normalized data were used for beta diversity analysis. Principle Coordinate Analysis (PCoA) was carried out using Bray-Curtis distances [7].

3. Results

3.1 Clinical examination

No mortality and abnormalities were observed in any of the animals from both the dose groups of the sweetener-treated groups as well as the controls. No signs of clinical toxicity were observed in animals receiving LD and HD of the two artificial sweeteners. Feces sampling showed normal fecal consistency. Figure 2 presents the food consumption and body weight values of female (A, C) and males (B, D)

animals from the different sweetener treatment groups relative to control animals respectively. The body weights of the animals and food consumption rate remained roughly the same throughout the 28-day study. The table with body weights and food consumption values can be found in the Supplementary material (see Supplementary Table S3).

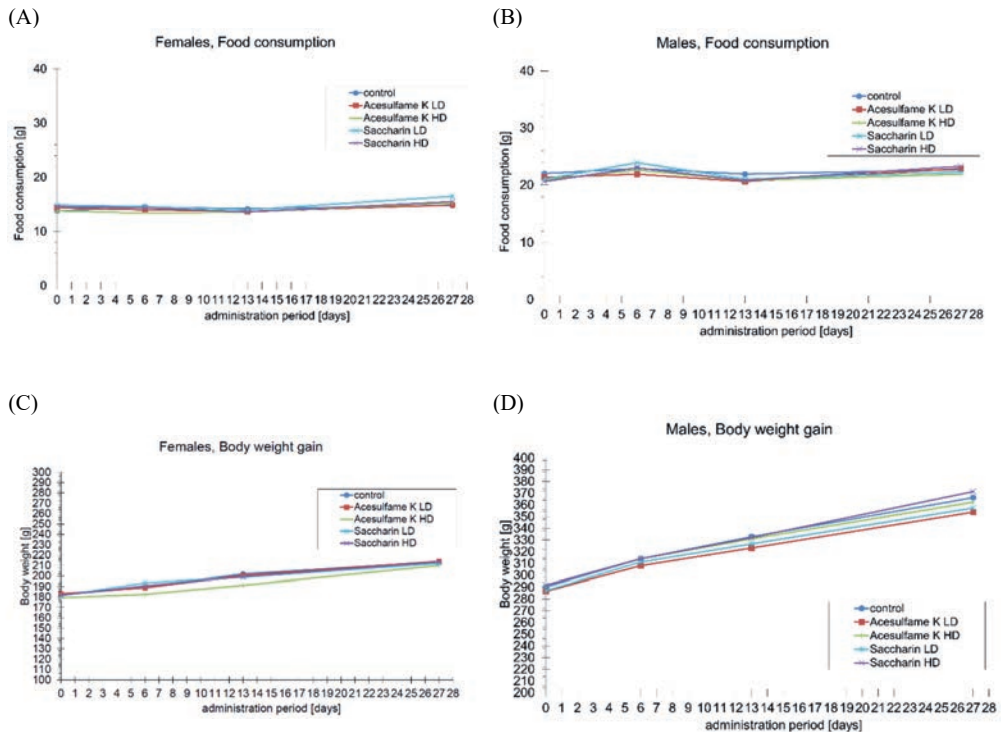


Figure 2: Line plots representing food consumption (g) and body weight gain (g) in female (A, C) and males (B, D) animals respectively, from the controls and different sweetener treatment groups from days 0, 6, 13 and 27. Changes in body weight and food consumption could be compared with control group and baseline values or day 0. Please refer to the legend to interpret the color coding of the samples from controls and the two sweeteners' treatments groups.

3.2 Diversity Analysis

Results from alpha and beta diversity analysis for the fecal samples from controls and artificial sweetener-administered rats are shown in Figures 3(A) and 3(B) respectively. Alpha diversity analysis, performed using the Shannon true diversity algorithm, was separated for both the sexes and dose levels for each sweetener treated group and controls. Shannon true diversity (see boxplot) depicts the diversity of different bacteria taxa that are prevalent in a specific condition or treatment group. The bigger the boxes in the plot, the higher is the variability between the samples from individual animals of a specific treatment group. Also, the higher the diversity in a specific treatment group, the higher is the presence

of different bacterial taxa. The dots falling outside the boxes demonstrate the most as extreme values, which are however accepted as normal high variations. In control groups from males and females, the variability in males was larger than in females.

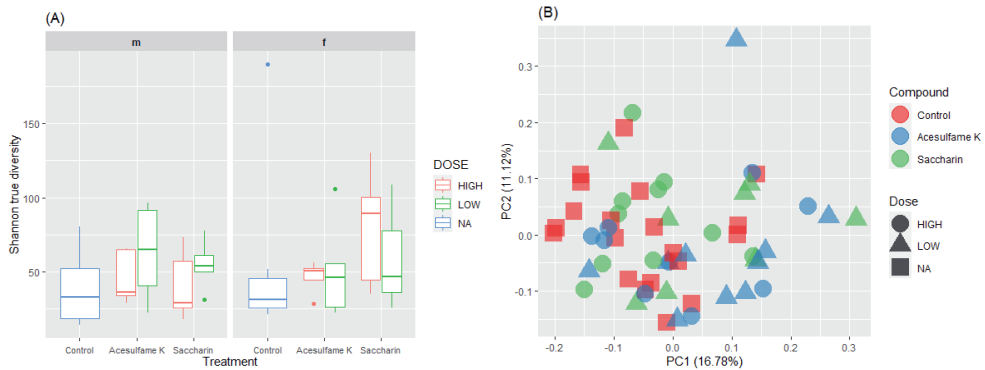


Figure 3: Diversity analysis of bacterial families from different treatments; (A) Alpha diversity analysis using Shannon true diversity index showing differences in bacterial diversity within a treatment group/condition. Dose groups are indicated in different colors, where HD is coded in red, LD in green and NA in blue (B) PCoA/Beta diversity analysis using Bray–Curtis distance matrix, showing limited differences in bacterial diversities between controls (in red), acesulfame potassium (in blue) and saccharin (in green) and the dose levels are indicated in different shapes.

Samples from female rats treated with acesulfame potassium show a similar alpha diversity compared to the control group irrespective of the dose levels. The same was observed for samples from male HD group, whereas samples from males treated with acesulfame potassium LD showed higher alpha diversity and higher variability compared to the corresponding control group as shown in Figure 3(A). Samples from female animals treated with both doses of saccharin showed higher variability than male animals. The males of the saccharin treatment groups possessed a similar alpha diversity as the control groups. In contrast to females, saccharin treated males possessed higher diversity compared to control group. Overall, only a slight increase in alpha diversity of males treated with both the sweeteners were observed and interestingly more in the LD group. Overall, it can be stated that few if any treatment related changes were observed.

Bray-Curtis distance-based beta diversity analysis, as depicted in the PCoA plot in Figure 3(B), are consistent with the observations from the alpha diversity analysis. Bray-Curtis is a rank-based PCoA analysis using a non-phylogenetic distance matrix, that represents different bacterial taxa that are present between different treatment groups or conditions. The clustering analysis, as shown in the PCoA plot in Figure 3(B), indicates that no treatment-specific clusters can be observed irrespective of the dose groups of the two artificial sweeteners. No distinct clusters were observed in the two treatment groups compared to controls, although the spread of the data points is large. According to the beta diversity analysis, the bacterial diversity in the sweeteners treatment group and control group seem similar.

3.3 Relative Abundance Analysis

A stacked bar plot was used to represent the relative abundances of different dominant bacterial families across the samples from the two dose groups of the artificial sweetener-treated groups and the controls (shown in Figure 4). Every color in the stacked bar plot depicts a specific bacterial family. The stacked bar plot shows the relative levels of different gut (fecal) bacterial families with respect to one another. The inter-individual variability can be distinctly observed in all the treatment and control groups. From a bird's eye view, a clear difference in the relative levels of the presented bacterial families between the two sexes in both control group and sweeteners-treated group is visible.



Figure 4: Stacked bar plot showing group indicators or core bacterial families that were detected in specific treatment groups. Individual animal variability can be easily observed. Dose groups and sexes for controls and each treatment group were separated. In treatment groups with sample size of less than 5 rats, fecal sample collection was not possible from all the five animals, hence for example in saccharin females LD and acesulfame potassium HD females, only three and four bars can be seen respectively, as samples from only three and four rats could be obtained from the respective treatment groups.

Relative abundances of control group males and females show apparent inter-individual variability in the 16S bacterial compositions. In females at the HD level, a small change in bacterial relative abundances could be observed for both artificial sweetener treatments compared to control. For males, such a response was not clearly visible. The *Verrucomicrobiaceae* family seems to be an influential factor as it appeared to be highly fluctuating between males and females and also within samples from individual animals. This also resulted in relative impact on the other dominant bacterial families. All in all, the occurrence of different bacterial families in the acesulfame potassium and saccharin treatment groups seem comparable to controls with an exception of one specific bacterial family. This has also been confirmed by plotting a differential abundance analysis volcano plot for the treatment groups relative to controls with p-value < 0.05 (see Supplementary figure S2). No obvious effect on the 16S bacterial composition in both artificial sweetener treatment groups could be observed in males, whereas

in females a clear variability in the bacterial abundances could be observed, predominantly in the *Verrucomicrobiaceae* family.

3.4 Fecal Metabolome analyses

PCA for samples from male and female Wistar rats treated with different doses of acesulfame potassium (in green) and saccharin (in blue) along with control groups (in red) are shown in Figures 5(A) and 5(B). The two dose levels have been represented in different shapes (i.e., LD in triangles and HD in circles) and the control groups as 'NA' or square symbol, for easier identification. In neither males nor females, a clear treatment-specific cluster could be observed. Both artificial sweetener treatment groups fall in the same space as samples from the control group for both the sexes. Both principal components PC1 and PC2 do not demonstrate sweeteners-treatment specific clusters compared to the control group. The spread of the data points is large in all the treatment and control groups.

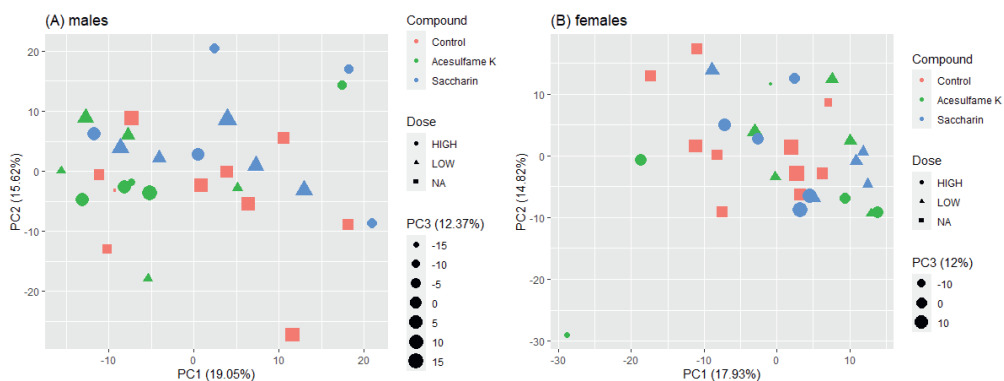


Figure 5: Principal component analysis (PCA) of fecal metabolomes of samples from day 28 of (A) males and (B) females of different treatments, dose groups and sex. Acesulfame potassium (in green) and saccharin (in blue) along with control groups (in red) are shown. The two dose levels have been represented triangles for LD group, circles for HD and the control groups as 'NA' or squares.

As PCA only represents a holistic overview of effects of the treatment groups, further analysis of the fecal metabolite profiles for both sweetener treatment groups for both sexes was performed.

3.4.1 Fecal metabolite profiles of acesulfame potassium treatment

Further analysis of several metabolites that were measured in the fecal samples of controls and both the doses of acesulfame potassium and saccharin treated rats, revealed altered metabolites for each of the sexes. Tables 2(A) and 2(B) represent the list of metabolites that were significantly altered (p -value < 0.05) in acesulfame potassium treated male and female animals, respectively, relative to the corresponding control group, keeping the HD group as standard for the search as it is expected to find most changed metabolites in the HD group.

Only a small number of significantly changed metabolites was observed in fecal samples from both the sexes treated with acesulfame potassium. Minor differences in the metabolite classes that were

significantly altered in males and females could be observed. In males, metabolites predominantly belonging to amino acids, carbohydrates, lipids, fatty acids and related classes were changed at p-value < 0.05. Compared to females, males show a slightly stronger effect on the fecal metabolite levels and more apparent differences between the two sexes were observed in metabolites belonging to carbohydrates and their derivative classes. The acesulfame potassium HD group clearly shows more significant changes in the metabolites than the acesulfame potassium LD group.

Table 2: Overall/total statistically significantly downregulated (yellow) and upregulated (red) fold change values of measured feces metabolites compared to the diet controls in feces (day 28, p-value < 0.05) of (A) male (d28) and (B) female (d28) Wistar rats after acesulfame potassium LD and HD treatment for 28 days and p values of individual metabolites have been added in separate columns.

(A)

Metabolite	Class	Acesulfame K HD		Acesulfame K LD	
		m28	p value	m28	p value
Tryptophan	Amino acids	0.57	0.02	0.84	0.15
Creatinine	Amino acids related	0.26	0.01	0.32	0.09
Sarcosine	Amino acids related	0.55	0.01	0.45	0.04
Dehydroalanine	Amino acids related	0.62	0.04	0.59	0.11
myo-Inositol	Carbohydrates and related	0.44	0.03	0.40	0.34
Xylose	Carbohydrates and related	0.55	0.00	0.66	0.57
Glucose-1-phosphate	Carbohydrates and related	0.41	0.00	0.58	0.21
Glucuronic acid	Carbohydrates and related	0.67	0.05	0.46	0.17
1,2-Anhydribose	Carbohydrates and related	1.72	0.01	1.06	0.41
2-Hydroxypentacosanoic acid	Complex lipids, fatty acids and related	1.10	0.02	0.83	0.25
Succinate	Energy metabolism and related	0.54	0.02	0.58	0.20
Glycerol-2-phosphate	Miscellaneous	0.55	0.03	0.67	0.18
bis-Glycerol phosphate	Miscellaneous	0.52	0.00	0.49	0.06
Cytosine	Nucleobases and related	0.73	0.01	0.98	0.38
Cucurbitacin	Unknown	1.59	0.03	0.83	0.99
Glutamate	Unknown	1.77	0.04	1.60	0.00
Kynurenic acid	Unknown	0.25	0.04	0.86	0.70
Creatinine	Unknown	0.51	0.04	0.59	0.22

(B)

Metabolite	Class	Acesulfame K HD		Acesulfame K LD	
		f28	p value	f28	p value
Serine	Amino acids	2.98	0.01	2.33	0.14
Octadecanol	Complex lipids, fatty acids and related	0.70	0.03	0.92	0.75
Hexadecanol	Complex lipids, fatty acids and related	0.56	0.03	1.06	0.70
Tetradecanol	Complex lipids, fatty acids and related	0.46	0.05	0.79	0.54
Serotonin	Hormones, signal substances and related	1.84	0.02	1.12	0.23
Stigmastanol, total	Miscellaneous	0.55	0.02	0.78	0.19
Glycine, lipid fraction	Miscellaneous	0.80	0.03	0.76	0.06
Adenine	Nucleobases and related	0.56	0.03	0.48	0.02
2,3-Dimethyl-5-phytylquinol	Unknown	0.65	0.04	1.22	0.46

1,25-Dihydroxy-vitamin D3	Unknown	0.80	0.01	1.17	0.08
Pipecolic acid	Unknown	3.23	0.01	3.82	0.02
Pyridoxal	Unknown	1.49	0.01	1.61	0.14
N2-Acetylhistidine	Unknown	3.32	0.02	0.90	0.41
Carnosine	Unknown	2.72	0.03	1.41	0.06
N-Acetylcytidine	Unknown	4.06	0.01	2.76	0.03
Uric acid	Unknown	2.39	0.03	3.42	0.06
p-Hydroxybenzoic acid	Vitamins, cofactors and related	3.39	0.04	1.50	0.16

3.4.2 Fecal metabolite profiles of saccharin treatment

The list of significantly altered fecal metabolites from samples belonging to saccharin LD and HD treated males and females are shown in Tables 3(A) and 3(B), using the changes observed in the HD group as standard for the search. In the saccharin HD group of males, more metabolites were statistically significantly changed compared to controls than in the saccharin HD female group. Further, statistically significant changes in saccharin LD groups of both sexes were smaller compared to the respective HD groups. The majority of the significantly changed metabolites belonged to the classes of amino acids, complex lipids and fatty acids and their derivatives in both the sexes upon saccharin treatments. The difference between the two sexes lies in the significant alteration of bile acids in female but not male rats upon saccharin HD treatment. As shown in Table 3(A), clearly a larger number of significantly changed metabolites was obtained after the administration of saccharin in males than females.

Table 3: Overall/total statistically significantly downregulated (yellow) and upregulated (red) fold change values of measured feces metabolites compared to the diet controls in feces (day 28, p-value < 0.05) of (A) male (d28) and (B) female (d28) Wistar rats after saccharin LD and HD treatment for 28 days and p values of individual metabolites have been added in separate columns.

(A)

Metabolite	Class	Saccharin HD		Saccharin LD	
		m28	p value	m28	p value
Glutamate	Amino acids	0.45	0.04	1.39	0.16
beta-Alanine	Amino acids related	2.91	0.02	1.15	0.13
Fucose	Carbohydrates and related	0.43	0.04	1.07	0.38
2-Hydroxypalmitic acid	Complex lipids, fatty acids and related	2.14	0.04	3.13	0.06
Myristic acid	Complex lipids, fatty acids and related	1.40	0.02	1.47	0.23
Eicosaenoic acid	Complex lipids, fatty acids and related	0.78	0.03	1.15	0.95
Eicosadienoic acid	Complex lipids, fatty acids and related	0.61	0.03	0.55	0.19
Azelaic acid (Dicarboxylic acid; C9:0)	Complex lipids, fatty acids and related	0.55	0.01	1.45	0.28
Fucoesterol, total	Miscellaneous	1.52	0.05	1.20	0.09
Resorcinol	Miscellaneous	1.38	0.04	1.20	0.27
threo-Sphinganine 3TMS	Unknown	1.42	0.05	1.36	0.40

18-Hydroxy-11-deoxycorticosterone	Unknown	1.90	0.04	1.07	0.36
2,3-Dimethyl-5-phytylquinol	Unknown	1.50	0.05	1.54	0.08
beta-/gamma-Tocotrienol	Unknown	1.21	0.03	1.78	0.00
Hexoses and Inositol + Chlorid-Addukt	Unknown	1.80	0.02	1.21	0.02
N-Acetylserine	Unknown	0.09	0.03	0.73	0.28
epsilon-Acetyllysine	Unknown	0.56	0.01	0.92	0.61
gamma-Carboxyglutamate	Unknown	1.61	0.04	1.49	0.48
Nicotinamide	Vitamins, cofactors and related	0.62	0.05	0.93	0.65

(B)

Metabolite	Class	Saccharin HD		Saccharin LD	
		f28	p value	f28	p value
Tyrosine	Amino acids	0.52	0.04	1.14	0.83
Ornithine	Amino acids related	0.68	0.04	1.73	0.12
1,2-Anhydroribose	Carbohydrates and related	1.79	0.02	2.33	0.14
Eicosadienoic acid	Complex lipids, fatty acids and related	1.55	0.04	1.16	0.91
Serotonin	Hormones, signal substances and related	1.88	0.05	0.99	0.78
Ethanolamine	Miscellaneous	0.78	0.02	0.92	0.74
Adenosine	Nucleobases and related	2.01	0.04	6.43	0.04
Deoxycholic acid	Bile acids and related	2.22	0.00	1.28	0.55
Lithocholic acid	Bile acids and related	1.65	0.01	1.09	0.29
α-Muricholic Acid	Bile acids and related	3.69	0.00	1.50	0.47
β-Muricholic Acid	Bile acids and related	2.83	0.01	2.28	0.34
ω-Muricholic Acid	Bile acids and related	4.03	0.00	1.67	0.22
putative Lithocholic acid OTMS ME	Unknown	1.21	0.04	1.09	0.23
putative Deoxycholyglycine	Unknown	1.86	0.00	1.25	0.26
putative β-Muricholic acid 3TMS ME	Unknown	2.63	0.01	2.58	0.63
Pipecolic acid	Unknown	2.77	0.02	3.39	0.07
Asparagine	Unknown	0.48	0.01	1.12	0.84
N-Methylglutamate	Unknown	0.45	0.00	0.89	0.16
Pregnenolone sulfate	Unknown	1.61	0.04	1.70	0.37

As males, similar change in the fecal metabolome could be observed in the saccharin-treated female animals. However, different to males, an upregulation in the levels of certain primary bile acids (alpha and beta-muricholic acid) and secondary bile acids (omega-muricholic acid, lithocholic acid) in saccharin HD treated females, was observed.

3.5 Plasma Metabolome Analysis

To investigate the possible effects of the artificial sweeteners on the plasma metabolite profiles of rats treated with acesulfame potassium or saccharin, samples from the study days 7, 14 and 28 were analyzed. PCA conducted similar to the fecal metabolome data, showed minimal treatment-based clustering compared to controls in both sweetener groups for both sexes (supplementary figure S1). To

examine the data for subtle changes fold change levels of individual plasma metabolites that were significantly altered upon the administration of artificial sweeteners, were examined in detail.

3.5.1 Plasma metabolite profiles of acesulfame potassium treatment

A list of significantly altered plasma metabolites, their respective metabolite classes and their relative fold change levels compared to controls is shown in Table 4(A) for acesulfame potassium treated males, using the changes observed in the HD group as the basis for comparison with the LD as it is expected to find most changed metabolites in the HD group. Compared to the rest of the metabolite classes, a metabolite of the bile acid group show clear and significant change in acesulfame potassium treated male animals, in particular the glycine conjugated bile acids. Primary glycine conjugated bile acid (i.e. glycochenodeoxycholic acid), secondary glycine bile acid conjugates (i.e. glycodeoxycholate and glyoursodeoxycholic acid) as well as the secondary bile acids (i.e. omega-muricholic acid) show a significant downregulation at both day 14 and day 28 of the acesulfame potassium HD treatment group.

Table 4: Overall/total statistically significantly downregulated (yellow) and upregulated (red) fold change values of measured plasma metabolites compared to the diet controls in blood plasma (days 7, 14 and 28, p-value < 0.05) of (A) male (d7, d14 and d28) and (B) female (d7, d14 and d28) Wistar rats after acesulfame potassium treatment LD and HD for 7, 14 and 28 days and p values of individual metabolites have been added in separate columns.

(A)

Metabolite	Class	Acesulfame K HD					Acesulfame K LD						
		m7	p value	m14	p value	m28	p value	m7	p value	m14	p value	m28	p value
Alanine	Amino acids	0.87	0.03	0.87	0.00	1.05	0.54	0.99	0.52	0.93	0.36	0.99	0.91
Phenylalanine	Amino acids	0.89	0.04	0.90	0.00	1.02	0.93	0.83	0.00	0.85	0.04	0.90	0.33
Indole-3-propionic acid	Amino acids related	0.88	0.01	0.85	0.03	1.00	0.87	0.97	0.42	1.02	0.36	0.92	0.51
Glycodeoxycholate	Bile acids and related	0.28	0.20	0.16	0.01	0.09	0.01	0.60	0.35	0.65	0.57	0.32	0.09
Glyoursodeoxycholic acid	Bile acids and related	0.78	0.99	0.15	0.03	0.21	0.01	0.50	0.42	0.52	0.23	0.19	0.00
ω-Muricholic Acid	Bile acids and related	0.10	0.04	0.18	0.01	0.49	0.10	0.45	0.27	0.30	0.10	0.74	0.64
Glycochenodeoxycholic acid	Bile acids and related	0.51	0.25	0.17	0.03	0.08	0.01	0.51	0.28	0.77	0.88	0.32	0.10
Glucuronic acid	Carbohydrates and related	0.53	0.02	0.66	0.02	0.79	0.16	0.86	0.51	1.05	0.67	0.79	0.30
Hexoses	Carbohydrates and related	1.63	0.03	1.59	0.03	0.92	0.24	1.47	0.01	1.30	0.02	0.87	0.48
Dodecanol	Complex lipids, fatty acids and related	1.35	0.02	1.04	0.49	2.63	0.04	1.07	0.40	0.73	0.57	1.14	0.44
Adrenaline (Epinephrine)	Hormones, signal substances and related	2.08	0.02	1.52	0.01	6.13	0.02	2.49	0.01	1.93	0.02	2.83	0.02

(B)

Metabolite	Class	Acesulfame K HD					Acesulfame K LD						
		f7	p value	f14	p value	f28	p value	f7	p value	f14	p value	f28	p value
Lysine	Amino acids	0.82	0.01	0.94	0.23	0.78	0.01	0.92	0.27	0.90	0.21	0.92	0.68
Ketoleucine	Amino acids related	0.76	0.03	0.83	0.03	1.01	0.98	0.93	0.60	0.85	0.06	0.79	0.61
Ethanolamine plasmalogen (C39:5)	Complex lipids, fatty acids and related	1.05	0.43	1.21	0.00	1.13	0.04	0.88	0.13	0.97	0.53	0.96	0.37
Succinate	Energy metabolism and related	0.87	0.43	0.90	0.01	0.88	0.02	0.93	0.95	0.85	0.22	0.96	0.58

The list of significantly regulated plasma metabolites upon acesulfame potassium administration in female rats can be seen in Table 4(B). The acesulfame potassium HD group showed a higher number of altered metabolites in the plasma matrices in both males and females compared to the acesulfame

potassium LD group. But the changes at both dose levels are so few that they are below the false discovery rate or FDR. Inconsistent to males, plasma bile acids levels did not change in females upon acesulfame potassium administration. No treatment related effect is observed for the LD groups.

3.5.2 Plasma metabolite profiles upon saccharin treatment

Shown in Table 5(A) is the list of significantly changed plasma metabolites in male animals at d7, d14 and d28 of the study. Amino acids and related metabolites show a significant downregulation in saccharin HD treated males, more apparent in samples from days 7 and 14. Amongst the other classes that were observed to be significantly altered by saccharin treatment in males, bile acids show a significant and strong downregulation in both HD and LD groups. Primary bile acids (alpha-muricholic acid), secondary bile acids (lithocholic acid) as well as conjugated primary bile acids (glycochenodeoxycholic acid) showed a significant downregulation in HD and LD groups. Plasma hippuric acid, which is a known key-metabolite for gut microbiota associated metabolism, showed a significant decrease in both LD and HD saccharin treatment groups [11, 19, 20]. Additionally, carbohydrates and signal substances and related classes appeared to be significantly influenced by HD saccharin administration including in males an increase in histamine. Overall, compared to all the other significantly altered plasma metabolites upon saccharin administration, a clear and strong effect in fold changes of plasma bile acid levels was observed in males.

Table 5: Overall/total statistically significantly downregulated (yellow) and upregulated (red) fold change values of measured plasma metabolites compared to the diet controls in blood plasma (days 7, 14 and 28, p-value < 0.05) of (A) male (d7, d14 and d28) and (B) female (d7, d14 and d28) Wistar rats after saccharin LD and HD treatment for 7, 14 and 28 days and p values of individual metabolites have been added in separate columns.

(A)

Metabolite	Class	Saccharin HD						Saccharin LD					
		m7	p value	m14	p value	m28	p value	m7	p value	m14	p value	m28	p value
Alanine	Amino acids	0.85	0.02	0.68	0.00	1.12	0.38	1.02	0.50	1.18	0.07	1.02	0.58
Methionine	Amino acids	0.82	0.03	0.79	0.03	1.01	0.54	0.94	0.30	0.94	0.79	1.07	0.05
Phenylalanine	Amino acids	0.83	0.02	0.85	0.00	1.03	0.57	0.85	0.06	0.90	0.13	0.99	0.54
Phosphocreatine	Amino acids related	0.70	0.01	0.45	0.00	0.74	0.00	0.71	0.05	0.57	0.05	1.05	0.76
Ornithine	Amino acids related	0.85	0.01	0.77	0.00	0.90	0.80	0.81	0.25	1.00	0.62	1.04	0.75
Indole-3-lactic acid	Amino acids related	1.41	0.02	0.94	0.94	1.15	0.02	1.20	0.12	0.96	0.98	0.93	0.83
Lithocholic acid	Bile acids and related	0.45	0.04	0.50	0.01	0.53	0.01	0.52	0.05	0.44	0.02	0.59	0.03
α -Muricholic Acid	Bile acids and related	0.40	0.01	0.15	0.02	0.10	0.11	0.47	0.18	0.09	0.10	0.03	0.01
Glycochenodeoxycholic acid	Bile acids and related	0.30	0.49	0.17	0.01	0.25	0.02	0.13	0.00	0.09	0.03	0.12	0.01
Xylitol	Carbohydrates and related	1.65	0.01	1.21	0.08	1.64	0.03	1.51	0.13	1.88	0.00	2.09	0.10
Lysophosphatidylcholine (C20:4)	Complex lipids, fatty acids and related	0.87	0.91	0.79	0.00	0.86	0.03	0.83	0.26	0.72	0.02	0.79	0.00
Pyruvate	Energy metabolism and related	0.74	0.05	0.39	0.00	1.11	0.71	1.16	0.64	1.47	0.21	0.62	0.66
Histamine	Hormones, signal substances and related	2.42	0.02	2.68	0.00	1.29	0.09	1.65	0.04	3.39	0.03	0.66	0.88
Phosphate (inorganic and from organic phosphates)	Miscellaneous	0.88	0.00	0.83	0.00	1.07	0.49	0.89	0.48	0.99	0.38	0.99	0.71
Hippuric acid	Miscellaneous	0.73	0.04	0.56	0.00	0.66	0.03	0.69	0.36	0.66	0.08	0.55	0.01
Uracil	Nucleobases and related	0.86	0.02	0.81	0.01	0.89	0.54	1.00	0.22	1.01	0.75	0.78	0.28

(B)

Metabolite	Class	Saccharin HD						Saccharin LD					
		f7	p value	f14	p value	f28	p value	f7	p value	f14	p value	f28	p value
3-Hydroxyisobutyrate	Amino acids related	0.78	0.14	0.77	0.02	0.77	0.02	0.90	0.54	0.75	0.01	0.86	0.00
Cholic acid	Bile acids and related	0.19	0.04	0.28	0.28	0.00	0.03	1.16	0.56	0.57	0.79	0.38	0.35
Chenodeoxycholic acid	Bile acids and related	0.27	0.05	0.17	0.23	0.01	0.02	0.56	0.25	0.30	0.26	0.27	0.32
Taurocholic acid sodium salt	Bile acids and related	1.74	0.05	2.92	0.00	1.18	0.39	2.70	0.02	1.75	0.02	1.73	0.26
α -Muricholic Acid	Bile acids and related	0.08	0.01	0.15	0.07	0.13	0.03	0.79	0.39	0.21	0.05	0.30	0.29

Taurodeoxycholate	Bile acids and related	2.83	0.00	2.46	0.00	1.35	0.12	1.64	0.01	1.39	0.15	1.70	0.49
1,5-Anhydrosorbitol	Carbohydrates and related	0.54	0.01	0.66	0.04	0.68	0.03	0.61	0.04	0.83	0.17	0.64	0.08
Phosphatidylcholine (C16:1,C18:2)	Complex lipids, fatty acids and related	0.77	0.02	0.70	0.05	1.17	0.79	0.77	0.04	0.72	0.02	1.11	0.94
Pyruvate	Energy metabolism and related	0.55	0.00	0.48	0.00	0.62	0.39	0.65	0.23	0.58	0.32	0.74	0.19
Lactate	Energy metabolism and related	0.73	0.02	0.57	0.01	0.80	0.42	1.01	0.55	0.80	0.79	0.94	0.49
beta-Sitosterol, total	Miscellaneous	0.62	0.03	0.69	0.01	0.90	0.52	0.68	0.14	0.68	0.06	0.85	0.48
Campesterol, total	Miscellaneous	0.67	0.02	0.66	0.01	0.90	0.63	0.73	0.11	0.62	0.07	0.83	0.74

The list of significantly altered plasma metabolites in female Wistar rats treated with saccharin HD and LD is shown in Table 5(B). Compared to males, females showed no apparent changes in metabolites belonging to hormones and related classes, highlighting sex-specific effects. Nevertheless, consistent changes were observed in plasma bile acid levels in females. Especially primary bile acids (cholic acid, chenodeoxycholic acid and alpha-muricholic acid) were observed to be significantly downregulated in saccharin HD treated females, whereas taurine conjugated primary (taurocholic acid) and secondary (taurodeoxycholate) bile acids were observed to be significantly upregulated at days 7 and day 14 of saccharin HD treated females. Apart from the bile acid class of metabolites, metabolites belonging to complex lipids, fatty acids, energy metabolites, vitamins and their derivatives showed significant changes upon saccharin treatment in females albeit only marginally but significantly. Overall, saccharin affected plasma metabolite levels in both males and females to a larger extent than what was observed upon acesulfame potassium treatment with especially the bile acid levels in both sexes being affected.

Table 6: Tables 6(A) and 6(B) show percentage levels of significantly altered plasma and fecal metabolites from acesulfame potassium HD and saccharin HD treated animals respectively at p-value <0.05, from a total number of 620 and 253 total fecal and plasma metabolites respectively.

(A)

	Acesulfame potassium HD, males				Acesulfame potassium HD, females			
	Plasma		Feces		Plasma		Feces	
	7d	14d	28d	28d	7d	14d	28d	28d
Total metabolites	253	253	253	620	253	253	253	620
% of sig. changed metabolites	9.49	12.64	9.09	7.90	4.74	8.30	4.74	3.70

(B)

	Saccharin HD, males				Saccharin HD, females			
	Plasma		Feces		Plasma		Feces	
	7d	14d	28d	28d	7d	14d	28d	28d
Total metabolites	253	253	253	620	253	253	253	620
% of sig. changed metabolites	13.04	22.13	15.02	8.55	10.28	15.41	6.32	6.12

4 Discussion

We investigated if two well-known artificial sweeteners, acesulfame potassium and saccharin, alter the intestinal (fecal) microbiota community composition and/or the plasma and fecal metabolomes of male and female Wistar rats in a 28-day oral toxicity study. Major findings of our research include the

following: 1. The sweeteners did not appear to induce changes in the gut microbiota and consequently fecal metabolic profiles also showed very few alterations. 2. Plasma metabolites showed minimal changes in all the measured metabolite classes except for a number of bile acids that were significantly changed, particularly in the Saccharin treatment group. 3. Sex-specific differences were observed for conjugated primary and secondary bile acids in the Saccharin treatment group. 4. In Ace K treated males, reductions in glycine conjugated bile acids were observed. 5. Key metabolites (incl. hippuric acid and indole derivatives) that are known to be associated with gut microbiome showed no relevant change in both the sweetener treatments. 7. Overall, there were no changes in the plasma metabolome considered to be adverse, rather indicating an adaptation to the sweeteners.

4.1 Microbiome analysis

From the alpha and beta diversity analyses, we could not observe any treatment-specific influence of both the dose groups of acesulfame potassium in both male and female rats compared to the respective controls. This finding is in line with the work from Lobach *et al.* 2019 and Uebanso *et al.* 2017 who demonstrated that acesulfame potassium at the maximum acceptable daily intake (ADI) levels of 15 mg/ kg body weight (8 times lower than the highest dose tested in the present study) did not alter the gut microbiota [24, 29]. Likewise, the selected doses for saccharin treatment, being 4 and 20 times higher than the ADI of 5 mg/ kg body weight established by Serrano *et al.* 2021 and Ruiz-Ojeda *et al.* 2019 [22, 23], also did not alter the bacterial diversity compared to the controls. Serrano *et al.* 2021 made a similar observation when an even higher dose of saccharin (250 mg/kg body weight) was supplemented and did not induce any gut microbiota changes in both mice and humans [22]. Consistently, the work of Ruiz-Ojeda, *et al.* 2019 also showed lack of alteration in the total numbers of anaerobic microbes upon dosing ~90 mg saccharin to rats, but they did observe a depletion in specific anaerobic microbes in the cecal content [23]. Consistent to this finding, our study demonstrated very few significant alterations in the 16S bacterial compositions. We did observe however an overall increased intra-group variability in the artificial sweetener-treatment groups. It is uncertain if higher levels of fluctuation in the bacterial family *Verrucomicrobiaceae* are treatment related, as this bacterial family is also observed to be highly variable in the controls. Similar to our observations, Eshar *et al.* 2014 also observed a high inter-individual variability in *Verrucomicrobiaceae* family in rabbits [30]. However, for other bacterial families, high variability has not been extensively explored.

With respect to the limitations of the research work presented here, it need to be taken into account that there is a lack of high resolution 16S sequencing data up to species or genus taxonomic levels. Such data would have enabled us to look deeper into potential causes of metabolic changes in saccharin treatment group and their possible associations with the gut composition. Another minor disadvantage would be the low sample size in two of the treatment groups, including saccharin female LD and acesulfame females HD groups with only 3 and 4 fecal samples obtained out of 5.

4.2 Metabolome analysis

When working with a high content technology such as metabolomics, a certain number of changes relative to the controls are expected to occur by chance. Therefore, changes in metabolites are not always necessarily indicative of a causal relationship with the treatment. Table 6 lists the percentage of changed metabolites for all HD treatment groups. Using a p-value of 0.05, it can be expected that up to 5% of the metabolites may be changed by chance. Our data thus indicate that for the HD acesulfame potassium and saccharin males, a weak treatment related effect on both fecal and plasma metabolite is likely. Interestingly, for females the number of changes in the plasma metabolome were only higher on days 7 and 14, which may suggest an adaptation or reversibility. This is in line with the observation that the number of changes in the 28-day fecal metabolome was also not higher than what could have been expected based on natural variation. However, as we know that some metabolite classes are more predictive for microbiome related changes in the metabolome than the others, an in-depth analysis of the type of metabolites that were changed was performed.

In males treated with acesulfame potassium, fecal metabolites predominantly belonging to amino acids, carbohydrates, lipids, fatty acids and related classes were changed. When comparing these metabolites with previously identified key indicators of microbiome-associated changes in rats (based on administering different classes of antibiotics in 28-day studies using Wistar rats, as published in Murali *et al.* 2021, Behr *et al.* 2018 and Behr *et al.* 2019), we observed that in our present study that none of these metabolites were significantly altered at p value < 0.05 in acesulfame potassium treated rats. It would therefore seem that acesulfame potassium treatment has only a small influence, if any, on the fecal metabolome of Wistar rats.

Samples from animals treated with acesulfame potassium consisted of plasma metabolome profiles showed a higher number of significantly altered metabolites compared to feces (>10% of total significantly changed metabolites), with clearer effect in the HD group. In both males and females, the dominant classes of plasma metabolites that showed significant changes are amino acids, complex lipids, fatty acids and their derivatives. Bile acids, however, were significantly changed only in acesulfame potassium treated males. Primary glycine conjugated bile acids (i.e., glycochenodeoxycholic acid), secondary glycine bile acid conjugates (i.e., glycodeoxycholate and glyoursodeoxycholic acid) as well as the secondary bile acid (i.e., omega-muricholic acid) show a significant downregulation at both day 14 and day 28 of the acesulfame potassium HD treatment group at p value < 0.05. Glycine conjugated bile acids show a more prominent and significant effect in plasma than feces of males treated with acesulfame potassium HD and in male than female plasma. This clear alteration in glycine-conjugated bile acids in males over females highlight a potential sex-dependent effect of the treatment. This could suggest a reduction of gut bacterial deconjugation of glycine-conjugated primary and secondary bile acids to their respective unconjugated forms. This could be

explained by a reduced dehydroxylation reaction, leading to lower levels of secondary bile acids o-MCA in the plasma of acesulfame potassium treated males. The work published by Bian *et al.* 2017 report a pronounced impact of Saccharin on the mouse gut metabolites with pro-inflammatory effects in liver, with the help of metabolomics [5]. It is, however, also possible that the changes in bile acids observed in the plasma are related to a reduced reabsorption as a consequence of treatment. Additionally, the altered glycine conjugated bile acids could also mean potential impairment in conjugation activity of the liver. As acesulfame potassium is bioavailable, it cannot be excluded that the observed changes in the plasma metabolome could have been caused by liver toxicity. Therefore, using the in-house database MetaMapTox, the plasma metabolome of acesulfame potassium was compared with the predefined patterns for liver toxicity [18, 31]. Based on this comparison, no hits for liver toxicity could be observed (data not shown) and an intestinal-related effect appears to be more likely.

In addition to the above-mentioned bile acids, indole-3-propionic acid (IPA), one of the key gut microbiome-derived metabolites, has been observed to be reduced in the plasma of acesulfame potassium HD treated males [11, 19, 20]. In this study we noted that this metabolite was also reduced in plasma samples from days 7 and 14 but not on day 28. This may be interpreted as evidence for a real, albeit temporary, effect on microbiome functionality during the initiation of treatment which is gradually changed towards the end of the study. In females, however, none of the typical key metabolites were altered upon treatment and the number of significantly changed plasma metabolites with a p-value of 0.05 in females was below the FDR (false discovery rate). Our observations could be explained by assuming a potential gut microbiota change which was not observable by the currently used community analysis method (e.g., more subtle microbiome changes at species level), or by a change of metabolic competence of the gut bacterial communities present. This also indicates higher sensitivity of the metabolomics approach compared to the 16S (V3-V4 region) gene sequencing method.

The majority of significantly changed fecal metabolites in HD saccharin treated rats belonged to the classes of amino acids, complex lipids and fatty acids and their derivatives. The difference between the two sexes lies in the significant alteration of bile acids. An upregulation in the levels of certain primary bile acids (alpha and beta-muricholic acid (α & β -MCA)) and secondary bile acids (omega-muricholic acid (Ω -MCA), lithocholic acid (LCA) and deoxycholic acid (DCA)). Compared to controls a slight increase in certain primary bile acids and secondary bile acids could be observed in feces of saccharin treated females. Accumulation of secondary bile acids in the feces, which are products of gut bacterial deconjugation of primary bile acids and a further dehydroxylation reaction, shows a possible impairment in the reabsorption of the secondary bile acids DCA and LCA. Furthermore, an accumulation of MCA- α and - β could potentially mean a slight impairment of conjugation activity in the liver, which apparently must have led to their higher levels in the feces of saccharin HD treated female rats. This significant effect on the fecal bile acids in females combined with the absence of a

change of gut microbial composition could indicate a systemic/host specific change, or a more subtle adaptation of gut microbiome functionally. Overall, however, from a quantitative point of view when compared to previously published work in Behr *et al.* 2018 and Behr *et al.* 2017 using antibiotic administration on Wistar rats, fecal bile acid levels in saccharin treated rats showed only a low magnitude of change. In conclusion, saccharin treatment HD group showed a clear sex-dependent effect but overall did not show a prominent impact on the fecal metabolomes in both sexes.

Compared to feces, the plasma metabolome of saccharin treated rats showed a more prominent impact as a larger number of metabolites (above the false discovery rate) were significantly changed compared to controls. Changes were observed in metabolites belonging to the following classes: amino acids, bile acids, lipids, fatty acids, carbohydrates, energy metabolism and their derivatives. Amongst the typical microbiome-associated key metabolites known from Behr *et al.* 2019 and Murali *et al.* 2020, bile acids, hippuric acid and indole derivative show a significant alteration in the plasma of saccharin HD treated males, however, compared to antibiotic administration, the fold change levels of these metabolites are rather low. This indicates that saccharin had a more prominent effect on the gut microbiota and associated metabolites than acesulfame potassium, which points at different mechanisms and also dose levels. Amongst the other classes that were observed to be significantly altered in plasma of saccharin treatment in males, bile acids show a clear and strong downregulation in both HD and LD groups. Primary bile acids (α -MCA), secondary bile acids (LCA) as well as conjugated primary bile acids (glycochenodeoxycholic acid) and conjugated secondary bile acid (tauro lithocholic acid) showed a significant downregulation in HD and LD groups. A clear reduction in conjugated bile acids in the plasma of males suggests a potential impairment in bacterial deconjugation activity and a consequent downregulation in secondary bile acids also indicate an additional impairment of gut bacterial dehydroxylation activity. Another potential cause could be an impairment in reabsorption of deconjugated and secondary bile acids. Significant alterations in these bile acids show a potential impact of saccharin on the gut microbial functions, although certainly not as high as upon antibiotic administration [7, 12, 13]. Although the fecal microbiota of saccharin treatment showed no clear difference compared to controls, subtle changes in their biochemistry may be responsible. In addition, our current research focused on the colon microbial communities so there is a possibility that the microbial population and metabolomes of small intestines may have been altered. Additionally, we have not determined the gut microbial population up to species level, which may reveal more subtle changes.

Compared to males, plasma metabolomes of females show lesser alterations upon saccharin administration. Significantly changed metabolites such as bile acids and 3-hydroxyisobutyrate are known to be associated with gut microbial functionality, and for females, too, a small but appreciable effect is observed. Primary bile acids and some taurine conjugated primary and secondary bile acids were increased on days 7 and 14.

Taking into account these clear albeit limited changes in the plasma metabolome, the question needs to be answered if these are associated with the microbiome or could have a systemic origin. Both sweeteners are bioavailable but are rapidly excreted and not metabolized [32-34]. To evaluate a potential systemic contribution to the plasma metabolome, we investigated, also for saccharin, if any form of liver toxicity could have been involved in the results obtained. Therefore, we used the MetaMapTox database to compare the plasma metabolome of saccharin treated animals with the pre-defined patterns for liver toxicity, as published by van Ravenzwaay *et al.* 2012, van Ravenzwaay *et al.* 2016, Kamp *et al.* 2012 and Sperber *et al.* 2019 [17, 18, 28, 31]. This comparison did not indicate any association with liver toxicity. This is in line with the work reported by Jo *et al.* 2017, in which no significant effect could be observed in mice treated with saccharin up to dose levels of 4,000 mg/kg for 7 days [35]. It is of interest to note that similar small alterations in plasma bile acid levels, also with sex-specific differences, were observed in Behr *et al.* 2019 upon oral administration of 0.5% carboxymethyl cellulose (CMC) in a similar experimental set-up (28-day study using Wistar rats) [12]. In this case, too, there were no obvious changes in the microbiome composition and there were no signs or indications of liver toxicity.

5 Conclusions

The results indicate that overall, the artificial sweeteners induce very minor changes in the gut microbiota according to the diversity- and relative abundance analyses. In line with this, fecal metabolic profiles of sweeteners treated animals also showed very limited alterations. In contrast, the plasma metabolomes of the sweeteners showed more profound alterations, saccharin being more potent than acesulfame potassium. Both compounds have specific effects on especially bile acids. Differences between males and females in acesulfame potassium treated group, were observed for conjugated primary and secondary bile acids, an upregulation in these plasma metabolites was observed in females, a downregulation in males. In acesulfame potassium treated males, larger alterations in glycine conjugated primary and secondary bile acids were observed compared to females. Previously established plasma biomarkers known to be associated with altered gut composition (indole derivatives, hippuric acid) did not show any change, in principle confirming the findings of our gut bacterial composition analysis [7, 12, 19]. Thus, in absence of any overall changes in the fecal- microbiota and fecal metabolome, there was a clear change particularly in conjugated bile acid levels in plasma. The MetaMapTox database used to compare and predict associations of the two sweeteners with any form of liver toxicity and did not indicate any liver-specific mode of action, nor in fact with any toxicological mode of action metabolome profile in MetaMapTox. Overall, there were no indications that the plasma metabolome changes observed should be considered as adverse. It remains to be elucidated if the observed changes are related to a subtle change in the biochemistry of the gut microbiome, minor changes of the microbiome at species level, or perhaps associated with the reabsorption of bile acids. Taking this into consideration, follow up studies using the 16S sequencing data with an in-depth

metagenomic analysis would promote a better resolution and a higher degree of information to ascertain a potential cause for the observed changes in the plasma metabolome and if these could be associated with subtle changes in the microbiome. This would not only provide better compositional data but it would also give insight into the functional aspects of both gut microbiota and their gene expression profiles as well as elucidate the importance of such changes for the host.

6 Declaration of conflicting interests

The authors declare that there are no conflicts of interest.

7 Acknowledgments

We cordially like to thank all the technical assistance from the animal facility technicians including Mr. Gunter Rank and the rest of the team, headed by Burkhard Flick as well as Irmgard Weber and the technicians from the lab of clinical chemistry at BASF SE, Ludwigshafen and the analytical support provided by BASF Metabolome Solutions, Berlin. We extend our sincere gratitude to Dr. Philipp Ternes who played an important role in performing additional 16S sequencing analysis, which is presented in the Supplementary data. Furthermore, we thank the discussion panel from the ELUMICA science monitoring team, and our project partners from Wageningen University and Research and ETH Zurich for extensive scientific discussions. Also, a big thanks to the Metabolome team at the Experimental Toxicology Department in BASF and the group of BMS Berlin GmbH. This research received an external funding from the Long-range Research Initiative (LRI), which is an initiative from the European Chemical Industry Council. Our research is extensively reviewed by an External Science Advisory Panel from Cefic-LRI.

Appendix A. Supplementary data

Supplementary data to this article can be found online at <https://doi.org/10.1016/j.fct.2022.113123>.

References

1. Zimmermann, M., et al., *Mapping human microbiome drug metabolism by gut bacteria and their genes*. Nature, 2019. **570**(7762): p. 462-467.
2. Clarke, G., et al., *Gut Reactions: Breaking Down Xenobiotic-Microbiome Interactions*. Pharmacol Rev, 2019. **71**(2): p. 198-224.
3. Dave, M., et al., *The human gut microbiome: current knowledge, challenges, and future directions*. Translational Research, 2012. **160**(4): p. 246-257.
4. Suez, J., et al., *Non-caloric artificial sweeteners and the microbiome: findings and challenges*. Gut Microbes, 2015. **6**(2): p. 149-55.
5. Bian, X., et al., *Saccharin induced liver inflammation in mice by altering the gut microbiota and its metabolic functions*. Food Chem Toxicol, 2017. **107**(Pt B): p. 530-539.
6. Wang, Q.P., et al., *Non-nutritive sweeteners possess a bacteriostatic effect and alter gut microbiota in mice*. PLoS One, 2018. **13**(7): p. e0199080.
7. Murali, A., et al., *Elucidating the Relations between Gut Bacterial Composition and the Plasma and Fecal Metabolomes of Antibiotic Treated Wistar Rats*. Microbiology Research, 2021. **12**(1): p. 82-122.
8. Agus, A., J. Planchais, and H. Sokol, *Gut Microbiota Regulation of Tryptophan Metabolism in Health and Disease*. Cell Host Microbe, 2018. **23**(6): p. 716-724.
9. Clayton, D.H., et al., *Host defense reinforces host-parasite cospeciation*. Proc Natl Acad Sci U S A, 2003. **100**(26): p. 15694-9.
10. Clayton, T.A., et al., *Pharmacometabonomic identification of a significant host-microbiome metabolic interaction affecting human drug metabolism*. Proc Natl Acad Sci U S A, 2009. **106**(34): p. 14728-33.
11. Behr, C., et al., *Impact of lincosamides antibiotics on the composition of the rat gut microbiota and the metabolite profile of plasma and feces*. Toxicol Lett, 2018. **296**: p. 139-151.
12. Behr, C., et al., *Analysis of metabolome changes in the bile acid pool in feces and plasma of antibiotic-treated rats*. Toxicol Appl Pharmacol, 2019. **363**: p. 79-87.
13. de Bruijn, V., et al., *Antibiotic-Induced Changes in Microbiome-Related Metabolites and Bile Acids in Rat Plasma*. Metabolites, 2020. **10**(6).
14. Zierer, J., et al., *The fecal metabolome as a functional readout of the gut microbiome*. Nat Genet, 2018. **50**(6): p. 790-795.
15. van Ravenzwaay, B., et al., *The use of metabolomics for the discovery of new biomarkers of effect*. Toxicol Lett, 2007. **172**(1-2): p. 21-8.
16. van Ravenzwaay, B., et al., *Use of 'omics to elucidate mechanism of action and integration of 'omics in a systems biology concept*. Mutat Res, 2012. **746**(2): p. 95-6.
17. van Ravenzwaay, B., et al., *Metabolomics as read-across tool: A case study with phenoxy herbicides*. Regul Toxicol Pharmacol, 2016. **81**: p. 288-304.
18. van Ravenzwaay, B., et al., *Metabolomics: a tool for early detection of toxicological effects and an opportunity for biology based grouping of chemicals-from QSAR to QBAR*. Mutat Res, 2012. **746**(2): p. 144-50.
19. Behr, C., et al., *Gut microbiome-related metabolic changes in plasma of antibiotic-treated rats*. Arch Toxicol, 2017. **91**(10): p. 3439-3454.
20. Behr, C., et al., *Microbiome-related metabolite changes in gut tissue, cecum content and feces of rats treated with antibiotics*. Toxicol Appl Pharmacol, 2018. **355**: p. 198-210.
21. Bian, X., et al., *The artificial sweetener acesulfame potassium affects the gut microbiome and body weight gain in CD-1 mice*. PloS one, 2017. **12**(6): p. e0178426.
22. Serrano, J., et al., *High-dose saccharin supplementation does not induce gut microbiota changes or glucose intolerance in healthy humans and mice*. Microbiome, 2021. **9**(1): p. 11.
23. Ruiz-Ojeda, F.J., et al., *Effects of Sweeteners on the Gut Microbiota: A Review of Experimental Studies and Clinical Trials*. Adv Nutr, 2019. **10**(suppl_1): p. S31-S48.
24. Uebanso, T., et al., *Effects of Low-Dose Non-Caloric Sweetener Consumption on Gut Microbiota in Mice*. Nutrients, 2017. **9**(6).
25. Green, J.M. and M.D. Owen, *Herbicide-resistant crops: utilities and limitations for herbicide-resistant weed management*. J Agric Food Chem, 2011. **59**(11): p. 5819-29.

26. Marksteiner, J., et al., *Bile acid quantification of 20 plasma metabolites identifies lithocholic acid as a putative biomarker in Alzheimer's disease*. *Metabolomics*, 2018. **14**(1): p. 1.
27. Walk, T.B., et al., *System and method for analyzing a sample using chromatography coupled mass spectrometry*. 2011, Google Patents.
28. Sperber, S., et al., *Metabolomics as read-across tool: An example with 3-aminopropanol and 2-aminoethanol*. *Regul Toxicol Pharmacol*, 2019. **108**: p. 104442.
29. Lobach, A.R., A. Roberts, and I.R. Rowland, *Assessing the in vivo data on low/no-calorie sweeteners and the gut microbiota*. *Food Chem Toxicol*, 2019. **124**: p. 385-399.
30. Eshar, D. and J.S. Weese, *Molecular analysis of the microbiota in hard feces from healthy rabbits (*Oryctolagus cuniculus*) medicated with long term oral meloxicam*. *BMC Vet Res*, 2014. **10**: p. 62.
31. Kamp, H., et al., *Application of in vivo metabolomics to preclinical/toxicological studies: case study on phenytoin-induced systemic toxicity*. *Bioanalysis*, 2012. **4**(18): p. 2291-301.
32. Magnuson, B.A., et al., *Biological fate of low-calorie sweeteners*. *Nutr Rev*, 2016. **74**(11): p. 670-689.
33. Renwick, A.G., *The metabolism of intense sweeteners*. *Xenobiotica*, 1986. **16**(10-11): p. 1057-71.
34. Renwick, A.G., *The disposition of saccharin in animals and man--a review*. *Food Chem Toxicol*, 1985. **23**(4-5): p. 429-35.
35. Jo, J.H., et al., *Investigation of the Regulatory Effects of Saccharin on Cytochrome P450s in Male ICR Mice*. *Toxicol Res*, 2017. **33**(1): p. 25-30.





CHAPTER 6:

GENERAL DISCUSSION

6.1. Overview results and key findings

Bacteria make up the majority of the intestinal microbiota, outnumbering eukaryotes and archaea by 2-3 orders of magnitude [1]. It is estimated that in a typical human host the most prominent bacterial phyla are Bacteroidetes and Firmicutes, followed by Proteobacteria, Verrucomicrobia and Actinobacteria [1]. Because rodents, specifically rats, are at the present state-of-the-art still used as the gold standard to assess chemical safety for humans, it is of importance to note that the rat and human gut microbiota are rather similar, allowing comparison [2, 3]. There are, however, inter-species differences in the gut composition, which may result in differences in gut metabolic function, making it necessary to understand the underlying relationships between gut microbiota composition and gut metabolic functionality. Currently, most research on chemically induced dysbiosis focuses exclusively on microbiota composition as an indicator of potential adversity [4], while metabolic endpoints (such as metabolic activity and metabolite production) may in fact be more relevant to assess potential adverse effects related to changes of the microbiota.

As a first step in elucidating the relationships between gut microbiota composition and metabolic functionality in the host, a comprehensive correlation analysis between the gut bacterial communities and fecal or plasma metabolites was performed to elucidate their interdependence. In **Chapter 2**, the effects of six different antibiotics and a 20% diet restriction, on the gut microbiome in a 28-day oral study with young adult Wistar rats were described. The antibiotics studied (streptomycin sulfate, roxithromycin, sparfloxacin, vancomycin, clindamycin and lincomycin hydrochloride) belong to different classes and hence represent diverse activity spectra inducing different changes in the composition of the gut microbiota. This study demonstrated a close connection between the gut microbiota and the fecal metabolome while the correlations between the gut (fecal) bacterial families and rat plasma metabolites were much weaker. Bile acids had the most significant and strongest correlations with the gut microbial families [5]. Dietary restriction did not induce any gut microbial perturbations and showed very marginal influence on the fecal metabolome.

Several plasma biomarkers that are associated with gut microbial perturbations, such as, indole derivatives and hippuric acid could be associated with the presence or absence of commensal bacterial families [6-8]. The correlations obtained in the study are comprehensive but also very complex and indicate several possible microbiota-metabolite relationships as there are multiple bacterial strains responsible for a specific metabolic function. Overall, this study showed that gut microbiome changes may indeed interfere with metabolism and could conceivably change how drugs or other chemicals are metabolized in the intestine when administered in such a situation [5]. Hence, a combination of 16S bacterial community analysis and metabolome profiling could help to unravel the consequences of microbiota changes and modifications for metabolism and metabolite production.

In **Chapter 3**, two additional antibiotics, tobramycin and colistin sulfate were orally administered to young adult Wistar rats for a period of 28 days to address their effects on the gut microbiome. The antibiotics were selected to induce gut dysbiosis [9]. The selected high doses were as high as possible without inducing systemic toxicity and the low doses were selected to be ten times lower than the high doses. Particularly, tobramycin had a strong and significant impact on the gut composition as well as the fecal metabolome, whereas colistin has much weaker effects. Significant changes in the levels of fecal bile acids upon tobramycin exposure indicated a clear dysbiosis induced by both doses of this antibiotic. The plasma metabolome showed far less alterations compared to the fecal metabolome, but the plasma biomarkers associated with a perturbed gut microbiota were all significantly changed, including indole derivatives, hippuric acid and bile acids. These metabolites were only marginally changed upon exposure of the rats to colistin sulfate, overall validating less impact of both the doses of colistin sulfate administered, on the gut microbiome and associated metabolites.

The significant microbiota and metabolome changes observed following tobramycin treatment, however, were not associated with apparent adverse effects, and showed no form of organ-specific toxicity. This conclusion was based on BASF's in-house database, MetaMapTox (MMT), which was used to compare the plasma metabolome of tobramycin-treated rats with more than a hundred pre-defined plasma metabolome patterns for toxicity including various types of liver and kidney toxicity and found no apparent association [10, 11]. The results of this study indicate that it is possible to identify and characterize substances that may alter the gut microbiome using plasma metabolome profiling, based on consistent changes in plasma metabolite patterns among the antibiotics. Another key finding from this study was a high variability of one specifically abundant bacterial family, *Verrucomicrobiaceae*, within the control animals. This observation has been previously noted by several other researchers and has been pointed out in previously published work [12]. However, further investigations and comparison of fecal metabolomes of control animals with and without this bacterial family, confirmed that this family has no apparent associated metabolite alterations, proving their commensal nature.

To understand the long-term consequences of antibiotic exposure on the gut microbiome it is essential to investigate its potential ability of spontaneous restoration following cessation of antibiotic treatment without any therapeutic interventions. The results of studies on this recovery are presented in **Chapter 4**. Two poorly bioavailable carbapenem antibiotics (meropenem trihydrate and doripenem hydrate) were orally administered for 28 days to young adult Wistar rats to elucidate the connection between the perturbed microbiota and metabolites [13]. Clear effects on the microbiota and associated fecal metabolites could be observed for both antibiotic treatments, with clear alterations in the fecal bile acids, indicating gut dysbiosis. Furthermore, the plasma metabolome, including previously established plasma key biomarkers, showed significant changes in these key metabolite levels upon exposure to both the

antibiotics. In addition, the spontaneous recovery of the gut microbiota and metabolomes in doripenem-exposed rats was studied at one and two weeks after the treatment was stopped.

Bacterial diversity fully recovered two weeks post doripenem antibiotic cessation, which was consequently also observed for the fecal metabolites. However, in the plasma metabolome, specifically in the high dose group, several metabolites showed indications of overcompensation, resulting in changes in the opposite direction than what was observed during the treatment itself, suggesting an ongoing recovery or a newly established stable state. Thus, this study provides insights into the connections between the microbiome and metabolome and demonstrates that both microbiome and metabolome can spontaneously recover from antibiotic treatment.

In further studies we applied the established technologies to assess the effects of two artificial sweeteners on the gut microbiota as well as on fecal and plasma metabolomes. **Chapter 5** presents the effects of acesulfame potassium and saccharin on the fecal bacterial composition and metabolomes of young adult Wistar rats following 28 days of oral administration [14]. Both sweeteners overall had only minor effects on the microbiota and fecal metabolome indicating that the doses given appear not to affect the gut microbiome. However, few alterations in the plasma metabolome, specifically in the bile acid levels were observed upon exposure of the rats to both sweeteners, with more pronounced effects for saccharin. Based on comparison to the pre-defined metabolic patterns on BASF's in-house database, MMT, none of these changes in the plasma metabolites showed any indications of organ specific toxicity, indicating a lack of adverse effects. Also, none of the plasma key metabolites that are known to be associated with a perturbed gut microbiome were altered upon exposure to either of the sweeteners. For further investigation, a metagenomic analysis or *in vitro* transport studies may highlight the gene expressions of gut bacteria or other modes of action that might have resulted in the changes in plasma bile acid levels induced by the artificial sweeteners.

6.2. General Discussion and future perspectives

To increase our mechanistic understanding of how the gut microbiome may influence host health, integration of the existing knowledge of gut microbiota with its functionality, in terms of metabolic capacity and the associated production of metabolites, is needed. The objectives of this thesis were to elucidate associations between gut bacteria and the production of metabolites for the host. The experimental strategy involved an *in vivo* approach changing the composition of the microbiome and studying the associated fecal and plasma metabolites in rats. Given the complexity of the system, a combination of omics technologies was applied to obtain functional and mechanistic understanding of the complex dynamics of host-microbiome interactions.

In the current thesis, 10 different antibiotics were selected based on the pre-existing literature taking three main criteria into consideration. Firstly, these compounds should be known to elicit a perturbation

in the gut composition. Secondly, these compounds should not be systemically bioavailable or their bioavailability in the system should be low thus avoiding the induction of any form of systemic toxicity that would change the plasma metabolome. The selected compounds consisted of antibiotics, food additives, and were administered orally for 28 days to young adult Wistar rats from which the blood and feces were sampled for metabolome analyses and the feces was also collected for 16S bacterial profiling. To assess the effects of exposure to these compounds on the microbiota composition, taxonomic profiling of DNA, isolated from feces samples, was performed and quantitative bacterial profiling was performed using qPCR to quantify the absolute count of bacterial loads. In addition, to quantify the impact of altered microbial communities on the metabolic output, Mass Spectrometry-based metabolomics was performed on feces and blood plasma samples. Together with the metabolome analyses, a comprehensive profile of metabolic functionality of intestinal microbial communities was generated enabling characterization of how these were differentially affected by chemical modulation.

The field of gut microbiota and its metabolic capabilities has gained significant attention in the last decade. However, there are still many unknowns about the (de)toxification abilities of the gut microbes, and even more about these abilities when the microbiota is altered as a result of exposure to different chemicals. Some of the most important questions that still remained unanswered in this field and are of interest for future considerations are the following.

1. Defining the inter-species and inter-individual baseline variability.
2. Higher taxonomic resolution for the identification of gut microbiota.
3. Sensitive methods to elucidate gut microbiota metabolic functionality.
4. The gut microbiome as critical effect for chemical risk assessment.
5. Drawing conclusions from the metabolome changes in terms of host well-being.
6. Alternative methods to elucidate gut microbial functionality.
7. Are the metabolome changes only a result of gut microbial dysbiosis?
8. Spontaneous restoration of gut microbiota and derived metabolites without therapeutic interventions.

In the following sections these topics are discussed in some further details and related future perspectives are presented.

6.2.1. Defining the inter-species and inter-individual baseline variability

High inter-species as well as inter-individual variabilities of the gut bacterial diversity need to be extensively explored in order to understand the translation of information between rodent model organisms to humans better. It has been well established that the gut microbial population of each individual consists of a unique profile distinct from that of the others [15]. Although the most dominant

phyla, the Bacteroidetes followed by Firmicutes remain relatively constant across all the baseline human gut (fecal) samples, the proportions of other less abundant phyla such as Proteobacteria, Actinobacteria and Faecalibacteria were observed to vary based on the on diet, age, gender, use of drugs, environmental exposure to contaminants [16]. These variations may even result in inter-individual variability in studies where effects on the microbiota are studied. However, this problem could be resolved by performing studies using model organisms under controlled environmental conditions and genetic backgrounds, which is difficult for human studies for obvious reasons.

Despite that, rodent animal models have been observed to have high inter-individual variability even under controlled environments that cannot be explained by cohort and caging effects, similar to what was observed in **Chapters 2-5**. Young adult Wistar rats of the age group 70 ± 1 days were acclimatized for a week, in an air-conditioned room at a temperature of 20-24 °C, a relative humidity level of 30-70%, and a 12 h light/12 h dark cycle. Ground Kliba mouse/rat maintenance diet was used for feeding throughout the course of the study and this diet along with drinking water were available *ad libitum* except 16-20 h before blood sampling. Parameters including food consumption and body weights were determined before the start of the treatment and further on the days 6, 13, and 27 of the study.

In chapters **Chapter 2-5**, a high inter-individual variability even within the control groups have been noticed, especially in the relative abundances of one specific bacterial family, *Verrucomicrobiacea*, as highlighted in **Chapter 3**. To understand the potential functional effects of these high variations, the feces metabolome profiles of control samples with high abundances of this family were compared to the samples with low abundances of the family and no functional differences could be spotted between the two groups. This indicated that this family appears to be a commensal species and hence its presence or absence may not drastically influence the metabolic output of the gut microbiota.

When a combined relative abundances stacked bar plot for control samples from studies conducted over a span of seven years was plotted, a high variability of the *Verrucomicrobiacea* family was observed between different studies where this family was abundant to a varying extent in control samples from studies conducted over a span of seven years (Figure 6.1). This fluctuation could be a result of a possible technical bias between studies as the DNA sequencing and 16S bacterial community profiling followed by data analyses were performed separately. Furthermore, in order to analyze the meanings of these high variations between individual samples, it is important to establish historic ratios of gut microbes that colonize healthy host guts [17]. This step is necessary before conducting any dietary intervention or cohort studies in order to define a 'normal' and healthy microbiota.

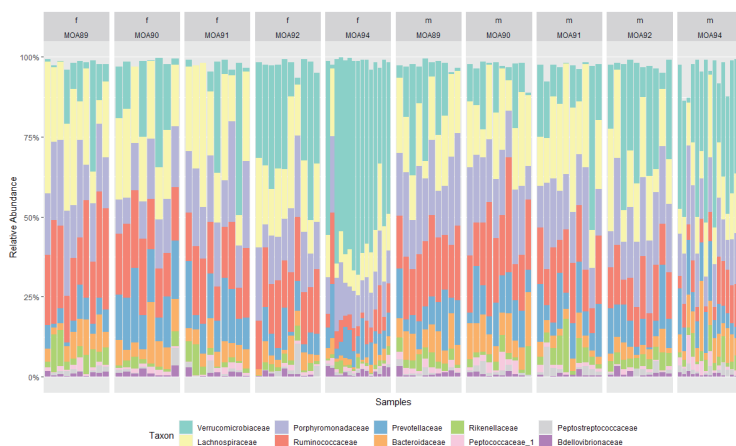


Figure 6.1: Combined relative abundances stacked bar plots of gut (fecal) samples from studies conducted over a span of seven years. The different color coding refers to different bacterial families as depicted.

Therefore, it is necessary to establish the baseline inter-individual variability in the intestinal microbiota to understand if changes induced by external factors lie within the natural biological variation or not. Hence control feces samples of rats (belonging to a similar age group) from different times of the year from both the sexes, making up to a total of at least 200 samples need to be collected and further used for a deep 16S rRNA gene sequencing analysis. Data processing and bioinformatic analyses of all the samples must be conducted together for all the samples in order to avoid any technical bias. The use of high throughput, deeper sequencing data and an easier ability of bioinformatics pipelines to integrate datasets is a must to establish the historical control range of baseline variability of normal gut microbiota composition of model organisms under controlled environments for better interpretations of microbiome data. Therefore, better definition of baseline inter-species as well as inter-individual variabilities of the gut bacterial composition will facilitate the detection of relevant chemical-induced changes and also facilitate inter-species extrapolations. Furthermore, for humans, better insight into the influence of different factors such as age, diet, disease state, gender and other confounders on baseline gut microbiota variability also remains an important topic for further studies.

6.2.2. Higher taxonomic resolution for the identification of gut bacteria

The importance of high resolution 16S sequencing data with taxonomic assignments up to species or strain levels may provide a clearer insight into the individual functionalities of the intestinal bacteria. At the present state-of-the-art 16S rRNA gene sequencing is widely used to determine the microbial diversity within a specific biological specimen or site. Next Generation Sequencing (NGS) technology has been extensively adopted to identify and characterize bacterial species. However, as the read lengths used for NGS platforms is short, only a subset of the gene is sequenced, which means that the resolution of the 16S profiling is somewhat restricted to the targeted variable regions (such as V3-V4), as many

bacteria might share the same amplified region [18, 19]. This will lead to reliable taxonomic assignments up to higher levels such as order or family but not beyond that, as observed in **Chapters 2-5**. Any assignments beyond these levels were inaccurate and error-prone and therefore the results did not allow studying of the gut bacteria functions at lower taxonomic levels such as species or strain level. The majority of the associations between the gut bacterial families and the fecal or plasma metabolites, as presented in **Chapter 2**, hint towards potential relationship between the two. However, since there are multiple bacterial strains responsible for a particular function, these direct one-to-one correlations may not necessarily answer the question of causality between the gut families and specific metabolic changes.

Recently, a high throughput sequencing using the full-length genes (~1500 bp) has gained a lot of attention in providing taxonomic resolution at species and strain levels [20]. This method seems to be more sophisticated and provides more accurate results at species level and avoids any type of subtle nucleotide substitutions. Literature suggests that sequencing platforms that rely on targeted regions of the 16S gene are unable to match the taxonomic accuracy when compared to sequencing the full 16S gene and the latter was able to resolve the issue of divergent intragenomic copy polymorphisms of the marker gene that are highly prevalent in the bacterial taxa that are isolated from the human gut microbiota [20]. Hence, there might be a need to use different approaches to circumvent the problem of taxonomic resolution by either opting for full-length 16S sequencing platforms or methods like whole genome shotgun sequencing methods and DNA microarray-based detection [21]. A higher taxonomic resolution of the gut bacteria may also be useful in defining meaningful correlations between the gut strains and feces/plasma metabolites and distinguish overlapping and unique functions of phylogenetically related taxa.

Another approach may be microbial RNA sequencing in combination with mass spectrometry-based metabolomics to understand the operations of the gut microbiota at a mechanistic level. With the transcriptomics approach using the RNA isolated from cecal and fecal samples, important genes that represent essential metabolic pathways could be identified [22]. Following which, mass spectrometry may be used to confirm the end products of the pathway components to verify the expression and activity of the genes involved.

Further, *in vitro* methods of culturing important gut microbiota and linking them to various health risks and diseases is gaining a lot of attention as *in vitro* models may provide an overall insight into essential microbiome responses. One important factor to be noted is that the cultivation media need to be carefully selected in order to successfully isolate the necessary strain [23]. However, because NGS technology cannot distinguish between live or dead bacteria, it is important to check the bacterial cell viability. However, it is also important to be noted that the majority of the gut taxa are still unculturable [24, 25] although they are metabolically and functionally active in the gut environment.

Clinically relevant gut bacterial isolates (such as a well-known gut microbiota-associated pathogen *Clostridium difficile*) may also be used for 16S rRNA based identification and further molecular and biochemical testing. Hence, not only omics-based approaches but also their integration with molecular assays may be used to confirm the biochemical functions of these vital bacterial strains. Further, targeting a set of genes that constitute a pathway rather than one single gene would yield more robust results. This also holds for metabolome analysis where the detection of multiple intermediates of a given pathway is likely to improve confidence compared to only measuring the end product. All together linking a specific metabolic conversion or pathway with (a) specific bacterial strain(s) remains an important topic for future research with several challenges.

6.2.3. Sensitive methods to elucidate gut microbiota metabolic functionality

In order to connect the microbiota and their metabolic functions better, also a metagenomics approach may be of use that determines the gene expression profiling of the individual bacteria. It is known that there are thousands of microbial species residing in the human gastrointestinal tract and these species are prominently bacteria. These gut bacteria are known to play an essential role in regulating host metabolism, the immune system, in protecting against harmful pathogens and in maintaining homeostasis [26]. Various molecular techniques have been developed to study these functions that the gut microbiota possess, such as integrated omics approaches using taxonomic and metabolomic methods. As established in **Chapters 2-5**, it is well known that the intestinally originating bacteria contribute to various important metabolic pathways such as formation of secondary bile acids, tryptophan metabolism, formation of short chain fatty acids, and several others. However, the gut microbial metabolic functionality can not only be studied by integrating 16S rRNA gene sequencing with metabolomics, but it is also necessary to understand the underlying biochemical mechanisms and/or genes that link the presence or absence of a certain microbe to the presence or absence of a certain microbiota-derived metabolite or metabolic pathway and this approach may also facilitate detection of pathways that consist of contributions from different bacteria.

Metagenomics is an approach that characterizes all the genes belonging to a community as a result of randomly sequencing ('shotgun') the DNA extracted for a particular sample [26, 27]. This functional metagenomics approach can be used to isolate rather novel genes from the unculturable fraction of the gut microbiota and can be used to reveal the complex behind the crosstalk between both microbial communities and the host organism. So, in order to obtain a high-resolution description of the host-bacterial interactions, whole-metagenome shotgun analysis could be performed. This is accomplished by analyzing the complete genome of all the microbes present in a specific sample [28]. This analysis would also help to establish species- or genus-specific metabolic functions of the gut microorganisms. Although promising this method identifies the presence of genes but cannot be used to identify microbial activity or gene expression. To address this shortcoming, a metatranscriptomics approach

may be used [29]. This approach may be used to determine the gene expression activity of gut communities [26]. Identifying the metabolic functions is done by the metabolomics approaches also used in the present thesis.

Another method developed is the *in vitro* model called PolyFermS platform to mimic the fermentation process that occurs in the human gut [30]. This model comprises a first-stage inoculum reactor seeded with immobilized fecal microbiota and is further used to continuously inoculate parallel operating systems in order to mimic the different sections of human colon to facilitate functional investigations [31].

6.2.4. The gut microbiome as critical effect for chemical risk assessment

Toxicological risk assessment of chemicals is the process to determine the extent of adverse health effects in humans or other target organisms that may be exposed to a particular chemical [32]. Based on the risk, a chemical is classified as the following categories: reprotoxic, teratogenic, skin irritant, organ toxic, carcinogen and several others. In recent years, the effects of several different compounds such as agricultural chemicals, pharmaceuticals and others, have been observed on the gut microbiota and the host. For risk assessments of chemical compounds, adverse or toxicological endpoints of observed changes in the gut microbiome and metabolomes may also need to be analyzed. Food, xenobiotics and environmental chemicals could potentially affect the gut microbiota by causing gut perturbations of certain bacterial taxa, consequently leading to host diseases [33]. Conversely, the gut microbiota composition may also have an influence on the nutrient uptake and intestinal permeability hereby effecting the xenobiotic uptake. Several studies have determined that antibiotic treatments actively affect gut permeability in rodent models, which may in turn lead to a differential uptake of given compounds and their overall toxic or beneficial effects on the gut and host [34]. This suggests that the gut microbiota likely can influence the toxicity of ingested xenobiotics. Such interventions such as exposure to drugs or food additives may have distinct effects on the gut microbiota composition and functions, as observed in **Chapters 2-5**, and these changes may or may not be adverse. Other agriculturally relevant compounds such as various fungicides, herbicides and insecticides have been recently shown to affect the gut microbiota composition, but their underlying functional mechanisms are to a vast extent still unexplored [35-37]. In addition, gut microbiota may convert the xenobiotics leading to more or less potent metabolites, such as is for example the case for the conversion of daidzein to its more potent estrogenic metabolite S-equol [38, 39].

In vivo animal studies such as the ones mentioned in **Chapters 2-5**, may be used to study essential interactions between the gut bacteria and host for chemical risk assessment. But the translation of knowledge to humans should be performed with caution due to obvious physiological species differences. Therefore, it may be necessary to adopt germ-free models colonized with gut bacterial communities isolated from humans in order to represent a comparable model system [40]. Another

important aspect that has also been already mentioned above is to understand the baseline inter-individual variability in order to interpret the inter-species and inter-individual differences in the risk assessments of chemicals between animal studies. Elucidating the full range of effects of chemicals on the gut microbiota as well as the gut microbial transformations of the respective chemicals or the overall host metabolome may provide new insights about the effects of diet, drugs and pollutants on human health and diseases [41].

In **Chapter 4**, the ability of spontaneous restoration of both the gut microbial community as well as the metabolome have been analyzed one and two weeks post antibiotic cessation. Although the recovery of both feces and plasma metabolomes were observed to be slower than that of the microbiota, there was indeed a hint towards a recovery process as several metabolites were back to their control levels while others showed indications of overcompensation, resulting in changes in the opposite direction than what was observed during the treatment itself. Studies like these may also help in understanding if an adaptation to a continuous (unintended) exposure of toxic substances in humans is possible. The exposure may be in extremely low doses but repeated, as a result of a dietary or occupational exposure. Therefore, the research question that needs to be answered is to what extent are these induced changes in the microbiota biologically relevant for the host organism. This knowledge would be essential to elucidate the physiological consequences of these alterations and their meaning with regards to toxicity or adversity and provide insight into to what extent these effects should become part of standard risk assessment guidelines. The potential consequences of gut microbiota related metabolic alterations for human health will be discussed to some further extent in the next section.

6.2.5. Drawing conclusions from the metabolome changes in terms of host well-being

Understanding the relevance of metabolome changes for the host is important to understand the consequences of changes in terms of adversity. The use of molecular technologies such as metabolomics, is important to understand the responses, in terms of metabolite changes, to external stimuli such as diet and environmental factors. Metabolomes include endogenous and exogenous small molecules that may originate from the diet, microbial products, drugs, dietary supplements and many others. With the help of rapidly growing integrated omics technologies, several essential metabolic markers have been identified and characterized that are associated with the gut microbiota composition and resulting dietary impact on the host metabolic functions [42]. As the metabolomes mirror the end-products of several different cellular and physiological-level processes, they may be related to host health and disease. To this end, static or dynamic clinical biomarkers may be selected, where dynamic biomarkers are important to understand the clinical response that may include disease progression and association to a particular treatment and static biomarkers are the ones that are able to predict a clinical response based on the physiological state of a patient [43]. Several biomarkers have been established

and associated to diseased conditions but what is still missing is the ability to understand the consequences for human health based on the extent of changes in the overall metabolome.

Recent studies have shown that high fat diets promote growth of endotoxin producing bacteria and inhibit the levels of bacteria that are known to protect the gut barrier. Further, they are known to alter the Firmicutes to Bacteroidetes ratio and this results in higher levels of lipopolysaccharides in the blood and hence, consequently triggers inflammation [44]. Gut microbiota produces endotoxins that mediate diet-induced metabolic syndromes such as obesity, diabetes and hypertension [45-47]. These results indicate that these diseases may be circumvented by targeting specific gut microbial populations via dietary interventions that specifically promote the growth of bacteria that protect the gut-barrier functions and therefore, suppress the harmful pathogenic strains that produce endotoxins. Another promising method would be to manipulate the gut microbiota via fecal microbiota transplantation (FMT) as a therapeutic method [48, 49]. FMT is the process of administering fecal slurry solution from a healthy donor into the gastrointestinal tract of a diseased recipient in order to trigger a change in the recipient's gut composition and consequently confer benefit to host health. Diseases such as inflammatory bowel disease, metabolic syndrome, autoimmune disorders, among others may be targeted for FMT-based therapy [48].

Other studies focus on the interactions between the gut microbiome and the host immune system and the role of the microbiota in the development of different immune-mediated diseases such as inflammatory bowel syndrome, autoimmune diseases, cancer, cardiometabolic diseases and several others [50]. Another study used G-protein coupled receptors to identify gut microbial metabolites and found that histamine production by *Morganella morganii* or *Lactobacillus reuteri* increased colonic motility [51]. A further observation was that certain Bacteroides strains may produce the essential amino acid phenylalanine and when the serum concentration of this amino acid is greater than 1mM, it may result in phenylketonuria.

The effects of different compounds on the different metabolite levels, specifically, the levels of bile acids, as observed in **Chapters 2-5**, do not however address the meanings of these changes in terms of host health. In order to understand the consequences of changes in the kinetics of bile acids, it may be important to additionally conduct histopathological analysis of the liver combined with liver function tests, in a situation where an indication of liver-associated toxicity is predicted [52]. Another important aspect could be conducting more of such controlled animal studies and add them to the MMT database in order to keep the database updated and have more precision in finding organ-associated toxicity patterns of new test compounds. This would strengthen the prediction of adverse effects in humans using *in silico* methods in terms of risk assessment.

Adverse outcome pathways (AOPs) have gained attention in order to elucidate the underlying mechanisms of toxic events relevant for the risk assessment of chemicals. Drug-induced liver injuries

(DILI) such as cholestasis result from an altered bile acid pool including a higher accumulation of bile acids in the host system. Therefore, in order to bridge the gaps in the mechanistic understanding behind the progression of DILI, AOPs provide the link between the molecular initiating event, a series of intermediate steps and an adverse outcome as a result of the event relevant for risk assessment [53]. Therefore, AOPs have been introduced for several bile acid associated disorders such as cholestatic liver injury focusing the bile salt export pump (BSEP) with inhibition of this export pump as the molecular initiating event for cholestasis [54]. BSEP is known to be essential for the export of Bas and an inhibition of BSEP may result in an accumulation of systemic Bas leading to either homeostatic response to regulate the bile acid pool by removing Bas and their products or to the induction of an array of deteriorative changes leading to cell death [55]. Transcriptomics analysis of human hepatoma monolayers (HepaRG) and liver cultures subjected to cholestatic drugs and a BA mix, together with subsequent pathway analysis showed that the available AOP on cholestatic liver injury could be used for predicting intrahepatic drug-induced cholestasis [55, 56]. Other studies have highlighted the use of AOPs for other kinds of DILIs including liver fibrosis and liver steatosis [57, 58].

Overall, AOPs need to be continually updated by taking into account newly obtained data (structural, multi-omics, *in vitro* and *in vivo* data) and it is therefore necessary to elucidate the important meanings behind the extent of changes caused to the metabolomes, that result from gut microbiota perturbations and be able to draw conclusions about the adversity of these changes with respect to host health. It will also help to analyze the changes induced by different compounds via the gut bacterial community, from a regulatory perspective.

6.2.6. Alternative methods to elucidate gut microbial functionality

It is also of importance to note that the results presented in this thesis were based on *in vivo* 28-day studies in young adult Wister rats. However, in modern toxicology there is also a need to consider new approach methodologies. That implies that it is also important to discuss the possibility to move towards use of alternative strategies including *in vitro* and/or *in silico* tools to promote more animal-free experiments in the future. *In vitro* methods are generally used to perform studies in a highly controlled manner without using animals. Simple cell-line based models maybe used to study cellular process whereas to understand crosstalk between different cell types, *ex vivo* methods such as using functional tissues or organs isolated from an organism may be used. Combining knowledge generation from *in vivo* and *in vitro* approaches may provide a mechanistic understanding of the gut microbiota mediated metabolic functionality. A possible strategy may be to develop *in vitro* gut models using for example 1) anaerobically incubated rat feces to study microbial metabolism as well as effects on microbial composition and 2) Caco-2 cell layer transwell systems in order to study effects on absorption processes in the gut that may eventually also modify metabolome patterns in feces and plasma. In addition, these *in vitro* studies my help to better understand the underlying modes of action of selected test compounds

in a controlled environment. This approach could also help in better understanding inter-individual and inter-species differences by mimicking the *in vivo* situation using pooled fecal samples of rats or human in small batch incubations that may allow to study the inter-individual and interspecies variations. Further, a specific class of metabolites such as the bile acids and their transportation across an intestinal cell layer could be targeted which would be of interest given that bile acids appeared to play a significant role in the altered metabolomes of the fecal and plasma samples from rats exposed to the model compounds of the present study.

In a recently reported study [59], the effects of antibiotics on bile acids was studied using *in vitro* models combined with integrated metabolomics and 16S rRNA sequencing in order to investigate to what extent such *in vitro* methodologies could elucidate the effects observed in the *in vivo* studies as published in **Chapters 2-5**. The 16S rRNA analysis of the *in vitro* fecal samples incubated with different antibiotics – tobramycin, colistin sulfate, meropenem trihydrate or doripenem hydrate revealed colistin sulfate to induce the least alterations in the gut microbiota, consistent with the *in vivo* data (**Chapter 3**). Also, in line with the *in vivo* data, in the *in vitro* fecal incubations, tobramycin appeared to have the strongest effect with a significant reduction of *Verrucomicrobiaceae* and an increase in *Lachnospiraceae*. Further, the *in vitro* anaerobic fecal incubations with tobramycin showed an increase in the taurine conjugated primary bile acid, TCA, corroborating the *in vivo* experiments and confirming that tobramycin inhibits TCA deconjugation. The *in vitro* studies also revealed that when extra TCA was added to the *in vitro* incubations with control fecal microbial samples deconjugation by the fecal microbiota was highly efficient [59].

Additionally, *in vitro* experiments were performed using a Caco-2 cell layer in a transwell model to study the intestinal reuptake of intestinal bile acids [60]. This Caco-2 cell line is able to differentiate into cells that are present in the small intestinal cell layer and this cell line can be used to evaluate transport and reuptake of intestinal bile acids. The results obtained when Caco-2 cell-based transport of bile acids was studied, indicated that the transportation of the taurine/glycine conjugated primary bile acids TCDCA and GCDCA were observed to be faster than that of the taurine/glycine conjugated primary bile acids TCA and GCA as a result of higher passive diffusion rates across the barrier for dihydroxy bile acids compared to trihydroxy bile acids [60]. The experiments also showed that when Caco-2 cells were preincubated with tobramycin, the transportation of four different primary bile acids (TCA, TCDCA, GCA and GCDCA) as well as that of six different conjugated secondary bile acids (including GLCA, GUDCA, GDCA, TLCA, TUDCA and THDCA), was lower. This indicated an inhibitory effect of the antibiotic on the apical sodium-dependent bile acid transporter (ASBT), which is normally located at the apical membrane of enterocytes and is responsible for reabsorption of the bile acids back to the liver [60]. Therefore, these *in vitro* studies showed that the effects of tobramycin on host bile acid homeostasis as detected in the 28-day *in vivo* study (**Chapter 3**) should not only be

ascribed to an effect on the intestinal microbiota but can in part also be ascribed to an effect of tobramycin administration on the process of bile acid reuptake.

Furthermore, as another new approach methodology, a physiologically based kinetic model (PBK) may be used to predict the levels of bile acids *in vivo*, using *in vitro* data to define the PBK model parameters, thus providing new *in silico* strategies for which some proofs-of-principle to promote more animal-free experiments are already available [61]. Such PBK models can also be of use to extrapolate responses from animals to humans for risk-assessment strategies (Figure 6.2). Already established PBK models for humans and rats may be used and may be modified to include the different sections of the intestines to allow smooth prediction of adverse effects resulting from *in vivo* doses based on the *in vitro* data.

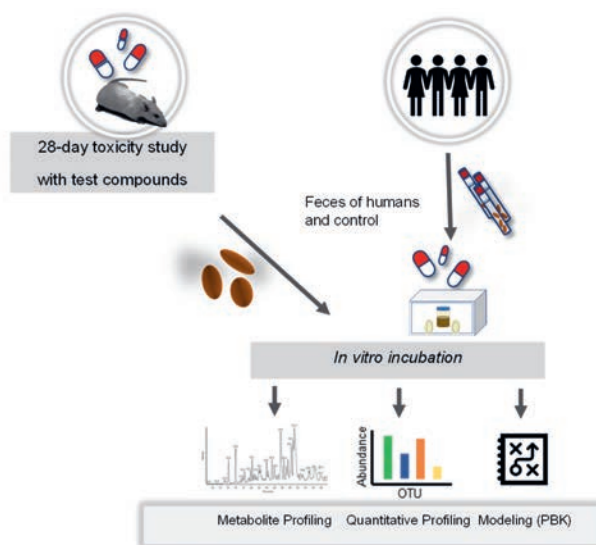


Figure 6.2: A combined schematic diagram of *in vitro* and *in silico* methods that may be used in combination with the *in vivo* approach used in the present thesis in order to predict adverse effects by new approach methodologies.

In vitro approaches will also be of use to evaluate gut bacterial enzyme-specific biotransformation capabilities. This strategy may involve incubating rat or human fecal samples from treated and untreated groups and further exposed to different chemical probes that are known to be biotransformed by human intestinal bacteria [41, 62]. Further, with the help of integrated taxonomic profiling and metabolomics analyses the correlations between *in vitro* biotransformations of reference compounds and specific bacterial families or strains may be defined thereby enabling definition of a metabolic activity-based fingerprint of the functionality of the microbiota. Alternatively isolated bacterial strains may be incubated. Hence, approaches like these may help understand the extent to which metabolic functions may vary between individual gut bacteria and promote an understanding of these bacterial biotransformation processes in improving human health.

6.2.7. Are the metabolome changes only a result of gut microbial dysbiosis?

As already shown by the example of tobramycin discussed in the previous section, effects on the host metabolome may not always be a result of microbiota perturbation but can also stem from other modes of action. The changes induced on the metabolome of the host upon dietary intervention, as observed in **Chapters 3-5**, were assumed to stem from an altered gut microbiota. As mentioned earlier, the antibiotics and their dose levels used were selected to induce a dysbiosis in the gut composition and produce low or no systemic effects on the host. As any form of systemic effects would hinder interpretation of the effects on the metabolomes, especially the blood metabolite changes, drugs and their doses were selected to exclude any systemic toxicity. However, it may not be ignored that compounds studies may, even when they are not systemically available, still have a local effect on the intestinal cells so that not all the metabolite changes are a result of an altered microbiota. This observation was made in **Chapter 5**, where artificial sweeteners were administered to young adult Wistar rats and although no significant change was observed in the gut bacterial composition, there were however changes in certain metabolites, specifically in blood plasma. It is therefore a necessity to understand if these observed changes in the plasma metabolome are actually related to a subtle change in the gut microbiota at species level or perhaps associated with for example the intestinal reabsorption of bile acids into the systemic circulation. Such effects on gut epithelial cells and their metabolic pathways or transporters may provide additional modes of action by which the host metabolome may be affected. Future studies using *in vitro* models for intestinal tissue seem to be the way forward to elucidate such modes of action. Beyond Caco-2 cell lines, there are other kinds of artificial gut model systems such as the simulator of the human intestinal microbial ecosystem (SHIME), that has been developed to mimic the enzymatic and physicochemical environment of the stomach, small and large intestines [63]. This model may be used to determine the systemic bioavailability of different compounds. And further mucin-coated microspheres may be included in these models to enable close resemblance to the human colon and can be used to study the effects of substances on the gut ecosystem [64].

Further, gut-on-a-chip models may be used for host-microbe interaction studies that take intestinal physiology into account [65]. In addition, platforms using primary cells have been recently developed to translate the characteristics of entire organs such as organoid (enteroid) 3D shaped systems, among others [66]. The organoids consist of monolayers of cells, a mucosal lumen, cell debris and outwardly proliferations regions enriched with stem cells and the 3D shaped intestinal systems mimic the topology and physiology of an actual intestinal tract [67]. These models may allow controlled regulation of gut ecosystems which is difficult to achieve when using *in vivo* animal studies and may focus on different ranges of variables depending on the research question. All in all, rapid progression in this field allows newer opportunities to further investigate the functional capabilities of the gut and its microbiome.

6.2.8. Spontaneous restoration of gut microbiota and derived metabolites without therapeutic interventions

Any impairment to the gut microbiota may lead to long term implications such as loss of homeostasis that may further impact host well-being. It is well known that severe diseases such as inflammatory bowel disease, metabolic syndrome, autoimmune disorders, neurological diseases, among others are directly or indirectly influenced by a dysbiotic gut or vice versa. Use of probiotics or lactic acid producing bacteria (LAB) like *Lactobacillus* and *Bifidobacteria* have been widely reported in the last decades as a method to restore the gut communities [68]. In addition, prebiotics consist of enrichment ingredients like non-starch polysaccharides and oligosaccharides that are known to be undigestible by humans but they help in stimulating vital metabolic activities that are possessed by LAB species and in turn may help the physiological well-being of the host [69]. Despite these efforts, not much research is conducted on the restoration capabilities of microbiota-derived metabolites post-treatment cessation. Hence, it is important to be able to elucidate long term compositional and functional effects (including antibiotic resistance) of compounds such as antibiotics that are known to alter the gut microbiota.

In **Chapter 5**, a potential ability of gut microbiota to spontaneously recover one and two weeks post antibiotic cessation has been reported. Not only the gut microbiota but this tendency to spontaneously restore was also observed for the metabolomes, more evidently in fecal than plasma metabolomes. The plasma metabolites showed an overcompensation effect two weeks post antibiotic cessation. This overcompensation effect may lead to a complete restoration of the metabolite changes back to baseline or control levels in a more prolonged study design. Therefore, these results may hint that there may be little need for therapeutic interventions such as FMT or the use of probiotics and prebiotics, for restoration of the intestinal microbiome. In humans however, several other variables may play a role in the spontaneous ability of gut microbiota reconstitution such as host health, exposure to drugs, genetics, age, immune system and several others. Therefore, the spontaneous restoration ability may be validated further with the help of humanized rodent models [70]. These models would help avoid any form of obvious inter-species differences between rodents and humans and be able to simulate and represent the complexity of human physiology.

6.3. Conclusions

The metabolic capacity of intestinal microbiota is well-studied, yet there are a lot of unknowns regarding its role in chemical (de)toxification. In the field of regulatory toxicology, the metabolic capacity of liver and other important organs is of huge interest whereas gut-mediated metabolism is often poorly characterized. Hence, this knowledge gap has led to more attention towards not only the composition dynamics of the gut microbiota but also its metabolic functionality upon exposure to chemical compounds, such as, food additives, drugs, etc. To investigate the complex bidirectional crosstalk between the gut microbes and the host, where the compounds affect the gut microbiome and in turn the microbiota affects the metabolism of the compounds, an integrated omics approach, combining taxonomics and metabolomics, appears to provide a promising tool. Measurement of metabolites compliment the gut bacterial profiling, hereby enabling definition of important correlations that may provide a first impression on the metabolic interplay between the gut microbiota and host organism. The observations made in this thesis emphasize the fact that although the fecal metabolome provides an image of the metabolic output of the gut (fecal) microbiota, the blood plasma metabolome may serve as a tool to identify a microbial perturbation. Another major highlight was the individuality of the gut microbiota composition within control rats that were maintained in a controlled environment, indicating the importance of a longitudinal study to determine the historical baseline variability of gut microbes from an untreated or control group from both sexes and not only for rats but also for human. These results obtained in this thesis also indicate that there is a need for better understanding of the consequences of the gut dysbiosis and metabolism for human health in order to facilitate use of the outcomes in toxicological risk assessment strategies of chemical substances.

References

1. Sender, R., S. Fuchs, and R. Milo, *Revised estimates for the number of human and bacteria cells in the body*. PLoS biology, 2016. **14**(8): p. e1002533.
2. Li, D., et al., *Microbial biogeography and core microbiota of the rat digestive tract*. Scientific reports, 2017. **7**(1): p. 1-16.
3. Wos-Oxley, M.L., et al., *Comparative evaluation of establishing a human gut microbial community within rodent models*. Gut microbes, 2012. **3**(3): p. 234-249.
4. DeGruttola, A.K., et al., *Current understanding of dysbiosis in disease in human and animal models*. Inflammatory bowel diseases, 2016. **22**(5): p. 1137-1150.
5. Murali, A., et al., *Elucidating the Relations between Gut Bacterial Composition and the Plasma and Fecal Metabolomes of Antibiotic Treated Wistar Rats*. Microbiology Research, 2021. **12**(1): p. 82-122.
6. Behr, C., et al., *Gut microbiome-related metabolic changes in plasma of antibiotic-treated rats*. Archives of Toxicology, 2017. **91**: p. 3439-3454.
7. Behr, C., et al., *Impact of lincosamides antibiotics on the composition of the rat gut microbiota and the metabolite profile of plasma and feces*. Toxicology letters, 2018. **296**: p. 139-151.
8. Behr, C., et al., *Microbiome-related metabolite changes in gut tissue, cecum content and feces of rats treated with antibiotics*. Toxicology and Applied Pharmacology, 2018. **355**: p. 198-210.
9. Murali, A., et al., *Connecting Gut Microbial Diversity with Plasma Metabolome and Fecal Bile Acid Changes Induced by the Antibiotics Tobramycin and Colistin Sulfate*. Chemical Research in Toxicology, 2023. **36**(4): p. 598-616.
10. Mattes, W., et al., *Detection of hepatotoxicity potential with metabolite profiling (metabolomics) of rat plasma*. Toxicology letters, 2014. **230**(3): p. 467-478.
11. Sperber, S., et al., *Metabolomics as read-across tool: An example with 3-aminopropanol and 2-aminoethanol*. Regulatory Toxicology and Pharmacology, 2019. **108**: p. 104442.
12. Eshar, D. and J.S. Weese, *Molecular analysis of the microbiota in hard feces from healthy rabbits (*Oryctolagus cuniculus*) medicated with long term oral meloxicam*. BMC veterinary research, 2014. **10**: p. 1-9.
13. Murali, A., et al., *Gut Microbiota as Well as Metabolomes of Wistar Rats Recover within Two Weeks after Doripenem Antibiotic Treatment*. Microorganisms, 2023. **11**(2): p. 533.
14. Murali, A., et al., *Investigating the gut microbiome and metabolome following treatment with artificial sweeteners acesulfame potassium and saccharin in young adult Wistar rats*. Food and Chemical Toxicology, 2022. **165**: p. 113123.
15. Fontana, A., et al., *Gut microbiota profiles differ among individuals depending on their region of origin: an Italian pilot study*. International journal of environmental research and public health, 2019. **16**(21): p. 4065.
16. Claesson, M.J., et al., *Composition, variability, and temporal stability of the intestinal microbiota of the elderly*. Proceedings of the National Academy of Sciences, 2011. **108**(supplement_1): p. 4586-4591.
17. King, C.H., et al., *Baseline human gut microbiota profile in healthy people and standard reporting template*. PloS one, 2019. **14**(9): p. e0206484.
18. Fuks, G., et al., *Combining 16S rRNA gene variable regions enables high-resolution microbial community profiling*. Microbiome, 2018. **6**(1): p. 1-13.
19. Numberger, D., et al., *Characterization of bacterial communities in wastewater with enhanced taxonomic resolution by full-length 16S rRNA sequencing*. Scientific reports, 2019. **9**(1): p. 9673.
20. Johnson, J.S., et al., *Evaluation of 16S rRNA gene sequencing for species and strain-level microbiome analysis*. Nature communications, 2019. **10**(1): p. 5029.
21. Sachse, K., et al., *DNA microarray-based detection and identification of Chlamydia and Chlamyphila spp*. Molecular and cellular probes, 2005. **19**(1): p. 41-50.
22. Rey, F.E., et al., *Dissecting the in vivo metabolic potential of two human gut acetogens*. Journal of Biological Chemistry, 2010. **285**(29): p. 22082-22090.

23. Średnicka, P., et al., *Effect of in vitro cultivation on human gut microbiota composition using 16S rDNA amplicon sequencing and metabolomics approach*. Scientific Reports, 2023. **13**(1): p. 3026.
24. Jin, H., et al., *Hybrid, ultra-deep metagenomic sequencing enables genomic and functional characterization of low-abundance species in the human gut microbiome*. Gut Microbes, 2022. **14**(1): p. 2021790.
25. Browne, H.P., et al., *Culturing of 'unculturable' human microbiota reveals novel taxa and extensive sporulation*. Nature, 2016. **533**(7604): p. 543-546.
26. Wang, W.-L., et al., *Application of metagenomics in the human gut microbiome*. World journal of gastroenterology: WJG, 2015. **21**(3): p. 803.
27. Sunagawa, S., et al., *Metagenomic species profiling using universal phylogenetic marker genes*. Nature methods, 2013. **10**(12): p. 1196-1199.
28. Jovel, J., et al., *Characterization of the gut microbiome using 16S or shotgun metagenomics*. Frontiers in microbiology, 2016. **7**: p. 459.
29. Chung, Y.W., et al., *Functional dynamics of bacterial species in the mouse gut microbiome revealed by metagenomic and metatranscriptomic analyses*. PLoS One, 2020. **15**(1): p. e0227886.
30. Zihler Berner, A., et al., *Novel Polyfermentor intestinal model (PolyFermS) for controlled ecological studies: validation and effect of pH*. PloS one, 2013. **8**(10): p. e77772.
31. Lacroix, C., T. De Wouters, and C. Chassard, *Integrated multi-scale strategies to investigate nutritional compounds and their effect on the gut microbiota*. Current opinion in biotechnology, 2015. **32**: p. 149-155.
32. Nielsen, E., G. Ostergaard, and J.C. Larsen, *Toxicological risk assessment of chemicals: A practical guide*. 2008: CRC Press.
33. Suez, J., et al., *Artificial sweeteners induce glucose intolerance by altering the gut microbiota*. Nature, 2014. **514**(7521): p. 181-186.
34. Tulstrup, M.V.-L., et al., *Antibiotic treatment affects intestinal permeability and gut microbial composition in Wistar rats dependent on antibiotic class*. PloS one, 2015. **10**(12): p. e0144854.
35. Xu, C., et al., *Changes in gut microbiota may be early signs of liver toxicity induced by epoxiconazole in rats*. Chemotherapy, 2015. **60**(2): p. 135-142.
36. Nasuti, C., et al., *Changes on fecal microbiota in rats exposed to permethrin during postnatal development*. Environmental Science and Pollution Research, 2016. **23**: p. 10930-10937.
37. Ackermann, W., et al., *The influence of glyphosate on the microbiota and production of botulinum neurotoxin during ruminal fermentation*. Current microbiology, 2015. **70**: p. 374-382.
38. Wang, Q., et al., *Use of physiologically based pharmacokinetic modeling to predict human gut microbial conversion of daidzein to S-Equol*. Journal of Agricultural and Food Chemistry, 2021. **70**(1): p. 343-352.
39. Wang, Q., et al., *Use of Physiologically Based Kinetic Modeling to Predict Rat Gut Microbial Metabolism of the Isoflavone Daidzein to S-Equol and Its Consequences for ERα Activation*. Molecular nutrition & food research, 2020. **64**(6): p. 1900912.
40. Zhang, L., et al., *Environmental spread of microbes impacts the development of metabolic phenotypes in mice transplanted with microbial communities from humans*. The ISME journal, 2017. **11**(3): p. 676-690.
41. Koppel, N., V. Maini Rekdal, and E.P. Balskus, *Chemical transformation of xenobiotics by the human gut microbiota*. Science, 2017. **356**(6344): p. eaag2770.
42. Tolstikov, V., et al., *Current status of metabolomic biomarker discovery: Impact of study design and demographic characteristics*. Metabolites, 2020. **10**(6): p. 224.
43. Kohler, I., et al., *Integrating clinical metabolomics-based biomarker discovery and clinical pharmacology to enable precision medicine*. European Journal of Pharmaceutical Sciences, 2017. **109**: p. S15-S21.
44. Zhang, C., et al., *Interactions between gut microbiota, host genetics and diet relevant to development of metabolic syndromes in mice*. The ISME journal, 2010. **4**(2): p. 232-241.
45. Turnbaugh, P.J., et al., *An obesity-associated gut microbiome with increased capacity for energy harvest*. nature, 2006. **444**(7122): p. 1027-1031.

46. Cani, P.D., et al., *Metabolic endotoxemia initiates obesity and insulin resistance*. Diabetes, 2007. **56**(7): p. 1761-1772.
47. Holmes, E., et al., *Human metabolic phenotype diversity and its association with diet and blood pressure*. Nature, 2008. **453**(7193): p. 396-400.
48. Borody, T.J. and A. Khoruts, *Fecal microbiota transplantation and emerging applications*. Nature reviews Gastroenterology & hepatology, 2012. **9**(2): p. 88-96.
49. Smits, L.P., et al., *Therapeutic potential of fecal microbiota transplantation*. Gastroenterology, 2013. **145**(5): p. 946-953.
50. Zheng, D., T. Liwinski, and E. Elinav, *Interaction between microbiota and immunity in health and disease*. Cell research, 2020. **30**(6): p. 492-506.
51. Chen, H., et al., *A forward chemical genetic screen reveals gut microbiota metabolites that modulate host physiology*. Cell, 2019. **177**(5): p. 1217-1231. e18.
52. Azer, S.A. and R. Hasanato, *Use of bile acids as potential markers of liver dysfunction in humans: A systematic review*. Medicine, 2021. **100**(41).
53. Vinken, M., *The adverse outcome pathway concept: a pragmatic tool in toxicology*. Toxicology, 2013. **312**: p. 158-165.
54. Vinken, M., et al., *Development of an adverse outcome pathway from drug-mediated bile salt export pump inhibition to cholestatic liver injury*. toxicological sciences, 2013. **136**(1): p. 97-106.
55. Gijbels, E., et al., *Robustness testing and optimization of an adverse outcome pathway on cholestatic liver injury*. Archives of Toxicology, 2020. **94**: p. 1151-1172.
56. Vinken, M., *In vitro prediction of drug-induced cholestatic liver injury: a challenge for the toxicologist*. Archives of toxicology, 2018. **92**(5): p. 1909-1912.
57. Horvat, T., et al., *Adverse outcome pathway development from protein alkylation to liver fibrosis*. Archives of toxicology, 2017. **91**: p. 1523-1543.
58. Mellor, C.L., F.P. Steinmetz, and M.T. Cronin, *The identification of nuclear receptors associated with hepatic steatosis to develop and extend adverse outcome pathways*. Critical reviews in toxicology, 2016. **46**(2): p. 138-152.
59. Zhang, N., et al., *In vitro models to detect in vivo bile acid changes induced by antibiotics*. Archives of Toxicology, 2022. **96**(12): p. 3291-3303.
60. Zhang, N., et al., *In vitro models to measure effects on intestinal deconjugation and transport of mixtures of bile acids*. Chemico-Biological Interactions, 2023. **375**: p. 110445.
61. de Bruijn, V.M., I.M. Rietjens, and H. Bouwmeester, *Population pharmacokinetic model to generate mechanistic insights in bile acid homeostasis and drug-induced cholestasis*. Archives of Toxicology, 2022. **96**(10): p. 2717-2730.
62. Fekry, M.I., et al., *The strict anaerobic gut microbe Eubacterium hallii transforms the carcinogenic dietary heterocyclic amine 2-amino-1-methyl-6-phenylimidazo [4, 5-b] pyridine (PhIP)*. Environmental microbiology reports, 2016. **8**(2): p. 201-209.
63. Molly, K., et al., *Validation of the simulator of the human intestinal microbial ecosystem (SHIME) reactor using microorganism-associated activities*. Microbial ecology in health and disease, 1994. **7**(4): p. 191-200.
64. Williams, C., et al., *Comparative analysis of intestinal tract models*. Annual review of food science and technology, 2015. **6**: p. 329-350.
65. Kim, H.J., et al., *Human gut-on-a-chip inhabited by microbial flora that experiences intestinal peristalsis-like motions and flow*. Lab on a Chip, 2012. **12**(12): p. 2165-2174.
66. Spence, J.R., *Taming the wild west of organoids, enteroids, and mini-guts*. Cellular and Molecular Gastroenterology and Hepatology, 2018. **5**(2): p. 159.
67. Dutton, J.S., et al., *Primary cell-derived intestinal models: recapitulating physiology*. Trends in biotechnology, 2019. **37**(7): p. 744-760.
68. Dinleyici, E.C., et al., *Effectiveness and safety of Saccharomyces boulardii for acute infectious diarrhea*. Expert opinion on biological therapy, 2012. **12**(4): p. 395-410.
69. Gauffin Cano, P., et al., *Bacteroides uniformis CECT 7771 ameliorates metabolic and immunological dysfunction in mice with high-fat-diet induced obesity*. 2012.

70. Ng, K.M., et al., *Recovery of the gut microbiota after antibiotics depends on host diet, community context, and environmental reservoirs*. *Cell host & microbe*, 2019. **26**(5): p. 650-665. e4.





CHAPTER 7:

SUMMARY

7.1. Summary

In the last decades, the gut microbiome and its influence on host health has been extensively studied. Hence, to elucidate the potential associations that govern interactions between the gut bacterial communities and the host, an integrative approach was used to yield knowledge about the gut metabolic capacity and its influence on the rodent microbiome. By identifying and quantifying alterations in targeted metabolites, along with the gut microbial perturbations induced by a chemical compound (such as drugs or non-caloric sweeteners), gut microbiota-associated metabolic functionality and its consequences for host metabolic patterns could be characterized. Rats, being the golden standard model for toxicological research, are commonly used to assess chemical safety in humans and were hence selected as the model organism for our experimental set up. The experimental strategy involved the use of well-defined test compounds that are known to induce gut microbial perturbations and carrying out a targeted metabolomics analysis of rat blood plasma and feces following 28 days oral exposure to the selected test compounds. A quantitative taxonomic profiling approach of feces and plasma samples was performed to connect the changes induced by chemical exposure in the microbiota with those observed for the metabolites.

In order to further expand the key knowledge from previously published work, the correlations between altered gut bacterial families and changes in the metabolites, induced by different antibiotics were investigated in **Chapter 2**. Antibiotics of different classes and activity spectra were used in this study to alter gut microbial composition and function. These perturbations in microbiota composition and metabolite patterns in both feces and plasma were then used to compute useful correlations to analyze how individual microbial families are responsible for the formation or conversion of fecal or plasma metabolites. The strongest correlations were found between 16S rRNA based identified bacterial families and fecal metabolites, mainly with bile acids, and their derivatives. Another key finding from this study was that the cecal and fecal metabolomes were highly comparable and therefore, as a more non-invasive matrix, feces may be preferred as the matrix to study the functional read-out that characterizes gut microbial perturbations.

Effects of two additional antibiotics belonging to different classes and activity spectra than the ones studied in **Chapter 1**, on the gut microbiota and associated feces and plasma metabolomes, were reported in **Chapter 3**. Tobramycin and colistin sulfate were each orally administered for 28 days to young adult Wistar rats and their subsequent gut (fecal) microbiota, and their feces and plasma metabolomes were analyzed to elucidate the gut microbial functionality. Tobramycin induced substantial changes in the gut microbiota as well as in the fecal metabolites, including the bile acid pool. Consistently, the plasma metabolome also exhibited alterations upon tobramycin administration, with significant changes in pre-established plasma biomarkers (i.e., hippuric acid, indole derivatives and bile acids) associated with gut microbial perturbations. However, in contrast to tobramycin, only marginal

effects on the gut (feces) microbiota and associated feces and plasma metabolomes were observed upon colistin sulfate exposure. Consistently, both fecal and plasma metabolome also overall did not reveal a profound effect upon exposure of the rats to colistin sulfate.

One specific change observed in the colistin treated microbiota was a profound reduction of the *Verrucomicrobiaceae* bacterial family, which appeared to be an effect induced by the antibiotic administration. However, the virtual absence of this bacterial family was also observed in four out of twenty control animals, suggesting that this reduction can equally well be related to a natural variability in the gut microbiota of young adult Wistar rats. Further analysis indicated that these microbes do not contribute to the approximately 600 fecal metabolites measured in the study, suggesting their commensal nature. Such inter-individual variabilities in the microbiome composition could further hamper the interpretation of test compound induced compositional changes in the gut microbiota. Therefore, better definition of baseline inter-species as well as inter-individual variabilities of the gut bacterial composition may further facilitate the detection of relevant chemical-induced changes and also facilitate inter-species extrapolations.

Furthermore, in **Chapter 4**, an insight into the recovering abilities of the gut bacterial families as well as the associated metabolites in doripenem-antibiotic perturbed animals was provided. With this study, spontaneous recovery and reconstitution of 16S rRNA based identified bacterial families as well as of the feces metabolome were observed two weeks after cessation of the doripenem treatment. In the plasma metabolome of two weeks post high dose doripenem cessation, an overcompensation mechanism was observed where the prior changed metabolites (when exposed to doripenem antibiotic) changed in the opposite directions two weeks after doripenem treatment was terminated. The results obtained from this study contribute to understanding the restoration abilities of the intestinal and metabolic homeostasis resulting from broad-spectrum antibiotic exposure, without any therapeutic interventions. More extensive studies with prolonged durations post-antibiotic cessation may indicate if this overcompensation is indeed in the process of complete recovery or if it leads to a new stable state.

Finally, **Chapter 5** presents a case study to understand if two artificial sweeteners modify the fecal microbiota and the metabolomes, Wistar rats from both sexes were orally exposed for 28 days to acesulfame potassium (Ace-K) or saccharin. The dose levels selected for Ace-K were 2.5 and 8 times higher than the acceptable daily intake (ADI) for the sweetener. The doses of saccharin were selected to be 4 and 20 times higher than the ADI for saccharin. Both sweeteners exhibited only minor effects on the microbiota, and consequently the fecal metabolome. Saccharin however, significantly altered the plasma metabolome, with significant changes in the levels of bile acids in both sexes, indicating potentially perturbed bile acid kinetics in the gut, which was rather not apparent in the 16S rRNA based identified bacterial families changes and consequently in the fecal metabolome profiles. The absence of any changes observed in the microbiota composition may suggest an adaptive effect of the microbiota

themselves to the exposure to saccharin or perhaps a possible effect on another target than the gut microbiota. This suggests either that the microbiome adaptation may occur faster than changes in the gut microbial metabolic functionality, in response to a particular treatment, or the fact that the changes in the bile acids may be a result of another mode of action such as for example an effect on bile acid intestinal reuptake. Further studies with a higher resolution of 16S rRNA sequencing data, perhaps down to taxonomic levels of species or strains assignment, in combination with a metagenomics approach and/or *in vitro* studies on effects of saccharin on intestinal transport of bile acids could be used to explore the bacterial species or strains driving the metabolic outcome of saccharin in rats or elucidate a different mode of action that may be causing these saccharin induced changes in the plasma metabolomes other than the gut microbiota.

The aim of this thesis was to extend the knowledge of the intestinal microbial metabolic capacity of young adult rodent models with the help of multi-omics approaches. This objective was addressed with the help of 28-day oral rat studies following OECD 407 guidelines. Test compounds were selected to induce gut microbiota perturbations and low or no systemic toxicity in order to assess specific gut microbially derived metabolites. The key findings of this thesis include identification and validation of metabolic markers and understanding functional roles of specific bacterial families. It was also noted that the ability of the gut microbiota to spontaneously recover post antibiotic treatment was much faster than the restoration of metabolic functions without any external or therapeutic intervention. These results suggest that a combined analysis of microbiota and metabolomes certainly provide a firsthand impression of the gut microbial metabolic functionality. A further aspect that needs to be explored are the other modes of action that may be affecting the changes in the metabolomes than the gut microbiota. These key findings have been discussed and summarized in **Chapter 6**. Despite that however, there are limitations to this work that have also been highlighted in this chapter, where the areas have been highlighted where further research may be needed. One of the crucial limitations and topics for future results is the apparent inter-individual variability as well as the inter-species variability between rodent models and humans and thus how the results can be translated to human and consequently, be of use in the risk assessment strategies for chemicals in human beings. Further elucidation of what metabolome and microbiota changes will be adverse is also essential to allow future use of the results in human risk assessment.



ACKNOWLEDGEMENTS

Acknowledgements

Time sure flies! My doctoral journey is the best example of this phrase. It is indeed unbelievable that the journey is now officially finished, and I cannot be any prouder of it. Pursuing a PhD in the field of my dreams has finally been checked off from my life's to-do list that I wrote back when I was 15. No part of this journey could have been fulfilled without the valuable and precious presence of everyone involved, that accompanied me through major ups and mediocre downs during the last four years.

Foremost of all, I would like to thank my two main supervisors Prof. Dr. Bennard van Ravenzwaay and Prof. Dr. Ivonne Rietjens. You both have been really patient with me and have guided me while I was lost and taught me a lot of different things, for which I will be forever thankful. Ben, you being my 1st supervisor, have always been nothing but kind (sometimes tough on me when I deserved it) and have been a wonderful source of encouragement throughout my PhD life. Your support, guidance, constructive criticisms and immense knowledge in the field of Toxicology has really perked up my motivation to pursue my career and advance in this field. Other than that, I always loved to learn new facts and general knowledge about birds, languages, world geography, flights and what not! So, a heartfelt thanks to you for believing in me and giving me this wonderful opportunity!!

Thank you, Ivonne, for being an incredible 2nd supervisor, kilometers away from where I live, but still being a huge pillar throughout my PhD journey. Your expertise in the field, your consistent support and always being present whenever I needed have expanded my horizon in this field and also have made me better at scientific writing. Your promptness is one of the many things I would be ever thankful for despite of only being able to connect with you virtually after the whole pandemic situation. I am very proud to have worked with you and will cherish this time throughout my life. I would take this opportunity to also apologize to you if whenever I had put you under stress during the journey.

Another very important group of people are the team members from the ELUMICA project that I was proudly a part of. Big thanks to the former members, Dr. Katherine Hurley and Dr. Marta Baccaro for being a very integrative and supportive parts of the project and always supporting and guiding me with your expertise during the time we spent together as collaboration partners. I would extend my gratitude to Prof. Dr. Shana Sturla for being one of the major backbones of the project, all the way from Zürich! Our scientific exchanges were always very informative, and I got a lot to learn from you from our regular virtual meetups. Apart from your inexhaustive knowledge of toxicology, your cheerful personality always lit up the moods of everyone in the team, so thank you for that! Nina and Ally, how dare I forget you guys? I will always cherish our virtual and in-person (Koblenz days) meetings which included scientific discussions to naming our favorite desserts. I am pretty sure that you both will always be a part of my life now. Last but not the least, Helene (I got your name wrong again, haven't I?), it was nice to have met you, although brief but it was fun! I wish you a lot of success in your PhD and future endeavors and guess what, the world is small, maybe will cross paths again?

Varun, I am not sure how to put my gratitude in words for you. I would start with extending my sincere thanks to you for always being a great support throughout my PhD duration. I would learn something new almost every day from you and I still remember when I 'joked' with you saying that I owe my doctoral degree to you. Starting from those days when I didn't even know what a 'Package' in R meant to defending my thesis, I can surely say that I have grown and learnt a lot from you. I will always cherish the presence and support of you and your family (I still haven't met Advik, by the way) during my journey.

The next person who played a big role during my PhD time is Franziska. Although you joined the ELUMICA club 2 years after I did, I can be sure that you had one of the biggest roles during my tenure at TOX. So, I thank you for always being a limitless support in making crucial scientific decisions about the project to helping me with my posters, presentations and publications. Not only that but I had some really funny exchanges about different things with you that lightened up my mood once in a while. You always offered your hand whenever I was going through a stressful situation, which I will be forever thankful for. So, I am happy that we can continue to be colleagues working for RG/T!!

I would also like to extend my gratitude to the metabolome team: Hennicke, Philipp, Volker H., Tilmann, Peter, Volker S., Markus, Oliver, Michael, Frank, Olga, Regine, Saskia (Former), Barbara (Former), Eric (Former), Jana (Former) and Burkhard (Former). Thank you so much every one of you for being an active part of the project and for your expertise in the field of Toxicology. Regular meetings with the team really helped me discuss and decide the various aspects of the experiments, review the progress of the project, troubleshoot the issues, whenever necessary and being able to make crucial decisions related to the ELUMICA project. Saskia and Hennicke, I would like to add my gratitude to you for being an incredible support during the project and making my onboarding into my PhD journey really smooth. Thank you, Philipp and Hunter, for being patient with me and helping me whenever I needed your guidance the most and helping me make sense out of my data. I would always cherish our exchanges throughout my life.

The people of Mechanistic Toxicology department at TOX, especially Herr Rank, Anne and Burkhard have been a huge support in conducting the animal studies on my behalf and bearing with all the sudden changes that were made to the studies (via amendments). Also thank you for being patient with me and my endless sample collection and not even complaining once about it. I also appreciate that you could be easily 'bribed' with a box of Ferrero Rocher chocolates. Additionally, thanks to the Clinical Chemistry lab of Volker S, no number of thanks is justifiable for the incredible Irmgard (I really wanted to write Frau Weber, but she would hate me even more for it). Thank you, Irmgard, for warmly welcoming me to your lab and allowing me to trash all my 'shitty' samples all over your refrigerator. Thank you some of the lovely lab technicians from the lab – Sandra, Manuela, Daniela and Britta for

the amazing chit chats in pseudo-German and keeping me a good company whenever Irmgard was not around.

How do I forget the 3 angels of RG/T- Frau Blum, Christine and Martina for being such motherly figures and for the lovely exchanges. Thank you for always helping me out sort my travel planning and taking care of the reimbursements of poor me. Christine, I cannot thank you enough for being a wonderful laughing buddy whenever I needed one, especially when we talked about 'those voices' we hear often. I am happy that we can stay colleagues and cross each other's paths even after my doctoral journey is over.

Did I save the best for the last? I am forever grateful for the presence of café UT in my life. All the old and new Café UT guys – Nils, Livia, Alex, Pegah, Priyata, Carol, Nina, Eleonora, Andreas, Julia, Max, Jonas, Dunja (my Serbian SIIIS), Sabina, Pia, Sakshi, Emanoela, Luisa, Alina, Mathias, Konstantinos, big thanks for being a part of the best part of my PhD journey. Special thanks to Nils and Livia for being great master students and not judging me for being an amateur and tolerating me throughout their thesis periods and still being in touch with me regardless. Big thanks to Didunja, Pegah, Priyata and dearest Sabina (the OGs) for all our trashy to super deep talks. Thanks for being the best colleagues who have now turned into best of friends of my life. Thanks for being with me through my best and worst and still not judging me. Thanks for those fun car drives, wild girls trips, routine dinner dates and many more to come. Special thanks to Nina (my LU guardian) for welcoming me to Ludwigshafen and being an active part of my life and for always listening to me and giving me all the wonderful life advice I need. Thank you, Carol, for being present for me although our time together during my PhD was limited. I am glad that you and I can still continue to be colleagues and that you can shower your wisdom on me whenever we meet in person!!

Big thanks to friends who were like a family in Ludwigshafen, which is not the best city to be in, other than the fact that BASF is located there. But you guys - Diksha, Keerthi, Krishna, Paula, Vincent, Laura, Mihir, Yojia, Yosr and all of Laura's and Paula's random friends - made it so much better and feel like home. I will always cherish the memories of ours and I am glad that we can still remain in touch and be a part of each other's life's. Friends from Jena – Reema (my best friend who knows me to pieces), Chen and Kyoyoung – I sincerely thank you for being a part of my life for over 6.5 years and still not getting sick of me (don't you dare!). I will always remember how our paths first met and the influence we still have in each other's lives. Any number of words that I write to appreciate you is less, so I extend my sincere gratitude to you all. My German teacher for 3.5 years, David, thanks for making me more street smart and a bit more comfortable with my German knowledge. I don't mind when I speak wrong and that is because of you! I will always remember our funny exchanges to reading random texts in German and laughing about it. The German classes with you and Varun were like a mini break from the hardships and struggle I experienced during my PhD duration.

Thanks to some of the PhD students from TOX-WUR – Annelies, Katja and Veronique – who I only briefly interacted with. But the interactions were very interesting, knowledgeable and fun so thanks for always being available and for reaching out to me every once in a while and being this reassuring virtual presence. Many thanks to my new Manager, Jessica for giving me the opportunity to remain in BASF and be an integral part of the company and also thanks to the team for warmly welcoming me into their gang in Berlin.

And finally, I appreciate and honor the relentless support of *la Familia*. I thank you mom and dad for believing in me and trusting me to move miles away from you to pursue my teenage dreams. Nothing would be possible without your emotional, mental and financial support in order to send me all the way when many girls back in India were not even allowed to leave their hometowns due to safety concerns. Thanks for being generous with me and making me an independent woman in order to be where I am today. I am also grateful for our daily long calls, despite the distance, that pushes me to be better and look forward to my next trip to India. I appreciate you both, Akshaya, SG and little Aadhu for being an immense part of my highs and lows and still not giving up on me. Narasiman, I thank you for crossing paths with me in Ludwigshafen, showering me with all the love I didn't realize I needed and getting promoted from a mere boyfriend to my life partner (and a partner in crime). Thank you for making me a part of your family and introducing me to your parents and sis Nisha, who by the way are the coolest and make the best in-laws. Thank you for introducing me to your amazing circle and your world that helped (and still continues to help) me expand my horizon and become a better version of myself. Last but definitely not the least is a special thanks to Vaishnevi for being this kind soul for creating such a lovely thesis cover and making the whole process even more special.

And before I forget, my final gratitude goes to myself, for being optimistic, energetic and being myself throughout the doctoral tenure and for becoming an improved version and achieving the biggest desire of my teenage dreams ...



ABOUT THE AUTHOR

Curriculum Vitae



Aishwarya Murali was born on the 1st of September 1994 in New Delhi, India. In 2012, she obtained her high school diploma from A.S.N. Senior Secondary School, Mayur Vihar, Delhi. She moved to the southern part of India, Chennai, Tamil Nadu to pursue her Bachelors in Genetic Engineering. Following that, to continue her education in Microbiology, she moved miles away to Germany where she studied Master's at the prestigious Friedrich-Schiller Universität Jena, Thüringen, Germany. While pursuing Master's she also got the opportunity to work in a variety of specialized research groups at Leibniz-Institut für Naturstoff-Forschung und Infektionsbiologie, Max Planck Institute for Biogeochemistry and at the Max Planck Institute for Chemical Ecology, all situated in Jena, Germany. She then joined the Max Planck Institute for Chemical Ecology for her master thesis under the supervision of Prof. Dr. Wilhelm Boland and Dr. Tilottama Mazumdar. After graduating from the Masters program with 1.6 grade, she moved to Ludwigshafen am Rhein in 2019 to pursue her PhD research at the department of Experimental Toxicology and Ecology of BASF SE in Ludwigshafen, Germany. During her PhD, she focused on elucidating the effects of different compounds on the gut microbiota and related metabolomes using rat models under the supervision of Prof. Dr. Bennard van Ravenzwaay (Former Vice President of the Department at BASF) and Prof. Dr. Ivonne Rietjens (Head of the department of Toxicology at Wageningen University & Research). The research was conducted in collaboration with Wageningen University and ETH Zürich as a part of the Cefic-LRI funded ELUMICA (Elucidating the Intestinal Microbial metabolic Capacity) project. Additionally, she organized the monthly meetings with the ELUMICA team members and bi-annual meetings with the Cefic-LRI funding committee to coordinate the collaboration and discuss the scientific progress of the project. As of March 2023, she is working at BASF Services Europe GmbH, Berlin, Germany, as an Executive Professional in scientific writing of Toxicological reports of routine *in vitro* studies performed at BASF SE, Ludwigshafen am Rhein.

List of publications

This thesis

1. **Murali, A.**, Giri, V., Cameron, H. J., Behr, C., Sperber, S., Kamp, H., ... & van Ravenzwaay, B. (2021). Elucidating the Relations between Gut Bacterial Composition and the Plasma and Fecal Metabolomes of Antibiotic Treated Wistar Rats. *Microbiology Research*, 12(1), 82-122.
2. **Murali, A.**, Giri, V., Zickgraf, F. M., Ternes, P., Cameron, H. J., Sperber, S., ... & van Ravenzwaay, B. (2023). Connecting Gut Microbial Diversity with Plasma Metabolome and Fecal Bile Acid Changes Induced by the Antibiotics Tobramycin and Colistin Sulfate. *Chemical Research in Toxicology*, 36(4), 598-616.
3. **Murali, A.**, Zickgraf, F. M., Ternes, P., Giri, V., Cameron, H. J., Sperber, S., ... & van Ravenzwaay, B. (2023). Gut Microbiota as Well as Metabolomes of Wistar Rats Recover within Two Weeks after Doripenem Antibiotic Treatment. *Microorganisms*, 11(2), 533.
4. **Murali, A.**, Giri, V., Cameron, H. J., Sperber, S., Zickgraf, F. M., Haake, V., ... & van Ravenzwaay, B. (2022). Investigating the gut microbiome and metabolome following treatment with artificial sweeteners acesulfame potassium and saccharin in young adult Wistar rats. *Food and Chemical Toxicology*, 165, 113123.

Other Publications

1. Mazumdar, T., Teh, B. S., **Murali, A.**, Schmidt-Heck, W., Schlenker, Y., Vogel, H., & Boland, W. (2021). Transcriptomics reveal the survival strategies of *Enterococcus mundtii* in the gut of *Spodoptera littoralis*. *Journal of Chemical Ecology*, 47, 227-241.
2. Mazumdar T, Hänniger S, Shukla SP, **Murali A**, Bartram S, Heckel DG, Boland W. 8-HQA adjusts the number and diversity of bacteria in the gut microbiome of *Spodoptera littoralis*. *Front Microbiol.* 2023 Jan 18;14:1075557. doi: 10.3389/fmicb.2023.1075557. PMID: 36744087; PMCID: PMC9891463.
3. Zhang, N., Wang, J., Bakker, W., Zheng, W., Baccaro, M., **Murali, A.**, ... & Rietjens, I. M. (2022). In vitro models to detect in vivo bile acid changes induced by antibiotics. *Archives of Toxicology*, 96(12), 3291-3303.
4. Zickgraf, F. M., **Murali, A.**, & Landsiedel, R. (2023). Engineered nanomaterials (ENM) and the microbiome: implications for human health. *Current Opinion in Toxicology*, 100429.

Overview of training activities

Courses:

Basic Principles of Toxicology	LMU Munich, DE	04/2022
--------------------------------	----------------	---------

Seminars & Conferences:

ECETOC Microbiome Expert Workshop	Porto, PT	06/2019
Deutsche Gesellschaft für Hygiene und Mikrobiologie (DGHM) Conference	Leipzig, DE	03/2020
Beneficial Microbes Conference	Online	03/2021
EUROTOX Conference	Online	09/2021
Society of Toxicology (SOT) Conference	Online	03/2022

Optional activities:

Wrote & published technical ECETOC report	BASF, DE	04/2020
Wrote and pitched a creativity proposal	BASF, DE	01/2021
Wrote a joint report for Cefic-LRI	BASF, DE	11/2022

The research described in this thesis was financially supported by Cefic- Long-Range Research Initiative (Grant number: Cefic-C7) and BASF SE, Ludwigshafen am Rhein, Germany

Financial support from Wageningen University for printing this thesis is gratefully acknowledged.

Cover design and drawings by Vaishnevi Vasu, Dubai, UAE

Layout and printing by ProefschriftMaken | proefschriftmaken.nl

